

https://dspace.org/

Time-course changes in cell proliferation, cell differentiation and cell death in the avian, amphibian and mammalian brains

Pilani Nkomozepi

2019
https://hdl.handle.net/10539/34580

Downloaded from a DSpace repository. https://dspace.org/

TIME-COURSE CHANGES IN CELL PROLIFERATION, CELL DIFFERENTIATION AND CELL DEATH IN THE AVIAN, AMPHIBIAN AND MAMMALIAN BRAINS

Pilani Nkomozepi

0506135K

PhD Thesis

Supervisor: Professor Amadi Ogonda Ihunwo

Co-Supervisor: Professor Paul Robert Manger

A Thesis submitted to the Faculty of Health Sciences, University of the Witwatersrand,

in fulfilment of the requirements for the degree of Doctor of Philosophy.

March, 2019

DECLARATION

I, Pilani Nkomozepi declare that this thesis is my own, unaided work. It is being submitted for the Degree of Doctor of Philosophy at the University of the Witwatersrand, Johannesburg. It has not been submitted before for any degree or examination at any other University.

(Signature of candidate)

18th day of MARCH 2019

DEDICATION

I dedicate this work to

... My wife, Faith...

... My son, Zach...

... My Mom and Dad...

... My late aunt, Emeldah...

... My late grandparents, Edith and Davison...

... And to the Glory of God...

PUBLICATIONS ARISING FROM THIS THESIS:

1. Nkomozepi P, Mazengenya P and Ihunwo AO (2018). Changes in neurogenesis with post-hatching age in the male Japanese quail (*Cortunix Japonica*). *Acta Neurobiologiae Experimentalis*. 78, 173-186. (**Published**)

2. Nkomozepi P, Mazengenya P and Ihunwo AO (2019). Quantitative analysis of age-related changes in doublecortin (DCX) expression in the male Japanese quail (*Cortunix Japonica*) telencephalon. *International Journal of Developmental Neuroscience* (**In Press**).

3. Nkomozepi P, Mazengenya P and Ihunwo AO (2019). Age-related changes in Ki 67 and DCX expression in the BALB/c mouse (*Mus musculus*) brain. *International Journal of Developmental Neuroscience*. 72:36-47. (**Published**)

4. Nkomozepi P, Mazengenya P and Ihunwo AO (2019). Age- related changes in proliferation nuclear antigen (PCNA) and doublecortin (DCX) expression in the post-metamorphic South African clawed (*Xenopus laevis*) frog brain. Manuscript ready for submission.

PRESENTATIONS ARISING FROM THIS THESIS:

1. Nkomozepi P, Mazengenya P, Manger P and Ihunwo AO: Time-course changes in PCNA and DCX expression in the juvenile and adult Japanese quail brains. XXIV International Symposium on Morphological Sciences, 2nd -6th September, 2015, Istanbul, Turkey. [ORAL]

2. Nkomozepi P, Mazengenya P, Manger P and Ihunwo AO: Changes in neurogenesis with post-hatching age in the Japanese quail (*Cortunix Cortunix Japonica*) Brain. 13th annual meeting of the Society of Neuroscientists of Africa on 11th-14th June, 2017, Entebbe, Uganda [ORAL]

3. Nkomozepi P, Mazengenya P and Ihunwo AO: Quantitative analysis of age-related doublecortin expression in the telencephalon of male Japanese quail (*Cortunix Japonica*). American Society of Neurochemistry on 24th -28th March, 2018, Riverside, California, USA [POSTER]

ABSTRACT

This thesis presents a collection of four related studies that were designed to investigate the occurrence and dynamics of postnatal neurogenesis in animal species derived from three different vertebrate taxa: mammals, avians and amphibians. This work was prompted by the observation that non-mammalian vertebrates are able to regenerate functional neural tissue following injury or experimental ablation of whole or parts of the brain parts, in striking contrast to mammals where neural tissue is seldom replaced following injury. The origin of this remarkable difference is poorly understood but differences in patterns of neuronal stem cell proliferation and neurogenesis are thought to be involved. Therefore, this interclass work was designed to determine neurogenic compartments in the amphibian, avian and mammalian brain and to determine time-course (defined as the increasing chronological age across the different life-history stages of each animal) changes in neurogenic activity (neuronal stem cell proliferation, differentiation and neuronal incorporation) in each compartment. The African clawed frog (*Xenopus laevis*), Japanese quail (*Cortunix cortunix Japonica*) and BALB/c mouse (*Mus musculus*) were used in this study as representative models for the amphibian, avian and mammalian vertebrates respectively.

In study 1, a qualitatively evaluation proliferative sites and brains areas that incorporate new neurons in the Japanese quail brain at post-hatching ages 3 to 12 weeks was carried using immunohistochemical methods. Proliferating cells were observed mainly in the olfactory bulb ventricular lining, telencephalic ventricular zones and cerebellum. Fewer proliferating cells were also observed in the hypothalamus, thalamus and bed nucleus of the stria terminalis. Newly formed neuroblasts were observed incorporated into the olfactory bulb, telencephalon and cerebellum. Furthermore, these neuroblasts were observed throughout all the regions of the pallium (except for the entopallium and arcopallium); septal nuclei and striatum. Fewer neuroblasts were also observed in the hippocampus and bed nucleus of stria terminalis. The density of proliferating cells and neuroblasts in all brain areas declined with post-hatching age.

Since study 1 established that the telencephalon exhibited the highest neurogenic activity, study 2 was designed to quantitatively analyse how neuronal incorporation in the Japanese quail telencephalon changes with age and life-history stage. In all the eight areas of the telencephalon quantified, the numbers of neuroblasts were strongly negatively correlated with post-hatching age. Furthermore, the numbers of neuroblasts in the same brain areas were higher at juvenile compared to sub adult and adult life-history stages. This study revealed that neuronal incorporation in the quail telencephalon is widespread but declines with post-hatching age. In addition, the most dramatic decline in neuronal incorporation in the all the telencephalic areas quantified occurred from the 7th week just after the quails attained sexual maturity.

Study 3 was designed to qualitatively and quantitatively determine how age (1-12 weeks) and life-history stage affect neurogenesis in the male BALB/c mouse brain using immunohistochemical methods. Proliferating cells were mainly observed in the olfactory bulb, rostral migratory stream, sub ventricular zone of the lateral ventricle and the sub granular zones of the dentate gyrus. In addition, fewer proliferating cells were also observed in the neocortex, cerebellum and tectum. Newly formed neuroblasts were found similar brain regions as the proliferating cells except for the cerebellum and tectum. The numbers of both proliferating and newly formed cells sharply decreased with increasing age or progression through life-history stages in the all the neurogenic areas of the BALB/c mouse brain.

The objective of study 4 was to qualitatively and quantitatively determine how proliferating cells and newly formed neuroblasts in the post-metamorphic African clawed frog brain change with age and life-history stage. Proliferating cells were observed mainly in the ventricular linings of the olfactory bulb, telencephalon, ventral hypothalamus, preoptic region and metencephalon adjacent to the cerebellar granule cell layer. Newly formed cells were observed in the parenchyma of the olfactory bulb, telencephalon, ventral hypothalamus and cerebellum. In the telencephalon, newly formed cells were concentrated mainly in the striatal and septal areas although fewer cells were also observed in the lateral, medial and dorsal pallial areas. In all the quantified areas of the post-metamorphic brain of the African clawed frog, the numbers of proliferating and newly formed cells were strongly negatively correlated

with age. Furthermore, both these cells were higher in the juvenile frogs compared to sub adult and adult frogs.

In conclusion, this work established that the ventricular lining is the main site of neuronal birth in all the vertebrate species investigated. In the amphibian brain, neuronal birth takes place in the ventricular lining of the olfactory bulb, telencephalon, diencephalon and rhombencephalon. In the avian brain, neuronal birth is restricted to the ventricular lining of the olfactory bulb and telencephalon, and the cerebellum. In mammals, however, neuronal birth is restricted to the telencephalon, specifically the sub ventricular zone of the lateral ventricles, rostral migratory stream and the sub granular zone of the dentate gyrus. This reflects a phylogenetic reduction in the brains regions exhibiting proliferative activity.

Similarly, neuronal incorporation is more widespread in the amphibian and avian brains compared to the mammalian brain. In the amphibian brain, new neurons are incorporated in the olfactory bulb, telencephalon, diencephalon and cerebellum. In the avian brain, neuronal incorporation takes place mainly in different parts of the telencephalon, and to a lesser extent the olfactory bulb and cerebellum. In mammals, neuronal incorporation is mainly restricted to the olfactory bulb and the hippocampal dentate gyrus. It therefore appears that as vertebrates evolve, there is a reduction in the number of brain regions incorporating new neurons.

In addition, this work also revealed that neurogenesis decreases with age in all the vertebrates studied. In the amphibian and avian brains, the rate of neurogenesis is relatively stable during the juvenile period and then declines steeply during the transition from sub adult to adult life-history stages as the animal attains sexual maturity. In mammals, however, the decline in neurogenesis is very rapid and steep from early postnatal life to adulthood. Thus neurogenesis declines at a slower pace in the amphibian and avian brains compared to their mammalian counterparts.

ACKNOWLEDGEMENTS

Firstly, I wish to thank my LORD and SAVIOUR Jesus Christ for giving me the strength and will to complete this thesis. Without his sufficient Grace, I would not have managed to accomplish this.

I would also like to extend my profound gratitude and appreciation to my PhD supervisors, Professors Amadi Ogonda Ihunwo and Paul Robert Manger for their guidance and unwavering support without which I would not have been able to complete this work. I thank them for allowing me to use their laboratory facilities and invaluable experience.

I would also like to thank members of the Adult Neurogenesis Research Group for their assistance in all the experiments and data collection. I am also greatly indebted to Mrs Hasiena Ali for her patience, advice and assistance at every stage of this work. I will forever be grateful for the knowledge and technical experience I gained through working with you.

I would also like to acknowledge the Swiss South Africa Joint Research program, NRF and the University of Johannesburg for funding my studies. Without this valuable financial support, I would not have been able to complete this work.

Finally, I would to extend my gratitude to my wife Faith and my family for their unwavering support and encouragement throughout the duration of this study. May God continue to richly bless them.

TABLE OF CONTENTS

DECLARATION i
DEDICATION ii
PUBLICATIONS ARISING FROM THIS THESIS: iii
PRESENTATIONS ARISING FROM THIS THESIS iv
ABSTRACT v
ACKNOWLEDGEMENTS viii
TABLE OF CONTENTS ix
LIST OF TABLES xiii
LIST OF FIGURES xiv
LIST OF ABBREVIATIONS xviii
CHAPTER 1: INTRODUCTION AND LITERATURE REVIEW 1
1.1 BACKGROUND 2
1.2. HISTORICAL BACKGROUND 4
1.3 NEURAL STEM CELLS AND THE NEUROGENIC NICHE 5
1.3.1 Architecture of the sub ventricular zone and neuronal stem cell identity in mammals 6
1.3.2 Architecture of the sub granular zone and neuronal stem cell identity in mammals 8
1.3.3 Architecture of the ventricular zone and neuronal stem cell identity in avians 9
1.3.4 Architecture of the ventricular zone and neuronal stem cell identity in amphibians 11
1.4 NEUROGENESIS IN VERTEBRATES 14
1.4.1 Adult neurogenesis in the mammalian brain 16
1.4.2 Adult neurogenesis in the avian brain 18
1.4.3 Adult neurogenesis in the amphibian brain 20
1.5 FUNCTIONAL SIGNIFICANCE OF NEUROGENESIS 21
1.6 FACTORS AFFECTING VERTEBRATE NEUROGENESIS 23
1.6.1 Effect of age on vertebrate neurogenesis 23
1.6.2 Mechanisms of age-dependent changes in neurogenesis in vertebrates 24
1.7 EVOLUTIONARY PERSPECTIVES AND ANIMAL MODELS USED 29
1.8 AIM AND OBJECTIVES OF THE STUDY 41
1.8.1 Aim 41
1.8.2 Objectives 41

CHAPTER 2: CHANGES IN NEUROGENESIS WITH POST-HATCHING AGE IN THE MALE JAPANESE QUAIL (*CORTUNIX JAPONICA*) BRAIN 45
2.1 INTRODUCTION 46
2.2 METHODS 48
2.2.1 Experimental Animals 48
2.2.2 Tissue collection and processing 48
2.2.3 Immunohistochemistry 49
2.2.4 Data Analysis 50
2.3.1 Age-related changes in PCNA expression in the Japanese quail brain 51
2.3.2 Age-related changes in DCX expression in the Japanese quail brain 61
2.4 DISCUSSION 73
2.4.1 Methodological considerations 73
2.4.2 Ontogenetic considerations 74
2.4.3 Age - related changes in PCNA and DCX expression in different brain regions 75
2.5 CONCLUSION 78
CHAPTER 3: QUANTITATIVE ANALYSIS OF AGE-RELATED CHANGES IN DOUBLECORTIN (DCX) EXPRESSION IN THE MALE JAPANESE QUAIL (*CORTUNIX JAPONICA*) TELENCEPHALON. 79
3.1 INTRODUCTION 80
3.2 MATERIAL AND METHODS 82
3.2.1 Experimental animals 82
3.2.2 Tissue collection and processing 82
3.2.3 Immunohistochemistry for doublecortin 83
3.2.4 DCX quantification 84
3.2.5 Data Analysis 87
3.3 RESULTS 90
3.3.1 Distribution of DCX in the Japanese quail telencephalon 90
3.3.2 Age- related changes in DCX immunoreactivity in the Japanese quail telencephalon 95
3.3.3 Life-history stage related changes in DCX immunoreactivity in the Japanese quail telencephalon 100
3.4 DISCUSSION 104
3.5 CONCLUSION 107
CHAPTER 4: AGE-RELATED CHANGES IN KI-67 AND DCX EXPRESSION IN THE BALB/ C MOUSE (*MUS MUSCULUS*) BRAIN 108
4.1 INTRODUCTION 109

4. 2 MATERIALS AND METHODS 110
4.2.1 Animals 110
4.2.2 Tissue collection and processing 111
4.2.3 Immunohistochemistry 111
4.2.4 Data Analysis 112
4.3 RESULTS 114
4.3.1 Distribution of Ki-67 and DCX immunoreactive cells in the BALB/c mouse brain 114
4.3.2 Age-related changes in the number of Ki-67 and DCX immunoreactive cells in the BALB/c mouse brain 126
4.3.3 Life-history stage related changes in Ki-67 and DCX immunoreactivity in the BALB/c mouse brain 133
4.4 DISCUSSION 138
4.4.1 Distribution of Ki-67 and DCX immunoreactive cells in the BALB/c mouse brain 138
4.4.2 Age and life-history stage related changes in Ki-67 and DCX expression in the BALB/c mouse brain 140
4.5 CONCLUSION 142
CHAPTER 5: AGE- RELATED CHANGES IN PROLIFERATION NUCLEAR ANTIGEN (PCNA) AND DOUBLECORTIN (DCX) EXPRESSION IN THE POST-METAMORPHIC SOUTH AFRICAN CLAWED (*XENOPUS LAEVIS*) FROG BRAIN. 143
5.1 INTRODUCTION 144
5.2 MATERIALS AND METHODS 145
5.2.1 Animals 145
5.2.2 Tissue collection and processing 146
5.2.3 Immunohistochemistry 146
5.2.4 Data Analysis 147
5.3 RESULTS 149
5.3.1 Distribution of PCNA in the South African clawed frog 149
5.3.2 Distribution of DCX in the South African clawed frog 154
5.3.3 Age-related changes in the number PCNA and DCX-ir cells in the telencephalon 158
5.3.4 Life-history stage dependent changes in PCNA and DCX immunoreactivity in the telencephalon 163
5.4 DISCUSSION 168
5.4.1 Methodological considerations 168
5.4.2 PCNA and DCX expression in the *X. laevis* brain 169

5.4.3 Age and life-history stage dependent changes in PCNA and DCX expression 171
5.5 CONCLUSION 173
CHAPTER 6: GENERAL DISCUSSION AND CONCLUSIONS 174
6.1 Observations from the different vertebrate taxa studied 175
6.2 Limitations of the study 181
6.3 Recommendations 182
6.4 Conclusions 183
REFERENCES 185
APPENDICES 205

LIST OF TABLES

CHAPTER 2

Table 2.1: Age-related changes in PCNA immunoreactivity in the Japanese quail brain. **60**

Table 2.2: Age-related changes in DCX immunoreactivity in the Japanese quail brain. **72**

CHAPTER 4

Table 4.1: Age-related changes in Ki 67 expression in the BALB/C mouse brain... **119**

Table 4.2: Age-related changes in DCX expression in the balb/C mouse brain..... **123**

CHAPTER 5

Table 5.1: Age-related changes in PCNA immunoreactivity in the *X. laevis* brain. . **153**

Table 5.2: Age-related changes in DCX immunoreactivity in the *X. laevis* brain..... **157**

CHAPTER 6

Table 6.1: A comparison of proliferative brain areas among vertebrates studied. .. **177**

Table 6.2: A comparison of brain areas that incorporate new neurons among vertebrates studied..... **179**

LIST OF FIGURES

CHAPTER 1

Figure 1.1: Schematic diagram showing the brain and architecture of the ventricular zone in mammalian, avian and amphibian vertebrates. **13**

Figure 1.2: Sagittal and coronal schematic diagrams showing the neurogenic sites and migratory destinations of neuroblasts in the mammalian and avian brains **15**

Figure 1.3: Schematic diagram showing the different stages of the cell cycle and factors that regulate the cycle in eukaryotes. **28**

Figure 1.4: Schematic diagram showing the phylogenetic tree of vertebrates..... **32**

Figure 1.5: Photographs showing different vertebrate animal models used in this study..... **40**

CHAPTER 2

Figure 2.1: Photomicrographs showing distribution of PCNA-ir cells in the olfactory bulb and telencephalon of the Japanese quail brain. **51**

Figure 2.2: Photomicrographs showing distribution of PCNA-ir cells in the POM, thalamic nuclei, mesencephalic nuclei, cerebellar cortex and the Cbi of the Japanese quail brain. **55**

Figure 2.3: Photomicrographs showing the distribution of PCNA-ir cells the different parts of the brain of juvenile, subadult and adult Japanese quails. **57**

Figure 2.4: Photomicrographs showing type 1 and type 2 DCX-ir cells in the Japanese quail brain. **61**

Figure 2.5: Photomicrographs showing distribution of DCX-ir cells in the olfactory bulb and telencephalon of the Japanese quail brain. **65**

Figure 2.6: Photomicrographs showing Japanese brain sections through the POM, hypothalamus, mesencephalon and cerebellum. **68**

Figure 2.7: Photomicrographs showing the distribution of DCX-ir cells the different parts of the brain of juvenile, subadult and adult Japanese quails. **70**

CHAPTER 3

Figure 3.1: Photomicrographs of doublecortin stained coronal sections of the Japanese quail brain showing areas where DCX expression was quantified. **88**

Figure 3.2: Photomicrographs showing DCX expression in the Japanese quail telencephalon. **91**

Figure 3.3: Photomicrographs showing DCX expression in the Japanese quail telencephalon. **93**

Figure 3.4: Photomicrographs and graphs showing age-related changes in DCX expression in the pallium of the Japanese quail telencephalon. **96**

Figure 3.5: Photomicrographs and graphs showing age-related changes in DCX expression in the sub pallium of the Japanese quail telencephalon. **98**

Figure 3.6: Graphs representing changes in the numbers of round multipolar and fusiform DCX-ir cells at different life-history stages in the Japanese quail brain. **102**

CHAPTER 4

Figure 4.1: Photomicrographs showing distribution of Ki 67-ir cells in the telencephalon and olfactory bulb of BALB/c mouse brain. **116**

Figure 4.2: Photomicrographs showing distribution of Ki 67-ir cells in the corpus callosum, neocortex, cerebellum and inferior colliculus. **120**

Figure 4.3: Photomicrographs showing distribution of DCX-ir cells in the telencephalon and olfactory bulb of the BALB/c mouse brain. **124**

Figure 4.4: Photomicrographs and graphs showing age-related changes in numbers of Ki-67-ir in the different parts of the BALB/c mouse rostral migratory stream. **127**

Figure 4.5: Photomicrographs and graphs showing age-related changes in the numbers of Ki-67 and DCX-ir cells in the terminal portion of the BALB/c mouse rostral migratory stream **129**

Figure 4.6: Photomicrographs and graphs showing age-related chages in the numbers of Ki-67 and DCX-ir cells in the anterior part subventricular zone (SVZa) and the subgranular zone (SGZ) of the BALB/c mouse brain. ... **131**

Figure 4.7: Graphical representation of the life-history stage related changes in the numbers of Ki 67 and DCX-ir cells in the rostral migratory stream of the BALB/c mouse brain. **134**

Figure 4.8: Graphical representation of the life-history stage related changes in the numbers of Ki 67 and DCX-ir cells in the SVZa and SGZ of the BALB/c mouse brain.....**136**

CHAPTER 5

Figure 5.1: Photomicrographs showing the distribution PCNA-ir cells in the *X. laevis* brain. **151**

Figure 5.2: Photomicrographs showing the distribution of DCX-ir cells in the *X.laevis* telencephalon. **155**

Figure 5.3: Photomicrographs and graphs representing age-related changes in the numbers of PCNA-ir cells in the ventral and dorsal ventricular zones of the *X. laevis* telencephalon.....**159**

Figure 5.4: Photomicrographs and graphs representing age-related changes in the numbers of DCX-ir cells in the LP, MP, St and S of the *X. laevis* telencephalon. **161**

Figure 5.5: Graphs representing life-history stage related changes in PCNA immunoreactivity in ventral and dorsal ventricular zones of the *X. laevis* telencephalon. **164**

Figure 5.6: Graphs representing life-history stage related changes in DCX immunoreactivity in parenchyma of the *X. laevis* telencephalon. **166**

LIST OF ABBREVIATIONS

A, arcopallium

AM, aqueduct mesencephalicus

ANOVA, analysis of variance

ARC, agricultural research centre

BDNF, brain derived neurotropic factor

BLBP, brain lipid binding protein

BMP, bone morphometric protein

BrdU, 5-bromo-2'-deoxyuridine

BrdU-ir. 5-bromo-2'-deoxyuridine immunoreactive

BSTL, lateral part of the bed nucleus of the stria terminalis

CA, anterior commissure

CAK, cyclin activated kinase

CAS, central animal services

Cb, cerebellum

Cbi, nucleus cerebellum internum

CC, corpus callosum

CDK, cyclin dependent kinases

C-Fos, immediate early gene

C-Jun, immediate early gene

CNS, central nervous system

CP, caudoputamen

DAB, 3, 3′-Diaminobenzidine tetrachloride

DCX, doublecortin;

DCX-ir, doublecortin immunoreactive

DG, dentate gyrus

DIEN, diencephalon

DLA, nucleus dorsolateralis anterior thalami

DMA, nucleus dorsomedialis anterior thalami

DNA, deoxyribonucleic acid

DP, dorsal pallium

E, entopallium

EEG, electroencephalogram

EGF, endothelial growth factor

EGFR, endothelial growth factor receptor

ER, endoplasmic reticulum

EW, nucleus of Edinger-Westphal

FGF-2, fibroblast growth factor 2

FLM, fasciculus longitudinalis medialis

GCL, granule cell layer

GCt, griseum centrale

GFAP, glial fibrillatory acid protein

GL, granule cell layer

GLv, nucleus geniculatus lateralis, pars ventralis

GP, globus pallidus

^{3}H-thymidine, tritiated thymidine

H_2O_2, hydrogen peroxide

HA, hyperpallium apicale

HD, hyerpallium densocellulare

HL-RMS, horizontal limb of the rostral migratory stream

HP, hippocampus

HPA, hypothalamic pituitary axis

HYPOTHAL, hypothalamus

HVC, high vocal centre

IGF-1, insulin like growth factor 1

IL-6, interleukin 6

IM, nucleus isthmi, pars magnocellularis

IMM, intermediate medial mesopallium

III, third ventricle

IV, fourth ventricle

Ki 67, Kiel 67

Ki 67-ir, Kiel 67 immunoreactive

LaM, lamina mesopallialis

LFM, lamina frontalis suprema

LFS, lamina frontalis superior

LP, lateral pallium

LPS, lamina pallio-subpallialis

LSt, lateral striatum

LV, lateral ventricule

M, mesopallium

MED, medulla

MET, metencephalon

ML, molecular cell layer

MLd, nucleus mesensephalicus lateralis, pars dorsalis

Medial pallium

MSt, medial striatum

N, nidopallium

NCL, nidopallium caudolaterale

NCM, nidopallium caudomediale

NC, nidopalliun caudale

NEO, neocortex

NHI, National institute of health

NIII, oculomotor nerve

NF, Nieuwkoop and Faber

NSC, neuronal stem cell

OB, olfactory bulb

OBc-RMS, olfactory bulb core rostral migratory stream

OBV, olfactory bulb ventricle

OMN, oculomotor nucleus

ON, olfactory nerve

OPT, optical tract

OV, nucleus ovoidalis

PB, phosphate buffer

PCNA, proliferating nuclear cell antigen

PCNA-ir, proliferating nuclear cell antigen immunoreactive

PL, Purkinje cell layer

POM, nucleus preopticus medialis

PSA-NCAM, polysialated-neural cell adhesion molecule

Rt, nucleus rotundus

RMC, red nucleus magnocellular part

RMS, rostral migratory stream

S, septum

S100β, S100 calcium binding protein betta

SCZ, subcallosal zone

SEM, standard error of mean

SGZ, subgranular zone

SL, lateral septum

SM, medial septum

SOX-2, sex determining region Y-box 2

St, striatum

SVZ, subventricular zone

TECT, tectum

TGF, tumor growth factor

TNF-α, tumor necrosis factor alpha

TSM, tractus septo-mesencephalicus

Tu, nucleus tuberis

Tuj 1, neuron-specific class III β-tubulin

VEGF, vascular endothelial growth factor

VL-RMS, ventral limb of the rostral migratory stream

VZ, ventricular zone

CHAPTER 1: INTRODUCTION AND LITERATURE REVIEW

1.1 BACKGROUND

The morphology of the adult vertebrate brain was previously considered to be stable having neurons that were structurally fixed within existing neuronal circuits. This way, the adult vertebrate brain was thought to have the ability to process a lot of information without requiring any morphological changes, but being able to lose information when its structure was disrupted. In past few years, a lot of studies have provided evidence that neurons continue to be produced in the postnatal brain. It is now widely accepted that production of neurons, traditionally considered an embryological process, continues to take place in the adult invertebrate and vertebrate animal brain. The realization that the adult brain continues to produce new neurons and the subsequent characterization of neuronal stem cells has triggered substantial interest in the neuroscience field with the aim of searching for novel stem cell-based therapies for neurological and neurodegenerative diseases such as Alzheimer's disease.

Neurogenesis is a complex process involving neuronal stem cell proliferation, differentiation, migration, integration and possibly suppression of proliferation (Barnea and Pravosudov, 2011). Postnatal neurogenesis is a conserved trait that is observed across all vertebrate animals. In mammals, postnatal neurogenesis is only restricted to two canonical brain regions: the lateral telencephalic ventricle and the dentate gyrus of the hippocampus. Unlike mammals, non-mammalian vertebrates exhibit widespread postnatal neurogenesis. In addition, non-mammalian vertebrates also display a remarkable ability to regenerate functional neural tissue following experimental brain lesions such as ablation of whole or parts of the brain parts, in striking contrast to mammals where neural tissue is seldom replaced following injury. Of the non-mammalian vertebrates, anamniotes (fish and amphibians) exhibit the most widespread neurogenic and regenerative capacity.

Firstly, the fact that non-mammalian vertebrate brains display more neurogenic compartments and are more capable of regenerating and restoring function following experimental lesions naturally leads to the following questions: Is there a change in the number of neurogenic compartments with the transition from anamniote to

amniote vertebrates? What are the differences that enable non-mammalian vertebrates to regenerate neural tissue while mammals cannot? It appears there are selective evolutionary pressures which, through adaptation, led to a reduction in neurogenic compartments and regenerative capacity in mammals (Kaslin et al., 2008). The source of this striking difference is poorly understood but differences in patterns of neuronal stem cell proliferation and neurogenesis are most likely involved (Chapouton et al., 2007). Comparative investigations of this trait in species from different taxonomic classes are important in order to more fully understand the diversity and plasticity of postnatal neurogenesis. In addition, such an inter-class analysis of this trait may yield insights into why anamniotes such as fish and amphibians display more neurogenic and regenerative capacity than amniotes like mammals and birds. Furthermore, a comparative approach that analyses the distribution of proliferating cells, differentiation and neuronal incorporation in the brain of amphibians and birds may reveal mechanisms that can possibly be harnessed to stimulate regeneration of neural tissue within the central nervous system of mammals. This information is valuable if therapeutic interventions are to be pursued.

Secondly, some authors have argued that postnatal neurogenesis is a remnant of the developmental primary neurogenesis that is protracted in brain areas such as the hippocampus that continue to mature postnatally and only ceases when such areas are fully matured (Chapouton et al., 2007). This argument is supported by the fact that the process of postnatal neurogenesis and its regulation resembles that of primary neurogenesis. For instance, the nature and properties of embryonic neuronal stem cells in rodents and zebrafish correspond with those found in the adult (Chapouton et al., 2007). To test this hypothesis, changes in neurogenic sites were investigated at different postnatal ages.

This study investigated time-course changes in neurogenesis in the amphibian, avian and mammalian brains. In this study, time-course was defined as the increasing chronological age (in weeks) spanning the different life-history stages (i.e juvenile, sub adult and adult stages) of the animal. The African clawed frog (*Xenopus laevis*), Japanese quail (*Cortunix cortunix Japonica*) and BALB/c mouse (*Mus musculus*)

were used in this study as representative models for the amphibian, avian and mammalian vertebrates respectively.

1.2. HISTORICAL BACKGROUND

"*In the adult centres, the nerve paths are something fixed, ended and immutable. Everything may die, nothing may be regenerated*" (y Cajal, 1913).

This statement, coined by Cajal in 1913, anchored on the notion that brain functionality was dependent on molecular and dendritic plasticity, was so convincing that evidence to the contrary was ignored. This statement reflects one of the main paradigms in neuroscience which considered neurogenesis as a phenomenon restricted only to prenatal development (Balu and Lucki, 2009). However, the scientific community has now accepted that neurogenesis continues into adulthood in the central nervous system of all vertebrates.

Ezra Allen was the first to provide evidence that new nerve cells are produced in the adult mammalian brain, through demonstration of proliferative activity along the lateral ventricular lining of adult rats (Allen, 1912). Five decades later, Altman and Das (1965) using tritiated thymidine (^{3}H-thymidine), provided auto radiographic proof that neurogenesis takes place in the adult rat sub granular (SGZ) and sub ventricular (SVZ) zones. These findings were corroborated fifteen years later by Kaplan and Hinds (1977), who demonstrated the neuronal nature of the ^{3}H-thymidine labelled cells in the adult rat hippocampal dentate gyrus and olfactory bulb using the electron microscope. In spite of all the evidence provided by these earlier researchers, the neuroscience community was still skeptical for two reasons: Firstly, the evidence provided was not sufficient to dislodge a long held and widely believed dogma. Secondly, other studies had reported that ^{3}H-thymidine is also incorporated in cells undergoing DNA repair (Balu and Lucki, 2009; Ihunwo et al., 2016).

In the 1980's, Fernando Nottebohm rekindled interest in the phenomenon of neurogenesis when he demonstrated substantial neuronal recruitment in the song

nuclei of the adult canary brain (Nottebohm, 1980, 1984). During the same period, Nottebohm and colleagues reported the first proof of neuroblasts that had functionally integrated into the song control nuclei (Nottebohm, 1984, 2011). In the 1990's, Heather Cameron and Elizabeth Gould provided new evidence of hippocampal neurogenesis in adult rats (Cameron and Gould, 1994). During the same period, 5-bromo-3' deoxy-uridine (BrdU), a thymidine analog that is incorporated into the DNA of cycling cells in a similar manner to ^{3}H-thymidine was discovered. However, the advantage of BrdU over ^{3}H-thymidine is that it is detected immunohistochemically and can be used together with other markers to identify cellular phenotype (Balu and Lucki, 2009). Today, the concept of postnatal neurogenesis is firmly established having been demonstrated in both mammalian and non-mammalian vertebrates (Cayre et al., 2002; Lindsey and Tropepe, 2006; Kaslin et al., 2008).

1.3 NEURAL STEM CELLS AND THE NEUROGENIC NICHE

Neuronal stem cells (NSCs) have the capacity to renew themselves through mitosis and give rise to different central nervous system (CNS) cell types (Gage, 2000; Gage and Temple, 2013). Neuronal stem cells are housed in neurogenic niches. Neurogenic niches are microenvironments that morphologically and functionally support NSC (Ming and Song, 2011; Gage and Temple, 2013). These microenvironments control the activities of NSCs determining whether they should divide or be quiescent. In addition, neurogenic niche factors also direct the fate of the proliferating cells, that is, whether they should be neuronal or glial cells (Gage and Temple, 2013; Ihunwo et al., 2016). Neurogenic niches are made up of different components including NSCs, astrocytes, ependymal cells, microglia, endothelial cells and blood vessels (Aimone et al., 2014). In mammals, the neurogenic niches are the lateral ventricular SVZ and the SGZ of the hippocampal dentate gyrus (Ihunwo and Pillay, 2007; Bonfanti and Peretto, 2011; Bond et al., 2015). In non-mammalian vertebrates, the ventricular zones are the sole neurogenic niches (Cayre et al., 2002; García-Verdugo et al., 2002; Lindsey and Tropepe, 2006; Kaslin et al., 2008).

During vertebrate embryonic period, the majority of cells of the CNS originate from the multipotent stem cells situated along the ventricular lining. The ventricles are

formed through a process called neurulation in which the neurectoderm forms a neural tube. The pseudostratified columnar lining of the ventricles is called the ventricular zone (VZ). In addition, these pseudostratified columnar cells are the proliferative radial glia cells which differentiate into all cells of the CNS. Until recently, the VZ was understood to disappear prior to birth or hatching following the completion of CNS histogenesis and become the ependymal layer. However, it is now established beyond doubt that the VZ persists into adulthood in all vertebrates studied although with a reduced thickness (Alvarez-Buylla et al., 1998; García-Verdugo et al., 2002). In addition, the cells lining VZ retain their proliferative capacity and are structurally different from those found in non-proliferative ependymal layer. Furthermore, the proliferative cells in all non-mammalian vertebrate brains studied to date are situated in the lining of the VZ (Cayre et al., 2002; Lindsey and Tropepe, 2006; Chapouton et al., 2007; Kaslin et al., 2008).

In adult mammalian brains, however, the older embryonic proliferative VZ (now termed SVZ) comes to lie deeper to a newer VZ made up of non-proliferative ependymal epithelial cells (García-Verdugo et al., 2002). Therefore, the mammalian NSCs are located in the SVZ whereas the VZ is made up of epithelial ependymal cells that line the lumen of the ventricles. However, no equivalent of the mammalian SVZ has been found in all non-mammalian vertebrates investigated to date. A clear understanding of the identity of the NSCs and the structural organization of the neurogenic niche of each vertebrate class studied is therefore critical.

1.3.1 Architecture of the sub ventricular zone and neuronal stem cell identity in mammals

In the mammalian SVZ, three types of cells (A, B and C) are found (Figs 1.1 A & B; 2A). In addition to these, the mammalian VZ is lined by Type E cells (García-Verdugo et al., 2002; Quiñones-Hinojosa et al., 2006). Type A cells exhibit a smooth outline and a fusiform shaped body with a single or two processes, scant cytoplasm and a lot of lax chromatin in the nucleus. The cytoplasm of type A cells contain numerous free ribosomes, few rough endoplasmic reticulum, small dictyosomes and abundant microtubules. Each type A cell is joined to neighbouring cells by small junctional

complexes (García-Verdugo et al., 1998). Type A cells have the morphology described for migrating neuroblasts in the rostral migratory stream (RMS) (Lois and Alvarez-Buylla, 1994) and express PSA-NCAM and Tuj 1 antigens (García-Verdugo et al., 2002).

Type B cells exhibit an irregular outline, irregular nucleus with clumped (B2) or sparse (B1) chromatin and occasionally contact the ventricular lumen. The cytoplasm of type B cells contains many intermediate filaments, dense bodies and a few free ribosomes (García-Verdugo et al., 1998). Type B cells also have two processes: a basal and an apical process. The basal process is in direct contact with blood vessels whereas the apical process has a cilium which extends through the VZ to reach the ventricular lumen (Mirzadeh et al., 2008; Bond et al., 2015). In addition, type B cells express GFAP and vimentin antigens (García-Verdugo et al., 2002).

Type C are large spherical cells with a smooth outline. The nucleus of these cells are deeply invaginated, exhibit several small nucleoli and mostly lax chromatin. In addition, the cytoplasm of these cells possess several dictyosomes, fewer ribosomes compared to type A cells and lack intermediate filaments. Type C cells usually make contact with both types A and B cells (García-Verdugo et al., 1998; García-Verdugo et al., 2002).

Type E are cuboidal cells that form the ependymal monolayer separating the SVZ from the ventricular lumen. They exhibit many cilia, round or oval nuclei with occasional invaginations and an electron lucent cytoplasm with few organelles. The cytoplasm contains intermediate filaments, small dictyosomes, lipid droplets and abundant basally located mitochondria. A short apical process that resembles a short radial fibre may be found on the apical membrane of some these cells (García-Verdugo et al., 1998).

In summary, type B cells are quiescent GFAP positive radial glia like cells that differentiate into neurons for the olfactory bulb and oligodendrocytes for the corpus callosum (Bond et al., 2015). In addition, type B cells give rise to transient amplifying

cells (Type C) which in turn give rise to migrating neuroblasts (Type A) (Ming and Song, 2011; Ihunwo et al., 2016). Type A cells form chains and migrate via the RMS guided by scaffolding formed by astrocytic processes and blood vessels to reach the olfactory bulb (Mobley et al., 2014). Therefore, type B cells are the NSCs in the SVZ.

1.3.2 Architecture of the sub granular zone and neuronal stem cell identity in mammals

The SGZ is made up of 3 cell types: radial astrocytes (Type 1), horizontal astrocytes (Type 2) and D (Type D) cells. D cell are further divided into three sub types: D1 (intermediate progenitors), D2 and D3 (postmitotic neuroblasts) (Seri et al., 2004). Type 1 cells possess a large round or triangular cell body with one main radial process which penetrates the granule cell layer (GCL) to reach the molecular layer (ML) where it branches repeatedly and thin lateral processes that are intercalated with granule cells. Type 1 cells express nestin and GFAP but not S100β (Seri et al., 2004).

Type 2 cells possess a fusiform or elongated cell body with branching processes that run along the SGZ and short slender secondary processes that penetrate the GCL and hilus. Type 2 cells express GFAP, S100β and SOX 2 but do not express nestin (Seri et al., 2004).

Both types of astrocytes exhibit irregular cell contours and lightly staining cytoplasm containing numerous intermediate filaments, dark mitochondria, thin endoplasmic reticular cisterns and small Golgi apparatuses. In addition, these cells contain clusters of chromatin in their nuclei and are connected to neighbouring cells via gap junctions. However, type 1 astrocytes have more numerous organelles and lighter staining mitochondria than type 2 astrocytes (Seri et al., 2004).

Type D cells possess a small ovoid or round cell body with a smooth outline, dark scanty cytoplasm, many polyribosomes compared to astrocytes, lighter mitochondria

and larger endoplasmic reticulum than astrocytes (Seri et al., 2001). In addition, these cells usually appear in clusters of two to four cells and resemble previously reported dark staining small progenitors (Altman and Das, 1965; Kaplan and Bell, 1984; Cameron et al., 1993). Three sub types of these cells have been identified in the SGZ: D1, D2 and D3 (Seri et al., 2004). The D1 sub type possesses no processes and divides by mitosis to produce D2 cells. The D2 sub type possesses short processes that bifurcate either horizontally along the blades of the dentate gyrus or vertically pointing towards the hilus. In turn, D2 cells develop into D3 cells. The D3 sub type resembles immature neurons exhibiting a main radial process that penetrates the GCL to reach the molecular layer and a thinner process which projects to the hilus. In addition, D3 cells are located at the junction between the SGZ and GCL (Seri et al., 2004). All D cell sub types express PSA-NCM, DCX and TUC-4 but not GFAP. However, sub types D2 and D3 are not labelled with BrdU suggesting that they are post-mitotic cells (Seri et al., 2004).

In summary, the SGZ has two types of NSCs: radial glia like cells similar to the ones found in the SVZ (Type 1) and non-radial cells with basal processes (Type 2) which may also arise from Type 1 cells (Seri et al., 2004; Ming and Song, 2011). Both Type 1 and 2 NSCs give rise to intermediate progenitors (D1) which in turn give rise to migrating post mitotic neuroblasts (D2 and D3). Type 1 NSCs appear to exclusively give rise to neuroblasts whereas Type 2 gives rise to both neuroblasts and glia (Ming and Song, 2011; Bond et al., 2015).

1.3.3 Architecture of the ventricular zone and neuronal stem cell identity in avians

The ventricular lining of the avian telencephalon is heterogenous having monolayered as well as stratified parts (Figs 1.1 C & D; 2 B). The stratified parts are usually three to four cells thick and are situated along the ventral and dorsal reaches of the lateral ventricles. The rest of the ventricular lining is monolayered. The stratified epithelium is made up of three types of cells: A, B and E (Alvarez-Buylla et al., 1998; Alvarez-Buylla et al., 2002; García-Verdugo et al., 2002).

Type E cells are characterized by a long radial process containing abundant intermediate filaments, numerous mitochondria and scanty cytoplasm. The nucleus of type E cells contains two small nucleoli and several chromatin aggregates. The cytoplasm contains basal bodies, large mitochondria, clusters of free ribosomes, few endoplasmic reticulum cisterns and multiple dictyosomes. These cells also show microvilli and multiple cilia that face the ventricular lumen. These cells also exhibit strong adhesion complexes. The ultrastructure of these cells is comparable to that of ependymal cells present in the ventricular lining of all vertebrates studied to date (García-Verdugo et al., 2002).

Type B cells are prism shaped, containing an oval to irregular nucleus possessing lax chromatin and a prominent nucleolus. The cytoplasm of these cells has numerous polyribosomes, a large Golgi complex and small round mitochondria. Type B cells also have a specialized straight or slightly curved cilium facing the ventricular lumen and a thin radial expansion. These cells form junctional complexes with B and E cells (Alvarez-Buylla et al., 1998; García-Verdugo et al., 2002).

Type A cells possess a fusiform cell body containing an elongated nucleus with one or two large nucleoli. They have scanty cytoplasm with small dictyosomes, few rough endoplasmic reticulum cisternae, several polyribosomes and fewer mitochondria compared to type B cells. In addition, these cells have processes that are rich in microtubules and are usually associated with radial processes of the other cell types. However, Type A cells are not restricted to the ventricular zones as they are also found in the parenchyma of the telencephalon. Type A cells resemble migrating neuroblasts (Alvarez-Buylla et al., 1998; García-Verdugo et al., 2002).

Generally, the inactive areas of the VZ are made up of a single layer of type E whereas the active areas are stratified containing all three cell types (A, B and E). Therefore, it appears that the stratified parts of the avian VZ are the neurogenic "hot spots" described by Alvarez-Buylla (1990). In addition, studies combining ^{3}H-thymidine and electron microscopy have provided evidence that the B cell population

of the avian VZ represents the NSCs. These mitotically active cells give rise to type A migrating neuroblasts (Alvarez-Buylla et al., 1998).

1.3.4 Architecture of the ventricular zone and neuronal stem cell identity in amphibians

In a similar fashion as the avian VZ, the epithelial lining of the amphibian VZ is also heterogenous consisting of both monolayered and stratified areas (Bernocchi et al., 1990) (Figs 1.1 E & F)). In addition, the stratified areas of the amphibian VZ are made up of three types of cells: unipolar tanycytes, bipolar tanycytes and epithelial cells (Bernocchi et al., 1990). Unipolar tanycytes have a round nucleus, scare cytoplasm and a long apical radial process. On the other hand, bipolar tanycytes have a long extensive apical process and a basal process that extends to the ventricular lumen. Ventricular zone epithelial cells correspond to the classical ependymal cells (Bernocchi et al., 1990; Seki et al., 2011). However, the evidence available suggests that the two types of tanycytes could actually be one type that transits between unipolar and bipolar depending on proliferative activity (Polenov and Chetverukhin, 1993). Furthermore, both types of tanycytes express GFAP and vimentin and are believed to be the radial glia like NSCs that proliferate in the VZ (Lazzari et al., 1997; Ferretti and Prasongchean, 2015). Moreover, D'Amico et al. (2011) observed BLBP (brain lipid binding protein) labelled cell bodies of radial glial like cells in the ventricular lining and radial fibre extensions in the parenchyma of the amphibian telencephalon. These radial glia like cells usually appear in pairs or small clusters that are labelled with ^{3}H-thymidine following short term survival (Bernocchi et al., 1990).

In the amphibian telencephalon, the VZ is mostly monolayered except for the ventral and dorsal regions which are stratified. Similarly, the lining of the diencephalic ventricles is mainly monolayered except for that of the recessus preopticus (Bernocchi et al., 1990). The linings of the tectal and fourth ventricles are monolayered and pluristratified respectively (Bernocchi et al., 1990). In addition, the stratified areas of the VZ are made up of all three cell types whereas the monolayered parts consist of only epithelial or ependymal cells.

Figure 1.1: Schematic diagram showing the brain and architecture of the ventricular zone in mammalian (A & B), avian (C & D) and amphibian (E & F) vertebrates. In each species, the blue, green, red and grey colours in B, D and F represent proliferative cells, amplifying cells, migrating cells and ependymal cells respectively. Adapted and modified from Seki et al. (2011). See list of abbreviations for abbreviations used in this figure.

A

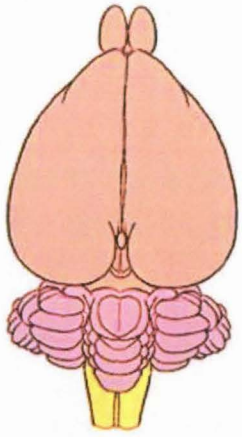

B

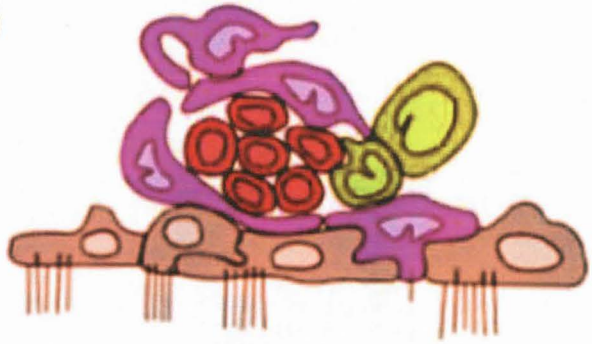

C

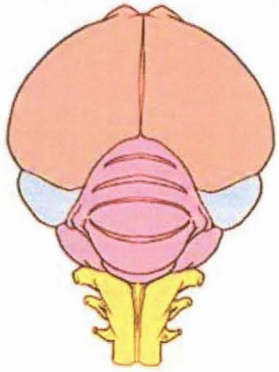

D

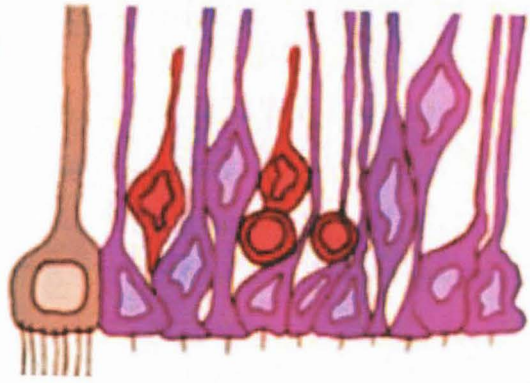

E

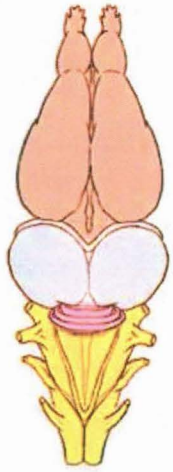

F

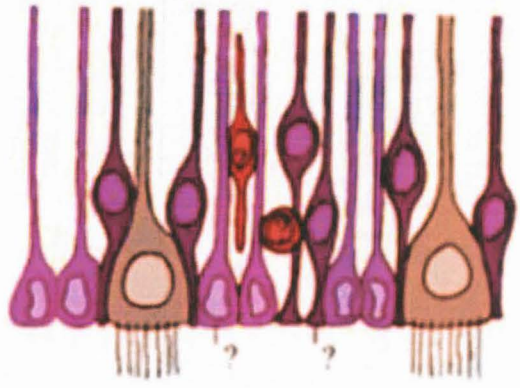

Figure 1.2: Sagittal and coronal schematic diagrams showing neurogenic sites and migratory destinations in the mammalian (A) and avian (B) vertebrates. Green regions indicate germinal zones and red dots indicate destinations of neuroblasts. Adapted and modified from Paredes et al. (2015). See list of abbreviations for abbreviations used in this figure.

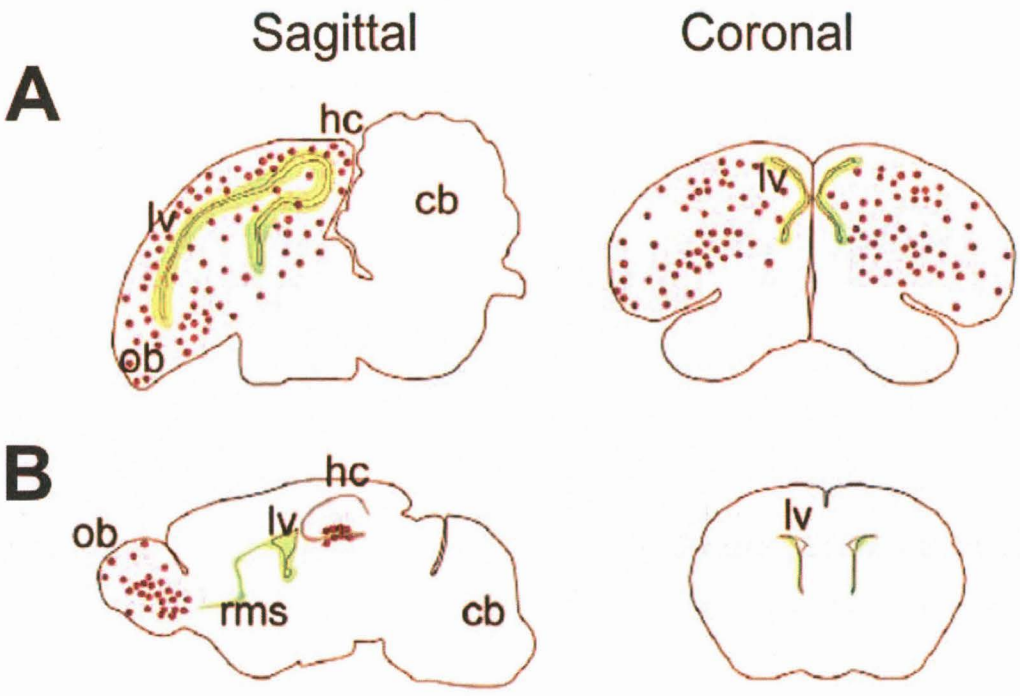
Sagittal
Coronal
A
hc
lv
cb
ob
lv
B
hc
ob
lv
rms
cb
lv

1.4 NEUROGENESIS IN VERTEBRATES

As already mentioned in previous sections, postnatal neurogenesis is a trait observed in all vertebrates studied to date. However, differences in characteristics of the process exist across all vertebrates. Generally, non-mammalian vertebrates display extensive neurogenesis compared to mammalian vertebrates. Specifically, neurogenesis is more extensive throughout the anamniote brain as shown by greater number of neurogenic compartments and the quantity of cells produced. On the contrary, neurogenesis in amniotes is mostly restricted to the telencephalon (Kaslin et al., 2008; Ferretti and Prasongchean, 2015).

1.4.1 Adult neurogenesis in the mammalian brain

Postnatal neurogenesis in the mammalian brain is restricted to the SVZ and SGZ of the telencephalon and to a lesser extent, the cerebellum (Pino et al., 2017). Although these two neurogenic microenvironments (SVZ and SGZ) are found within the mammalian telencephalon, differences exist with regard to: 1) the neuronal phenotype produced 2) their contact with ventricular surfaces or displacement in the parenchyma 3) the fate of the newly formed neurons, that is, whether they are destined for neuronal replacement in the olfactory bulb or growth of an existing neuronal circuit of the dentate gyrus (Grandel and Brand, 2013).

In the cerebellum, neurogenesis continues postnatally (Bonfanti and Peretto, 2011). Initially, postembryonic neurogenesis results in growth of the granular layer of the cerebellum. In rodents, a secondary neurogenic zone, the external granular layer, remains proliferative postnatally and generates neuroblasts that accumulate in the granular cell layer of the cerebellum. This process terminates when the cerebellum has reached its stable adult size (Altman, 1972; Grandel and Brand, 2013). However, production of neuroblasts and glioblasts in the cerebellum persists into adulthood in most mammals studied to date, although at a lower rate.

1.4.1.1 Proliferative areas in the mammalian brain

Under normal physiological conditions, NSCs have been identified in many brain areas but only those resident in the SVZ and SGZ have the capacity to produce new neurons (Gage, 2000; Gage and Temple, 2013; Pino et al., 2017). Neuronal stem cells in other areas of the CNS are also capable of proliferating but produce only neuroglia cells (Ming and Song, 2011; Bond et al., 2015). Neuronal stem cells have also been isolated from other brain areas outside the SVZ and SGZ such as the neocortex, diencephalon, brainstem or spinal cord. However, proliferation of NSCs in these regions is related to maintenance of precursor cell populations or production of neuroglia (Gage and Temple, 2013). Interestingly, when these NSCs are isolated from the non-neurogenic areas and transplanted to *in vitro* conditions simulating the SVZ or SGZ differentiate into neuroblasts. Indeed, NSCs isolated from the spinal cord differentiated into granule neurons after being transplanted to the SGZ (Shihabuddin et al., 2000). Similarly, NSCs from the SGZ developed into olfactory bulb interneurons following transplantation into the SVZ (Ming and Song, 2011). Conversely, when NSCs from either the SVZ or SGZ are transplanted into non-neurogenic microenvironments develop into neuroglia (Seidenfaden et al., 2006).

1.4.1.2 Migration and differentiation in mammalian brain

New neuroblasts produced in the SVZ migrate as chains via the RMS to reach the olfactory bulb where they are incorporated as inhibitory interneurons (Lois and Alvarez-Buylla, 1994). These neuroblast chains migrate through the RMS without the aid of astrocytes or axonal guides (García-Verdugo et al., 2002). Instead, these chains of newly formed neuroblasts migrate along glial tubes formed by astrocytes and their extensions (García-Verdugo et al., 2002). In mice, migration of neuroblasts from the SVZ to the olfactory bulb (a distance of approximately 5 mm) takes approximately 10–14 days (Whitman et al., 2009). On reaching the olfactory bulb, neuroblasts differentiate into either granule (95%) or periglomerular (5%) interneurons that synapse with mitral cells (Mobley et al., 2014). Granule neurons are GABAergic whereas periglomerular neurons are both GABAergic and dopaminergic (Mobley et al., 2014).

In the dentate gyrus, neuroblasts migrate short distances to reach the GCL where they differentiate into new granule neurons (Kempermann, 2011; Pino et al., 2017). These newly formed granule neurons are excitatory (using glutamate and aspartate neurotransmitters) and project to area CA3 of the Ammon's horn via the mossy fiber pathway (García-Verdugo et al., 2002).

1.4.2 Adult neurogenesis in the avian brain

Avian neurogenesis was extensively investigated in the song control system of songbirds such as the canary (Alvarez-Buylla et al., 1998; Nottebohm, 2011) and hippocampi of food storing or migratory birds such as sparrows or chickadees (Barnea and Nottebohm, 1994; LaDage et al., 2011). However, adult neurogenesis was studied in brains of few non-song birds including parrots (Mazengenya et al., 2018), doves (Ling et al., 1997; Chen et al., 2006), pigeons (Melleu et al., 2016; Meskenaite et al., 2016; Mazengenya et al., 2017), chicken (Mezey et al., 2012) and quails (Nikolakopoulou et al., 2006b; Balthazart et al., 2010; Bardet et al., 2012; Mouriec and Balthazart, 2013).Using ^{3}H-thymidine , Nottebohm and colleagues revealed abundant neuronal incorporation in the high vocal centre (HVc), a nucleus related to song learning in the canary brain (Goldman and Nottebohm, 1983; Nottebohm, 1984; Nottebohm, 1996). Since then several studies, using exogenous and endogenous markers demonstrated that new neurons are incorporated in most regions of the avian telencephalon such as the striatum, septum, nidopallium, mesopallium, hyperpallium and hippocampus (Boseret et al., 2007; Balthazart et al., 2008; Meskenaite et al., 2016; Mazengenya et al., 2017; Mazengenya et al., 2018). Outside the telencephalon, several investigations have revealed that neurogenesis also takes place in the cerebellum of most birds studied (Bardet et al., 2012; Mezey et al., 2012; Mazengenya et al., 2017; Mazengenya et al., 2018). However, no studies to date have reported neurogenesis in the hypothalamus, thalamus, optic tectum and brainstem of the avian brain under normal homeostasis (Chen et al., 2006).

1.4.2.1 Proliferative areas in the avian brain

Neuronal birth in all avian species investigated to date takes place in the lateral ventricular zones of the telencephalon. The VZ is the region where cells are labelled with ^{3}H-thymidine or BrdU following short survival times (Alvarez-Buylla et al., 1998; Nottebohm, 2011). The VZ labelling reveals that the distribution of the proliferative cells is not homogenous with mitotic activity being abundant in the dorsal and ventral "hot spots" of the VZ (Alvarez-Buylla et al., 1990; Alvarez-Buylla et al., 1998).

1.4.2.2 Migration and differentiation in the avian brain

Despite having been born in focused 'hotspots" of the ventricular lining, dispersal of the neuroblasts is more widespread in the telencephalon. These newly formed neurons reach target areas in the telencephalon through different migratory routes. Although migratory routes of neuroblasts in the avian telencephalon are not well understood, the direction of migration is generally rostral. In addition, a stream of ventrocaudally migrating neuroblasts has been reported underneath the caudal telencephalon (Alvarez-Buylla, 1990; Alvarez-Buylla and Kirn, 1997). Regardless of the migratory route used and the final destination, migration takes approximately 20-40 days (Alvarez-Buylla and Kirn, 1997). The most commonly held hypothesis is that neuroblasts initially follow a tangential migratory route before coursing radially guided by the radial glial scaffolding (Kaslin et al., 2008). The glial scaffolding is formed by the radial fibres that penetrate several millimeters into the parenchyma of the telencephalon (Alvarez-Buylla and Kirn, 1997). However, the fact that these radial fibres do not reach the pial surface of the avian telencephalon suggests that other mechanisms are also employed for migration (Kaslin et al., 2008). Possible mechanisms for migration include use of blood vessels as guides or chain migration as in the mammalian SVZ and RMS (García-Verdugo et al., 2002; Whitman et al., 2009). All cell types generated from the VZ of the avian telencephalon are either interneurons or long projecting neurons (Kirn et al., 1991; Alvarez-Buylla and Kirn, 1997; García-Verdugo et al., 2002).

1.4.3 Adult neurogenesis in the amphibian brain

Urodele and anuran amphibians also exhibit extensive proliferative and neurogenic activity in many brain areas including the telencephalon, diencephalon, mesencephalon and cerebellum (Wullimann et al., 2005; Raucci et al., 2006; D'Amico et al., 2011; Maden et al., 2013; Amamoto et al., 2016; Herrgen and Akerman, 2016). In addition, neurogenic activity has also been reported in other areas outside the amphibian brain including the olfactory mucosa, vemoronasal mucosa and retina (Lindsey and Tropepe, 2006; Grandel and Brand, 2013). Previous studies demonstrated proliferative activity in the amphibian brain using ^{3}H-thymidine, BrdU and PCNA techniques whereas the fate of these newly formed cells was demonstrated using DCX, BLBP and GFAP (Wullimann et al., 2005; Raucci et al., 2006; D'Amico et al., 2011; Maden et al., 2013; Thuret et al., 2015; Herrgen and Akerman, 2016; Moreno and González, 2017)

1.4.3.1 Proliferative areas in the amphibian brain

In the post-metamorphic amphibian brain, proliferative activity occurs mostly along the ventricular lining (Bernocchi et al., 1990; Filoni et al., 1995; Almli and Wilczynski, 2007; Cerri et al., 2009; D'Amico et al., 2011; Maden et al., 2013). In the dorsoventrally flattened ventricles of olfactory bulb and rostral telencephalon, proliferative activity is very high in the ventricular lining of the roof (Raucci et al., 2006; Maden et al., 2013). In the mid-telencephalon, proliferation activity is abundant mainly along the ventromedial aspects of the lateral ventricles adjacent to the sub pallial nuclei (Bernocchi et al., 1990; Almli and Wilczynski, 2007; Cerri et al., 2009; D'Amico et al., 2011).

In the diencephalon, the lining of the recessus preopticus exhibits high proliferative activity (Raucci et al., 2006). On the contrary, infundibular recess of the hypothalamus, habenular nuclei, anterior and ventromedial thalamic nuclei are characterized by low proliferative activity (Bernocchi et al., 1990; Raucci et al., 2006).

Low proliferative activity also takes place in the mesencephalon specifically the ventral portion of the tectal ventricles, lamina nucleus and ventricular area of the dorsal tegmentum (Raucci et al., 2006). In addition, low proliferative activity is also observed along the fourth ventricular wall adjacent to the granular layer of the cerebellum and in the granular layer of the cerebellum (Bernocchi et al., 1990; Raucci et al., 2006; D'Amico et al., 2011).

1.4.3.2 Migration and Differentiation in the Amphibian brain

New cells born in the amphibian brain VZ migrate to the parenchyma as revealed by pulse chase experiments using ^{3}H-thymidine or BrdU (Bernocchi et al., 1990; D'Amico et al., 2011). In anurans, BrdU immunopositive cells were only observed in the lining of the VZ two days post BrdU injection. However, BrdU immunopositive cells co-expressing either neuronal or oligodendrocyte markers were observed in the parenchyma of many brain regions including the pallium, sub pallium, hypothalamus and optic tectum at later time points (D'Amico et al., 2011). Similarly, BrdU labelling was restricted to the ventricular zones of the urodele brain shortly after BrdU injection but could be observed in the telencephalic parenchyma after 2 weeks where they co-express NeuN (Maden et al., 2013).

These observations suggest that newly born cells migrate away from their place of birth in VZ lining to reach the brain parenchyma. Indeed, through BrdU/DCX double labelling experiments, D'Amico et al. (2011) provided evidence that newly born neuroblasts migrate from the VZ to the brain parenchyma. Furthermore, the same authors also reported that these BrdU/DCX positive neuroblasts migrate radially along the BLBP positive processes of radial glial like cells (D'Amico et al., 2011).

1.5 FUNCTIONAL SIGNIFICANCE OF NEUROGENESIS

The exact function of the newly born neurons in the postnatal CNS remains unclear. Previously, neuroscientists believed that postnatal neurogenesis was only a remnant of embryonic development that has no functional significance in the adult animal.

Adult neurogenesis has been observed in several classes of invertebrate and vertebrate animals studied to date. The evolutionary conservation of this trait suggests that neurogenesis might have a fundamental biological function.

In mammals, newly formed neurons in the SGZ of the hippocampal dentate gyrus have been shown to form synapse with mature granule neurons (Hastings and Gould, 1999; Markakis and Gage, 1999). In comparison to mature granule neurons, these newly formed neurons exhibit unique structural and electrical properties such as lower thresholds for long term potentiation (Liu et al., 2000; Wang et al., 2000). Moreover, neurogenic activity occurs in brain areas that are important for learning and memory raising the possibility that this process could be related to memory acquisition thereby improving animal adaptation to its environment (Kempermann et al., 1997; Kempermann, 2011; Aimone et al., 2014). In rodents, factors that increase neurogenesis such as estrogens, physical activity and environmental enrichment have also been shown to result in enhanced execution of hippocampus dependent tasks (Kempermann et al., 1997; Van Praag et al., 1999; Kronenberg et al., 2006). Similarly, factors that decrease neurogenesis such as stress, adrenal corticosteroids and age also result in poor performance of hippocampal dependent tasks (Lupien et al., 2009; Aimone et al., 2014). In addition, SVZ neurogenesis which produces new olfactory interneurons has been reported to be essential in odor discrimination or olfactory learning (Mobley et al., 2014).

In birds, telencephalic neurogenesis has been shown to be related to a variety of functions including song learning in song birds and spatial learning or memory in migratory, food storing and homing birds (Kaslin et al., 2008; Barnea and Pravosudov, 2011; Barkan et al., 2016). In canaries, production and subsequent recruitment of new neuronal cells in the HVc possibly forms a cellular basis for the observed plasticity in song learning (Alvarez-Buylla et al., 1992; Kirn and Nottebohm, 1993; Nottebohm, 2011). Indeed, song stability in canaries has been observed in seasons when neurogenesis was low (Kirn and Nottebohm, 1993; Kirn, 2010). Similarly, hippocampal neurogenesis in food caching or storing birds such as chickadees, jays and sparrows or migratory or homing birds such as pigeons has

been shown to be correlated with spatial learning (Barnea and Nottebohm, 1994; Lee et al., 1998; Barkan et al., 2016; Meskenaite et al., 2016).

In amphibians, the widespread neurogenesis observed is thought to be related to continuous growth of the CNS particularly the sensory systems (Grandel and Brand, 2013). Indeed, the high neurogenic activity observed in amphibians is most likely related to the high demand of CNS processing power needed for the increasing sensory input as the body grows (Kaslin et al., 2008; Grandel and Brand, 2013).

1.6 FACTORS AFFECTING VERTEBRATE NEUROGENESIS

Postnatal neurogenesis in vertebrates is regulated bi-directionally by several extrinsic and intrinsic factors. These factors include neutrophins, anti-depressants, stress, opioids, hormones, physical activity, environmental enrichment, seasonal variation, hibernation, temperature, photoperiods, social status, sex differences, learning and age (Lindsey and Tropepe, 2006; Kaslin et al., 2008; Balu and Lucki, 2009; Barnea and Pravosudov, 2011; Ming and Song, 2011; Pino et al., 2017). For all vertebrates studied to date, consensus exists on the regulatory effect of age.

1.6.1 Effect of age on vertebrate neurogenesis

Age is a powerful internal regulator of postnatal neurogenesis in vertebrates. In addition, age-related decreases in the formation and incorporation neurons has been reported across all vertebrates studied to date. In mammals, age-related decline in neurogenesis has been reported in the SGZ (Kuhn et al., 1996; Nada et al., 2010; Encinas et al., 2011; Jinno, 2011; Aimone et al., 2014; Pino et al., 2017), SVZ (Enwere et al., 2004; Luo et al., 2006; Shook et al., 2012), RMS (Mobley et al., 2014), OB (Enwere et al., 2004; Kondo et al., 2010) and the sub callosal zone (SCZ) (Kim et al., 2012).

Similarly, age-dependent changes in avian neurogenesis have also been reported in the HVc of the canary (Alvarez-Buylla et al., 1994; Wilbrecht and Kirn, 2004) and zebra finch (DeWulf and Bottjer, 2002; Wang et al., 2002; Kim et al., 2006; Pytte et al., 2007), hippocampus of the migrating white-crowned sparrow (LaDage et al., 2011), telencephalon of the ring dove (Ling et al., 1997), hippocampus and olfactory bulb of homing pigeons (Meskenaite et al., 2016).

Although no quantitative studies exist on the effect of age, neurogenic activity has been shown to be higher in the juvenile compared to adult amphibians. Raucci et al. (2006) reported comparatively lower mitotic activity in the brains of early post-metamorphic froglets compared to their larval counterparts. Similarly, D'Amico et al. (2011) reported reduced proliferative and neurogenic activity in the adult compared to juvenile frog brains.

1.6.2 Mechanisms of age-dependent changes in neurogenesis in vertebrates

Age-dependent decline in neurogenesis could result from either cell or non-cell autonomous mechanisms or both (Hamilton et al., 2013).

1.6.2.1 Cell autonomous mechanisms

Cell autonomous changes are those that occur within the NSCs themselves. Two main control systems which are potential mediators of cell autonomous changes are: telomere shortening and cyclin dependent kinase (CDK) inhibition (Mandal et al., 2011). These control systems result in prolongation of the cell cycle and NSC entry into reversible or irreversible quiescence (Hamilton et al., 2013).

Telomere shortening occurs each time NSCs divide leading to senescence. However, telomerase activity opposes the telomere shortening effects of cell division (Bodnar et al., 1998). Telomerase, a member of the reverse transcriptase group of enzymes, is highly detectable in NSCs. Indeed, high telomerase activity was observed in the rodent SVZ-OB system (Caporaso et al., 2003). In addition, accelerated aging and significant suppression of SVZ neurogenesis occurs in

telomerase knockout mice (Wong et al., 2003; Ferrón et al., 2004). However, this suppression in neurogenesis can be reversed after restoration of telomerase activity (Jaskelioff et al., 2011).

Analysis of the cell cycle in NSCs is important in order to understand how CDK inhibition regulates neurogenesis. The cell cycle consists of four sequential stages namely: G1 (Gap 1 stage), S (Synthesis-stage, DNA synthesis), G2 (Gap 2 stage) and M (Mitotic stage) (Boxem, 2006). After the M stage, cells either re-enter the cycle by proceeding to G1 or exit the cycle and enter the G0 phase (Gap 0). The G1 stage involves cell growth and preparation for DNA synthesis. If the conditions are ideal, the cell proceeds to the S-phase. In the S-phase, the cell starts DNA synthesis, which results in replication of DNA. The S-phase is followed by the G2 phase where the cell continues to grow in preparation for mitosis. Finally, the cell enters the M-phase in which mitosis occurs (Boxem, 2006) (Fig 1.3).

The cell cycle is intimately and precisely controlled by the activity of CDKs (Sherr and Roberts, 1999; Boxem, 2006). CDKs are only active when they are coupled with cyclins. Cyclins are cell cycle regulatory proteins whose name originates from their periodic synthesis and degradation during the cell cycle. On activation by cyclin, CDKs become cyclin activated kinases (CAKs) whose activity allows the cell to progress through the stages of the cell cycle. At the end of each cell cycle, cyclins are degraded, leading to inactivation of their coupled CDKs. Inhibition of CDKs therefore result in no progression through the cycle (Sherr and Roberts, 1999) (Fig 1.3).

Two families of CDK inhibitors are believed to be responsible for the observed age-related decline in neurogenesis. These are the INK4 and Cip/Kip families. The INK4 is a tumor suppressor family and consist of the following members: $P16^{INK4a}$, $P15^{INK4b}$, $P18^{INK4c}$ and $P19^{INK4d}$ (Kim and Sharpless, 2006). It has been reported that increased expression of INK4 results in age-dependent suppression in NSC proliferation (Molofsky et al., 2006). Conversely, a reduction in the expression of $P16^{INK4a}$ attenuates age-dependent decline in NSC proliferation. In addition,

transcription factors Bmil and Hmga 2 which suppress expression of $P16^{INK4a}$, promote NSC proliferation and attenuate age-related decline in neurogenesis (Molofsky et al., 2003; Molofsky et al., 2006; Nishino et al., 2008).

The Cip/Kip family consist of the following family members: $p21^{Walf\ 1/Cip}$, $p27^{\ Kip\ 1}$and $p57^{\ Kip\ 2}$(Kim and Sharpless, 2006; Hamilton et al., 2013). Similarly, expression of P21 promotes age-related decrease in progenitor cell proliferation. Indeed, expression of P21 resulted in aging of the rodent cerebellum (Legrier et al., 2001). Conversely, P21 knockout mice show no age-related decline in NSC proliferation (Kippin et al., 2005).

Figure 1.3: Schematic diagram showing the different stages of the cell cycle and factors that regulate the cycle in eukaryotes. Adapted from Boxem (2006). See list of abbreviations for abbreviations used in this figure.

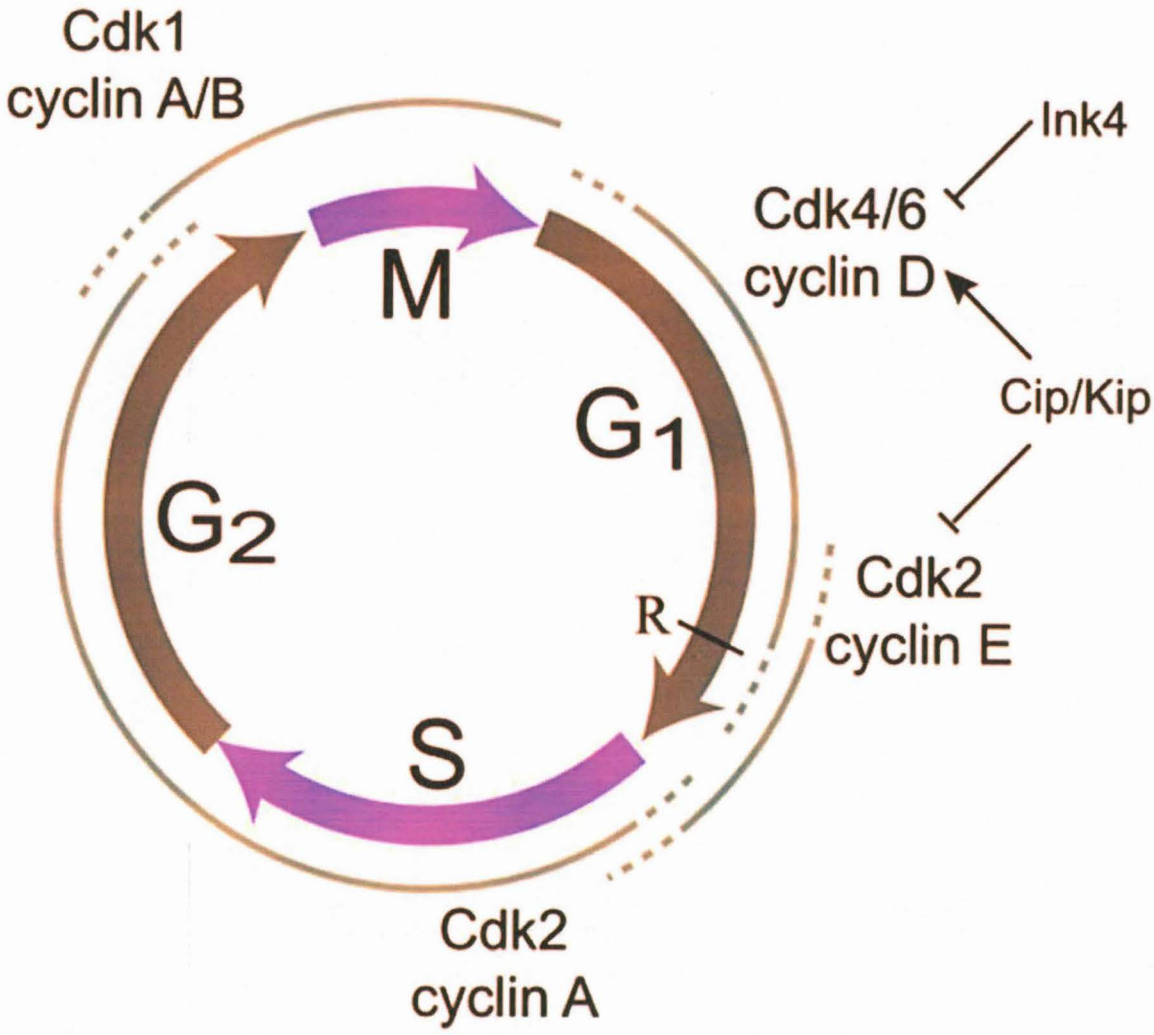
Cdk1
cyclin A/B
Ink4
Cdk4/6
cyclin D
Cip/Kip
M
G1
G2
R
Cdk2
cyclin E
S
Cdk2
cyclin A

1.6.1.2 Non-cell autonomous mechanisms

Non-cell autonomous mechanisms include all changes in the neurogenic microenvironments that result in reduced trophic support of NSCs. These changes result in either an increase in neurogenesis inhibiting factors or a decrease in signals promoting neurogenesis (Hamilton et al, 2013). The majority of these factors were identified from neurogenesis research in rodents. Ephrins, epidermal growth factors (EGFs), fibroblast growth factors (FGFs), vascular endothelial derived factors (VEGFs), insulin-like growth factor-1 (IGF-1), brain derived neurotropic factor(BDNF), sonic hedgehog, notch and Wnts are some of the neurogenesis promoting signals that decrease with age (Aimone et al., 2014; Bond et al., 2015; Pino et al., 2017). On the other hand, neurogenesis inhibiting factors that increase with age include bone morphometric proteins (BMPs), corticosteroids and pro-inflammatory cytokines such as tumor necrosis factor-alpha (TNF- α), interleukin-6 (IL-6) (Cameron and Gould, 1994; Aimone et al., 2014; Bond et al., 2015). Interestingly, exogenous infusion or blockage of some of these factors result in attenuation of the impaired neurogenesis (Jin et al., 2003; Enwere et al., 2004).

In addition, several other changes in the neurogenic niches including alterations in blood borne factors, cerebrospinal fluid composition, ventricular stenosis leading to loss of ependymal cells and lipid droplet accumulation in the ependyma are also potential culprits (Villeda et al., 2011; Baird et al., 2012; Shook et al., 2012).

1.7 EVOLUTIONARY PERSPECTIVES AND ANIMAL MODELS USED

The majority of postnatal neurogenesis research work was done using mammalian animal models. Consequently, almost all general theories on vertebrate neurogenesis are derived from mammalian work. However, neurogenesis in non-mammalian vertebrates have largely been ignored. A comparative analysis of postnatal neurogenesis in animal models from different vertebrate taxa is significant in revealing differences in regional and temporal distribution of this trait. In this study, neurogenesis was investigated in the brains of the African clawed frog, Japanese

quail and BALB/c mouse as animal model representatives of the amphibian, avian and mammalian vertebrate classes respectively.

Ancestral amphibians evolved from fish approximately 360 million years ago (Barker et al., 2011). In turn, urodele and anuran amphibians separated from each other around 350 million years ago from a common amphibian ancestor. In this study, we used an anuran (African clawed frog) as the amphibian model because studies have shown that anurans and not urodeles most likely represent the evolutionary path from which reptiles and mammals emerged from (Kuhn and Eisch, 2014). Furthermore, paleontological evidence shows that the paths leading to birds and mammals diverged several million years ago when the amphibian ancestors gave rise to two parallel evolutionary paths: one leading to reptiles and birds and the other one leading to mammals (Barnea and Pravosudov, 2011) (Fig 1.4).

The Japanese quail and the BALB/c mouse were chosen as representative models of the avian and mammalian animals respectively because as short-lived species all the life-history stages can easily be studied within a relatively short period of time. Another reason for selection of the animal models used in this study is that they widely available and are easy to breed and rear under laboratory conditions.

Figure 1.4: Schematic diagram showing the phylogenetic tree of vertebrates. Figure adapted from Kuhn and Eisch (2014).

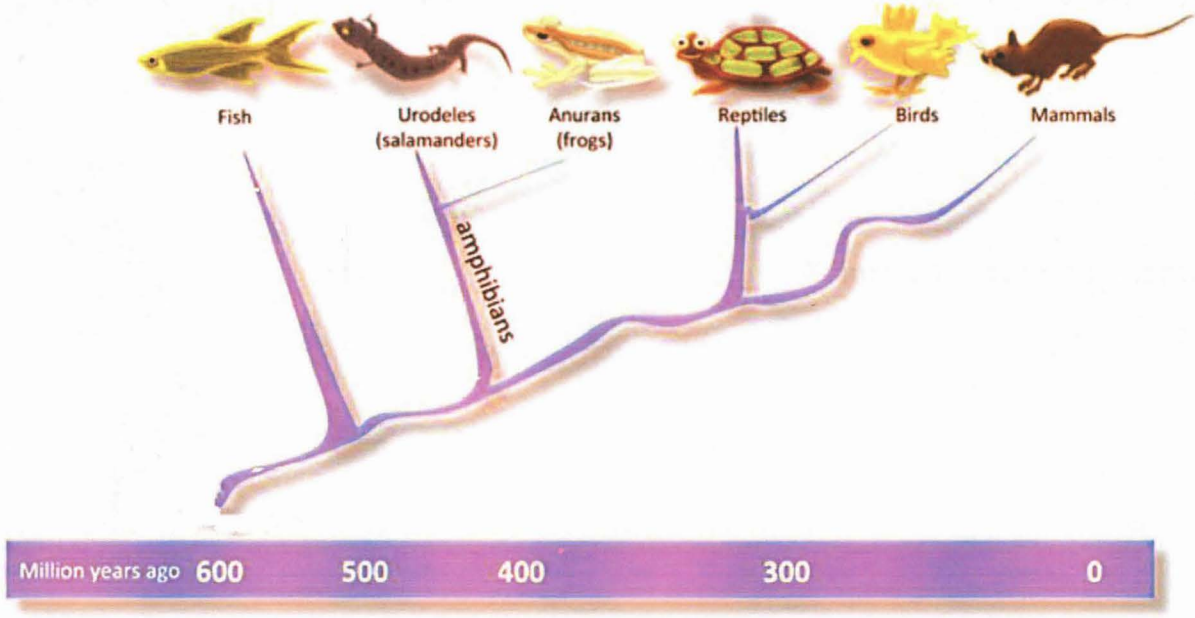
Fish
Urodeles
(salamanders)
Anurans
(frogs)
Reptiles
Birds
Mammals
amphibians
Million years ago
600
500
400
300
0

1.7.1 BALB/c mice

1.7.1.1 Scientific classification

The BALB/c mouse (Fig 1.5 A) belongs to class mammalia, order rodentia, family muridae, genus *mus*, sub genus *mus* and species *m. musculus*

1.7.1.2 Habitat and geographic distribution

The BALB/c mouse is a close relative of the house mouse. The BALB/c is the popularly used species belonging to the genus *mus* in laboratory research. These mice are able to survive under a wide range of environmental conditions including homes, commercial buildings, open fields and agricultural land. BALB/c mice usually live under laboratory conditions. Although they are omnivorous, BALB/c mice also feed on plant material.

1.7.1.3 General characteristics and behaviour

BALB/c mice can easily be identified by their pointed snout, small round ears, a long tail and a white colour coat. Females usually have five pairs of mammary glands whereas their male counterparts do not have nipples. Males have a large pair of testes which can be retracted close to the body. Like all other members of the genus *mus*, BALB/c mice can run, walk and stand using all four limbs. In addition, BALB/c mice can also jump, climb and swim. However, when feeding or fighting, they usually lift their forelimbs while tripoding on their hind legs and long tail. BALB/c mice are thigmotactic as they have a tendency to keep in close contact with upright surfaces or walls.

Mice are nocturnal and usually avoid bright light. In captivity, BALB/c mice sleep for an average of 12.5 hours daily. In the wild, mice live close to food sources in hidden places usually in nests built from soft materials. In natural populations, mice usually live in small groups and are territorial. Usually each group is comprised of one dominant male, several females and young mice. The social behaviour of mice in

natural populations is not rigid but is largely dependent on food, water and space availability (Frynta et al., 2005). This dynamism enables mice to live in a wide variety of environments ranging from sandy areas to buildings.

Depending with the environment, mice display commensal and non-commensal forms of social behaviour. Commensal behaviour is mostly displayed in mouse populations that inhabit urban areas and buildings where food is in large supply (Frynta et al., 2005). These environments are characterized by short home ranges and high population densities. Under these circumstances, territorial behaviour is abolished and individuals have a social hierarchy. In commensal populations, social units are usually composed of one male and two or more related females that breed and nurse cooperatively, thereby increasing reproductive success (Frynta et al., 2005; Szenczi et al., 2012). On the other hand, non-commensal behaviour is displayed by mice that live wild and open fields (Gray and Hurst, 1997; Szenczi et al., 2012). These environments are characterized by limited food and large home ranges. Compared to commensal populations, female to female and male to male aggression is very high in non-commensal populations (Gray and Hurst, 1997; Frynta et al., 2005). In both populations, males aggressively defend their territories against intrusion. To avoid intrusion, males usually mark their territories with urine. As a result, sexually mature males usually leave their birth places to form new territories. However, females generally stay within their birth territory.

Mice are opportunistic rather than seasonal breeders. The gestation period in mice is usually 19 to 21 days and at term they give birth to an average of 6-8 pups. The pups are born without fur, ears and sight. However, the ears are formed by the 4th day, fur appears by the 6th day and eyes are open by the 13th day after birth. Juvenile pups feed on breast milk before they are weaned around 21 days after birth. Usually, male and female mice reach sexual maturity or puberty between 5 weeks to 6 weeks of age when they become adults. The lifespan of BALB/c mice is one year and four years in the wild and in captivity respectively (Miller et al., 2002).

1.7.2 Japanese quail

1.7.2.1 Scientific classification

The Japanese quail (Fig 1.5 B) belongs to class aves, order galliformes, family phisianidae, genus *cortunix* and species c. *japonica*

1.7.2.2 Habitat and geographic distribution

Japanese quails are a member of the old world quail populations found in eastern Asia. Some populations also inhabit several countries in Africa including Egypt, Kenya, Madagascar, Malawi, Namibia and Tanzania. However, their breeding sites are mainly located in Eastern and Central Asia. Japanese quails are a ground-living species that inhabit areas of dense vegetation to avoid predation. The quail's natural habitat includes grassy fields, bushes along the river banks and grain farms (Buchwalder and Wechsler, 1997). In addition, Japanese quails also live in open habitats including steppes, meadows and dry mountain slopes in close proximity to water sources. Quails mainly feed on grass seeds such as white millet and panicum and small invertebrates including insects and their larvae.

1.7.2.3 General characteristics and behaviour

Both sexes of quail chicks have the same colour of plumage (Hubrecht and Kirkwood, 2010). Although both sexes have a predominantly brown coloured plumage in adulthood, the colour of the throat and breast plumage is sexually dimorphic. In females, the breast feathers are pale littered with dark spots. In contrast, the breast plumage in males is reddish brown with no dark spots (Hubrecht and Kirkwood, 2010).

Socially, quails display both monogamous and polygamous relationships (Bennett G Galef and White, 1998). In addition, Japanese quails are seasonal breeders with breeding activity peaking during the summer. During this period, the testes of the

quails enlarge and testosterone production reaches its peak (Akbar and Qureshi, 2012). When mating, the male usually deposits semen into the cloaca of a receptive female. If fertilization takes place, the female will lay eggs usually just before dusk (Mills et al., 1997). Egg incubation, lasting about 17 days, is carried out by the female quail and commences when the last egg in the batch is laid (Ainsworth et al., 2010). During this period, the female becomes increasingly aggressive and intolerant to male quails. Just before the egg hatching, the female eventually chases the male off the nest. Therefore, females are the sole providers of parental care of the juvenile quails (Correa et al., 2011). Japanese quails attain sexual maturity between 5 to 6 weeks of age and have an average life span of 4 years in captivity.

Based on their inability to distinguish different carbohydrates, quails were previously thought to have an underdeveloped gustatory sense. However, new evidence shows that quails have a preference for sugar containing solutions over simple water or salty solutions (Mills et al., 1997). In addition, quails also possess an olfactory epithelium in their nasal cavity and prominent olfactory bulbs. Indeed, a few studies have shown that quails are able to avoid pesticides and lectin, a food contaminating toxin, using olfaction alone (Mills et al., 1997). Furthermore, quails have very large eyes which enable them to have frontal eye filed overlap. Moreover, they have also been reported to possess colour vision and therefore able to perceive more than form or shape (Mills et al., 1997). Although not much is known about the quail's auditory sense, they are able to distinguish more than 28 different calls used by other quails. Each call is dependent on the circumstances and elicits certain behaviours (Mills et al., 1997). These vocalizations appear after 5 weeks of development and are non-learned. Crowing in males has been shown to speed the maturation of the female ovaries and females exposed to this crowing reach sexual maturity earlier than those non-exposed (Mills et al., 1997).

1.7.3 African Clawed frog

1.7.3.1 Scientific classification

The African clawed frog (Fig 1.5 C) belongs to class amphibian, family pipidae, genus xenopus and species *x. laevis*.

1.7.3.2 Habitat and geographic distribution

The African clawed frog is mainly resident in ponds, wetlands, rivers and lakes in arid and semi-arid south eastern parts of Sub Saharan Africa. In addition, fewer introduced populations are also found in Europe, North and South America.

1.7.3.3 General characteristics and behaviour

African clawed frogs have a smooth, slippery skin that is olive grey or brown in colour dorsally and cream in colour ventrally. Every season, they shed and consume their skin. African clawed frogs do not have a tongue and teeth. They use their claws to break pieces of food and use their hands to shove the food into the mouth (Maddin et al., 2009). African clawed frogs are scavengers and prey on anything living or dead.

African clawed frogs reproduce by fertilising the eggs laid by the female outside the body. Females usually lay eggs during the period between winter and spring. Following fertilisation, pre-metamorphic development (embryo to tadpoles) of *x. laevis* takes approximately 6 to 8 weeks (Nieuwkoop and Faber (NF) stages 1-55). After 8 weeks, metamorphosis (NF stages 55-66) takes place for approximately 4-5 days when the tadpole transforms into a froglet. This change involves resorption of the tadpole tail and development of the limbs. The juvenile period is approximately 10 months, followed by the sub adult period stretching from 10 to 12 months. African clawed frogs attain sexual maturity at approximately 12 months of age when they

become adults. African clawed frogs have a life span around 15 years in the wild and 25 to 30 years in captivity.

African clawed frogs do not have ears but use lateral lines on the sides and under aspect of their bodies to sense movements and vibrations. They also employ their very sensitive fore digits, keen olfactory sense and the lateral line system to find food. Anuran amphibians also demonstrate significant learning ability and display considerable navigational abilities when they migrate seasonally in search for food or between breeding ponds.

Figure 1.5: Photographs showing different vertebrate animal models used in this study. A) BALB/c mouse, B) Japanese quail and C) African clawed frog.

A



B



C

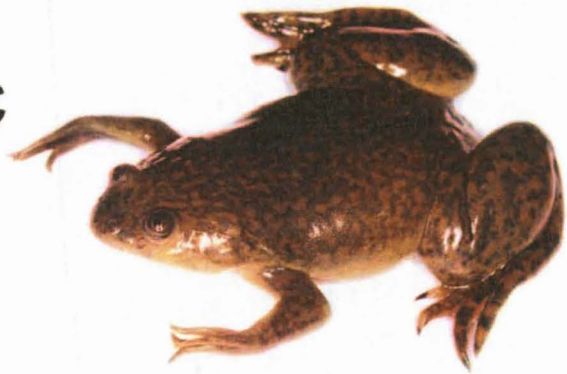

1.8 AIM AND OBJECTIVES OF THE STUDY

1.8.1 Aim

The aim of the study was to determine time-course changes in cell proliferation, differentiation and cell death in the mammalian, avian and amphibian brains. In the current study, time-course was defined as the increasing chronological age spanning different life-history stages of the animal. However, changes in cell death could not be determined using the initial technique that was proposed for this study and the exorbitant cost of the likely alternate technique.

1.8.2 Objectives

1.8.2.1 To qualitatively determine proliferative sites in the BALB/c mouse, Japanese quail and African clawed frog brain using Ki-67 and PCNA immunohistochemistry.

1.8.2.2 To qualitatively determine areas of the BALB/c mouse, Japanese quail and African clawed frog brain that incorporate newly formed neurons using DCX immunohistochemistry.

1.8.2.3 To qualitatively and quantitatively determine how cell proliferation and neuroblast incorporation change with chronological age in the BALB/c mouse, Japanese quail and African clawed frog brain.

1.8.2.4 To qualitatively and quantitatively determine how cell proliferation and neuroblast incorporation change with life-history stages in the BALB/c mouse, Japanese quail and African clawed frog brain.

To achieve these aims, the research was divided into four studies.

Study 1: Changes in neurogenesis with post-hatching age in the male Japanese quail (*Cortunix japonica*) brain

The objective of this study was to qualitatively evaluate proliferative sites and brains areas that incorporate new neurons in the Japanese quail brain at post-hatching ages 3 to 12 weeks using PCNA and DCX immunohistochemistry respectively. PCNA-ir cells were observed mainly in the olfactory bulb ventricular lining, telencephalic ventricular zones and cerebellum. Fewer PCNA-ir cells were also observed in the hypothalamus, thalamus and bed nucleus of the stria terminalis. In telencephalic ventricular zones, PCNA-ir cells were concentrated ventrally and dorsally adjacent to the mesopallium and medial striatum, respectively. DCX-ir cells were observed in the olfactory bulb, telencephalon and cerebellum. Furthermore, DCX-ir cells were scattered throughout the pallium except for the entopallium and arcopallium; septal nuclei and striatum. Fewer DCX-ir cells were also observed in the hippocampus and bed nucleus of stria terminalis. The density of PCNA-ir cells and DCX-ir cells in all brain areas declined with post-hatching age. Findings from this study reveal that cell proliferation appears to be restricted to the ventricular zones whereas neuronal recruitment is more widespread in the olfactory bulb, telencephalon and cerebellum. In addition, post-hatching neuronal incorporation appears to be absent in the diencephalon and mesencephalon.

Study 2: Quantitative analysis of age-related changes in doublecortin (DCX) expression in the male Japanese quail (*Cortunix Japonica*) telencephalon.

Since the high density of PCNA-ir cells in the dorsal and ventral reaches of the telencephalic ventricles precluded quantification, only DCX-ir cells were quantified in this study. The objective of this study was therefore to quantitatively determine how DCX expression in the Japanese quail telencephalon changes with post-hatching age (3-12 weeks) and life-history stage. Bipolar and multipolar DCX-ir cells were

observed in the entire telencephalon except for the entopallium and arcopallium. In addition, DCX expression in all the eight telencephalic areas quantified was strongly negatively correlated with post-hatching age. Furthermore, numbers of bipolar and multipolar DCX-ir cells were higher in the juvenile compared to sub adult and adult quails. This study revealed that neuronal incorporation in the quail telencephalon is widespread but declines with post-hatching age. In addition, the most dramatic decline in neuronal incorporation in the all the telencephalic areas quantified occurred from the 7th week just after the quails attained sexual maturity.

Study 3: Age-related changes in Ki-67 and DCX expression in the BALB/ c mouse (*Mus musculus*) brain.

The objective of this study was to qualitatively and quantitatively determine how age (1-12 weeks) and life-history stage affect neurogenesis in the male BALB/c mouse brain. To achieve this, Ki-67 and DCX immunohistochemistry was used to assess changes in cell proliferation and neuronal incorporation respectively. Ki-67 expression was mainly observed in the olfactory bulb, RMS, SVZ of the lateral ventricle and the SGZ of the dentate gyrus. In addition, fewer Ki-67 positive cells were also observed in the neocortex, cerebellum and tectum. DCX was expressed in similar regions as Ki-67 except for the cerebellum and tectum. Both Ki-67 and DCX expression sharply decreased with increasing age or progression through life-history stages in the SVZ, RMS and SGZ of the BALB/c brain.

Study 4: Age- related changes in proliferation nuclear antigen (PCNA) and doublecortin (DCX) expression in the post-metamorphic African clawed (*Xenopus laevis*) frog brain.

The objective of this study was to qualitatively and quantitatively determine how PCNA and DCX expression in the post-metamorphic African clawed frog brain changes with age and life-history stage. In this study, PCNA and DCX were used as proxies for neuronal stem cell proliferation and neuronal incorporation respectively. PCNA-ir cells were observed mainly in the ventricular linings of the olfactory bulb,

telencephalon, ventral hypothalamus, preoptic region and metencephalon adjacent to the cerebellar granule cell layer. DCX-ir cells were observed in the parenchyma of the olfactory bulb, telencephalon, ventral hypothalamus and cerebellum. In the telencephalon, DCX-ir cells were concentrated mainly in the striatal and septal areas although fewer cells were also observed in the lateral, medial and dorsal pallial areas. PCNA-ir and DCX-ir cells in the telencephalic areas were then quantified and correlated with age and life-history stage. PCNA-ir and DCX-ir in all the telencephalic areas quantified were strongly negatively correlated with age. Furthermore, PCNA-ir and DCX-ir cells were higher in the juvenile froglets compared to sub adult and adult frogs. This study revealed that neuronal stem cell proliferation and neuronal incorporation in the *X. laevis* brain is widespread but declines with age. In addition, the most dramatic decline in neurogenesis in all the telencephalic areas quantified occurred during the period of transition from sub adult to adult life-history stages.

CHAPTER 2: CHANGES IN NEUROGENESIS WITH POST-HATCHING AGE IN THE MALE JAPANESE QUAIL (*CORTUNIX JAPONICA*) BRAIN

2.1 INTRODUCTION

Across all vertebrate species, the central nervous system harbours constitutively active neuronal progenitors that are responsible for producing new neurons throughout life (Alunni and Bally-Cuif, 2016). The process through which new neurons are formed from these progenitors is termed neurogenesis and involves cell proliferation, differentiation, migration and integration of the newly formed neurons into the existing neuronal circuitry (Barnea and Pravosudov, 2011). In mammalian adult brains, neurogenesis is restricted to the sub granular zone of the hippocampus and the sub ventricular zone of the lateral ventricle (Kaslin et al., 2008). On the other hand, in avian brains new neurons are generated along the walls of the lateral ventricle and migrate radially to be integrated into different circuits of the telencephalon (Vellema et al., 2010; Hall et al., 2014).

The songbird species such as the canary and zebra finch have been used extensively in post-hatching neurogenesis studies (Nottebohm, 1984; Brenowitz, 2004; Nottebohm, 2011; Brenowitz and Larson, 2015). Although neurogenesis in songbird brains was observed to be widespread, the focus of most studies has been almost exclusively on neuronal recruitment and integration into telencephalic circuits involved in song production (Alvarez-Buylla et al., 1992; Boseret et al., 2007; Balthazart et al., 2008; Nottebohm, 2011; Balthazart and Ball, 2016). However, songbirds constitute only about 2% of all avian species (Ling et al., 1997). Furthermore, previous studies have revealed that the neurogenesis observed in the telencephalon is not only specific to songbirds but also occurs in other avian species belonging to other orders such as ring doves (Ling and Cheng, 1995; Ling et al., 1997), pigeons (Melleu et al., 2013; Melleu et al., 2016; Meskenaite et al., 2016; Mazengenya et al., 2017) chicken (Nikolakopoulou et al., 2006a; Mezey et al., 2012) and quails (Nikolakopoulou et al., 2006b; Balthazart et al., 2010; Bardet et al., 2012; Mouriec and Balthazart, 2013).

Neurogenesis in the avian brain has been shown to be regulated by several internal and external factors including levels of circulating sex steroids (e.g testosterone, estradiol), variations in day length, seasonal changes and age (DeWulf and Bottjer,

2002; Yamamura et al., 2011; Mouriec and Balthazart, 2013; Barker et al., 2014; Guigueno et al., 2016; Meskenaite et al., 2016).

Age-related decline in the production and recruitment of neuronal cells has been reported in the telencephalon and song control nuclei of canaries (Alvarez-Buylla et al., 1994) and zebra finches (DeWulf and Bottjer, 2002; Wang et al., 2002; Pytte et al., 2007). In addition, neurogenesis was reported to decline with age in the telencephalic ventricular zones of the ring doves (Ling et al., 1997), hippocampus and olfactory bulb of the pigeon (Meskenaite et al., 2016), and the telencephalon of the chicken (Mezey et al., 2012). Interestingly, Mouriec and Balthazart (2013) reported an age-dependant decline in cell proliferation in the medial preoptic nucleus (POM) of the Japanese quail brain during the pre-pubertal stages (PND 1 to 43) which was followed by an increase in cell proliferation at puberty (PND 44 to 56).

The majority of neurogenesis studies in quails focussed on the sex steroid sensitive areas like the POM (Bardet et al., 2012), intermediate medial mesopallium and lateral septal nucleus (Nikolakopoulou et al., 2006b) with little attention given to neurogenesis in other quail brain areas like the telencephalon. The aim of the present study was therefore to determine the effect of post-hatching age on cell proliferation and neuronal recruitment in the male Japanese quail (*Cortunix japonica*) brain. Japanese quails are precocial birds that belong to the order galliformes. In addition, male quails exhibit crowing, a testosterone dependent behaviour. However, crowing is considered a non-learned vocalisation in contrast to the learned song of songbirds. To achieve this aim, proliferating cell nuclear antigen (PCNA) and DCX were used to assess cell proliferation and neuronal recruitment respectively in the quail brains.

2.2 METHODS

2.2.1 Experimental Animals

Thirty male Japanese quails with post-hatching ages ranging from 3 to 12 weeks obtained from the agricultural research centre (ARC, Irene, South Africa) were used in this study. All animals were treated and used according to the guidelines of the University of the Witwatersrand Animal Ethics Committee which correspond with those of the National Institute of Health (NIH) for care and use of animals in scientific experimentation. All protocols were approved by the University of the Witwatersrand Animal Ethics Screening Committee (AESC/2012/53/01).

Throughout their life, the birds were maintained on a photoperiod simulating long days (16L: 8D) with access to food and water *ad libitum.* During the first 3 weeks after hatching, chicks were kept in mixed groups in brooder cages at 30°C. Temperature was then progressively reduced to room temperature by the 5th week. From post hatching age 3 weeks, 3 birds were collected every week up until the 12th week. The quails were allocated to groups according to their sexual maturity as follows: juvenile (sexually immature, 3-5 weeks old, n= 9), sub adult (sexually matured, 6-8 weeks old, n=9) and adult (sexually active, 9-12 weeks old, n=12).

2.2.2 Tissue collection and processing

All birds were given a dose of heparin (1ml i.m) 5 min prior to euthanasia to prevent blood clotting followed by an intraperitoneal injection of Euthapent (0.5 – 1 ml/kg). Animals were then perfusion-fixed transcardially, initially with 0.9 % cold saline solution, followed by 4 % paraformaldehyde in 0.1 M phosphate buffer (PB, pH 7.4) solution. After perfusion, brains were carefully removed from the skull, post-fixed overnight in 4 % paraformaldehyde in 0.1M PB, weighed before being transferred into 30% sucrose in 0.1M PB until equilibration. The brains were sectioned in a coronal plane at 50 µm using a cryostat (Shandon Cryotome E, Thermo Fischer scientific, UK) at -24 ℃ and repeated series of 5 sections were collected free-floating into 24 multi-well plates containing 0.1 M PB. The first series of sections was mounted on gelatin- coated slides before staining with 1 % cresyl violet for

anatomical orientation, the second one for PCNA and the third one for DCX immunohistochemistry. The remaining two series were stored in a cryoprotectant solution at -20°C for future use.

2.2.3 Immunohistochemistry

Brain sections were pre-treated for 30 min at room temperature under gentle shaking with an endogenous peroxidase inhibitor solution [0.1 M PB, 100% methanol and 30% H_2O_2 in the ratio 49.2: 49.2: 1.66]. Following three 10-min rinses in 0.1 M PB, the sections were subsequently pre-incubated in a blocking buffer solution [3 % normal horse serum or 3 % normal rabbit serum, 2 % bovine serum albumin, 0.25 % Triton X-100 in 0.1 M PB] for 2 h under gentle shaking at room temperature to prevent non-specific binding. Sections were then transferred into a primary antibody solution [1:500, mouse anti-PCNA (clone PC 10; NCL-L-PCNA, Novocastra, UK) or 1: 300, goat anti-DCX (C-18: SC-8066, Santa Cruz Biotechnology, Inc, USA), in the blocking buffer solution] and were incubated for 48 h at 4 °C under gentle shaking. Following incubation, sections were subjected to three 10-min rinses in 0.1 M PB before being incubated in secondary antibody solution [1:1000 biotinylated anti-mouse IgG (Novocastra, UK) or 1: 1,000 dilution of biotinylated anti-goat IgG (BA-5000; Vector Laboratories, USA) in blocking buffer solution] for 2 h at room temperature under gentle shaking. Following three 10-min rinses in 0.1 M PB, the sections were incubated in an avidin-biotin solution [1: 125 A and 1: 125 B (Vector Laboratories) in 0.1 M PB] for 1 h. The sections were then transferred into three 10-min 0.1 M PB rinses before being placed in a solution containing 0.05% 3, 3 Di-amino-benzidine tetrachloride (DAB) in 0.1 M PB for 5 min. To each 1 ml of this solution, 3.3 µl of 30% H_2O_2 were added, and chromatic precipitation was visually monitored under a low power stereomicroscope.

Development was subsequently stopped by placing the sections in 0.1 M PB, followed by a final 10-min rinse in 0.1 M PB. Sections were mounted on 0.5% gelatinised slides, left to dry overnight, dehydrated in a graded series of alcohols, cleared in xylene and cover slipped with DPX. To ensure that non-specific staining was not affecting the results, control sections taken at random were processed in the

same manner, but either the primary or the secondary antibody was omitted. No labelled cells were observed in either case.

2.2.4 Data Analysis

Sections were analysed qualitatively with both low and high power microscopy to yield a comparative description of the distribution of PCNA and DCX-immunoreactive (ir) cells. Brain structures were identified based on the atlas of the quail or chicken brain (Baylé et al., 1974; Kuenzel and Masson, 1988; Puelles, 2007) and we adopted the nomenclature by the Avian Brain Forum (Reiner et al., 2004). High power microscopic observation was used to determine the relative densities of stained structures throughout the different regions of the brain. The relative densities of immunostained structures were visually compared and recorded on a scale ranging from absent (-) to low (+) to moderate (++) to high (+++). A second observer was used to eliminate observer bias (Chawana et al., 2013; Mazengenya et al., 2018).

High resolution microscopic images were digitally captured using an AxioCam HRC digital camera on a Zeiss Axioplan 2 compound microscope and a Zeiss Discovery SteREO v20 Stereomicroscope connected to a PC running Axiovision software. Composite images were prepared with the Adobe Photoshop 7.0 software (Adobe Systems, Mountain View, CA). No pixelation adjustment or manipulation of the captured images was undertaken, except for the adjustment of contrast, brightness and levels.

2.3 RESULTS

We report here changes in PCNA and DCX immunoreactivity from post-hatching age 3 weeks to 12 weeks.

2.3.1 Age-related changes in PCNA expression in the Japanese quail brain

2.3.1.1 Olfactory bulb

In juvenile quails, a high density of PCNA-ir cells was observed in the ependymal and sub ependymal lining of the olfactory ventricles (Figs 2.1A and B). In addition, a few PCNA-ir cells were observed extending dorsally into the hyperpallium densocellulare (HD) (Fig 2.1 C). The distribution of PCNA-ir cells in the OB of sub adult and adult quails was similar to that observed in juvenile quails except that no PCNA-ir cells were observed extending into the HD in adult quails older than 9 weeks (Figs 2.3 A-C, Table 2.1).

2.3.1.2 Telencephalon

In the juvenile telencephalon, a high density of PCNA-ir cells was observed throughout the rostrocaudal extent of the lateral ventricles (Figs 2.1 D-L). In the ventricular zones, PCNA-ir cells were mostly abundant ventrally adjacent to the medial striatum (Mst) and dorsally adjacent to the mesopallium (M) (Figs 2.1 D and E). In addition, a few PCNA-ir cells were observed in the M (arrows in Fig 2.1 E) of quails aged 3 and 4 weeks. However, no PCNA-ir cells were observed in the rest of the pallial areas. In the sub pallium, a low density of PCNA-ir cells was observed in the Mst adjacent to the lateral ventricles (Figs 2.1 H and I). Fewer cells were also observed in the bed nucleus of stria terminalis (BSTM and BSTL) (arrows in Fig 2.1 L).

The distribution of PCNA-ir cells in the telencephalon of sub adult and adult quails was similar to that observed in the juvenile group although the density of PCNA-ir

cells was lowest in the adult group (Figs 2.3 D-I). However, no PCNA-ir cells were observed in the pallial areas of the sub adult and adult quails. In addition, PCNA-ir cells were absent in the BSTM and BSTL of adults older than 9 weeks or in the Mst of adult quails (Table 2.1).

Figure 2.1: Photomicrographs showing distribution of PCNA-ir cells in the olfactory bulb and telencephalon of the Japanese quail brain. (A) Low power photomicrograph showing distribution of PCNA-ir cells in the OB. (B) High power photomicrograph showing distribution of PCNA-ir cells along the olfactory bulb ventricular lining. (C) High power photomicrograph showing PCNA-ir cells (black arrows) extending from the OB to the HD. (D) Low power image showing distribution of PCNA-ir cells long the lining of the lateral ventricle of the rostral telencephalon. (E) High power image showing distribution PCNA-ir cells along the lining of the lateral ventricle adjacent to the M (black arrows showing PCNA-ir cells in the M). (F) High power image showing distribution PCNA-ir cells in the lining of the lateral ventricle adjacent to the N. (G) Low power image showing distribution of PCNA-ir cells long the lining of the lateral ventricle of the mid telencephalon. (H) Photomicrograph showing an increase in PCNA-ir cells on the ventral reach of the lateral ventricular zones adjacent to Mst. (I) High power image showing PCNA-ir cells in the Mst (black arrows) adjacent to the lateral ventricle. (J) Low power photomicrograph showing distribution of PCNA-ir cells long the lining of the lateral ventricle of the caudal telencephalon (insert shows part of the lateral ventricle magnified in figure K). (K) High power image showing distribution of PCNA-ir cells along the lateral ventricular lining of the caudal telencephalon. (L) High power photomicrograph showing the distribution of PCNA-ir cells in the BSTL (black arrows). Scale bars: J= 500μm and applies to A, D, G; L=50 μm and applies to B, C, E, F, I, K and H=200μm. See list of abbreviations for abbreviations used in this figure.

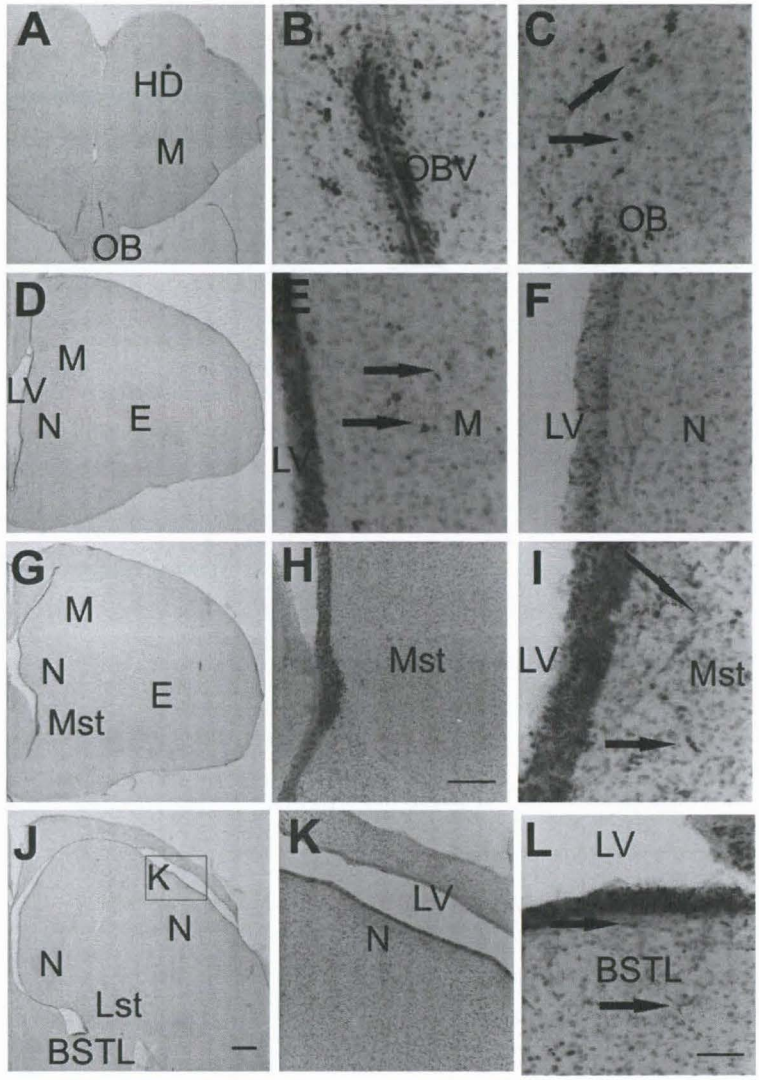
A
HD
M
OB
B
OBV
C
OB
D
M
LV
N
E
E
M
LV
F
LV
N
G
M
N
E
Mst
H
Mst
I
LV
Mst
J
K
N
N
Lst
BSTL
K
LV
N
L
LV
BSTL

2.3.1.3 Diencephalon

In the hypothalamus of juvenile quails, medium densities of PCNA-ir cells were observed in the POM (Figs 2.2 A & 2.3 J-L), nucleus paraventricularis (PVN), nucleus ventromedialis hypothalami (VMN) and nucleus tuberis (Tu). In the thalamus, low densities of PCNA-ir cells were observed in nucleus rotundus (Rt), nucleus ovoidalis (OV), nucleus dorsolateralis anterior thalami (DLA), nucleus dorsomedialis anterior thalami (DMA) and nucleus geniculatus lateralis pars ventralis (GLv) (Fig 2.2 B). A low density of PCNA-ir cells was also observed lining the ventricular zones of the 3rd ventricle of the diencephalon. The pattern of expression of PCNA in the diencephalon of sub adult and adult quails was identical to that observed in juvenile quails although the density of PCNA-ir cells appeared to decline with age (Table 2.1).

2.3.1.4 Mesencephalon and optic tectum

In the juvenile mesencephalon, a high density of strongly stained PCNA-ir cells was observed in the oculomotor nucleus (OMN) and red nucleus magnocellular part (RMC) located ventral to the OMN (Figs 2.2 C-D & 2.3 M-O). In addition, a high density of small weakly staining PCNA-ir cells were also observed in the Gct (Fig 2.2 C). Furthermore, a low density of PCNA-ir cells were observed in the lining of the aqueduct mesencephalicus. The distribution of PCNA-ir cells in the mesencephalon of sub adult and adult groups was similar to that of the juvenile groups. However, the density of PCNA-ir cells was lowest in the adult group. In the optic tectum, no PCNA-ir cells were observed at all age-groups (Table 2.1).

2.3.1.5 Cerebellum

In the cerebellum of juvenile quails, a high density of PCNA-ir cells was observed in the Purkinje and granule cell layers of the cerebellum (Figs 2.2 E & 2.3 P-R). In addition to this, fewer PCNA-ir cells were also found in the nucleus cerebellum internum (Cbi) situated on either side of the cerebellar recess of the fourth ventricle (Fig 2.2 F).

A similar pattern of PCNA expression was observed in sub adult quails although the number of PCNA-ir cells decreased with age. In the adult quails, fewer PCNA-ir cells were observed in the cerebellar layers whereas no PCNA-ir cells were observed in the Cbi (Table 2.1).

Figure 2.2: Photomicrographs showing distribution of PCNA-ir cells in the POM (A), thalamic nuclei (B), mesencephalic nuclei (C, D) nuclei, cerebellar cortex (E) and the Cbi (F) of the Japanese quail brain. Inserts in figures C and D represent high magnifications of the Gct and OMN respectively. Scale bars: F= 200 µm and applies to images A-F; inserts in C and D = 20 µm. See list of abbreviations for abbreviations used in this figure.

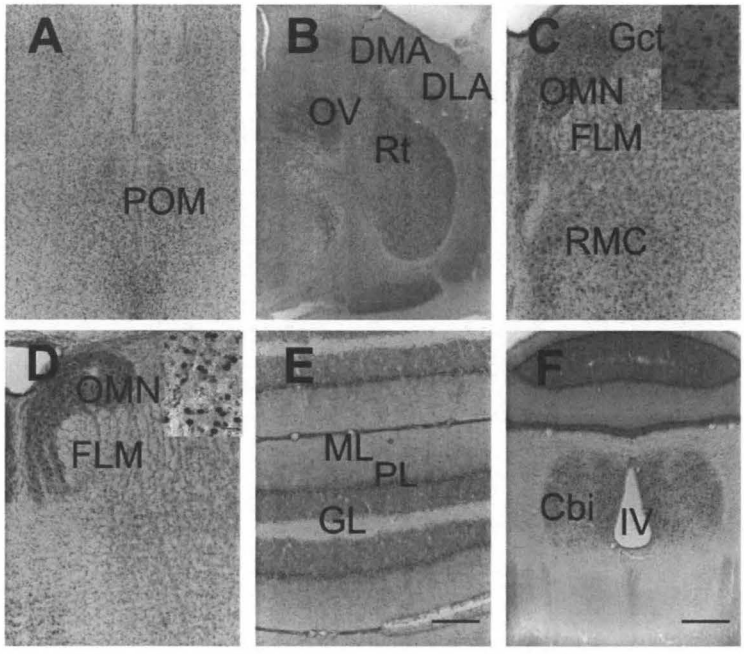
A
POM
B
DMA
DLA
OV
Rt
C
Gct
OMN
FLM
RMC
D
OMN
FLM
E
ML
PL
GL
F
Cbi
IV

Figure 2.3: Photomicrographs showing the distribution of PCNA-ir cells the different parts of the brain of juvenile (A, D, G, J, M and P), sub adult (B, E, H, K, N and Q) and adult (C, F, I, L, O and R) Japanese quails. Ventricular lining of OB (A-C), ventricular lining adjacent to M (D-F), ventricular lining adjacent to Mst (G-I), POM (J-L), OMN (M-O) and CB (P-R). Scale bars: C= 200 µm and applies to A and C; R= 50µm and applies to D-Q. See list of abbreviations for abbreviations used in this figure.

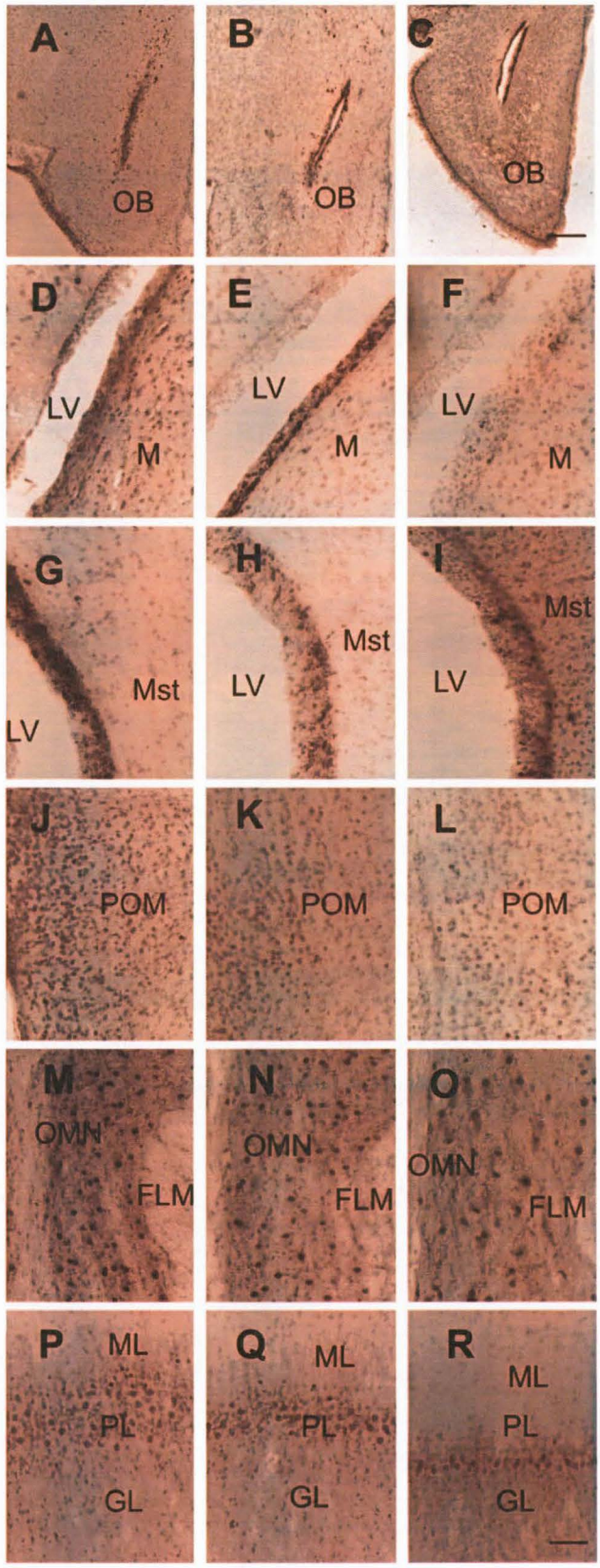
A
OB
B
OB
C
OB
D
LV
M
E
LV
M
F
LV
M
G
Mst
LV
H
Mst
LV
I
Mst
LV
J
POM
K
POM
L
POM
M
OMN
FLM
N
OMN
FLM
O
OMN
FLM
P
ML
PL
GL
Q
ML
PL
GL
R
ML
PL
GL

2.3.2 Age-related changes in DCX expression in the Japanese quail brain

2.3.2.1 General observations

Two main types of DCX-ir cells were observed in the Japanese quail brain. Type 1 cells were round multipolar cells that displayed spherical or triangular shapes with cytoplasm filled with DCX and pale nuclei devoid of DCX staining. Long DCX-ir fibres extending from the cell bodies were also observed (Fig 2.4 A). Type 1 pattern of staining was mostly observed in the pallial (towards the external surface) and striatal parts of the telencephalon. In addition, smaller type 1 cells were observed in the cerebellum.

Type 2 cells were either unipolar or bipolar cells that displayed elongated DCX-ir cell bodies with long fibres originating from one or both ends. Furthermore, the cell bodies of type 2 cells displayed elongated pale staining nuclei (Fig 2.4 B). Type 2 staining pattern was mostly observed in the pallial areas adjacent to the lateral ventricles, striatum, septum, and cerebellar cortex.

Table 2.1: Age-related changes in PCNA immunoreactivity in the Japanese quail brain

			Post-hatching age									
			3weeks	4weeks	5weeks	6weeks	7weeks	8weeks	9weeks	10weeks	11weeks	12weeks
Olfactory Bulb	OBV		+++	+++	+++	++	++	++	++	+	+	+
Telencephalon	LV		+++	+++	+++	+++	+++	+++	++	++	++	++
	Pallium	HA	-	-	-	-	-	-	-	-	-	-
		HD	-	-	-	-	-	-	-	-	-	-
		M	-*	-*	-	-	-	-	-	-	-	-
		N	-	-	-	-	-	-	-	-	-	-
		E	-	-	-	-	-	-	-	-	-	-
		A	-	-	-	-	-	-	-	-	-	-
		HP	-	-	-	-	-	-	-	-	-	-
	Sub pallium	MSt	-**	-**	-	-	-	-	-	-	-	-
		Lst	-	-	-	-	-	-	-	-	-	-
		GP	-	-	-	-	-	-	-	-	-	-
		SL	-	-	-	-	-	-	-	-	-	-
		SM	-	-	-	-	-	-	-	-	-	-
		BSTM	+	+	+	+	+	+	+	-	-	-
		BSTL	+	+	+	+	+	+	+	-	-	-
Diencephalon	Hypothal	POM	++	++	++	+	+	+	+	+	+	+
		PVN	+	+	+	+	+	+	+	+	+	+
		VMN	+	+	+	+	+	+	+	+	+	+
		Tu	+	+	+	+	+	+	+	+	+	+
	Thalamus	Rt	+++	+++	+++	++	++	++	++	+	+	+
		OV	+++	+++	+++	++	++	++	++	+	+	+
		DLA	++	++	++	+	+	+	+	+	+	+
		DMA	++	++	++	+	+	+	+	+	+	+
		GLv	+++	+++	+++	++	++	++	++	+	+	+
Mesencepalon		Gct	+++	+++	+++	++	++	++	++	++	+	+
		OMN	+++	+++	+++	++	++	++	++	++	+	+
		RMC	++	++	++	+	+	+	+	+	+	+
Optic Tectum			-	-	-	-	-	-	-	-	-	-
Cerebellum		Cb	+++	+++	+++	++	++	++	+	+	+	+
		Cbi	+++	+++	+++	++	++	++	+	+	+	+

+++ High density, ++ medium density, + low density, - absent. PCNA-ir cells in the mesopallium (*) and medial striatum (**). See list of abbreviations for abbreviations used in the table.

Figure 2.4: Photomicrographs showing type 1 (A) and type 2 (B) DCX-ir cells in the Japanese quail brain (black arrows). Scale bar: B = 20 µm and also applies to A.

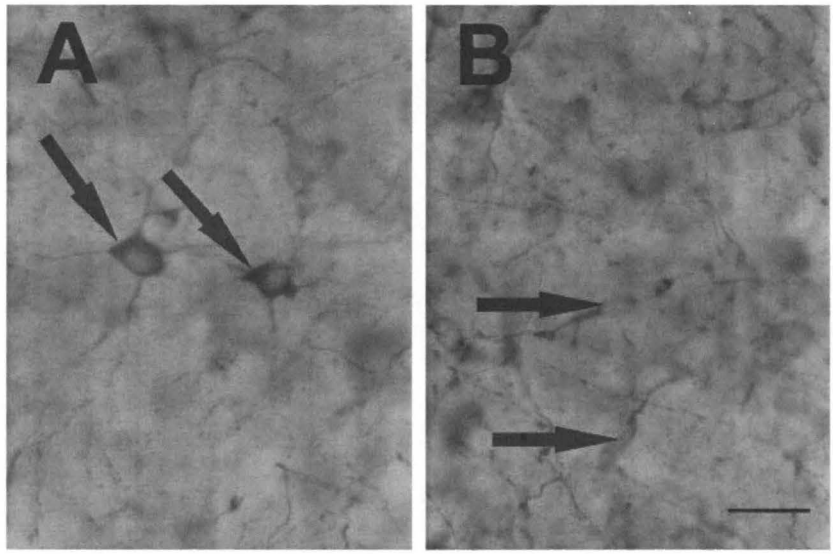
A
B

2.3.2.2 Olfactory bulb

In juvenile quails, the OB was intensely stained with a compact plexus of DCX-ir fibres interspersed with small round or fusiform (types 1 and 2) weakly staining cell bodies in the ependymal and sub ependymal linings of the olfactory ventricles (Figs 2.5 A-B & 2.7A). In addition, a dense network of DCX-ir fibres extended dorsally into the HD (Fig 2.5 C). The pattern of DCX staining in the OB of sub adult and adult animals was identical to that observed in juvenile animals although there was a marked decline in the density of DCX-ir cells and fibres with age (Figs 2.7 A-C). In contrast to juvenile and sub adult quails, no DCX-ir fibres were observed extending into the HD in adult quails.

2.3.2.3 Telencephalon

In juvenile quails, the highest density of DCX-ir cells and fibres were observed in the pallial part (HA, HD, M & N) of the telencephalon although the density of positive cells varied across different pallial areas (Figs 2.5 D-N). Type 1 cells were mostly observed near the external surfaces of the pallium whereas type 2 cells were observed near the lateral ventricles. The HA, HD, M and N were densely populated by types 1 and 2 DCX-ir cells. A much higher density of types 1 and 2 DCX-ir cells was observed on the ventral aspect of the nidopallium caudale (NC). In addition, a high density of DCX-ir fibres was observed in the pallial areas adjacent to the lateral ventricles with highest densities observed in the M and Mst. The hippocampus (HP) had the lowest density of DCX-ir cells in the pallium (Figs 2.5 G and H). However, DCX-ir elements (cells or fibres) were absent in the entopallium (Figs 2.5 D and K) and arcopallium.

In the sub pallium, a high density of types 1 and 2 cells was observed in the Mst (Figs 2.5 D, G and I) and Lst (Figs 5 G, J and K). A low density of type 2 cell bodies was also observed in the Septum (SL & SM) (Figs 2.5 J, I and M) and in the bed nucleus of stria terminalis (BSTM & BSTL) (Figs 2.5 N). However, no DCX-ir cells or fibres were observed in the globus pallidus (Fig 2.5 G).

Throughout the entire telencephalon, the lateral ventricular walls were lined up with a high density of DCX-ir elements. The distribution of DCX-ir cells in the pallium of sub adult and adult quails was similar to that observed in juvenile quails except that there was a reduction in the density of DCX-ir elements with age (Figs 2.7 D-I, Table 2.2). Similarly, the density of DCX-ir elements declined with age in the sub pallium of sub adult and adult quails (Figs 2.7 J-O, Table 2.2). However, no DCX-ir elements were observed in the BSTM and BSTL of adult quails older than 9 weeks (Table 2.2).

Figure 2.5: Photomicrographs showing distribution of DCX-ir cells in the olfactory bulb and telencephalon of the Japanese quail brain. (A) Low power photomicrograph showing distribution of DCX-ir cells in the OB. (B) High power photomicrograph showing distribution of DCX-ir cells along the OB. (C) High power photomicrograph showing DCX-ir cells (black arrows) extending from the OB to the HD. (D) Low power image showing distribution of DCX-ir cells in the rostral telencephalon, E-high power image showing distribution DCX-ir cells in the M. (F) High power image showing distribution DCX-ir cells in the N. (G) Low power image showing distribution of DCX cells in the mid telencephalon. (H) Photomicrograph showing DCX-ir cells in the HP (black arrows). (I) High power image showing DCX-ir cells in the Mst. (J) Low power photomicrograph showing distribution of DCX-ir cells in the caudal telencephalon. (K) High power image showing distribution of DCX-ir cells in the Lst near the lateral striatal-entopallial junction. (L) High power photomicrograph showing the distribution of DCX-ir cells in the SL (black arrow). (M) High power photomicrograph showing the distribution of DCX-ir cells in the SM (black arrow). (N) High power photomicrograph showing the distribution of DCX-ir cells in the BSTL (black arrow). Scale bars: J= 500µm and applies to A, D, G; N =50 µm and applies to B, C, E, F, H, I, K, L, M. See list of abbreviations for abbreviations used in this figure.

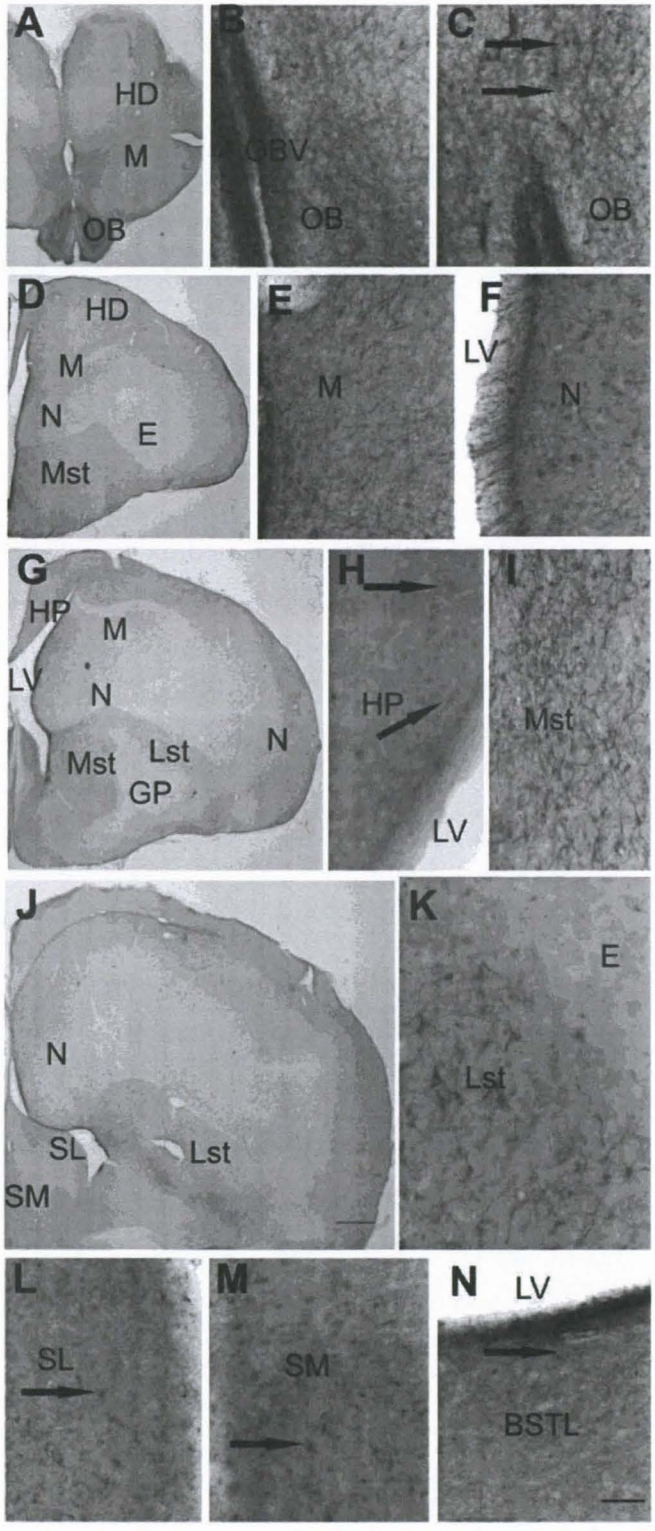
A
HD
M
OB
B
OBV
OB
C
OB
D
HD
M
N
E
Mst
E
M
F
LV
N
G
HP
M
LV
N
Mst
Lst
N
GP
H
HP
LV
I
Mst
J
N
SL
Lst
SM
K
E
Lst
L
SL
M
SM
N
LV
BSTL

2.3.2.4 Diencephalon, mesencephalon and optic tectum

At all ages studied, no type 1 nor type 2 DCX-ir cells were observed in the ventricular or parenchymal areas of the diencephalon, mesencephalon and optic tectum (Figs 2.6 A-C).

2.3.2.5 Cerebellum

A high density of small bipolar DCX-ir cells (Type 2) were observed in the granular and Purkinje layers of the juvenile quail cerebellar cortex (Figs 2.6 D, F and G). In addition, a few type 2 cells with long fibres were also observed in the molecular layer of the cerebellum (Figs 2.6 D and E).

In the sub adult and adult quail cerebellar cortex, the pattern of DCX-ir cells was similar to that observed in juvenile although the densities declined with age (Figs 2.7 P-R, Table 2.2). However, no type 1 or type 2 DCX-ir cells were observed in the Cbi at all ages studied (Fig 2.6 H).

Figure 2.6: Photomicrographs showing Japanese brain sections through the POM, hypothalamus, mesencephalon and cerebellum. DCX-ir cells were absent in the POM (A), hypothalamus (B), mesencephalon (C) and Cbi (H). DCX-ir cells were observed in all the layers (ML, PL and GL) of the cerebellar cortex (D, E, F and G). Scale bars: G= 20 µm and applies to E and F; H = 200 µm and applies to A, B, C and D. See list of abbreviations for abbreviations used in this figure.

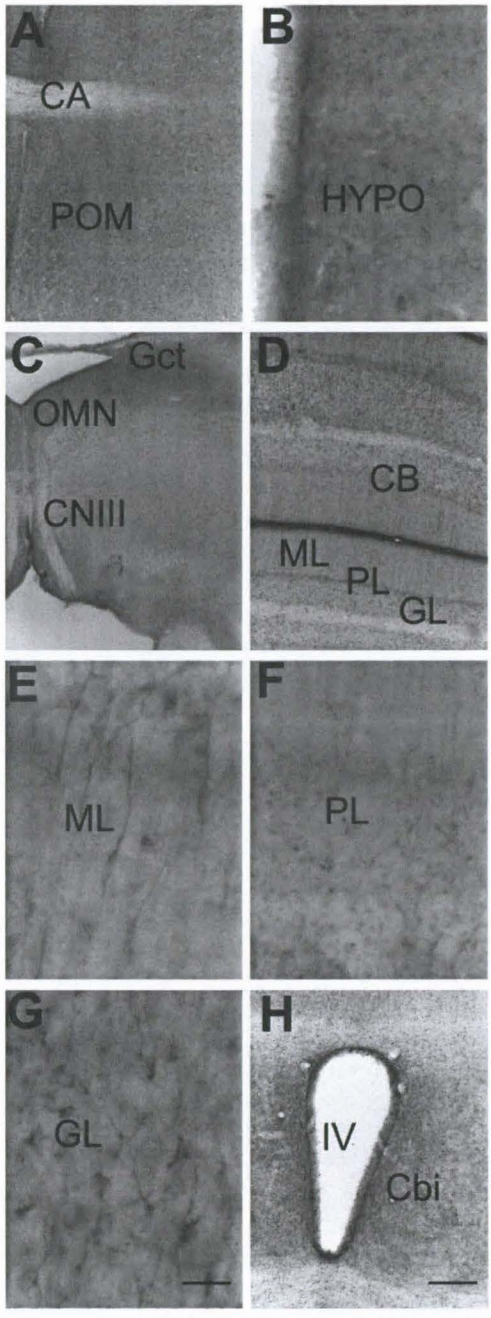
A
CA
POM
B
HYPO
C
Gct
OMN
CNIII
D
CB
ML
PL
GL
E
ML
F
PL
G
GL
H
IV
Cbi

Figure 2.7: Photomicrographs showing the distribution of DCX-ir cells the different parts of the brain of juvenile (A, D, G, J, M and P), sub adult (B, E, H, K, N and Q) and adult (C, F, I, L, O and R) Japanese quails. OB (A-C), M (D-F), N (G-I), Mst (J-L), Lst (M-O) and CB (P-R). Scale bars: C= 200 µm and applies to A and C; R= 50µm and applies to D-Q. See list of abbreviations for abbreviations used in this figure.

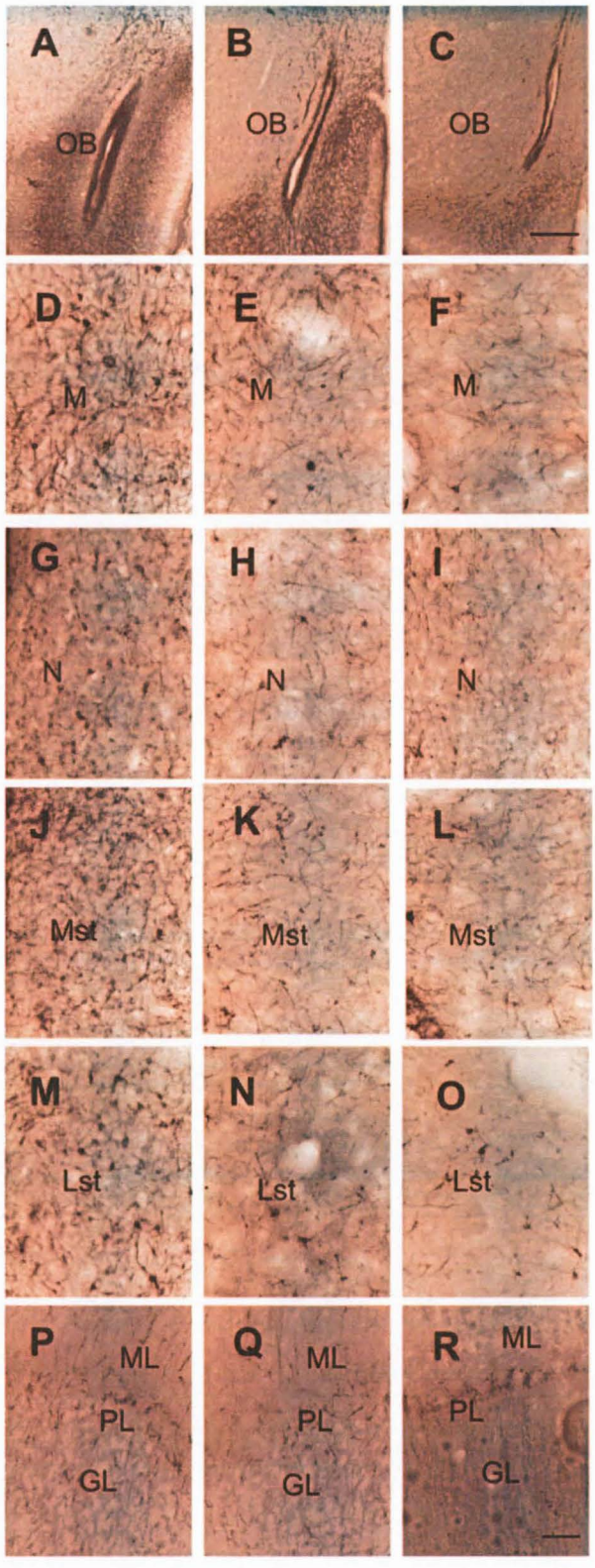
A
OB
B
OB
C
OB
D
M
E
M
F
M
G
N
H
N
I
N
J
Mst
K
Mst
L
Mst
M
Lst
N
Lst
O
Lst
P
ML
PL
GL
Q
ML
PL
GL
R
ML
PL
GL

Table 2.2: Age-related changes in DCX immunoreactivity in the Japanese quail brain

			Post-hatching age									
			3weeks	4weeks	5weeks	6weeks	7weeks	8weeks	9weeks	10weeks	11weeks	12weeks
Olfactory Bulb	OB		+++	+++	+++	+++	++	++	++	+	+	+
Telencephalon	LV		+++	+++	+++	+++	+++	+++	++	++	+	+
	Pallium	HA	+++	+++	+++	++	++	++	+	+	+	+
		HD	+++	+++	+++	+++	+++	+++	++	++	++	++
		M	+++	+++	+++	+++	+++	+++	++	++	++	++
		N	+++	+++	+++	+++	+++	+++	++	++	++	++
		E	-	-	-	-	-	-	-	-	-	-
		A	-	-	-	-	-	-	-	-	-	-
		HP	++	++	+	+	+	+	+	+	+	+
	Sub pallium	MSt	+++	+++	+++	+++	+++	+++	++	++	+	+
		Lst	+++	+++	+++	++	++	++	+	+	+	+
		GP	-	-	-	-	-	-	-	-	-	-
		SL	++	++	++	+	+	+	+	+	+	+
		SM	+	+	+	+	+	+	+	+	+	+
		BSTM	+	+	+	+	+	+	+	-	-	-
		BSTL	+	+	+	+	+	+	+	-	-	-
Diencephalon	Hypothal	POM	-	-	-	-	-	-	-	-	-	-
		PVN	-	-	-	-	-	-	-	-	-	-
		VMN	-	-	-	-	-	-	-	-	-	-
		Tu	-	-	-	-	-	-	-	-	-	-
	Thalamus	Rt	-	-	-	-	-	-	-	-	-	-
		OV	-	-	-	-	-	-	-	-	-	-
		DLA	-	-	-	-	-	-	-	-	-	-
		DMA	-	-	-	-	-	-	-	-	-	-
		GLv	-	-	-	-	-	-	-	-	-	-
Mesencepalon		Gct	-	-	-	-	-	-	-	-	-	-
		OMN	-	-	-	-	-	-	-	-	-	-
		RMC	-	-	-	-	-	-	-	-	-	-
Optic tectum			-	-	-	-	-	-	-	-	-	-
Cerebellum		Cb	+++	+++	+++	++	++	++	+	+	+	+
		Cbi	-	-	-	-	-	-	-	-	-	-

+++ High density, ++ medium density, + low density of DCX-ir type 1 and 2 cells only. See list of abbreviations for abbreviations used in the table.

2.4 DISCUSSION

Our study used PCNA and DCX to investigate cell proliferation and neuronal incorporation in the Japanese quail brain and to determine how these processes change with post-hatching age.

2.4.1 Methodological considerations

2.4.1.1 Proliferating cell nuclear antigen

Proliferating cell nuclear antigen, also known as cyclin, is a protein associated with catalytic activity of DNA polymerase A and is critical to the extension of the DNA strand during replication (Balthazart and Ball, 2014b). PCNA is therefore expressed during the G1 and S phases of the cell cycle and not in G0 or resting phase. In addition, PCNA expression is highly conserved among eukaryotes (Charvet and Striedter, 2008) and has been employed in the current study as a marker of cell proliferation in the Japanese quail brain. PCNA immunolabelling was used previously in the avian brain to compare cell proliferation during ontogeny in birds that possess large (Parakeets) vs small (Bobwhite quails) brains in adulthood (Charvet and Striedter, 2008). Additionally, Bardet et al. (2012) and Mouriec and Balthazart (2013) also used PCNA to demonstrate age dependent changes in cell proliferation in the POM of Japanese quail brains. In the quail specifically, the pattern of PCNA staining was reported to coincide with BrdU labelling observed after injections with short survival times (Striedter and Charvet, 2008; Bardet et al., 2012) and therefore justifies its use as a marker of cell proliferation in the current study.

2.4.1.2 Doublecortin

DCX is a microtubule-associated protein that binds to microtubules, increasing their bundling and stabilization (Horesh et al., 1999). DCX controls the polymerization of the leading process and stabilization of the cytoskeleton during neuronal migration (Balthazart and Ball, 2014a, 2014b) thus playing a critical role in the positioning of new born neurons. However, mammalian studies have also shown that DCX is not

only a marker of neurogenesis but also relates to the extensive neuronal plasticity present in the adult brain (Nacher et al., 2001; Brown et al., 2003; Klempin et al., 2011; Kremer et al., 2013). Given the role of DCX in microtubule reorganization, DCX also supports the reorganization of the dendritic arbour, neurite outgrowth and synaptogenesis in plastic neurons.

The DCX antibody has been validated for both mammals and birds and it has been established that it is specific to the DCX protein (Balthazart et al., 2008; Balthazart and Ball, 2014b). In galliformes, DCX has been identified in the developing or post hatching brain of the chicken (Capes-Davis et al., 2005; Mezey et al., 2012) and Japanese quail (Balthazart et al., 2010). In this study, DCX immunolabelling was also used to investigate neuronal incorporation in the Japanese quail brain.

Two main types of DCX –ir elements were observed in this study. Type 1 cells were observed mostly near the external surfaces of the brain are presumably differentiating neurons that have reached their destination following migration since DCX expression begins in late mitotic neuronal precursors and extends in early post mitotic neurons (Brown et al., 2003; Balthazart et al., 2008). Type 2 cells were mostly observed in the telencephalic areas adjacent to the lateral ventricles and resemble migrating neurons with leading and trailing processes that will presumably transform into multipolar morphology on reaching their target area (Boseret et al., 2007; Mezey et al., 2012).

2.4.2 Ontogenetic considerations

Japanese quails are precocial birds and therefore require minimal parental care after hatching. For precocial birds it is vital to have a highly developed brain by the time of hatching especially sub telencephalic areas that are important for homeostatic processes and simple behavioural tasks (Mezey et al., 2012). Neurogenesis in the quail brain is therefore supposed to be complete before hatching (Tsai et al., 1981). In galliformes such as quails and chicks, neurogenesis starts at about 16-30% of hatching time and is presumed to be complete for the medulla by 30%, the tectum by 50% and the telencephalon by 50% of hatching time (Mezey et al., 2012). However,

Bardet et al. (2012) reported that neurons in most brain areas in the quail except for the telencephalon and the cerebellum are born and become post-mitotic before embryonic day 6 (E6). Even if neurogenesis persists throughout life in the telencephalon of adult birds, the bulk of neurons in this part of the brain are produced before E6 in quails (Bardet et al., 2012) and E7-E9 in chicks (Tsai et al., 1981). Our results reveal that the post hatch development of higher order brain areas such as the telencephalon and cerebellum is protracted in precocial birds in a similar way as observed in other birds and mammals.

2.4.3 Age - related changes in PCNA and DCX expression in different brain regions

2.4.3.1 Olfactory bulb

PCNA-ir and DCX-ir elements were observed in the olfactory bulb of juvenile, sub adult and adult quails. Our findings suggest that the lining of the olfactory ventricle is the birth site of neurons that are incorporated in the olfactory bulb. This is in contrast with the situation in mammals where neurons are born in the lateral ventricular zones and migrate through the rostral migratory stream to reach the olfactory bulb (Maheu et al., 2015). A qualitative analysis of the results revealed an age dependent decline in PCNA-ir and DCX-ir cells in the olfactory bulb especially in the sub adult and adult groups. A similar age dependent decline in DCX expression was also reported by Mezey et al. (2012) in chicks and Meskenaite et al. (2016) in pigeons. DCX-ir cells and fibres running between the OB and the HD have been previously observed in the adult chick (Mezey et al., 2012) and in the pigeon (Melleu et al., 2013). These fibres may represent an extensive network of newly generated neurons being continuously exchanged along the rostrocaudal extension of the olfactory pathways (Melleu et al., 2013). The presence of neuronal production and incorporation in the olfactory bulb of the quail is not surprising as this bird has been reported to have a keen sense of smell and is known to be able to detect the presence of certain pesticides, as well as avoid food containing a toxic chemical called lectin, using only the sense of smell (Mills et al., 1997).

2.4.3.2 Telencephalon

In the pallium, the majority of PCNA-ir cells observed throughout the rostrocaudal extent of the lateral ventricles appeared to decline with post-hatching age. PCNA-ir cells were mostly abundant ventrally and dorsally in the ventricular zones adjacent to the medial striatum and mesopallium respectively corresponding to the proliferative "hotspots" described by Alvarez-Buylla et al. (1990). In juvenile quails, very few PCNA-ir cells were also observed in the mesopallium and caudal part of the nidopallium adjacent to the lateral ventricles. Similarly, Bardet et al. (2012) reported presence of a few PCNA and BrdU labeled cells in the quail pallium and concluded that these could be slow cycling progenitors. Alternatively, the presence of PCNA-ir cells in the parenchyma may not be related to cell proliferation but to DNA repair in mature neurons as proposed by Essers et al. (2005). Apart from those few cells in the pallial parenchyma of juvenile quails, cell proliferation in the sub adult and adult Japanese quails appears to be restricted to the lateral ventricular zones.

DCX-ir cells were observed throughout the pallium except for the entopallium and the arcopallium. DCX expression in the pallium suggests that the Japanese quail, like other birds, continues to recruit neurons into the pallium throughout life although at a slower rate in adult as compared to juvenile and sub adult quails. The very low density of DCX-ir cells in the quail hippocampus throughout juvenile, sub adult and adult stages is not surprising given that spatial memory is not a major factor in the life of quails as it is in food storing birds (Mezey et al., 2012) or homing pigeons (Meskenaite et al., 2016).

In the sub pallium, PCNA-ir cells declined with post hatching age eventually disappearing in the medial striatum and in the bed nucleus of stria terminalis (BSTM and BSTL) in adult quails older than 9 and 10 weeks respectively. DCX expression ceased in the BSTL and BSTM at 11 weeks suggesting that these brain structures reach full maturation at 10 weeks after which no new neurons are incorporated. However, the striatum continues to express DCX throughout the juvenile, sub adult and adult ages. The observation that DCX is expressed in the septum and the striatum, areas where PCNA is not expressed, implies that there could be another

source for neurons that are added to these brain areas, presumably the adjacent lateral ventricles. Furthermore, our findings suggest that the septum continues to recruit neurons throughout the ages studied. This is contrary to the findings by Nikolakopoulou et al. (2006b) who reported an early maturation of the SL in the quail at post hatching day 20 (P20) using BrdU staining. They reported that about 50 % of BrdU-ir cells in the SL were of unknown phenotype as they neither co-expressed with neuronal nor glial markers. Since the SL is a steroid sensitive brain area, this population of BrdU-ir cells could be slow cyclin progenitors that are quiescent at P20 but may be reactivated at puberty when the level of circulating steroids increases as observed by Mouriec and Balthazart (2013).

2.4.3.3 Diencephalon

Given the fact that no type 1 or type 2 DCX-ir cells were observed in the diencephalon, the PCNA immunoreactivity observed in this region is presumably related to glial cell production. Additionally, Balthazart et al. (2010) also reported lack of DCX immunoreactivity in the adult quail POM. In support of our observation, Bardet et al. (2012) reported that neuronal production in this region of the quail brain is complete by embryonic day 6 and that further cell proliferation after this date is related to production of glial cells. However, attempts to test this hypothesis through double labelling experiments in birds is technically challenging because many antibodies available to identify glial cells in mammals either do not label any cell in birds or only label sub populations of glial cells in specific brain regions (Bardet et al., 2012).

2.4.3.4 Mesencephalon and Optic Tectum

As was the case with the diencephalon, no type 1 or type 2 DCX-ir cells were observed in these two regions of the quail brain. As a result, it can be concluded that the intense PCNA immunoreactivity observed in the oculomotor nucleus, griseum centrale and the red nucleus of the mesencephalon may not be related to neurogenesis but possibly related to glial cell production. No PCNA-ir or DCX-ir cells

were observed in the optic tectum of all the quails suggesting that this structure reaches full maturity before hatching.

2.4.3.5 Cerebellum

Our findings suggest that neuronal birth and incorporation continue to take place in the cerebellum of juvenile, sub adult and adult quails just like other birds species (Stamatakis et al., 2004; Bardet et al., 2012). The PCNA immunoreactivity observed in the Cbi of juvenile and sub adult quails may be related to glial cell production since no type 1 or type 2 DCX-ir cells were observed in that nucleus.

2.5 CONCLUSION

Post-hatch neuronal production appears to be restricted to olfactory and telencephalic ventricles whereas neuronal incorporation is restricted to telencephalon and cerebellum. In addition, both processes continue into adulthood and appear to decline with post hatching age beginning from the 6th week. Furthermore, sub telencephalic regions such as the diencephalon, mesencephalon and optic tectum appear to reach full maturity prior to hatching and post-hatching proliferation observed in these regions is most likely related to glial cell production.

CHAPTER 3: QUANTITATIVE ANALYSIS OF AGE-RELATED CHANGES IN DOUBLECORTIN (DCX) EXPRESSION IN THE MALE JAPANESE QUAIL (*CORTUNIX JAPONICA*) TELENCEPHALON.

3.1 INTRODUCTION

Most neurons in the vertebrate central nervous system are born before or shortly after birth. However, addition of new neurons to the brain continues into adulthood in both precocial and altricial vertebrates. The process through which new neurons are added to the brain is termed neurogenesis. In adult mammals, production of new neurons is restricted to the sub ventricular zone (SVZ) of the lateral ventricles and the sub granular zone (SGZ) of the hippocampus. Newly formed neurons in the SVZ and SGZ are incorporated into the olfactory bulbs and the granule cell layer of the hippocampal dentate gyrus respectively (Chawana et al., 2013; Olaleye and Ihunwo, 2014; Olude et al., 2014).

On the other hand, neurogenesis in the avian brain is more widespread than that observed in mammals. In adult birds, new neurons are born in the lining of the lateral ventricles and migrate radially to different parts of the brain parenchyma guided by radial cell processes where they integrate into existing neuronal circuits (Alvarez-Buylla and Nottebohm, 1988). To date, adult neurogenesis has been found in birds belonging to widely unrelated avian orders including canaries (Alvarez-Buylla and Kirn, 1997; Boseret et al., 2007; Nottebohm, 2011; Vellema et al., 2014; Balthazart and Ball, 2016), zebra finches (Kim et al., 2006; Barkan et al., 2007; Cattan et al., 2015), song sparrows (LaDage et al., 2011; Wada et al., 2014), black capped chickadees (Barnea and Nottebohm, 1994; Hoshooley and Sherry, 2004; Aitken, 2015; Guitar, 2016), reed warblers (Barkan et al., 2016), cowbirds (Guigueno et al., 2016), starlings (Absil et al., 2003; Hall et al., 2014), ring doves (Ling and Cheng, 1995; Ling et al., 1997; Zuo, 1998; Chen et al., 2006; Chen and Cheng, 2007), turtle doves (Barkan et al., 2016), pigeons (Melleu et al., 2013; Melleu et al., 2016; Meskenaite et al., 2016; Mazengenya et al., 2017), parrots (Mazengenya et al., 2018), chicken (Capes-Davis et al., 2005; Nikolakopoulou et al., 2006a; Mezey et al., 2012) and quails (Nikolakopoulou et al., 2006b; Balthazart et al., 2010; Bardet et al., 2012; Mouriec and Balthazart, 2013; Nkomozepi et al., 2018).

However, the majority of neurogenesis studies in Japanese quails focused on sex steroid sensitive areas of the brain like the preoptic area (Balthazart et al., 2010; Bardet et al., 2012; Mouriec and Balthazart, 2013) and lateral septal nucleus (SL) (Nikolakopoulou et al., 2006b) in relation to sexual behavior. Neurogenesis in the

Japanese quail telencephalon has largely been ignored, despite its critical involvement in learning and memory tasks such as imitation, filial imprinting, discriminative taste aversion learning and passive avoidance learning. Indeed, significant increases in synaptic density and plasticity have been observed in the hippocampus (HP), intermediate medial mesopallium (IMM) and medial striatum (MSt) following passive avoidance learning tasks in the domestic chick, a species closely related to the Japanese quail (Ünal et al., 2002). In addition, Dermon et al. (2002) and Nikolakopoulou et al. (2006a) also reported changes in neurogenesis in the chick HP, IMM and MSt following passive avoidance training. Furthermore, passive avoidance learning has also been shown to increase expression of immediate early genes c-fos and c-jun in the IMM and MSt (Freeman and Rose, 1999). Similarly, filial imprinting in the chick has been shown to increase c-fos and c-jun expression in the hyperpallium apicale (HA), the dorsal HP and the IMM (McCabe and Horn, 1994). Moreover, lesion of the chick hyperpallium densocellure (HD) with ibotenic acid resulted in impaired visual imprinting (Nakamori et al., 2013).

Given the importance of the galliform telencephalon in learning and memory tasks, this study was aimed at identifying neurogenic areas in the Japanese quail telencephalon and to quantitatively determine how neurogenesis in these areas changes with post-hatching age spanning different life-history stages. This study was a continuation from our previous study described in Chapter 2 above which qualitatively established that neurogenesis decreases with post-hatching age in the Japanese quail brain (Nkomozepi et al., 2018). To achieve the aim of the current study, doublecortin (DCX) was used in this study as a marker for neurogenesis in Japanese quail telencephalon. DCX is a microtubule-associated protein that is expressed in migrating neuroblasts (Balthazart and Ball, 2014b). In the avian brain, DCX was reported to co-express with more than 70% of new BrdU positive migrating neuroblasts confirming that it is an accurate proxy for neurogenesis (Boseret et al., 2007; Balthazart et al., 2008). Additionally, DCX expression has been reported in the telencephalon of the zebra finch (Kim et al., 2006); canary (Boseret et al., 2007; Balthazart et al., 2008), pigeon (Meskenaite et al., 2016; Mazengenya et al., 2017), chicken (Capes-Davis et al., 2005; Mezey et al., 2012) and quail (Nkomozepi et al., 2018) brains.

Previous studies in the ring dove (Ling et al., 1997), zebra finch (DeWulf and Bottjer, 2002; Kim et al., 2006) and pigeon (Meskenaite et al., 2016) have shown that neurogenesis declines with age.

3.2 MATERIAL AND METHODS

3.2.1 Experimental animals

The study was carried out using thirty male Japanese quails age ranging 3-12 weeks obtained from the Agricultural research centre (Irene, South Africa). All protocols were approved by the University of the Witwatersrand Animal Ethics Screening Committee (AESC/2012/53/01) and animals were treated according to the guidelines which correspond with those of the NIH for care and use of animals in scientific experimentation. The birds were maintained on a photoperiod stimulating long summer days (16L: 8D) with access to food and water *ad libitum.* During the first 3 weeks after hatching, chicks were kept in mixed groups in brooder cages at a temperature of 30°C. Temperature was then progressively reduced to room temperature by the 5th week. From post hatching age 3 weeks, 3 birds were sacrificed and brains collected every week up until the 12th week.

3.2.2 Tissue collection and processing

All birds were given a dose of heparin (1-10 ml, i.m depending on animal size) 5 min prior to overdose to prevent blood clotting and then euthanized with an intraperitoneal injection of Euthapent (0.5 – 1 ml/kg). Animals were then perfusion-fixed transcardially, initially with 0.9% cold saline solution, followed by 4% paraformaldehyde in 0.1 M phosphate buffer (pH 7.4) solution. Following perfusion, Brains were carefully removed from the skull, post-fixed overnight in 4% paraformaldehyde in 0.1M PB (pH 7.4), weighed before being transferred into 30% sucrose in 0.1M phosphate buffer (PB) until equilibration. The brains were coronally sectioned at 50 µm using a cryostat at -24℃ and repeated series of 5 sections were collected free-floating into 24 multi-well plates containing 0.1 M PB (pH 7.4). One series of sections was mounted on gelatin-coated slides before staining with 1 % cresyl violet for anatomical orientation and

another one was used for DCX immunohistochemistry. The rest were stored in a cryoprotectant solution at -20℃ for future use.

3.2.3 Immunohistochemistry for doublecortin

Brain sections were pre-treated for 30 min at room temperature under gentle shaking with an endogenous peroxidase inhibitor solution [0.1 M PB, 100% methanol, 30% H_2O_2 in the ratio 49.2: 49.2 1.66]. Following three 10-min rinses in 0.1 M PB, the sections were subsequently pre-incubated in a blocking buffer solution [3% normal rabbit serum, 2% bovine serum albumin, 0.25% Triton X-100 in 0.1 M PB] for 2 h under gentle shaking at room temperature to prevent non-specific binding. Sections were then transferred into a primary antibody solution [1: 300, goat anti-DCX (Santa Cruz), in the blocking buffer solution] and were incubated for 48 h at 4 ° C under gentle shaking. Following incubation, sections were subjected to three 10-min rinses in 0.1 M PB before being incubated in secondary antibody solution [1: 1,000 dilution of biotinylated anti-goat IgG (BA-5000; Vector Laboratories, Burlingame, Calif., USA) in 3% 3% normal rabbit serum and 2% bovine serum albumin in 0.1 M PB] for 2 h at room temperature under gentle shaking. Following three 10-min rinses in 0.1 M PB, the sections were incubated in an avidin-biotin solution [1: 125 A reactive and 1: 125 B reactive (Vector Laboratories) in 0.1 M PB] for 1 h.

The sections were then transferred into three 10-min 0.1 M PB rinses before being placed in a solution containing 0.05% 3, 3' di-amino-benzidine tetrachloride (DAB) in 0.1 M PB for 5 min. To each 1 ml of this solution, 3.3 µl of 30% H_2O_2 were added, and chromatic precipitation was visually monitored under a low power stereomicroscope.

Development was subsequently stopped by placing the sections in 0.1 M PB, followed by a final 10-min rinse in 0.1 M PB. Sections were mounted on 0.5% gelatinised slides, left to dry overnight, dehydrated in a graded series of alcohols, cleared in xylene and cover slipped with DPX. To ensure that non-specific staining was not affecting the results, control sections taken at random were processed in the

same manner, but either the primary or the secondary antibody was omitted. No labelled cells were observed in either case.

3.2.4 DCX quantification

All sections were first qualitatively surveyed using a microscope to identify brain areas expressing DCX. The numbers of bipolar and multipolar DCX-ir cells were then quantified separately in eight selected brain areas expressing DCX throughout the ages studied. The quantification of DCX-ir cells was done using computer assisted image analysis by the first author who was blind to the ages of the animals. Sections were digitized using a Leica 1C550 video camera linked to a Leica DM500 microscope (x40 objective) and DCX-ir cells in each camera field (0.3298mm (*h*) x 0.2473 (*l*) mm or 0.0816 mm^2) were counted using the cell counter function of ImageJ (Schneider et al., 2012). Only DCX-ir cells containing a clear unstained nucleus surrounded by stained cytoplasm were counted. The camera field for quantification was placed in a standardized manner based on predefined anatomical landmarks (ventricles or prominent fibre tracts) (Balthazart et al., 2008; Yamamura et al., 2011; Bardet et al., 2012).

Composite images were prepared with the Adobe Photoshop 7.0 software (Adobe Systems, Mountain View, CA). No pixelation adjustments or manipulations of the captured images were undertaken, except for the adjustment of contrast and brightness. Brain structures were identified based on the atlas of the chicken brain (Kuenzel and Masson, 1988; Puelles, 2007) and we used the nomenclature adopted by the avian brain forum (Reiner et al., 2004).

The following brain areas were quantified:

Hyperpallium densocellulare (HD)

Quantification was done in one field at two rostrocaudal levels. The rostral level was in a section corresponding to plate A11.2 of the chicken brain atlas (Kuenzel and Masson, 1988) and the caudal level was in a section 250µm caudal to the rostral one. The quantification field was placed one camera length from the external surface

of the brain midway between the lamina frontalis superior (LFS) and lamina frontalis suprema (LFM) (Fig 3.1 A).

Intermediate medial mesopallium (IMM)

DCX-ir cells were quantified in the IMM at two rostrocaudal levels. The rostral level was in the same section as that used for the HD whereas the caudal level was situated 250μm caudal to the rostal one. At each rostrocaudal level, two quantification fields were used. The first quantification field was situated ventral to the lamina mesopallialis (LaM) and lateral to the lateral ventricle. The second quantification field was placed one camera length along the LaM from the first quantification field (Fig 3.1 A).

Hippocampus (HP)

DCX-ir cells were quantified in the hippocampus at two rostrocaudal levels. The rostral level was in a section corresponding to plate A8.2 of the chicken brain atlas (Kuenzel and Masson, 1988) whereas the caudal level was in a section situated 250 μm caudal to the rostral one. At each level, two quantification fields were used. The first one was placed between the interhemispheric line and the lateral ventricle. The second field was placed immediately adjacent and positioned one height dorsally and one length laterally (Fig 3.1 B).

Nidopallium (N)

In the nidopallium, DCX-ir cells were quantified in two fields at three rostrocaudal levels. Rostral, intermediate and caudal levels were situated in sections corresponding to plates A11.2, A8.2 and A7.6 of Kuenzel and Masson (1988) respectively. At each rostrocaudal level, the first quantification field was placed one camera length from the lateral edge of the lateral ventricle midway between the LaM and LPS (Lamina pallio-subpallialis). The second quantification field was placed at a point one camera length medial to the external surface of the brain and one camera height ventral to the LaM (Figs 3.1 A, B and C).

Medial striatum (MSt)

DCX-ir cells were quantified in two adjacent fields at two rostrocaudal levels in the MSt. The rostral level corresponded to plate A8.2 of the chicken brain atlas of Kuenzel and Masson (1988) whereas the caudal level was situated 250µm caudal to the rostral one. At each level the first quantification field was placed lateral to the edge of the lateral ventricle and ventral to the LPS. The second quantification field was placed at a point that was one camera height ventral to LPS and one camera length lateral to the edge of the lateral ventricle (Fig 3.1 B).

Lateral striatum (LSt)

In the LSt DCX-ir cells were quantified in one camera field at two rostrocaudal levels in the same sections as for the MSt. At both levels, the quantification field was placed in a region just ventral to the LPS and medial to the entopallial-lateral striatal junction (Fig 3.1 B).

Lateral septum (SL)

DCX-ir cells in this structure were quantified in one field at two rostrocaudal levels that were 250µm apart. The rostral level was situated in a section corresponding to plate A8.2 of Kuenzel and Masson (1988). At both levels, the quantification field was precisely placed to cover the entire bulge of the lateral septal nucleus into the lateral ventricle (Fig 3.1 B).

Medial septum (SM)

DCX-ir cells were quantified in one field at two rostrocaudal levels in the same sections as the LSt. At each level, the camera field was initially placed between the lateral ventricle and the interhemispheric line. The field was then moved two camera lengths ventrally along the interhemispheric line to reach the quantification field (Fig 3.1 B).

3.2.5 Data Analysis

Where multiple quantification fields were used at the same or different rostrocaudal levels of the same brain area, DCX- ir cell counts were averaged. The Shapiro-Wilks normality test was used to test the normality of data in all the variables. For all the variables, the data followed a normal distribution ($P>0.05$). To determine the relationship between age and the number of DCX- ir cells in each brain area quantified, counts of round multipolar and fusiform bipolar cells were pooled. Pearson's correlation test was used to test the correlation between the DCX- ir counts for each brain area and age.

To determine how DCX-ir counts differed in each brain area with life-history stage, birds were divided into juvenile (sexually immature, 3-5 weeks old, n=9), sub adult (sexually mature, 6-8 weeks old, n=9) and adult (sexually active, 9-12 weeks, n= 12) groups based on their sexual maturity. Group means were computed and compared separately for bipolar and multipolar DCX-ir cells using one-way analysis of variance (ANOVA) followed by Bonferroni *post hoc* test. All analyses were performed using Prism 5 software (Graphpad software, CA). All results were expressed as means ± standard deviation and a significance level of $P<0.05$ was used.

Figure 3.1: Photomicrographs of doublecortin stained coronal sections of the Japanese quail brain showing areas where DCX expression was quantified (dark rectangular boxes). Sections corresponding to plate A 11.2 (A); A 8.2 (B) and A 7.6 (C) of Kuenzel and Masson (1988). Scale bar =300 µm and applies to all images. See list of abbreviations for abbreviations used in this figure.

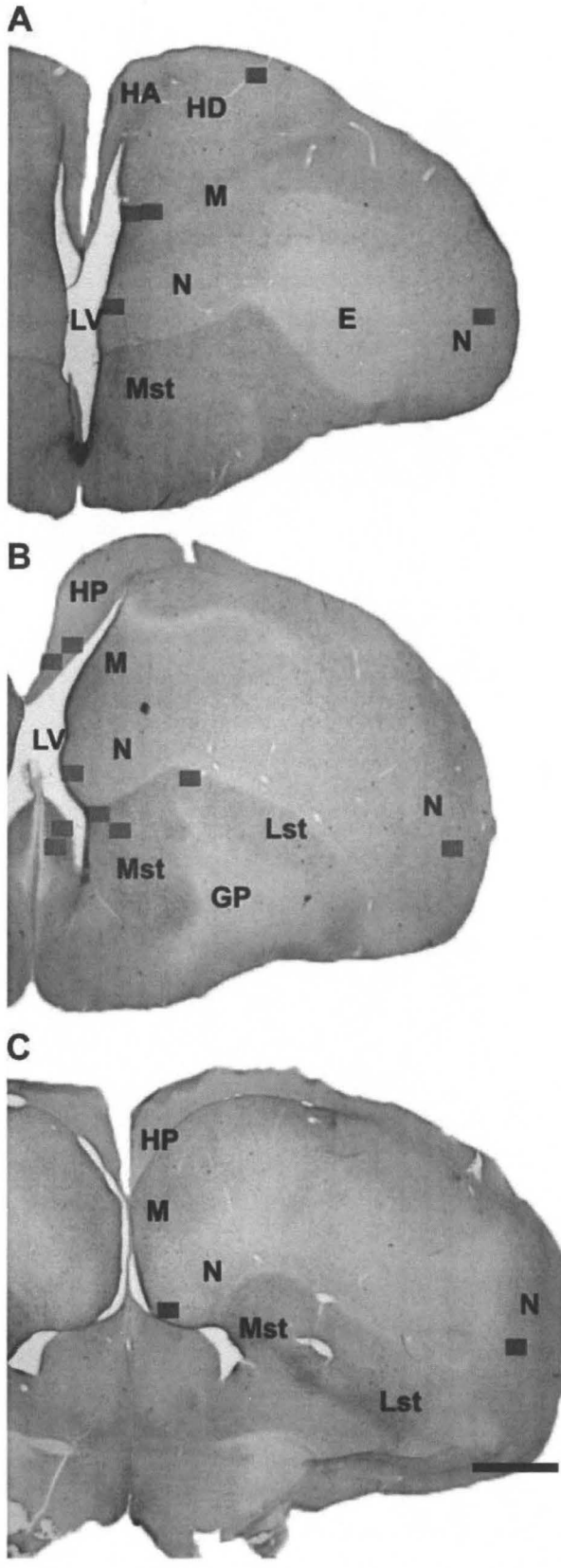
A
HA
HD
M
N
LV
E
N
Mst
B
HP
M
LV
N
N
Lst
Mst
GP
C
HP
M
N
N
Mst
Lst

3.3 RESULTS

3.3.1 Distribution of DCX in the Japanese quail telencephalon

The pattern of DCX immunoreactivity in the Japanese quail telencephalon was consistent across all the ages studied although the densities of labelled cells varied. Thus the following description applies to all ages studied. Two main types of DCX-ir cells were observed: elongated bipolar cells with long processes and round multipolar cells (Figs 3.2 A and B). DCX-ir cells were observed throughout the telencephalon except for the entopallium (E), arcopallium (A) and globus pallidus (GP). In the pallium, a high density DCX-ir cells and fibres was observed in the lateral ventricular zones, HA (Figs 3.2 C), HD (Fig 3.2 C), M (Figs 3.2 C to D & 3.3 A) and N (Figs 3.2 D & 3.3 B to D) at all the ages studied. In addition, a lower density of DCX-ir elements were observed in the HP (Fig 3.3 A). In the sub pallium, a high density of DCX-ir cells and fibres were observed in the MSt (Figs 3.3 B & D) and LSt (Fig 3.3 C). The SM (Fig 3.3 D) and SL (Figs 3.3 B &D) were also populated by a low density of DCX-ir cells. Generally, high densities of bipolar DCX-ir cells were concentrated in telencephalic areas closest to the lateral ventricular zones compared to the areas further from the ventricles. Conversely, a high density of multipolar DCX-ir cells was observed near the external surfaces of the telencephalon compared to periventricular regions.

Figure 3.2: Photomicrographs showing DCX expression in the Japanese quail telencephalon. (A) Arrows showing round multipolar DCX ir cells; (B) Arrows showing fusiform round multipolar DCX-ir cells; (C) Low power image showing DCX expression in the hyperpallium apicale (HA), hyperpallium densocellulare (HD) and mesopallium (M); (D) low power image showing DCX expression in the mesopallium ventrale (MV), mesopallium dorsale (MD) and nidopallium (N). Scale bar in B = 20 μm and applies to A, in D = 100 μm and applies to C.

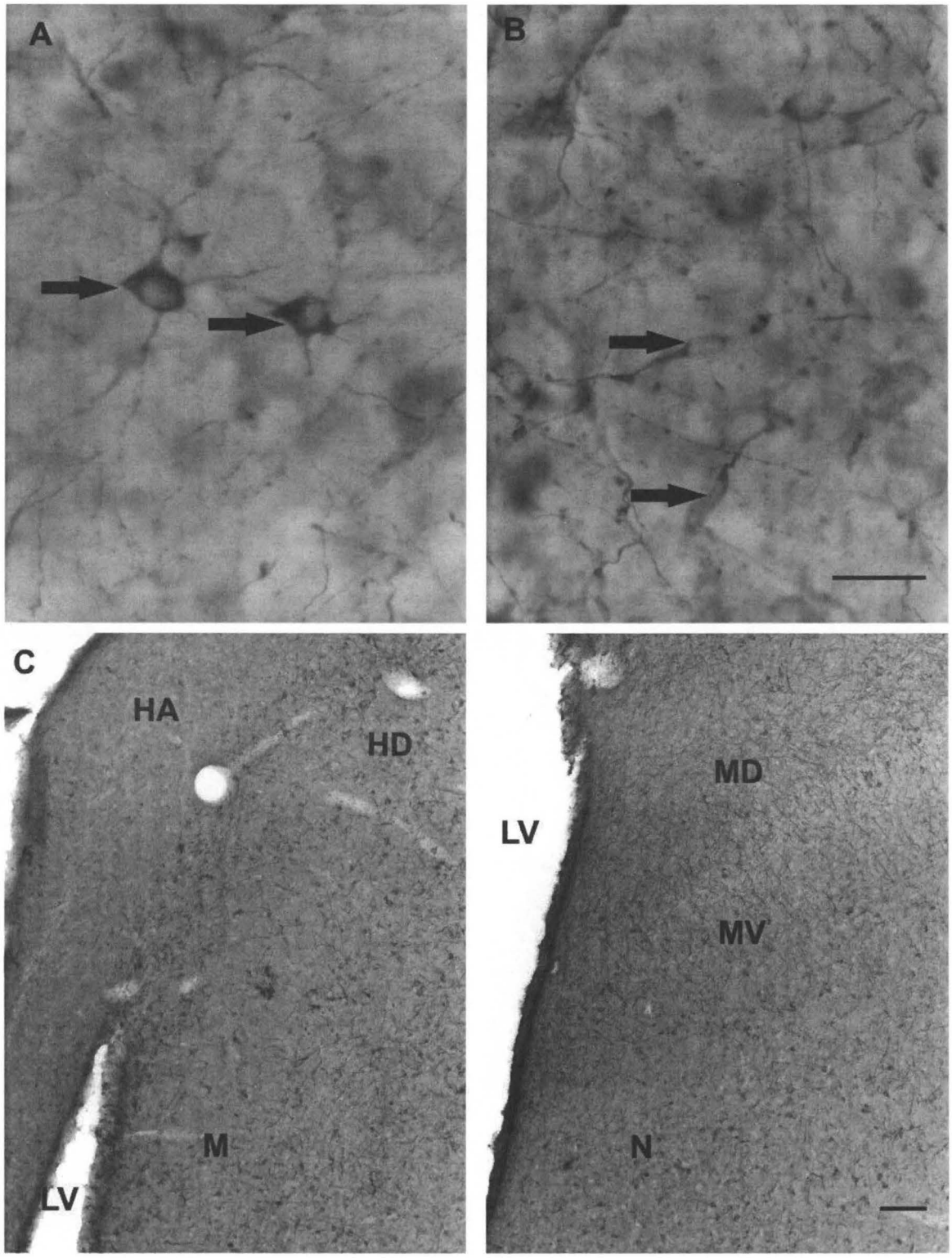
A
B
C
HA
HD
M
LV
LV
MD
MV
N

Figure 3.3: Photomicrographs showing DCX expression in the Japanese quail telencephalon. (A) low power image showing DCX expression in the hippocampus (HP) and mesopallium; (B) low power image showing DCX expression in the nidopallium (N), medial straiatum (Mst) and the lateral septal nucleus (SL); (C) Low power image showing DCX expression in the nidopallium and lateral striatum (Lst); (D) low power image showing DCX expression in the nidopallium, medial straitum, medial septal nucleus (SM) and the lateral septal nucleus (SL). Arrow shows the tractus-septo-mesencephalicus (TSM). Scale bar in D = 100 μm and applies to all images.

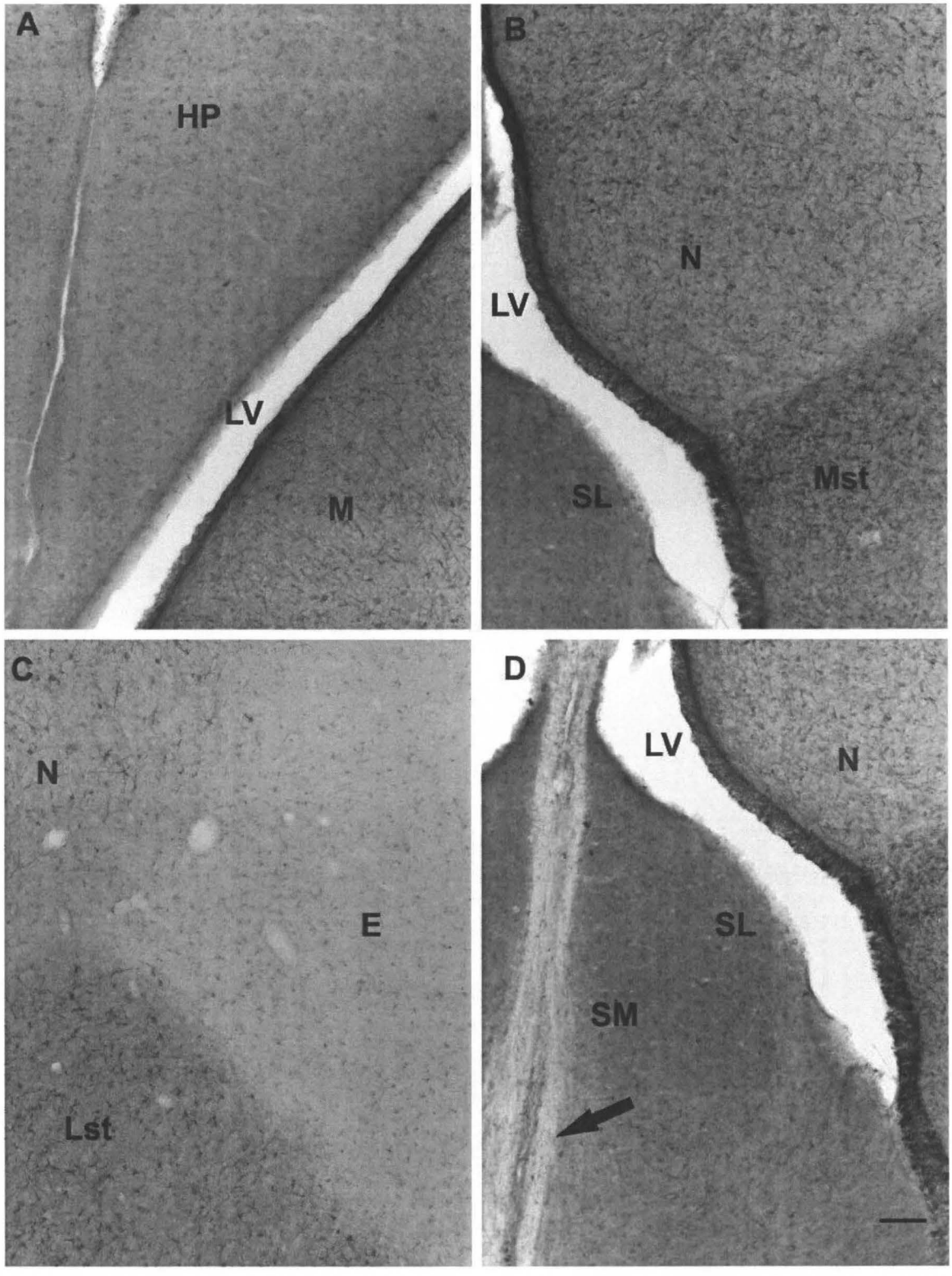
A
HP
LV
M
B
N
LV
SL
Mst
C
N
E
Lst
D
LV
N
SL
SM

3.3.2 Age- related changes in DCX immunoreactivity in the Japanese quail telencephalon

Generally, the density of DCX-ir cells within the quail telencephalon decreased with age even though the pattern of distribution remained the same. High densities of DCX-ir cells were observed in the HD, IMM, N, MSt and LSt. Moreover, Pearson's correlation analysis revealed strong negative relationships between age and the total number of DCX- ir cells in the HD (r = -0.9561; P<0.0001, Figure 3.4A), IMM (r = - 0.9905; P<0.0001, Figure 3.4C), N (r = - 0.9824; P<0.0001, Fig 3.4D), MSt (r = - 0.9850; P<0.0001, Fig 3.5A) and LSt (r = - 0.9979; P<0.0001, Fig 3.5B). In spite of the low densities of DCX-ir cells, Pearson's correlation test revealed strong negative correlations between age and DCX-ir cell counts in the HP (r = - 0.9711; P<0.0001, Fig 3.4B), SM (r = - 0.9904; P<0.0001, Fig 3.5C) and SL (r = - 0.9744; P<0.0001, Fig 3.5D). The most drastic decline took place between 5 and 6 weeks in the HD (Fig 3.4A), HP (Fig 3.4B) and SL (Fig 3.5D); and between 6 and 7 weeks in the IMM (Fig 3.4C), N (Fig 3.4D) and MSt (Fig 3.5A). However, the decline in the numbers of DCX-ir cells with age was more uniform in the LSt (Fig 3.5B) and SM (Fig 3.5C).

Figure 3.4: Photomicrographs and graphs showing age-related changes in DCX expression in the pallium of the Japanese quail telencephalon. The number of DCX-ir cells sharply decreased with age in the HD (A), HP (B), IMM (C) and N (D). In each figure, the photomicrographs represent the same brain region in the youngest (3 weeks old) and the oldest (12 weeks old) animals used in this study. Scale bar in D= 20μm and applies to all photomicrographs. Error bars correspond to the standard error of the mean (SEM). See list of abbreviations for abbreviations used in this figure legend.

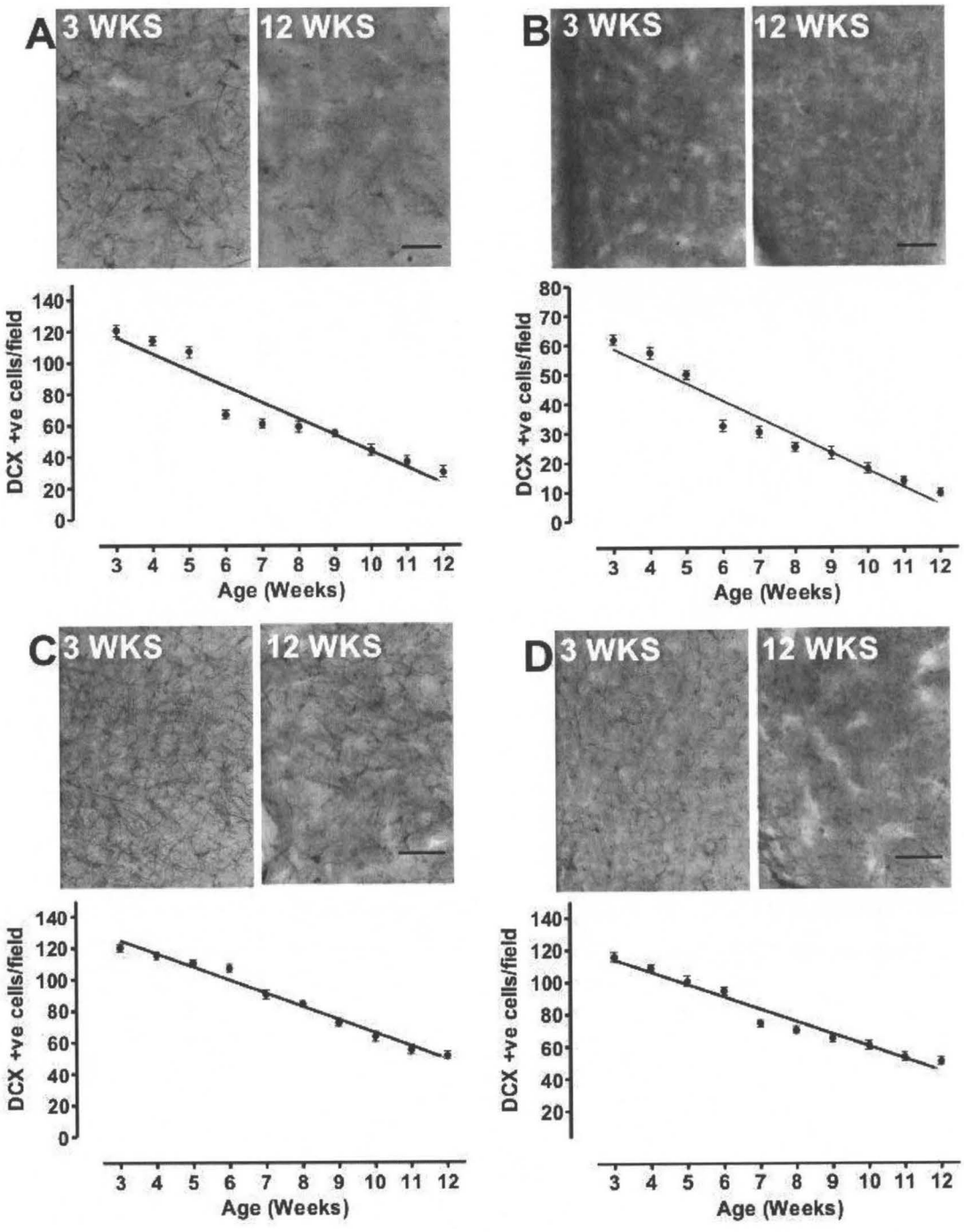
A
3 WKS
12 WKS
DCX +ve cells/field
Age (Weeks)
B
3 WKS
12 WKS
DCX +ve cells/field
Age (Weeks)
C
3 WKS
12 WKS
DCX +ve cells/field
Age (Weeks)
D
3 WKS
12 WKS
DCX +ve cells/field
Age (Weeks)

Figure 3.5: Photomicrographs and graphs showing age-related changes in DCX expression in the sub pallium of the Japanese quail telencephalon. The number of DCX-ir cells sharply decreased with age in the Mst (A), Lst (B), SM (C) and SL (D). In each figure, the photomicrographs represent the same brain region in the youngest (3 weeks old) and the oldest (12 weeks old) animals used in this study. Scale bar in D= 20μm and applies to all photomicrographs. Error bars correspond to the standard error of the mean (SEM). See list of abbreviations for abbreviations used in this figure legend.

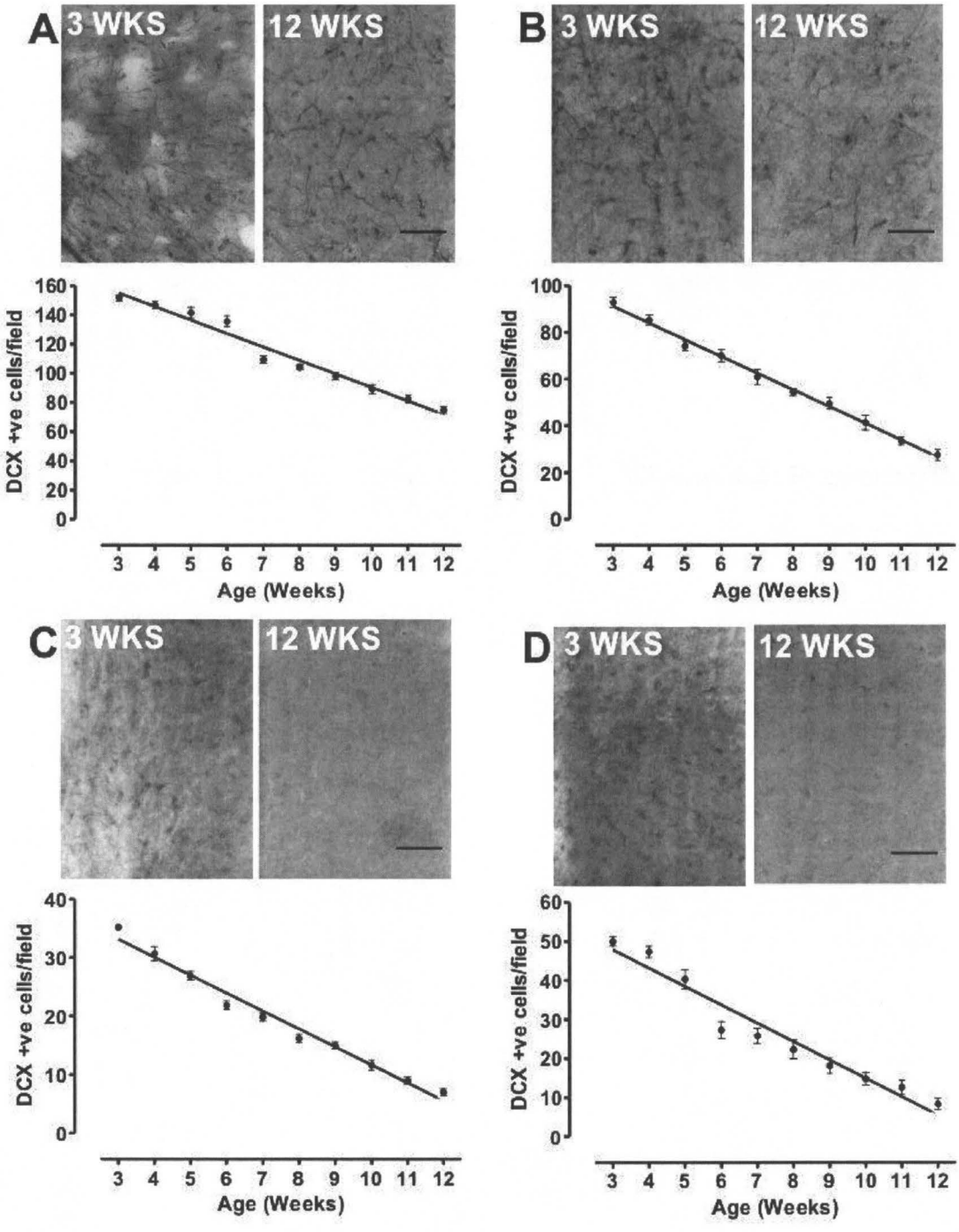
A
3 WKS
12 WKS
DCX +ve cells/field
160
140
120
100
80
60
40
20
0
3 4 5 6 7 8 9 10 11 12
Age (Weeks)
B
3 WKS
12 WKS
DCX +ve cells/field
100
80
60
40
20
0
3 4 5 6 7 8 9 10 11 12
Age (Weeks)
C
3 WKS
12 WKS
DCX +ve cells/field
40
30
20
10
0
3 4 5 6 7 8 9 10 11 12
Age (Weeks)
D
3 WKS
12 WKS
DCX +ve cells/field
60
50
40
30
20
10
0
3 4 5 6 7 8 9 10 11 12
Age (Weeks)

3.3.3 Life-history stage related changes in DCX immunoreactivity in the Japanese quail telencephalon

The number of round multipolar DCX-ir cells were significantly higher in the juvenile group compared to sub adult and adult groups in the HD (F=456.5; P<0.0001, Fig 3.6A), HP (F=106.9; P=0.0005, Fig 3.6B), IMM (F=182.9; P<0.0001, Fig 3.6C), N (F=103.5; P=0.0005, Fig 3.6D), MSt (F=96.6; P=0.0006, Fig 3.6E), LSt (F=107.2; P=0.0005, Fig 3.6F), SL (F=274.0; P<0.0001, Fig 3.6G) and SM (F=128.5; P=0.0003, Fig 3.6H).

Between juvenile and sub adult life-history stages, *post hoc* analysis revealed that the number of round multipolar DCX-ir cells declined significantly by approximately 20% in the IMM (P<0.0001) & the MSt (P<0.01); 30% in the Lst (P<0.01) & the N (P=0.0005), 40 % in the SM (P=0.0003) and 50% in the HD (P<0.0001), the HP (P=0.0005) & the SL (P<0.0001). Similarly, number of round multipolar DCX positive cells declined by approximately 30% in the N (P<0.01) & the MSt (P<0.01); 35% in the HD (P<0.0001) & the Lst (P<0.01; 45% in the IMM (P<0.001) and 50% in the SM (P<0.01) & the SL (P<0.01) between sub adult and adult life-history stages. However, no statistically significant differences were found in the HP between the sub adult and adult life-history stages (P>0.005).

The number of fusiform bipolar DCX-ir cells were also significantly higher in the juvenile group compared to the sub adult and adult groups in the HD (F=174.2; P<0.0001, Fig 3.6A), HP (F=148.8; P=0.0002, Fig 3.6B), IMM (F=162.8; P=0.0001, Fig 3.6C), N (F=103.1; P=0.0005, Fig 3.6D), MSt (F=96.3; P=0.0007, Fig 3.6E), Lst (F= 101.7; P=0.0006, Fig 3.6F), SL (F=282.3; P<0.0001, Fig 3.6G) and SM (F=86.8; P=0.0009, Fig 3.6H).

Bonferroni *post hoc* analysis revealed that the number of fusiform bipolar DCX positive cells decreased significantly by approximately 20% in the N (P<0.01) & the MSt (P<0.01); 30% in the Lst (P<0.01) & the SM (P<0.01); 40 % in the HD (P<0.0001); 50% in HP (P=0.0002) and 60% in the SL (P<0.0001) between juvenile and sub adult life-history stages. However, no statistically significant differences were

found in the IMM between the juvenile and sub adult life-history stages (P>0.05). Similarly, fusiform bipolar DCX positive cells declined by approximately 20% in the MSt (P<0.01); 25% in the N (P<0.01); 35% in the IMM (P<0.0001) and 45% in the Lst (P<0.01) & the SM (P<0.01) between sub adult and adult life-history stages. However, no statistically significant differences were found in the HD, HP and SL between the sub adult and adult life-history stages (P>0.005).

Figure 3.6: Graphical representation of life-history stage related differences in the numbers of round multipolar and fusiform DCX-ir cells in the Japanese quail telencephalon. Generally, the number of DCX-ir cells was significantly higher in juvenile group compared to the sub adult and adult groups in the HD (A), HP (B), IMM (C), N (D), MSt (E), LSt (F), SM (G) and SL (H). In turn, the number of DCX-ir cells was higher in the sub adult compared to adult group in HD (A), HD (B), IMM (C), N (D), MSt (E), LSt (F), SM (G) and SL (H). Error bars correspond to the SEM. *P<0.01. **P<0.001 ***P<0.0001 #P>0.005. See list of abbreviations for abbreviations used in this figure legend.

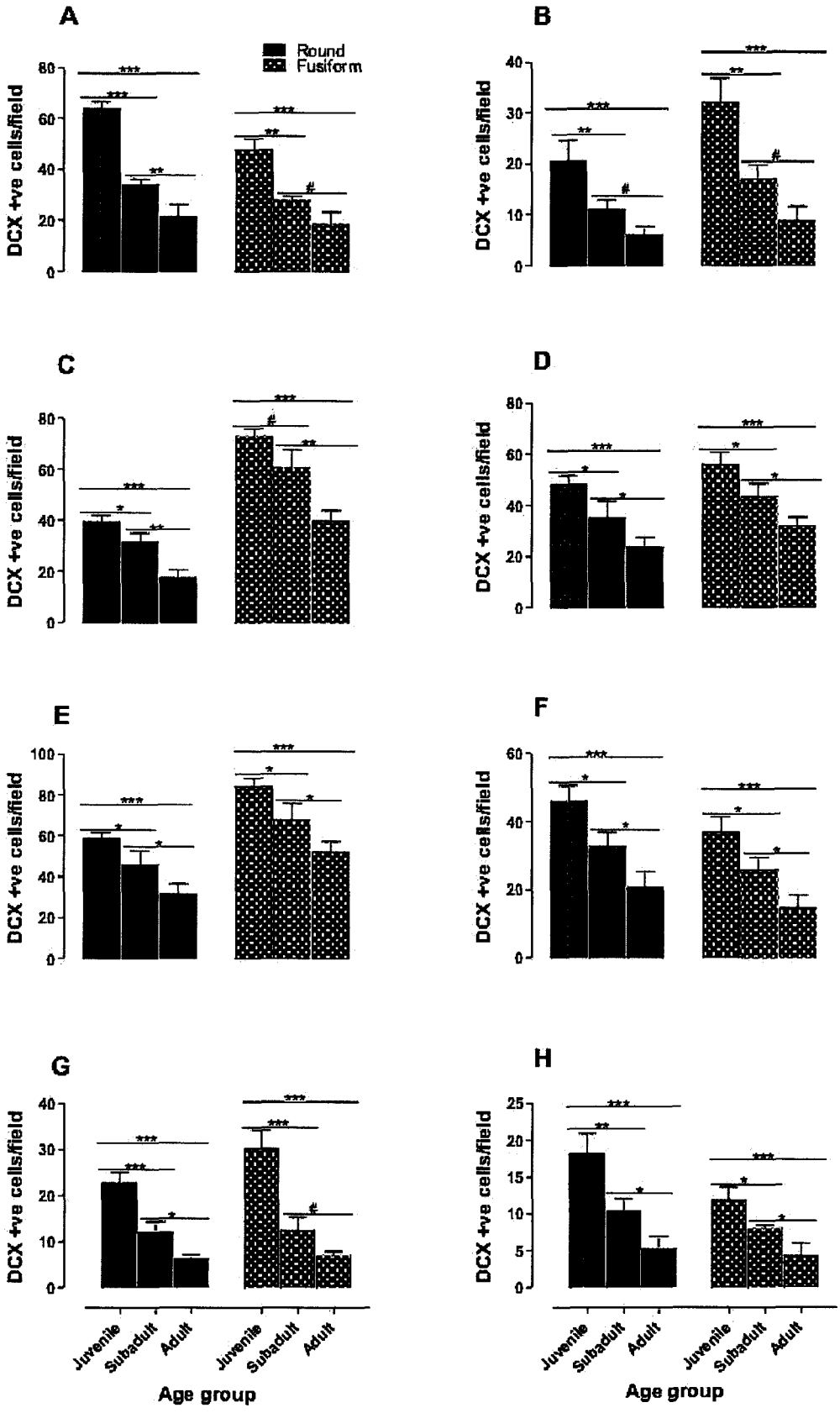
A
B
C
D
E
F
G
H
Round
Fusiform
DCX +ve cells/field
Juvenile
Subadult
Adult
Age group

3.4 DISCUSSION

In this quantitative study, DCX immunolabelling was used to investigate neuronal recruitment in the Japanese quail brain and to determine how this process changes with post hatching age spanning different life history stages. Doublecortin is a microtubule associated protein that controls polymerisation of the leading process and stabilisation of the neuroblast cytoskeleton during migration (Horesh et al., 1999). DCX, therefore, plays a critical role in neuronal migration from the birth site to positioning at the recruitment site.

Two main types of DCX-ir cells were observed in the telencephalon: elongated bipolar cells, presumably corresponding to migrating neuroblasts, and round multipolar cells representing neuroblasts that have recently arrived at the recruitment site (Boseret et al., 2007; Balthazart et al., 2008; Yamamura et al., 2011). These DCX-ir cells were observed throughout the whole telencephalon except in the entopallium, arcopallium and globus pallidus across all the ages studied indicating widespread neuronal incorporation in the Japanese quail brain. The pattern and distribution of DCX immunoreactivity observed in this study corresponds with the findings from studies in the chicken (Capes-Davis et al., 2005; Mezey et al., 2012), pigeon (Melleu et al., 2013; Melleu et al., 2016; Meskenaite et al., 2016; Mazengenya et al., 2017), zebra finch (Kim et al., 2006) and canary (Boseret et al., 2007; Balthazart et al., 2008). In addition, if DCX is an accurate proxy for neuronal incorporation, findings from this study also resonate with those of Ling et al. (1997) in the ring dove brain. However, our findings are contrary to the conclusion made by Tsai et al. (1981), using thymidine auto radiographic analysis that neurogenesis in the chick telencephalon ceases prior to hatching. This study shows that the Japanese quail, in spite of being a precocial bird, continues to add new neurons to the brain in a similar way as other birds studied to date. Moreover, it can be concluded that the entopallium, arcopallium and globus pallidus of the quail brain presumably reach their stable gross structures before hatching which explains why they do not recruit any more neurons after hatching.

What then is the significance of neurogenesis in the Japanese quail brain? A few studies have shown that neurogenesis in the chick telencephalon, a close relative of the Japanese quail, is related to learning and memory. Dermon et al. (2002) reported

increased neuronal recruitment in the Mst and IMM, and cell proliferation in the adjacent ventricular zones following a passive avoidance learning task in chicks. In addition, passive avoidance learning was also shown to reduce neurogenesis in the chick hippocampus (Nikolakopoulou et al., 2006a). Furthermore, areas shown to have intense DCX immunoreactivity (HD, IMM, MSt) in this study also constitute the main components of thalamofugal pathways, a neural circuit essential for visual imprinting in chicks (Nakamori et al., 2013). Indeed, these areas have been shown to change the number of synapses or to change the expression of immediate early genes c-fos and c-jun or to increase glucose uptake following performance of learning and memory tasks (McCabe and Horn, 1994; Freeman and Rose, 1999; Ünal et al., 2002). These studies indicate that post hatching neurogenesis in the galliform brain might play a critical role in learning and memory tasks.

Although this study shows that neurogenesis persists throughout life, it decreases with increasing post-hatching age and progression through different life-history stages. In all the brain areas studied, post-hatching neurogenesis declined sharply with age especially during the transition from juvenile ages to sub adult ages where significant differences in DCX-ir numbers were found. Similarly, age-dependent changes in neuronal incorporation have been reported in the high vocal centre (HVc) of the canary (Alvarez-Buylla et al., 1994; Wilbrecht and Kirn, 2004) and zebra finch (DeWulf and Bottjer, 2002; Wang et al., 2002; Kim et al., 2006; Pytte et al., 2007) birds. In addition, age-dependent decline in neuronal incorporation has also been described in the hippocampus of the migrating white-crowned sparrow (LaDage et al., 2011), telencephalon of the ring dove (Ling et al., 1997), olfactory bulb and hippocampus of homing pigeons (Meskenaite et al., 2016).

Although the galliformes are precocial birds, significant structural and functional changes occur in their brains post hatching. From electroencephalography (EEG) studies, two broad phases of synaptogenesis have been identified in the galliform brain, synapse formation phase and synapse maturation phase (Atkinson et al., 2003). The synapse formation phase is characterised by an increase in the number of synapses whereas the synapse maturation phase is characterised by trimming and conversion of the immature synaptic networks into adult ones (Rostas et al., 1991). In galliformes, these two phases are separated temporally, making it easy to determine the time-course of developmental changes from juvenile to adult birds (Atkinson et

al., 2008). In addition, rapid growth in the juvenile phase gives the chick brain its full complement of synapses by 10-21 days post hatch. Thereafter, synaptic proliferation ceases and between 6-8 weeks progressive modification in the functional and structural properties of neural networks occurs without any overall increase in the number of synapses (Rostas et al., 1991; Atkinson et al., 2003; Atkinson et al., 2008). In the context of our findings, it appears that the rapid neurogenesis that occurs in the Juvenile ages caters for the need for increased numbers of synapses during the synapse formation phase until the gross structure of the quail brain is stable (Rostas et al., 1991; Atkinson et al., 2008). Neurogenesis, therefore, begins to decline during the sub adult ages which corresponds to the maturation phase of synapses (6-8 weeks) since no more neurons or synapses are required for this phase. This period of decline presumably reflects a stage when fine tuning of neuronal circuits takes place during the maturation phase.

Several trophic factors, including sex steroids and glucocorticoids, have been identified as potential mediators of age-dependant changes in neurogenesis (Cameron and McKay, 1999b; Absil et al., 2003; Soma et al., 2004; Brenowitz, 2013, 2015). Changes in blood levels of testosterone and corticosterone could be related to the observed age-dependent changes in neuronal incorporation in the Japanese quail brain.

Testosterone has been shown to increase neuronal incorporation in the song bird telencephalon including the high vocal centre (Balthazart et al., 2008; Yamamura et al., 2011; Brenowitz, 2013, 2015). In addition, testosterone is believed to increase the number of incorporated neurons by increasing their survival (Rasika et al., 1999; Spritzer and Galea, 2007). Although telencephalic areas and ventricular zones lack steroid hormone receptors, the trophic effects of testosterone on neurogenesis have been shown to be mediated via its aromatization to estradiol by aromatase (Chen et al., 2013). In turn, estradiol acts via brain derived neurotropic factor (BDNF) to increase neuronal production and incorporation (Tang and Wade, 2012; Brenowitz, 2013; Chen et al., 2013). However, immunoreactivity for both BDNF protein and aromatase enzyme in the avian brain have been reported to decline with post-hatching age (Mattson et al., 2004; und Halbach, 2010; Tang and Wade, 2016). In male Japanese quails, testosterone has been shown to peak during the sub adult period (between 6 to 8 weeks) and thereafter declining during the adult period

(Ottinger and Brinkley, 1979; Ottinger et al., 2004). This decline in serum testosterone levels at these life history stages might explain the decrease in neurogenesis observed in the adult compared to juvenile quail brain.
In addition, changes in glucocorticoid levels have also been shown to cause a reduction in neurogenesis, particularly production of hippocampal granule cells in aged rats (Cameron and McKay, 1999b; Montaron et al., 1999; Montaron et al., 2006). In addition, Newman et al. (2010) reported a decrease in production and survival of neuronal cells in the white crowned sparrow brain following chronic exposure to corticosterone. More specifically, corticosterone levels have been shown to be lower in juvenile quails compared to adults, increasing gradually with increasing age (Hazard et al, 2005). These changes in corticosterone levels at different life-history stages mirror the changes in neurogenesis taking place in the quail telencephalon at corresponding stages.

3.5 CONCLUSION

The Japanese quail brain, just like other birds studied to date, continues to recruit neurons in adulthood. Moreover, neurogenesis in the Japanese quail brain declines with post hatching age in a similar manner as that observed in mammals and other birds: that is juvenile peaking followed by a decline at sub adult and adult stages. Additionally, this decline observed in neurogenesis might also reflect the reduced capacity for behavioural plasticity observed in adult as compared to juvenile quails.

CHAPTER 4: AGE-RELATED CHANGES IN KI-67 AND DCX EXPRESSION IN THE BALB/ C MOUSE (*MUS MUSCULUS*) BRAIN.

4.1 INTRODUCTION

Neurogenesis in the mammalian brain was thought to be complete before or soon after birth. Today it is widely accepted that the mammalian brain, just like other vertebrates, continues to produce new neurons throughout life. The process through which new neurons are added to the brain after birth is termed postnatal or secondary neurogenesis (Thuret et al., 2015). To date, postnatal neurogenesis has been reported in the brains of several laboratory bred and wild living mammalian species including laboratory mice (Kondo et al., 2010; Nada et al., 2010; Encinas et al., 2011; Mobley et al., 2014), four striped mice (Olaleye and Ihunwo, 2014), rats(Kuhn et al., 1996; Jessberger et al., 2009), voles (Amrein et al., 2004), African giant rats (Olude et al., 2014), mole rats (Amrein et al., 2014), bats (Chawana et al., 2013), dogs (Fernández-Flores et al., 2018) and humans (Eriksson et al., 1998).

Neurogenesis is a complex multi-step process that involves proliferation of neuronal stem cells, differentiation, migration and integration into existing neuronal circuits (Barnea and Pravosudov, 2011). Under normal physiological conditions, new neurons are formed in the sub ventricular zone (SVZ) of the lateral ventricles and the sub granular zones (SGZ) of the hippocampal dentate gyrus of the mammalian brain (Ihunwo and Pillay, 2007). Neurons formed in the SVZ migrate long distances through the rostral migratory stream (RMS) to reach the olfactory bulb (OB) where they integrate into the local circuitry as granule cells and periglomerular cells (Mobley et al., 2014). On the other hand, neurons born in the SGZ travel short distances to integrate into the granule cell layer of the dentate gyrus (Nada et al., 2010; Amrein et al., 2014). However, other potential neurogenic sites have been reported in the mammalian brain including the hypothalamus, cortex, septum, subcallosal zone (SCZ), 3rd ventricle and 4th ventricle (Brown et al., 2003; Ihunwo and Pillay, 2007; Pierce and Xu, 2010; Kim et al., 2012; Lee and Blackshaw, 2012).

Several intrinsic and extrinsic factors have been shown to regulate neurogenesis including growth factors, hormones, physical activity, environmental enrichment, learning and age (reviewed by Aimone et al. (2014)). Although neurogenesis persists throughout life in the mammalian brain, several studies have identified chronological

age as one of the strongest of its regulators. In mice specifically, age-related decline in neurogenesis was reported in the SGZ (Kuhn et al., 1996; Nada et al., 2010; Encinas et al., 2011; Jinno, 2011), SVZ (Enwere et al., 2004; Luo et al., 2006; Shook et al., 2012), RMS (Mobley et al., 2014), OB (Enwere et al., 2004; Kondo et al., 2010) and the SCZ (Kim et al., 2012). However, these age-related studies focused only on neurogenesis at different phases of adulthood, that is young or early (1-3 months old), mid (6-12 months old) and late (20-24 months old) adulthood. Findings from such studies only represent changes at the tail end of postnatal neurogenesis and do not provide insight on how postnatal neurogenesis changes across different life history stages of the animal, that is juvenile, sub adult and adult stages. Given that age-related decreases in neurogenesis likely commences during early postnatal life, the current study analyzed age and life-history stage related changes in this process in the male BALB/c mouse brain. Ki-67 and DCX immunohistochemistry was used to assess changes in cell proliferation and neuronal incorporation respectively. Ki-67 is a chromosomal associated protein that is expressed during the cell cycle whereas DCX is a microtubule-associated protein which labels immature and migrating neuroblasts in the brain (Jinno, 2011; Balthazart and Ball, 2014b).

4. 2 MATERIALS AND METHODS

4.2.1 Animals

Male BALB/c mice obtained from the Central Animal Services, University of the Witwatersrand with ages ranging from 1 to 12 weeks (n=36) were used in this study. The animals were treated and used according to the guidelines of the University of the Witwatersrand Animal Ethics Committee which correspond with those of the National Institute of Health (NIH) for care and use of animals in scientific experimentation. All protocols were approved by the University of the Witwatersrand Animal Ethics Screening Committee (AESC/2014/35/A).

Throughout the study, the mice were maintained under a 12 hour: 12-hour light dark cycle with access to food and water *ad libitum.* For the 12 weeks, 3 mice were collected and sacrificed every week. The mice were randomly allocated to groups

according to their sexual maturity as follows: juvenile (1-5 weeks old, n= 15), sub adult (6-8 weeks old, n=9) and young adult (9-12 weeks old, n=12).

4.2.2 Tissue collection and processing

All animals were injected intraperitoneally with Euthapent (0.5 – 1 ml/kg). Animals were then perfused transcardially, initially with 0.9 % cold saline solution, followed by 4 % paraformaldehyde in 0.1 M phosphate buffer (PB, pH 7.4) solution. After perfusion, brains were carefully removed from the skull, post-fixed overnight in 4 % paraformaldehyde in 0.1M PB, weighed before being transferred into 30% sucrose in 0.1M PB until equilibration. The brains were sectioned in a sagittal plane at 50 µm using a cryostat (Shandon Cryotome E, Thermo Fischer Scientific, UK) at -24 ℃ and repeated series of 5 sections were collected free-floating into 24 multi-well plates containing 0.1 M PB. The first series of sections was mounted on gelatin- coated slides before staining with 1 % cresyl violet for anatomical orientation. The second and third series were used for Ki-67 and DCX immunohistochemistry respectively. The remaining two series were stored in a cryoprotectant solution at -20 ˚C for future use.

4.2.3 Immunohistochemistry

Brain sections were pre-treated for 30 min at room temperature under gentle shaking with an endogenous peroxidase inhibitor solution [0.1 M PB, 100 % methanol, 30% H_2O_2 in the ratio of 49.2: 49.2: 1.66 H_2O_2]. Following three 10-min rinses in 0.1 M PB, the sections were subsequently pre-incubated in a blocking buffer solution [3 % normal goat serum, 2 % bovine serum albumin, 0.25 % Triton X-100 in 0.1 M PB] for 2 h under gentle shaking at room temperature to prevent non-specific binding. Sections were then transferred into a primary antibody solution [1:1000, rabbit anti-Ki-67 (AB15580, Abcam, UK) or 1: 2000, rabbit anti-DCX (AB18723, Abcam, UK), in the blocking buffer solution] and were incubated for 48 h at 4 °C under gentle shaking. Following incubation, sections were subjected to three 10-min rinses in 0.1 M PB before being incubated in secondary antibody solution [1,000 dilution of biotinylated anti-rabbit IgG (BA-5000; Vector Laboratories, USA) in blocking buffer solution] for 2 h at room temperature under gentle shaking. Following three 10-min

rinses in 0.1 M PB, the sections were incubated in an avidin-biotin solution [1: 125 A and 1: 125 B (Vector Laboratories) in 0.1 M PB] for 1 h. The sections were then transferred into three 10-min 0.1 M PB rinses before being placed in a solution containing 0.05% 3, 3' di-amino-benzidine tetrachloride (DAB) in 0.1 M PB for 5 min. To each 1 ml of this solution, 3.3 µl of 30% H_2O_2 were added, and chromatic precipitation was visually monitored under a low power stereomicroscope.

Development was subsequently stopped by placing the sections in 0.1 M PB, followed by a final 10-min rinse in 0.1 M PB. Sections were mounted on 0.5% gelatinised slides, left to dry overnight, dehydrated in a graded series of alcohols, cleared in xylene and cover slipped with DPX. To ensure that non-specific staining was not affecting the results, control sections taken at random were processed in the same manner, but either the primary or the secondary antibody was omitted. No labelled cells were observed in either case.

4.2.4 Data Analysis

4.2.4.1 Qualitative analysis

Sections were analysed qualitatively with both low and high power microscopy to yield a comparative description of the distribution of Ki-67 and DCX-immunoreactive (-ir) cells. Anatomical brain structures were identified based on the Allen's reference atlas of the mouse brain (Dong, 2008). High power microscopic observation was used to determine the relative densities of Ki-67 and DCX immunostained structures throughout the different regions of the brain. The relative densities of immunostained structures were visually compared and recorded on a scale ranging from absent (-) to low (+) to moderate (++) to high (+++). A second observer was used to eliminate observer bias (Chawana et al., 2013; Mazengenya et al., 2017; Nkomozepi et al., 2018).

4.2.4.2 Quantitative analysis

The quantification of Ki-67 and DCX-ir cells was done using computer assisted image analysis by the first author (PN) who was blinded to the ages of the animals. Sections

were digitized using a AxioCam HRC video camera linked to a Zeiss Axioplan 2 microscope and Ki-67 and DCX-ir cells in each brain region of interest were manually counted using the cell counter function of ImageJ (Schneider et al., 2012). Ki-67 and DCX quantification was carried out in the following brain regions:

Sub ventricular zone and rostral migratory stream

Quantification of Ki-67 and DCX-ir cells was carried out in all the brain sections per animal exhibiting the complete SVZ- RMS- OB continuum (two sections in this case) following the method described by Li et al. (2009). The first brain section corresponded to sagittal level 15 (lateral 1.10 mm) of Allen's reference atlas of the mouse brain (Dong, 2008) and the second one was situated 250μm medial to the first section. For the SVZ, the enlarged region overlying the anterior horn of the lateral ventricle (SVZa) was quantified (Fig 4.1 A). For the RMS, three regions were quantified: the short vertical segment which descends ventrally from the SVZ (VL-RMS), the rostral horizontal extension of the RMS (HL-RMS) (Fig 4.1 A) and the terminal portion of the RMS in the centre of the olfactory bulb (OBc-RMS) (Fig 4.1B). In each of these brain regions, three quantification fields at a magnification of 100X (each one equal to 0.013 mm^2) were used per section.

Sub granular zone of the dentate gyrus

Ki-67 and DCX-ir cells were quantified in 6 corresponding sections/per animal (approximately 250μm apart) containing the dentate gyrus following a method modified from Obiorah et al. (2015). The first section was situated at a level corresponding to sagittal level 12 (lateral 1.725mm) of Allen's reference atlas of the mouse brain (Dong, 2008) and the rest were placed medial to the first one. In each section, all Ki-67 and DCX-ir in the SGZ of the entire dentate gyrus were quantified at a magnification of 40X.

High resolution microscopic images digitally captured with an AxioCam HRC digital camera on a Zeiss Axioplan 2 compound microscope were processed with the Adobe Photoshop 7.0 software (Adobe Systems, Mountain View, CA). No pixelation adjustment or manipulation of the captured images was undertaken, except for the adjustment of brightness and contrast.

4.2.4.5 Statistical analysis

Ki-67 and DCX-ir cell counts were averaged where multiple quantification fields were used at the same or different medio-lateral levels of the same brain region. The Shapiro-Wilks normality test was used to test the normality of data in all the variables. For all the variables, the data followed a normal distribution ($P>0.05$). The correlation between age and either Ki-67 or DCX-ir cell counts for each brain region was tested using Pearson's correlation analysis. For each brain area quantified, the mean counts of Ki-67 or DCX ir cells for each life-history stage were computed and compared using one-way analysis of variance (ANOVA) followed by Bonferroni's *post hoc* test. All analyses were performed using Graphpad prism 5 software (Graphpad software, CA). All results were expressed as means ± standard deviation and a significance level of $P<0.05$ was used.

4.3 RESULTS

4.3.1 Distribution of Ki-67 and DCX immunoreactive cells in the BALB/c mouse brain

The distributive pattern of Ki-67 and DCX-ir was similar across all the ages studied except for variations in the density of labelled cells (Tables 4.1 and 4.2). Thus the following description applies to all ages studied. Ki-67-ir cells were mainly observed in the sub ventricular zones (SVZ) of the lateral ventricles, the rostral migratory stream (RMS), olfactory bulbs (OB) and sub granular zone (SGZ) of the dentate gyrus.

In the SVZ, Ki-67-ir cells occupied the dorsal and ventral proliferative zones which were separated by the lateral ventricular bulge of the corpus striatum (Fig 4.1A). From the dorsal proliferative zone a band of Ki-67-ir cells (dorsal RMS) coursed along the dorsal border of the corpus striatum between the caudoputamen and the corpus callosum. In this region, some Ki-67-ir cells appeared to migrate from the dorsal RMS and traverse the substance of the corpus callosum to reach the neocortex (Fig 4.2A). Ki-67-ir cells from the ventral proliferative zone (ventral RMS) coursed along the ventral border of the corpus striatum between the nucleus

accumbens and the caudoputamen. The dorsal RMS and ventral RMS merged rostrally into one RMS before turning sharply upwards to enter the OB (Fig 4.1B). In the OB, Ki-67-ir cells were observed in all the five layers although they were mostly abundant in the granule cell layer (Fig 4.1C).

Figure 4.1: Photomicrographs showing distribution of Ki-67-ir cells in the telencephalon and olfactory bulb of the BALB/c mouse brain. (A) Ki-67-ir cells in the sub ventricular zone (SVZ) and the rostral migratory streams (dRMS & vRMS), (B) Ki-67-ir cells in terminal portion of the rostral migratory stream in the core of the olfactory bulb (OBc-RMS), (C) Ki-67-ir cells in the olfactory bulb (OB) and (D) Ki-67-ir cells in the dentate gyrus of the hippocampus (DG). The inserts in the upper right corner of each image represent higher magnification photomicrographs. In all images dorsal is to the top and rostral to the left. Squares a, b, c & d in photomicrographs A and B show brain regions where quantification was carried out. Squares in photomicrographs A (a), B, C and D show regions where the inserts were magnified from. Scale bar in A and B= 200μm; in C and D = 100 μm. Scale bar in all inserts= 20 μm. See list of abbreviations for abbreviations used on the figure.

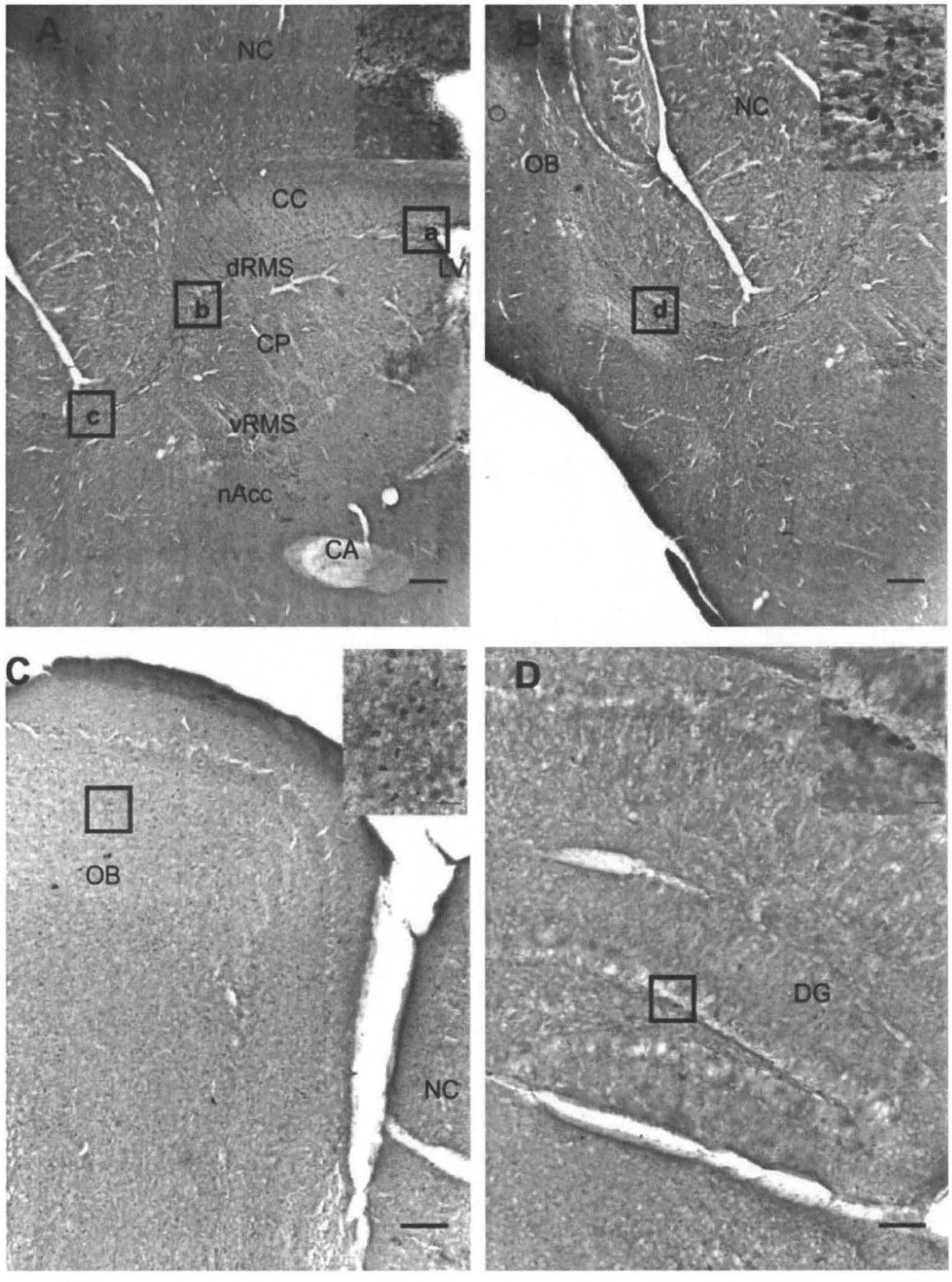
A
NC
CC
a
LV
dRMS
b
CP
c
vRMS
nAcc
CA
B
NC
OB
d
C
OB
NC
D
DG

Ki-67-ir cells were mostly observed in the SGZ, a region located between the granule cell layer and the hilus of the dentate gyrus of the hippocampus (Fig 4.1D). In addition, fewer Ki- 67-ir cells were observed in the granule cell layer of the dentate gyrus. Few Ki-67-ir cells were occasionally observed in the different layers of the neocortex (Fig 4.2B); the cerebellar cortex and peduncles (Fig 4.2C), superior and inferior colliculi of the tectum (Fig 4.2D). The density of Ki-67-ir cells decreased with advancing age (Table 4.1).

Table 4.1: Age-related changes in Ki-67 expression in the BALB/c mouse brain

	Postnatal age											
	1 week	2 weeks	3weeks	4weeks	5weeks	6weeks	7weeks	8weeks	9weeks	10weeks	11weeks	12weeks
OB	+++	+++	++	++	+	+	+	+	+	+	+	+
RMS	+++	+++	+++	+++	+++	+++	+++	+++	++	++	++	++
SVZ	+++	+++	+++	+++	+++	+++	+++	+++	++	++	++	++
SGZ	+++	+++	++	++	++	++	++	+	+	+	+	+
NC	+	+	+	+	+	+	+	+	+	+	+	+
TECT	++	++	++	+	+	+	+	+	+	+	+	+
DIEN	-	-	-	-	-	-	-	-	-	-	-	-
MES	-	-	-	-	-	-	-	-	-	-	-	-
MED	-	-	-	-	-	-	-	-	-	-	-	-
CB	++	++	++	++	++	++	++	+	+	+	+	+

+++ High density ++ medium density + low density - absent. See list of abbreviations for abbreviations used in the table.

Figure 4.2: Photomicrographs showing distribution of Ki-67-ir cells in the dorsal RMS & corpus callosum (A), neocortex (B), cerebellum (C) and inferior colliculus (D) of the BALB/c mouse brain. The inserts in the upper right corner of images B, C and D represent higher magnification photomicrographs of the respective region to demonstrate cellular morphology. In all images dorsal is to the top and rostral to the left. Squares in images B, C and D represent areas where images in inserts were obtained from. Black arrows show Ki-67-ir cells in the dRMS and white arrows show Ki-67-ir cells migrating through the corpus callosum. Scale bar in A = 20μm; in B = 100 μm; in C and D = 200 μm. Scale bar in inserts B, C and D = 20 μm. See list of abbreviations for abbreviations used on the figure.

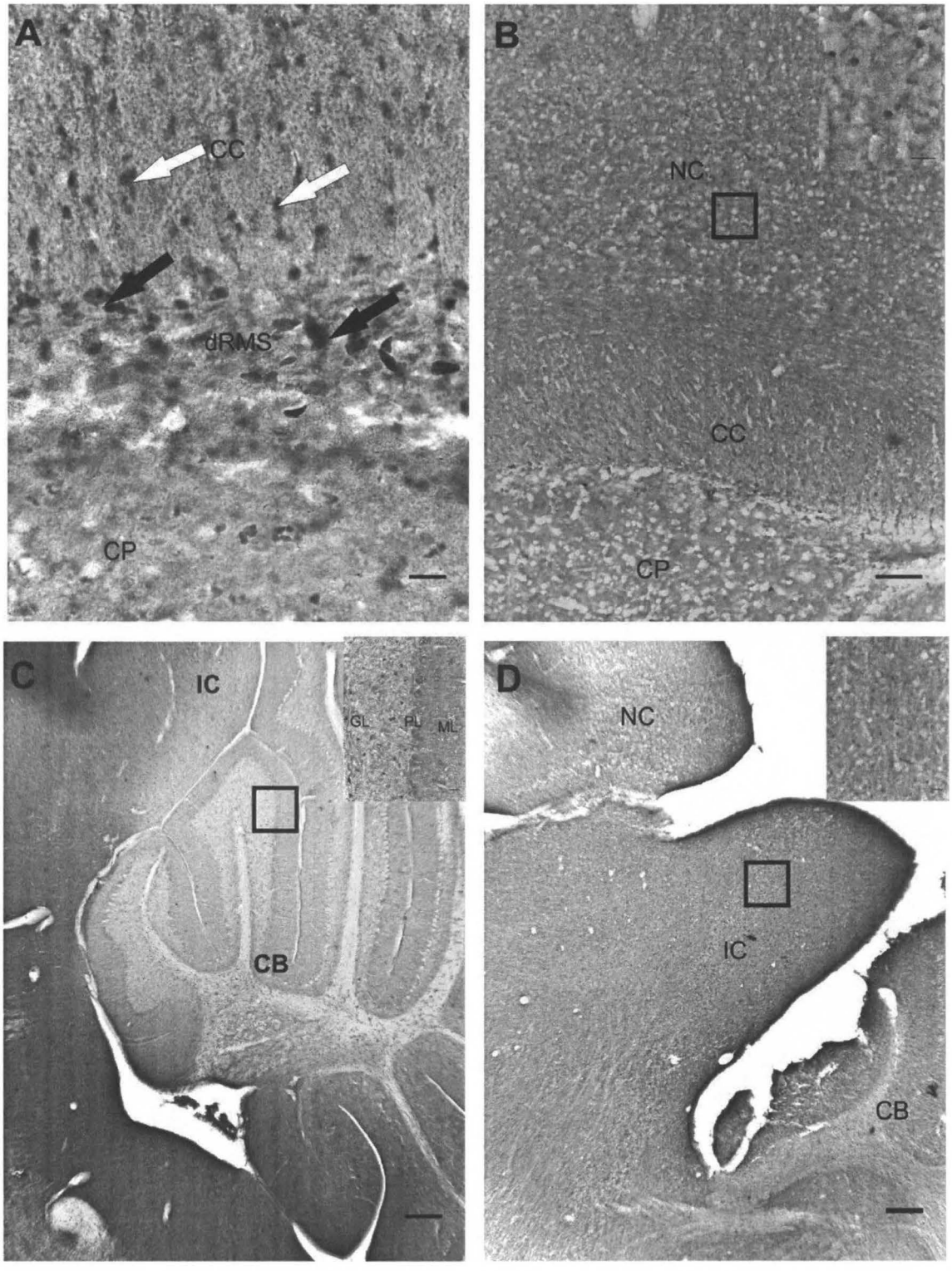
A
CC
dRMS
CP
B
NC
CC
CP
C
IC
GL
PL
ML
CB
D
NC
IC
CB

Similarly, DCX-ir cells were observed mainly in the SVZ of the lateral ventricles, RMS (Figs 4.3A & B), OB (Fig 4.3C) and SGZ (Fig 4.3D) at all ages studied. In these areas, DCX-ir cells were observed in corresponding locations as the Ki-67-ir cells. The majority of DCX-ir cells observed in the SVZ and RMS were bipolar in morphology with short leading processes and appeared to migrate from the SVZ towards the OB. In the OB, numerous small bipolar cells with short processes were observed in the granule cell layer (Insert, Fig 4.3C). In addition, fewer cells with longer processes were observed in the internal plexiform and glomerular layers of the OB.

In the dentate gyrus, DCX-ir cells were mostly observed in the SGZ and granule layer with their processes extending towards the granule cell layer and molecular layers respectively (Insert, Fig 4.3D). Fewer DCX-ir cells were occasionally observed in the layers of the neocortex (Fig 4.3E). The density of DCX-ir cells decreased with advancing age (Table 4.2).

Table 4.2: Age-related changes in DCX expression in the BALB/c mouse brain

	Postnatal age											
	1 week	2 weeks	3weeks	4weeks	5weeks	6weeks	7weeks	8weeks	9weeks	10weeks	11weeks	12weeks
OB	+++	+++	+++	+++	+++	+++	+++	+++	++	++	++	++
RMS	+++	+++	+++	+++	+++	+++	++	++	++	++	++	+
SVZ	+++	+++	+++	+++	+++	+++	++	++	++	++	++	++
SGZ	+++	+++	+++	+++	+++	++	++	++	++	+	+	+
NC	++	++	+	+	+	+	+	+	+	+	+	+
TECT	-	-	-	-	-	-	-	-	-	-	-	-
DIEN	-	-	-	-	-	-	-	-	-	-	-	-
MES	-	-	-	-	-	-	-	-	-	-	-	-
MED	-	-	-	-	-	-	-	-	-	-	-	-
CB	-	-	-	-	-	-	-	-	-	-	-	-

+++ High density ++ medium density + low density - absent. See list of abbreviations for abbreviations used in the table.

Figure 4.3: Photomicrographs showing distribution of DCX-ir cells in the telencephalon and olfactory bulb of the BALB/c mouse brain. (A) DCX-ir cells in the sub ventricular zone (SVZ) and the rostral migratory streams (dRMS & vRMS), (B) DCX-ir cells in the terminal portion of the rostral migratory stream that projects into the olfactory bulb (OBc-RMS), (C) DCX- ir cells in the olfactory bulb (OB), (D) DCX-ir cells in the dentate gyrus of the hippocampus (DG) and (E) DCX-ir cells in the neocortex (NC). The inserts in the upper right corner of each image represent higher magnification photomicrographs of each region to demonstrate cellular morphology. In all images dorsal is to the top and rostral to the left. Squares in photomicrographs A, B, C, D and E represent areas where images in inserts were obtained from. Scale bar in A and B= 200μm; in C and D = 100 μm. Scale bar in all inserts= 20 μm. See list of abbreviations for abbreviations used on the figure.

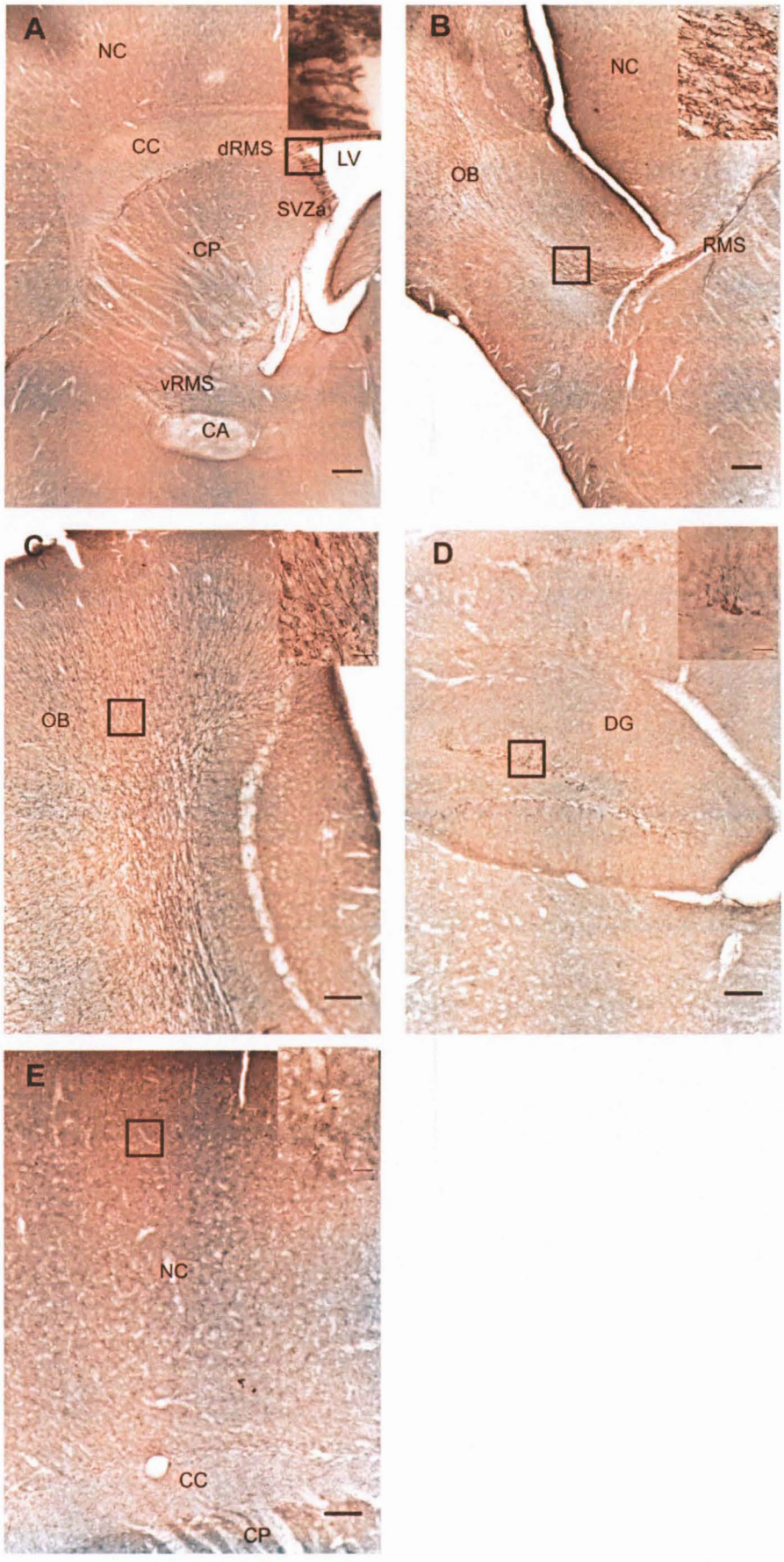
A
NC
CC
dRMS
LV
SVZa
CP
vRMS
CA
B
NC
OB
RMS
C
OB
D
DG
E
NC
CC
CP

4.3.2 Age-related changes in the number of Ki-67 and DCX immunoreactive cells in the BALB/c mouse brain

Pearson's correlation analysis revealed that the number of Ki-67-ir cells sharply declined with postnatal age in the VL-RMS (r =-0.9884; P<0.0001, Fig 4.4A), HL-RMS (r = -0.9910; P<0.0001, Fig 4.4C), OBc-RMS (r =-0.9951; P<0.0001, Fig 4.5A), SVZa (r = -0.9940; P<0.0001, Fig 4.6A) and SGZ (r =-0.9838; P<0.0001, Fig 4.6C)

Similarly, the number of DCX-ir cells decreased significantly with postnatal age in the VL-RMS (r =-0.9811; P<0.0001, Fig 4.4B), HL-RMS (r = -0.9830; P<0.0001, Fig 4.4D), OBc-RMS (r =-0.9858; P<0.0001, Fig 4.5B), SVZa (r =-0.9722; P<0.0001, Fig 4.6B) and SGZ (r =-0.9767; P<0.0001, Fig 4.6D).

Figure 4.4: Photomicrographs and graphs showing age-related changes in numbers of Ki-67-ir (A & C) and DCX-ir (B & D) cells in the different parts of the rostral migratory stream of the BALB/c mouse brain. The number of Ki-67-ir cells sharply decreased with age in the VL-RMS (A) and HL-RMS (C). Similarly, DCX-ir cells decreased with age in the VL-RMS (B) and HL-RMS (D). In each figure, the photomicrographs represent the same brain region in the youngest (1 week old) and the oldest (12 weeks old) animals used in this study. Scale bar in D= 20μm and applies to all photomicrographs. Error bars correspond to the standard error of the mean (SEM).

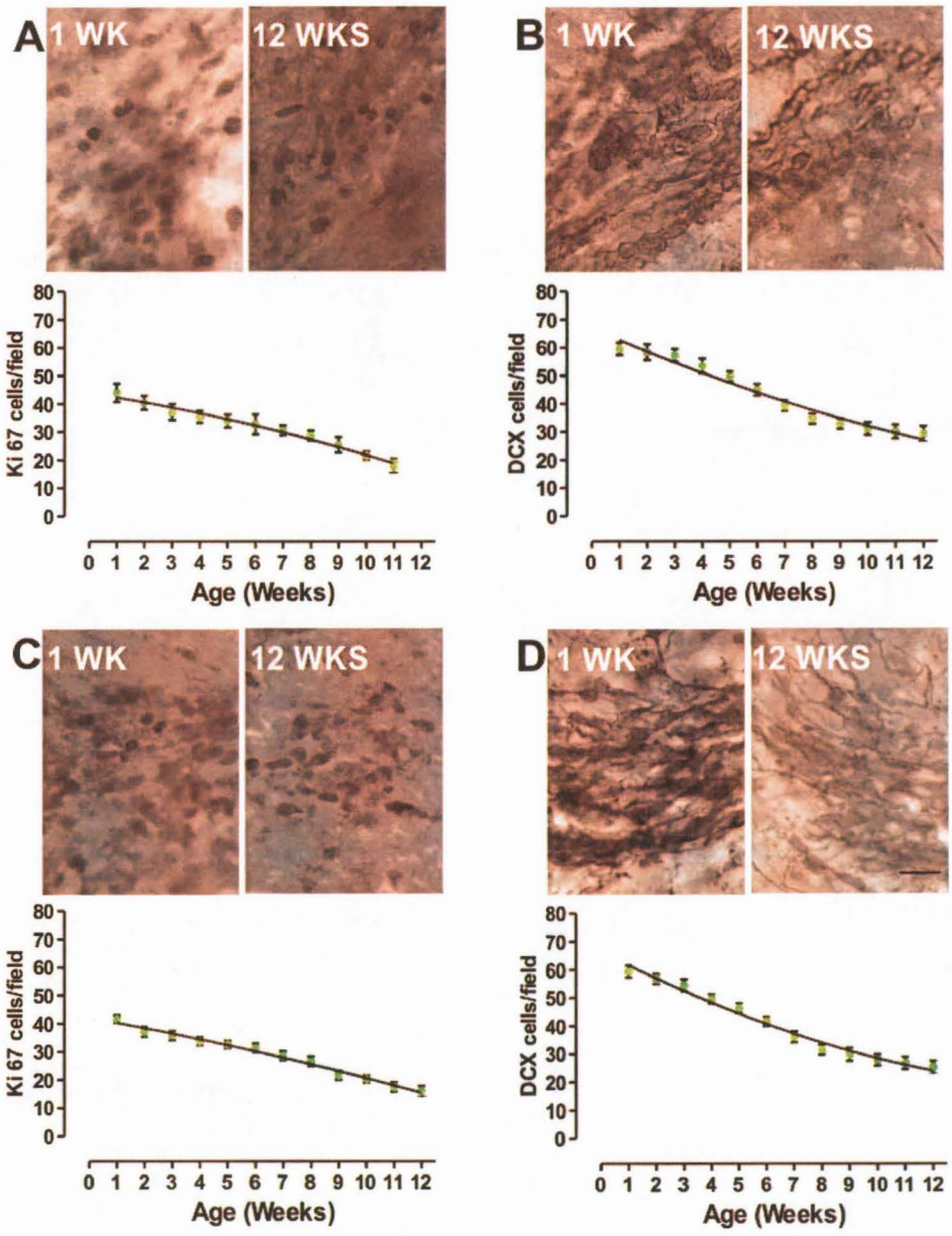
A
1 WK
12 WKS
Ki 67 cells/field
0 10 20 30 40 50 60 70 80
0 1 2 3 4 5 6 7 8 9 10 11 12
Age (Weeks)
B
1 WK
12 WKS
DCX cells/field
0 10 20 30 40 50 60 70 80
0 1 2 3 4 5 6 7 8 9 10 11 12
Age (Weeks)
C
1 WK
12 WKS
Ki 67 cells/field
0 10 20 30 40 50 60 70 80
0 1 2 3 4 5 6 7 8 9 10 11 12
Age (Weeks)
D
1 WK
12 WKS
DCX cells/field
0 10 20 30 40 50 60 70 80
0 1 2 3 4 5 6 7 8 9 10 11 12
Age (Weeks)

Figure 4.5: Photomicrographs and graphs showing age-related changes in the number of Ki-67-ir (A) and DCX-ir (B) cells in the terminal portion of the rostral migratory stream that extends into the core of the olfactory bulb (OBc-RMS) of the BALB/c mouse. The number of Ki-67-ir cells sharply decreased with age in the OBc-RMS (A). Similarly, DCX-ir cells decreased with age in the OBc-RMS (B). In each figure, the photomicrographs represent the same brain region in the youngest (1 week old) and the oldest (12 weeks old) animals used in this study. Scale bar in B= 20μm and applies to all photomicrographs. Error bars correspond to the standard error of the mean (SEM).

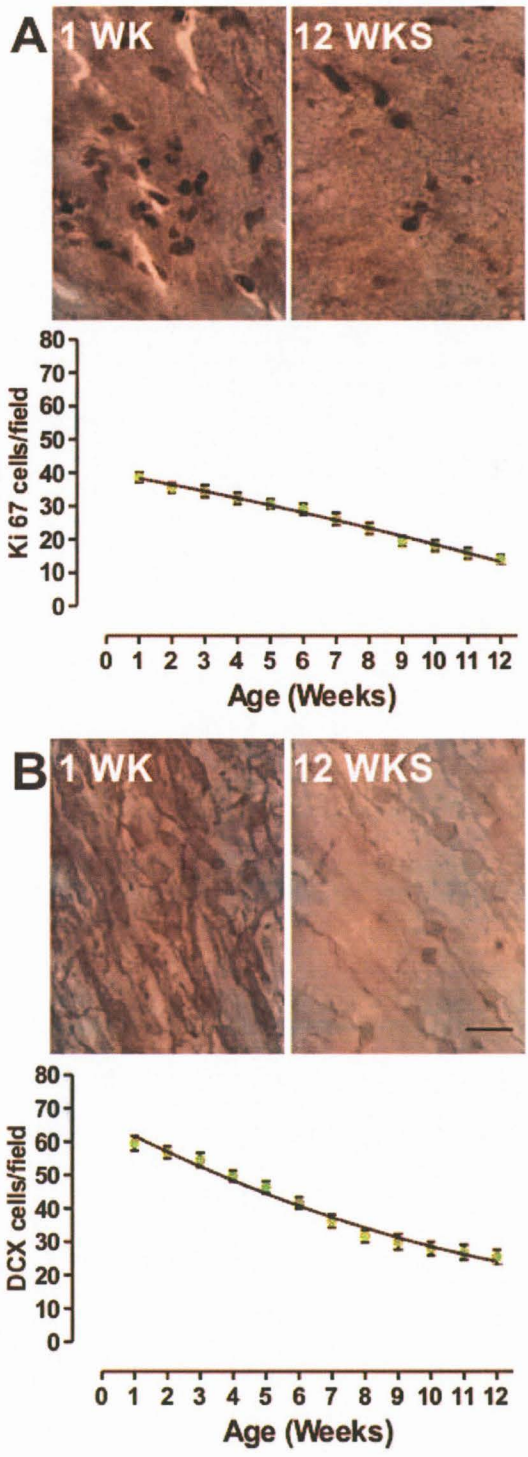
A
1 WK
12 WKS
Ki 67 cells/field
80
70
60
50
40
30
20
10
0
0 1 2 3 4 5 6 7 8 9 10 11 12
Age (Weeks)
B
1 WK
12 WKS
DCX cells/field
80
70
60
50
40
30
20
10
0
0 1 2 3 4 5 6 7 8 9 10 11 12
Age (Weeks)

Figure 4.6: Photomicrographs and graphs showing age-related changes in the number of Ki-67-ir (A & C) and DCX-ir (B & D) cells in the anterior part of the sub ventricular (SVZa) and sub granular (SGZ) zones of the BALB/c mouse brain. The number of Ki-67-ir cells sharply decreased with age in the SVZa (A) and SGZ (C). Similarly, DCX-ir cells decreased with age in the SVZa (B) and SGZ (D). In each figure, the photomicrographs represent the same brain region in the youngest (1 week old) and the oldest (12 weeks old) animals used in this study. Scale bar in D= 20μm and applies to all photomicrographs. Error bars correspond to the standard error of the mean (SEM).

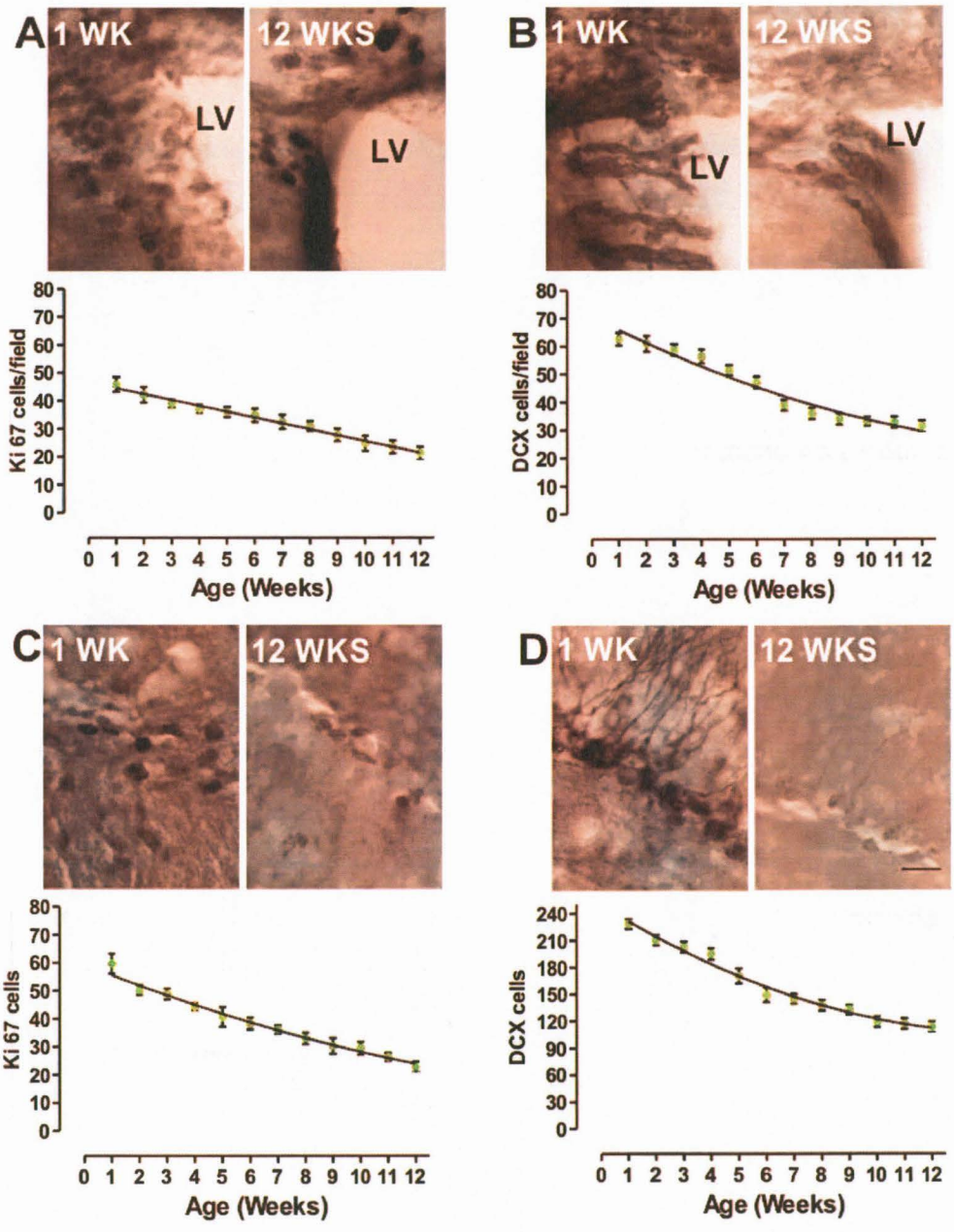
A
1 WK
12 WKS
LV
LV
Ki 67 cells/field
Age (Weeks)
B
1 WK
12 WKS
LV
LV
DCX cells/field
Age (Weeks)
C
1 WK
12 WKS
Ki 67 cells
Age (Weeks)
D
1 WK
12 WKS
DCX cells
Age (Weeks)

4.3.3 Life-history stage related changes in Ki-67 and DCX immunoreactivity in the BALB/c mouse brain

One-way analysis of variance (ANOVA) revealed significant differences in the number of Ki-67-ir cells at different life-history stages in the VL-RMS (F=137.7; P<0.0001, Fig 4.7A), HL-RMS (F=153.9; P<0.0001, Fig 4.7C), OBc-RMS (F=197.0; P<0.0001, Fig 4.7E), SVZa (F= 135.2; P<0.0001, Fig 4.8A) and SGZ (F=119.6; P<0.0001, Fig 4.8C). Between juvenile and sub adult life-history stages, Bonferroni *post hoc* analysis revealed that the number of Ki-67-ir cells significantly declined by approximately 20% in the VL-RMS (P<0.0001), HL-RMS (P<0.0001) & SVZa (P<0.0001) and approximately 25% in the OBc-RMS (P<0.0001) & SGZ (P<0.0001). Similarly, the numbers of Ki-67 positive cells declined by approximately 25% in the SVZa (P<0.0001) & SGZ (P<0.0001), approximately 30% in the VL-RMS (P<0.0001) and approximately 35% in the HL-RMS (P<0.0001) & OBc-RMS (P<0.0001) between the sub adult and adult life-history stages.

Using ANOVA, significant differences were found in the number of DCX-ir cells at different life-history stages in the VL RMS (F=134.5; P<0.0001, Fig 4.7B), HL-RMS (F=139.6; P<0.0001, Fig 4.7D), OBc-RMS (F=145.3; P<0.0001, Fig 4.7F), SVZa (F= 141.3; P<0.0001, Fig 4.8B) and SGZ (F=153.5; P<0.0001, Fig 4.8D). Bonferroni *post hoc* analysis revealed that the number of DCX-ir cells significantly declined by approximately 30% in the VL-RMS (P<0.0001), HL-RMS (P<0.0001), OBc-RMS (P<0.0001), SVZa (P<0.0001) and SGZ (P<0.0001) between the juvenile and sub adult life-history stages. Similarly, the numbers of DCX-ir cells declined by approximately 20% in the VL-RMS (P<0.0001), HL-RMS (P<0.0001), OBc-RMS (P<0.0001), SVZa (P<0.0001) and SGZ (P<0.0001) between sub adult and adult life-history stages.

Figure 4.7: Graphical representation of the life-history stage related changes in the number of Ki-67-ir (A, C &E) and DCX-ir (B, D & F) cells in the rostral migratory of the BALB/c mouse brain. The number of Ki-67-ir cells decreased with advancing life-history stages in the VL-RMS (A), HL-RMS (C) and OBc-RMS (E). Similarly, DCX-ir cells decreased with advancing life-history stages in the VL-RMS (B), HL-RMS (D) and OBc-RMS (F). Error bars correspond to the mean (SEM). ***$P<0.0001$.

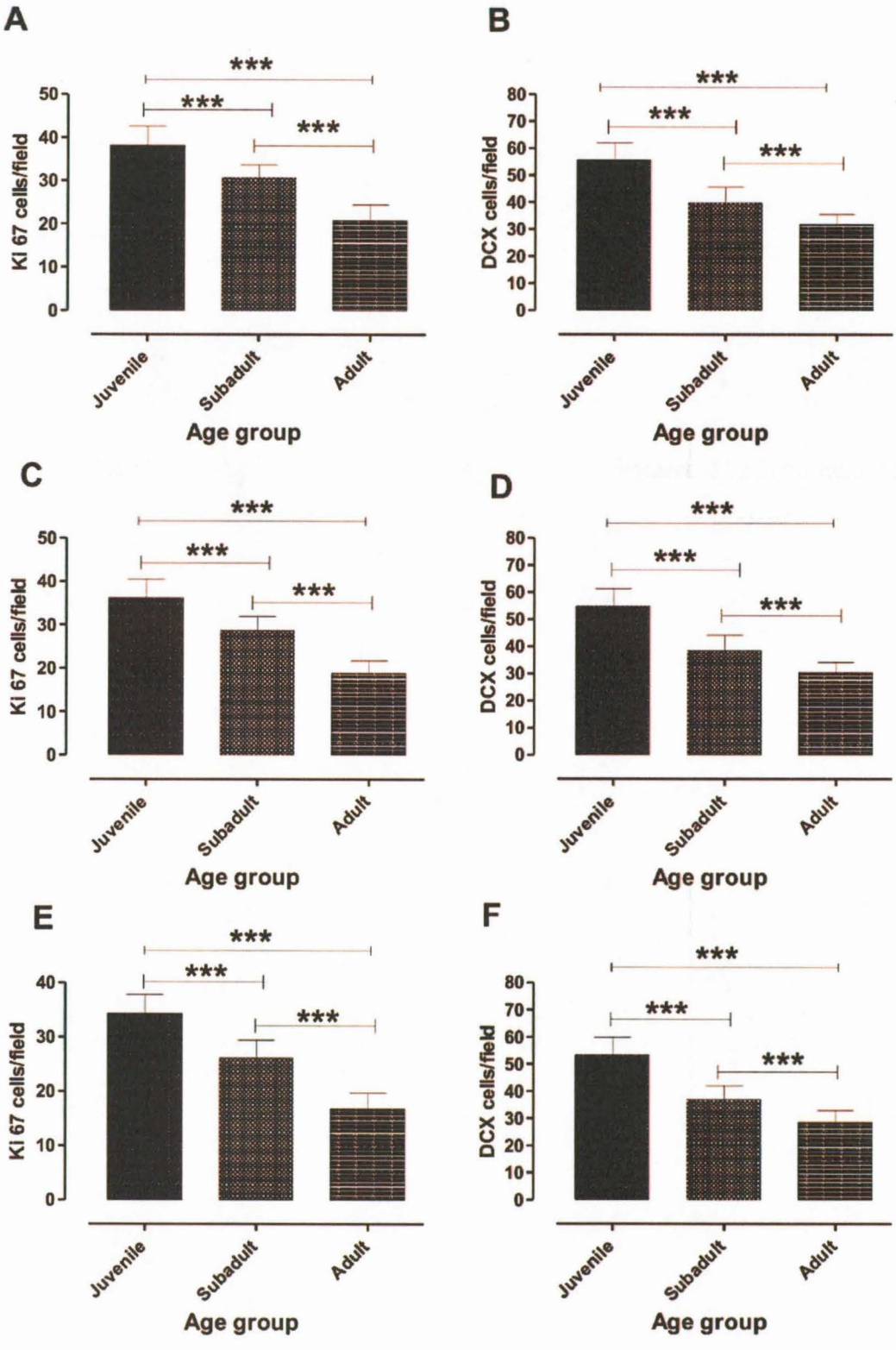
A
B
C
D
E
F
Ki 67 cells/field
DCX cells/field
***
Juvenile
Subadult
Adult
Age group

Figure 4.8: Graphical representation of the life-history stage related changes in the number of Ki-67-ir (A&C) and DCX-ir (B&D) cells the SVZa and SGZ of the BALB/c mouse brain. The number of Ki-67-ir cells decreased with advancing life-history stages in the SVZa (A) and SGZ (C). Similarly, DCX-ir cells decreased with advancing life-history stages in the SVZa (B) and SGZ (D). Error bars correspond to the standard error of the mean (SEM). ***P<0.0001.

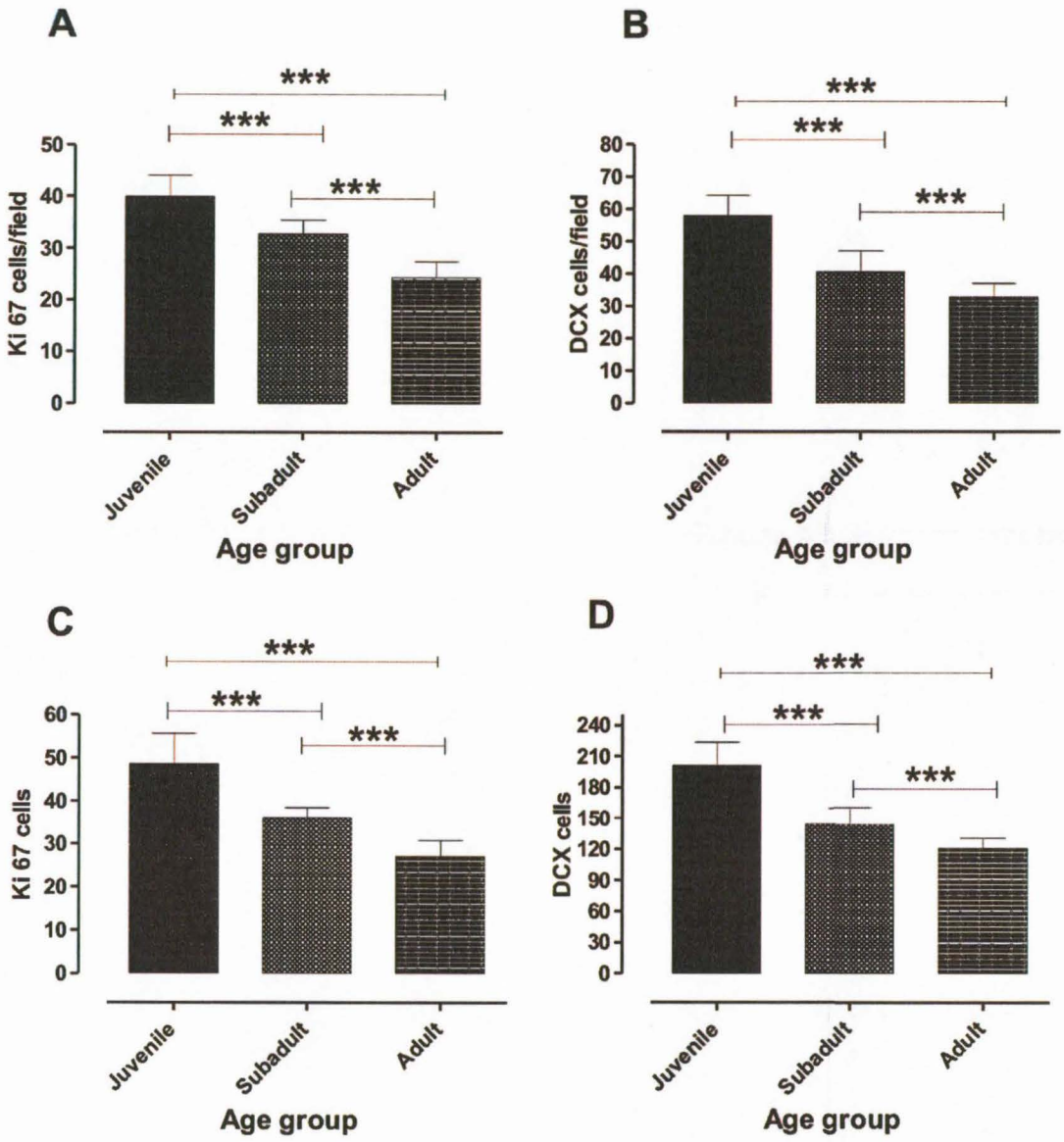
A
***
***
***
Ki 67 cells/field
50
40
30
20
10
0
Juvenile
Subadult
Adult
Age group
B
***
***
***
DCX cells/field
80
70
60
50
40
30
20
10
0
Juvenile
Subadult
Adult
Age group
C
***
***
***
Ki 67 cells
60
50
40
30
20
10
0
Juvenile
Subadult
Adult
Age group
D
***
***
***
DCX cells
240
210
180
150
120
90
60
30
0
Juvenile
Subadult
Adult
Age group

4.4 DISCUSSION

In the current study, Ki-67 and DCX immunohistochemistry was used to identify proliferating cells and immature neurons respectively in the BALB/c mouse brain. Ki-67, is a nuclear protein that is associated with ribosomal transcription and is found in the nucleus during interphase (Bullwinkel et al., 2006). However, during mitosis Ki-67 becomes associated with the surface of chromosomes (Balthazart and Ball, 2014b). Ki-67 is expressed during all active phases of the cell cycle (G1, S, G2 and mitosis) but is absent in cells that are not cycling (Go) (Scholzen and Gerdes, 2000). However, Ki-67 labelling is related to both neurogenesis and gliogenesis. DCX is a microtubule associated protein that controls polymerisation of the leading process and stabilisation of the neuroblast cytoskeleton during migration (Horesh et al., 1999). DCX, therefore, plays a critical role in the migration of immature neurons from the birth site to final positioning at the recruitment site.

4.4.1 Distribution of Ki-67 and DCX immunoreactive cells in the BALB/c mouse brain

Proliferating cells and immature neurons were observed at all ages in the sub ventricular zone of the lateral ventricles, rostral migratory stream, olfactory bulb and sub granular zone of the hippocampal dentate gyrus. Expression of both Ki-67 and DCX confirmed that these brain regions are indeed neurogenic sites and these findings extend earlier observations made by previous researchers in mammals (Kuhn et al., 1996; Enwere et al., 2004; Kondo et al., 2010; Nada et al., 2010; Encinas et al., 2011; Jinno, 2011; Kempermann, 2011; Mobley et al., 2014; Olaleye and Ihunwo, 2014; Olude et al., 2014; Fernández-Flores et al., 2018).

New neurons produced in the sub ventricular zone migrate along the lateral wall of the lateral ventricles and through the rostral migratory stream guided by the astrocytic scaffolding to reach the olfactory bulb where they differentiate into granule and periglomerular interneurons (Mobley et al., 2014). As the neuroblasts migrate through the rostral migratory stream, they retain their ability to proliferate (Mobley et al., 2014) and possibly explains the expression of Ki-67 in RMS observed in the current study.

In the olfactory bulb, mitral and tuft cells are born during embryonic development. However, granule and periglomerular interneurons are mainly born postnatally (Mirich et al., 2002). In fact, only about 25% of the bulbar interneurons are born prenatally (Bayer, 1983). The bulk of bulbar interneurons are born locally within the olfactory bulb before postnatal day 7. In addition, proliferation in the olfactory bulb after the first postnatal week is most likely related to production of glial cells as the SVZ and RMS become the major sources of new bulbar interneurons (Lemasson et al., 2005). Therefore, the Ki-67 expression in the olfactory bulb we observed in this study is most likely related to formation of neuroglia.

Within the hippocampus, Ki-67 and DCX-ir cells were also observed in the sub granular zone of the dentate gyrus at all ages investigated confirming the presence of neurogenesis in this region. In this region, new neurons are born in the sub granular zone, migrate a short distance and integrate into the granule cell layer.

In the neocortex, a few cells expressing Ki-67 and DCX were also observed. In addition, we observed Ki-67 cells migrating from the dorsal RMS through the corpus callosum to reach the neocortex (Fig 4.2A) suggesting that the proliferating cells and immature neurons observed in the cortex could have migrated from the dorsal RMS. These observations confirmed that the neocortex continues to recruit new neurons at all ages studied. Our observations are in agreement with the findings of other authors who have reported presence of neurogenesis in the mammalian neocortex (Ihunwo and Pillay, 2007; Chawana et al., 2013; Olude et al., 2014). In contrast to our findings, Olaleye and Ihunwo (2014) observed only DCX but not Ki-67 immunoreactivity in the four striped mouse neocortex. This variation could possibly reflect species (four striped mouse vs BALB/c mouse) and habitat (wild vs laboratory bred) specific differences.

Ki-67 but not DCX immunoreactivity was observed in the tectum and cerebellum. The proliferation observed in these brain regions is presumably related to production of neuroglial cells and not neurons since no immature neurons were observed.

4.4.2 Age and life-history stage related changes in Ki-67 and DCX expression in the BALB/c mouse brain

In this study, the number of proliferating cells and immature neurons in the SVZ and RMS significantly decreased with postnatal age and life history periods (i.e higher during juvenile periods and lower during adulthood) of the BALB/c mouse brain. Our results further revealed that there was no period during the first 12 postnatal weeks where neurogenesis was stable over extended periods defining life-history stages corresponding to juvenile, sub adult and adult. Age-related decreases in neurogenesis in the SVZ and RMS have been reported previously in laboratory mice (Enwere et al., 2004; Luo et al., 2006; Shook et al., 2012; Mobley et al., 2014), laboratory rats (Chen et al., 2003), the giant African rat (Olude et al., 2014) and more recently dogs (Fernández-Flores et al., 2018). These age-related decreases in neurogenesis in the SVZ and RMS have also been proposed to be functionally linked to the olfactory dysfunction that is observed during aging (Enwere et al., 2004). The decreases in neurogenesis in the SVZ and RMS with age are thought to be as a consequence of either a reduction in the neuronal stem cell proliferation (Kuhn et al., 1996; Tropepe et al., 1997; Enwere et al., 2004; Luo et al., 2006) or lengthening of the cell cycle (Tropepe et al., 1997; Maslov et al., 2004). The decline in cell proliferation observed in the SVZ and RMS has been reported to be related in part to a reduction in epidermal growth factor receptor (EGFR) signaling, fibroblast growth factor 2 (FGF 2) and transforming growth factor (TGF), all of which have been shown to decline with age (Jin et al., 2003; Enwere et al., 2004; Sun et al., 2006). Intracerebral infusions of FGF 2 or heparin binding EGF in aged rodents was reported to restore SVZ and RMS neurogenesis to levels found in young rodents (Jin et al., 2003). In addition, this ability to respond to exogenous factors suggests that neuronal stem cells in the SVZ and RMS become quiescent with aging but retain their capacity to form new neurons when appropriately stimulated. Furthermore, age dependent reductions in telomerase activity have also been implicated in age-related down regulation of neurogenesis in the SVZ. Caporaso et al. (2003) reported that the young rodent SVZ contains higher telomerase activity compared to the adults. Interestingly, telomerase activity appears to mirror proliferation levels in the SVZ (Caporaso et al., 2003).

In the SGZ of the dentate gyrus, a similar relationship between age or life-history stage and the number of proliferating cells or immature neurons was also observed. Similar age-related changes in hippocampal neurogenesis were previously reported in several mammals including laboratory mice (Kronenberg et al., 2006; Nada et al., 2010), wild mice (Amrein et al., 2004), laboratory rats (Drapeau et al., 2003; Jessberger et al., 2009) African giant rats (Olude et al., 2014), mole rats (Amrein et al., 2014) and Humans (Knoth et al., 2010). These observed age-related reductions in neurogenesis in the dentate gyrus could be functionally related to the spatial memory deficits observed in aged animals (Kuhn et al., 1996; Drapeau et al., 2003).

Although the exact mechanisms underlying age-related reductions in hippocampal neurogenesis are poorly understood, a few processes have been singled out. These include a reduction in the neuronal stem cell pool, reduced proliferation of neuronal stem cells or progenitors, reduced survival of neuronal stem cells or progenitors and reduced neuronal lineage commitment (Encinas et al., 2011). Encinas et al. (2011) reported division coupled conversion of neuronal stem cells into mature astrocytes in the hippocampus of aged rodents.

Several factors have been implicated in age-related down regulation of hippocampal neurogenesis among them glucocorticoids and growth factors such as insulin-like growth factor-1 (IGF-I), FGF-2 and vascular endothelial growth factor (VEGF). Glucocorticoid receptors are strongly expressed in the granule cells of the hippocampus and in neuronal stem cells (Garcia et al., 2004). During the early postnatal period, rodents have been shown to exhibit very low levels of circulating glucocorticoids and to be relatively resistant to stress (Sapolsky and Meaney, 1986). Incidentally, this early postnatal period is also associated with high levels of hippocampal neurogenesis (Bayer, 1983). Furthermore, previous studies have shown that glucocorticoid levels naturally rise with increasing postnatal age in rodents as the hypothalamic-pituitary-adrenal (HPA) axis matures (Sapolsky, 1992; Dalm et al., 2005) and this rise coincides with a reduction in the numbers of newly generated neurons (Cameron and Gould, 1994; Seki and Arai, 1995; Kuhn et al., 1996; Cameron and McKay, 1999a).The HPA axis matures during adolescence, thereby

providing increased levels of glucocorticoids which have drastic effects on hippocampal neurogenesis in adult animals (Lupien et al., 2009). Conversely, elimination of glucocorticoids by adrenalectomy increases proliferation of neuronal progenitors and formation of new neurons in the hippocampus (Cameron and McKay, 1999a; Montaron et al., 1999; Montaron et al., 2006).

Growth factors (IGF-I, FGF-2 and VEGF) increase neuronal stem cell proliferation in the hippocampal dentate gyrus and the concentration of these factors in serum or expression of their receptors in the hippocampus have reported to be reduced in adults and aged animals compared to juvenile animals (Lai et al., 2000; Jin et al., 2003; Shetty et al., 2005; Sun et al., 2006). In addition, intraventricular infusion of these growth factors were reported to increase neurogenesis in the adult or aging hippocampus (Lai et al., 2000; Jin et al., 2003; Sun et al., 2006; Rai et al., 2007).

4.5 CONCLUSION

Neurogenesis persists throughout the life-history periods of the BALB/c mouse in the sub ventricular zone of the lateral ventricles, rostral migratory stream, olfactory bulb, sub granular zone of the dentate gyrus and the neocortex. In addition, neurogenesis declines sharply with postnatal age in the SVZ, RMS and SGZ of the BALB/c mouse brain. Although cell proliferation persists in the tectum and cerebellum of the BALB/c mouse, it is presumably related to the production of neuroglia.

CHAPTER 5: AGE- RELATED CHANGES IN PROLIFERATION NUCLEAR ANTIGEN (PCNA) AND DOUBLECORTIN (DCX) EXPRESSION IN THE POST-METAMORPHIC SOUTH AFRICAN CLAWED (*XENOPUS LAEVIS*) FROG BRAIN.

5.1 INTRODUCTION

Neurogenesis is a process through which new neurons are added to the brain. This process involves progenitor cell proliferation, differentiation, migration and integration of the newly formed neuroblasts into the existing neuronal circuitry of target areas (Kaslin et al., 2008). Primary neurogenesis establishes the central nervous system during embryogenesis (Thuret et al., 2015). Secondary neurogenesis, however, refers to the continuous production and addition of new neurons to the brain after birth or hatching. Over the last few years, secondary neurogenesis has received a lot of attention having been found to be a common trait shared by all vertebrates. In mammals, secondary neurogenesis is restricted to the olfactory bulbs and the dentate gyrus of the hippocampus (Ihunwo and Pillay, 2007; Chawana et al., 2013; Olaleye and Ihunwo, 2014; Olude et al., 2014). However, this process is more widespread in the non-mammalian vertebrate brains including amphibians.

In amphibians, neurogenesis was widely studied during embryonic development of the brain (Chapman et al., 2006; Simmons et al., 2006; Simmons et al., 2008; Herrgen and Akerman, 2016; Moreno and González, 2017) or in relation to brain regeneration following experimental lesions (Endo et al., 2007; Parish et al., 2007; Maden et al., 2013; Kirkham et al., 2014; Amamoto et al., 2016). Reports from these studies demonstrate that neurogenesis takes place in both urodele and anuran amphibian brains under normal physiological or experimental conditions. However, a closer analysis of the available literature on amphibian neurogenesis reveals three main problems. Firstly, neurogenesis in anuran amphibians has mostly been studied in detail in the developing brain during the larval and pre-metamorphic stages. Secondary neurogenesis in the post-metamorphic anuran brain is either poorly understood or is not well documented. Secondly, most secondary neurogenesis studies focused mainly on mapping progenitor cell proliferation in the anuran brain. Indeed, cell proliferation has been mapped in pre and post metamorphic brains of the *X. laevis* (D'Amico et al., 2011; Herrgen and Akerman, 2016; Moreno and González, 2017), *R. esculenta* (Raucci et al., 2006; Cerri et al., 2009), *R. catesbiana* (Chapman et al., 2006; Simmons et al., 2006; Simmons et al., 2008) and *H. ceneria* (Almli and Wilczynski, 2007). However, progenitor cell proliferation constitutes only one stage of neurogenesis and provides no information on the fate of the newly formed cells

(neurons or glial cells). Thirdly, age dependent changes in neurogenesis have only been reported during the pre-metamorphic stages of development (Simmons et al., 2008; Thuret et al., 2015; Moreno and González, 2017). To date, no studies have quantitatively investigated changes in neurogenic activity in the post-metamorphic *X. laevis brain* across the major life-history stages, i.e juvenile, sub adult and adult stages.

Previous studies mostly relied on exogenous markers of neurogenesis such as titriated thymidine (H^3–thymidine) and more recently 5-bromo-2'-deoxyuridine (BrdU) (Bernocchi et al., 1990; Almli and Wilczynski, 2007; Simmons et al., 2008; D'Amico et al., 2011). Although these markers allow investigators to monitor survival of the newly formed cells, their usage is limited by their short half-lives as they become diluted with each successive cell division. In addition, BrdU has also been shown to induce DNA damage (Balthazart and Ball, 2014b). In this paper, we report a detailed neuroanatomical mapping of cell proliferation and neuronal incorporation in the brains of juvenile, sub adult and adult African clawed frogs (*Xenopus laevis*) using endogenous markers PCNA and DCX respectively. In addition, the current study also quantitatively describes how PCNA and DCX expression changes with age in the telencephalon of the post-metamorphic *X. laevis*.

5.2 MATERIALS AND METHODS

5.2.1 Animals

Forty-six post-metamorphic (juvenile, ages 8 to 20 weeks old, n = 34; sub adult, ages 36 to 44 weeks old, n= 6 and adult, 48 to 60 weeks old, n= 6) South African clawed frogs obtained from the African Xenopus Facility (Knysna, Western Cape, South Africa) were used in this study. The animals were housed at the Central Animal Services (CAS) of the University of the Witwatersrand. During this experimental period, the frogs were kept in tape water maintained at 25 ± 3°C, fed *ad libitum* and maintained on a 12:12 hr light-dark cycle. All experimental animals were handled according to the ethical principles for Animal Research approved by the University of the Witwatersrand Animal Ethics Screening Committee (AESC/2014/35/A), which

correspond with those of the National Institute of Health (NIH) for care and use of animals in scientific experimentation.

5.2.2 Tissue collection and processing

Following euthanasia by an intraperitoneal injection of Euthapent (0.5 – 1 ml/kg), the animals were decapitated and the heads were immersion fixed *in toto* in 4 % paraformaldehyde in 0.1 M phosphate buffer (PB, pH 7.4) solution. Brains were carefully removed from the skull, post-fixed overnight in 4 % paraformaldehyde in 0.1M PB, weighed before being transferred into 30% sucrose in 0.1M PB until equilibration. The brains were sectioned in a coronal plane at 20 µm using a cryostat (Shandon Cryotome E, Thermo Fischer scientific, UK) at -24 °C and repeated series of 5 sections were collected free-floating into 48 multi-well plates containing 0.1 M PB. The first series of sections was mounted on gelatin- coated slides and stained with 1 % cresyl violet for anatomical orientation. The second and third series were used for PCNA and DCX immunohistochemistry respectively. The remaining two series were stored in a cryoprotectant solution at -20 °C for future use.

5.2.3 Immunohistochemistry

Brain sections were pre-treated for 30 min at room temperature under gentle shaking with an endogenous peroxidase inhibitor solution containing 0.1 M PB, 100% methanol and 100% H_2O_2 in the ratio 49.2%: 49.2%:1.66%. Following three 10-min rinses in 0.1 M PB, the sections were subsequently pre-incubated in a blocking buffer solution [3 % normal horse serum or 3 % normal goat serum, 2 % bovine serum albumin, 0.25 % Triton X-100 in 0.1 M PB] for 2 h under gentle shaking at room temperature to prevent non-specific binding. Sections were then transferred into a primary antibody solution [1:500, mouse anti-PCNA (ab29, Abcam, USA) or 1: 500, rabbit anti-DCX (ab18723, Abcam, USA), in the blocking buffer solution] and were incubated for 48 h at 4 °C under gentle shaking. Following incubation, sections were subjected to three 10-min rinses in 0.1 M PB before being incubated in secondary antibody solution [1:1000 biotinylated anti-mouse IgG (Novocastra, UK) or 1: 1,000 dilution of biotinylated anti-rabbit IgG (BA-5000; Vector Laboratories, USA) in blocking buffer solution] for 2 h at room temperature under gentle shaking. Following

three 10-min rinses in 0.1 M PB, the sections were incubated in an avidin-biotin solution [1: 125 A and 1: 125 B (Vector Laboratories) in 0.1 M PB] for 1 h. The sections were then transferred into three 10-min 0.1 M PB rinses before being placed in a solution containing 0.05% 3, 3 di-amino-benzidine tetrachloride (DAB) in 0.1 M PB for 5 min. To each 1 ml of this solution, 3.3 µl of 30% H_2O_2 were added, and chromatic precipitation was visually monitored under a low power stereomicroscope.

Development was subsequently stopped by placing the sections in 0.1 M PB, followed by a final 10-min rinse in 0.1 M PB. Sections were mounted on 0.5% gelatine-coated slides, left to dry overnight, dehydrated in a graded series of alcohols, cleared in xylene and cover slipped with DPX. To ensure that non-specific staining was not affecting the results, control sections taken at random were processed in the same manner, but either the primary or the secondary antibody was omitted. No labelled cells were observed in either case.

5.2.4 Data Analysis

5.2.4.1 Qualitative analysis

Sections were analysed qualitatively with both low and high power light microscopy to yield a comparative description of the distribution of PCNA and DCX-immunoreactive (ir) cells. Brain structures were identified and nomenclature used according to the stereotaxic atlas of the CNS of *R. pipiens* (Wada et al., 1980). The relative densities of immunostained structures were visually compared and recorded on a scale ranging from absent (-) to low (+) to moderate (++) to high (+++). A second observer was used to eliminate observer bias (Chawana et al., 2013; Mazengenya et al., 2017; Nkomozepi et al., 2018)

5.2.4.2 Quantitative analysis

Quantification of PCNA and DCX-ir cells was carried out in areas of the telencephalon that exhibited high expression for these markers. The PCNA-ir cells were quantified in the ventral and dorsal reaches of the lateral ventricles whereas DCX-ir cells were quantified in the medial pallium (MP), lateral pallium (LP), septum

(S) and striatum (St) in all the animals studied. The quantification of PCNA and DCX-ir cells was done using computer assisted image analysis by the first author (PN) who was blinded to the ages of the animals. Sections were digitized using an AxioCam HRC digital camera linked to a Zeiss Axioplan 2 compound microscope (40X objective) and PCNA or DCX-ir cells in each camera field (0.0816 mm^2) were counted using the cell counter function of ImageJ (Schneider et al., 2012).

The camera field for quantification was placed in a standardized manner based on predefined anatomical landmarks guided by Nissl stained sections using the anatomical scheme of Moreno and González (2004) (for the S and St) and Westhoff and Roth (2002) (for the MP and LP). Briefly, four coronal sections of the telencephalon of each animal corresponding to plate figures 3, 5, 6 and 9 of the stereotaxic atlas of the CNS of *R. pipiens* (Wada et al., 1980) were used for quantification of PCNA-ir or DCX-ir cells. Representative photomicrographs of the *X. laevis* showing neurogenic activity were acquired using the AxioCam HRC digital camera and were prepared with the Adobe Photoshop 7.0 software (Adobe Systems, Mountain View, CA). No pixelation adjustment or manipulation of the captured images was undertaken, except for the adjustment of contrast and brightness.

5.2.4.3 Statistical analysis

For each animal, PCNA or DCX-ir counts obtained from different rostrocaudal levels of the same brain area quantified were averaged. The Shapiro-Wilks normality test was used to test the normality of data in all the variables. For all the variables, the data followed a normal distribution ($P>0.05$). The correlation between age and the mean PCNA or DCX-ir cell counts for each brain area quantified was tested using Pearson's correlation analysis. Furthermore, the mean counts of PCNA or DCX -ir cells for each brain area quantified at different life history stages (i.e juvenile, sub adult and young adult) were computed and compared using one-way analysis of variance (ANOVA) followed by Bonferroni's *post hoc* test. All analyses were performed using Graphpad prism 5 software (Graphpad software, CA). All results were expressed as means ± standard deviation and a significance level of $P<0.05$ was used.

5.3 RESULTS

5.3.1 Distribution of PCNA in the South African clawed frog

5.3.1.1 Olfactory bulb.

In the olfactory bulb of juvenile frogs, a high density of PCNA-ir cells were observed in the lining of the olfactory ventricles. More specifically, PCNA-ir cells were concentrated along the dorsal, medial and lateral walls of the olfactory ventricle (Fig 5.1 A). A similar pattern of PCNA immunoreactivity was observed in sub adult and adult frogs although the density was comparatively lower than that observed in juvenile frogs (Table 5.1).

5.3.1.2 Telencephalon

In the telencephalon, PCNA-ir cells were observed mainly in the lining of the lateral ventricle (Figs 5.1 B-F). In the rostral telencephalon, a high density of PCNA-ir cells were observed mainly in the ventricular walls adjacent to the dorsal, lateral and medial pallial areas dorsally and striatal and septal areas of the sub pallium ventrally. At mid-telencephalic levels, a high density of PCNA-ir cells was mainly concentrated along the ventral aspects of the lateral ventricles adjacent to the septum, nucleus accumbens and striatum. Furthermore, a few PCNA-ir cells were also observed in the parenchyma of the striatum (Fig 5.1 D). At more caudal levels, PCNA-ir cells were mainly aggregated in the ventricular lining adjacent to the DP and MP.

The distribution of PCNA-ir cells in sub adult and adult frogs was similar to that of juvenile frogs. However, the density of PCNA-ir cells in the juvenile frogs was comparatively higher than that observed in sub adult and adult frogs (Table 5.1).

5.3.1.3 Diencephalon

In juvenile frogs, no PCNA-ir cells were observed in the ventricular and parenchymal areas of the diencephalon except for a few cells seen in the preoptic area (POA) (Fig 5.1 F). In addition, a few PCNA-ir cells were also observed in the ventricular lining of the adjacent to the caudal parts of the ventral hypothalamus (VH). A similar pattern of PCNA expression was also observed in the diencephalon of sub adult and adult frogs (Table 5.1).

Figure 5.1: Photomicrographs showing the distribution PCNA-ir cells in the *X. laevis* brain. PCNA-ir cells were concentrated in the lining of the olfactory ventricles (A), telencephalic ventricles adjacent to the DP, MP, LP, St (B-E) and the 3rd (III) ventricle adjacent to the POA (F). Black arrows show PCNA-ir cells in the striatum. Scale bar in F = 20 µm and applies to A, B, C, D and E. See list of abbreviations for abbreviations used in the table.

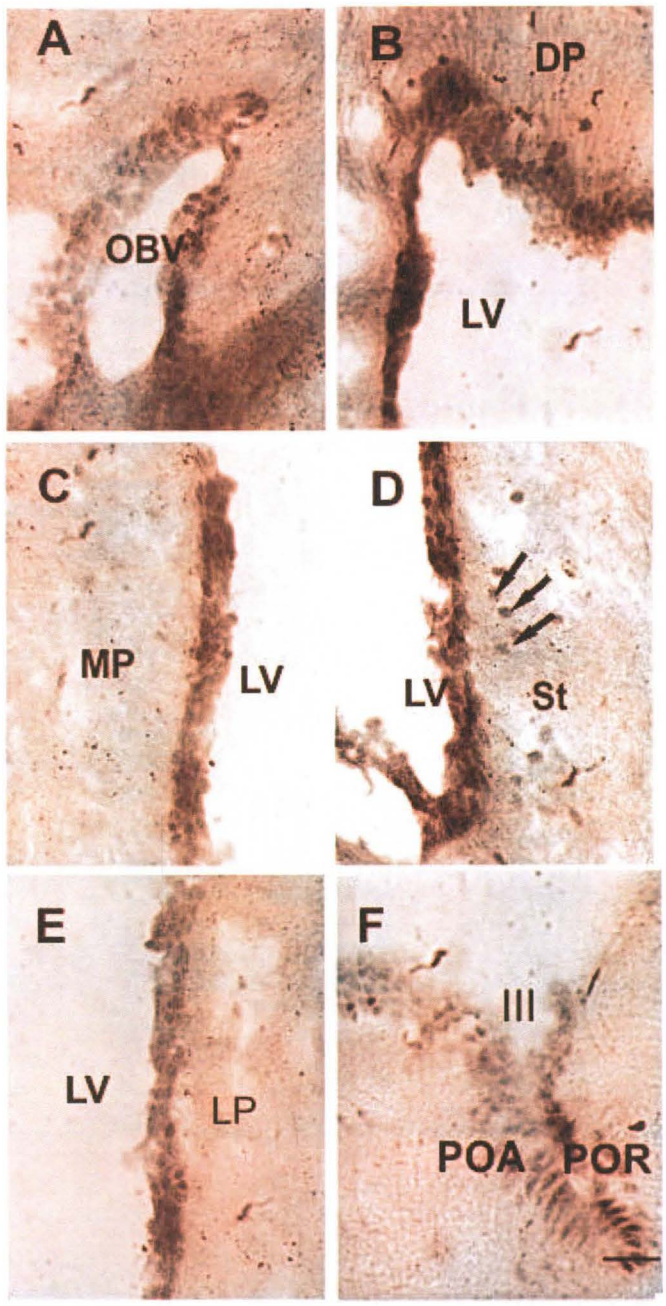
A
OBV
B
DP
LV
C
MP
LV
D
LV
St
E
LV
LP
F
III
POA
POR

Table 5.1: Age-related changes in PCNA immunoreactivity in the *X. laevis* brain

		Age															
		9 weeks	10 weeks	11 weeks	12 weeks	13 weeks	14 weeks	15 weeks	16 weeks	17 weeks	18 weeks	19 weeks	20 weeks	36 weeks	44 weeks	48 weeks	60 weeks
OB	OBV	+++	+++	+++	+++	+++	+++	+++	+++	+++	+++	++	++	++	++	++	++
	OB	-	-	-	-	-	-	-	-	-	-	-	-	-	-	-	-
TEL	LV	+++	+++	+++	+++	+++	+++	+++	+++	+++	+++	+++	+++	++	++	++	++
	MP	-	-	-	-	-	-	-	-	-	-	-	-	-	-	-	-
	LP	-	-	-	-	-	-	-	-	-	-	-	-	-	-	-	-
	DP	-	-	-	-	-	-	-	-	-	-	-	-	-	-	-	-
	St*	-	-	-	-	-	-	-	-	-	-	-	-	-	-	-	-
	S	-	-	-	-	-	-	-	-	-	-	-	-	-	-	-	-
DIE	3rd V	+	+	+	+	+	+	+	+	+	+	+	+	+	+	+	+
	POA**	-	-	-	-	-	-	-	-	-	-	-	-	-	-	-	-
	Hypo**	-	-	-	-	-	-	-	-	-	-	-	-	-	-	-	-
	Thal	-	-	-	-	-	-	-	-	-	-	-	-	-	-	-	-
MES	TECT	-	-	-	-	-	-	-	-	-	-	-	-	-	-	-	-
	MID	-	-	-	-	-	-	-	-	-	-	-	-	-	-	-	-
RHOM	4th V	+	+	+	+	+	+	+	+	+	+	+	+	+	+	+	+
	CB	++	++	++	++	++	++	++	++	++	++	++	+	+	+	+	+

+++ High density, ++ medium density, + low density, - absent. * Few PCNA-ir cells were observed in the striatum. ** PCNA-ir cells were only observed in the ventricle adjacent to the preoptic area and caudal part of the ventral hypothalamus. See list of abbreviations for abbreviations used in the table.

5.3.1.4 Mesencephalon and rhombencephalon

No PCNA-ir cells were observed in the mesencephalon of juvenile, sub adult and adult frogs. Additionally, the rhombencephalon, with the exception of the cerebellum, was devoid of PCNA-ir cells. In the cerebellum, PCNA-ir cells were observed in the granule cell layer across all age groups studied (Table 5.1). However, no PCNA-ir cells were observed in the molecular and Purkinje cell layers of the cerebellum.

5.3.2 Distribution of DCX in the South African clawed frog

5.3.2.1 Olfactory bulb.

In the olfactory bulb of juvenile frogs, a high density of DCX-ir cells were observed along the walls of the olfactory ventricles and parenchyma adjacent to the ventricles. Similarly, DCX-ir were also observed in the olfactory bulb of sub adult and adult frogs although the density was lower compared to that found in juveniles (Table 5.2).

5.3.2.2 Telencephalon

Across all age groups, high densities of DCX-ir cells were mainly concentrated along the lining of the telencephalic ventricles. Although DCX-ir cells were also observed in the ventricular lining, highest densities of these cells were observed ventrally in the ventricular lining adjacent to the sub pallium. Additionally, medium densities of DCX-ir cells were also observed in the parenchyma of the LP and MP (Figs 5.2 B and C). Furthermore, comparatively higher densities of DCX-ir cells were observed in the striatum, septum and nucleus accumbens (Figs 5.2D and F). Although the distribution of DCX-ir cells in the telencephalon was identical at all ages studied, the density of DCX-ir cells in the juvenile frogs was comparatively higher than that of sub adult and adult frogs (Table 5.2).

Figure 5.2: Photomicrographs showing the distribution of DCX-ir cells in the *X. laevis* telencephalon. A: Low power cross sectional photomicrograph of the mid-telencephalon; B, C, D, E and F: Showing the distribution of DCX-ir cells in the LP, MP, St, S and VH respectively at high power. White arrows in F show DCX-ir cells in the VH. Scale bar in A = 200 µm & in F = 20 µm and applies to B, C, D and E. See list of abbreviations for abbreviations used in this figure.

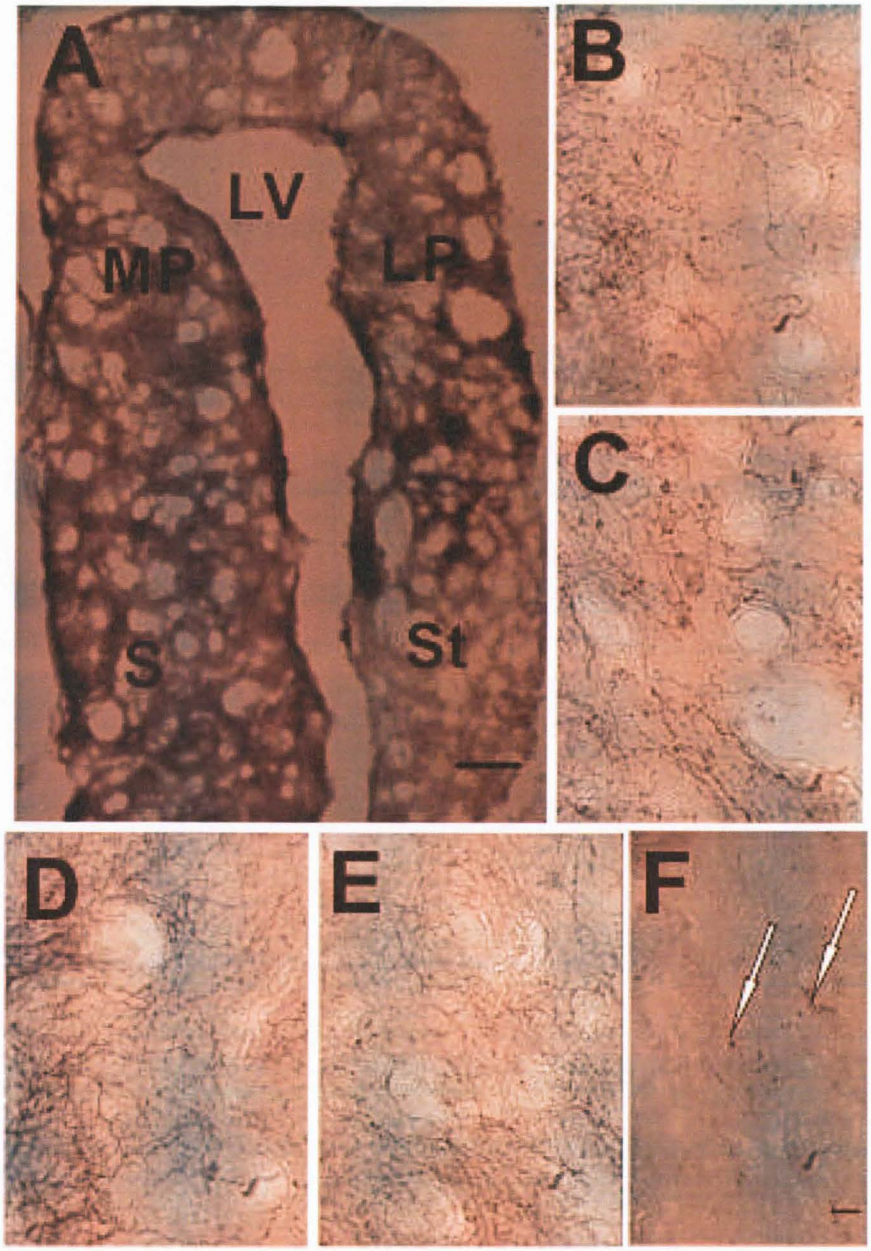
A
LV
MP
LP
S
St
B
C
D
E
F

Table 5.2: Age-related changes in DCX immunoreactivity in the *X. laevis* brain

		Age															
		9 weeks	10 weeks	11 weeks	12 weeks	13 weeks	14 weeks	15 weeks	16 weeks	17 weeks	18 weeks	19 weeks	20 weeks	36 weeks	44 weeks	48 weeks	60 weeks
OB	OBV	+++	+++	+++	+++	+++	+++	+++	+++	+++	+++	+++	+++	++	++	++	++
	OB	+++	+++	+++	+++	+++	+++	+++	+++	+++	+++	+++	+++	++	++	++	++
TEL	LV	+++	+++	+++	+++	+++	+++	+++	+++	+++	+++	+++	+++	++	++	++	++
	MP	+++	+++	+++	+++	+++	++	++	++	++	++	++	++	+	+	+	+
	LP	++	++	++	++	++	++	++	++	++	++	++	+	+	+	+	+
	DP	++	++	+	+	+	+	+	+	+	+	+	+	+	+	+	+
	St/Acc	+++	+++	+++	+++	+++	+++	+++	+++	+++	+++	+++	+++	++	++	++	++
	S	+++	+++	+++	+++	+++	+++	+++	+++	++	++	++	++	++	++	++	++
DIE	3rd V	-	-	-	-	-	-	-	-	-	-	-	-	-	-	-	-
	POA	+	+	+	+	+	+	+	+	+	+	+	+	+	+	+	+
	Hypo*	+	+	+	+	+	+	+	+	+	+	+	+	+	+	+	+
	Thal	-	-	-	-	-	-	-	-	-	-	-	-	-	-	-	-
MES	TECT	-	-	-	-	-	-	-	-	-	-	-	-	-	-	-	-
	MID	-	-	-	-	-	-	-	-	-	-	-	-	-	-	-	-
RHOM	4th V	-	-	-	-	-	-	-	-	-	-	-	-	-	-	-	-
	CB	++	++	++	++	++	++	++	++	++	++	++	++	+	+	+	+

+++ High density, ++ medium density, + low density, - absent. * DCX-ir cells observed only in the caudal part of the ventral hypothalamus. See list of abbreviations for abbreviations used in this table.

5.3.2.3 Diencephalon, mesencephalon and rhombencephalon

In the diencephalon, fewer DCX-ir cells were observed in the parenchyma of the POA and VH (Fig 5.2F) at all ages studied. In addition, DCX-ir cells were also observed in the granular cell layer of the cerebellum at all ages studied (Table 5.2).

5.3.3 Age-related changes in the number PCNA and DCX-ir cells in the telencephalon

Pearson's correlation analysis revealed that the number of PCNA-ir cells significantly decreased with age in the dorsal (r =-0.9817; P<0.0001; Fig 5.3A) and ventral (r = -0.9746; P<0.0001; Fig 5.3B) reaches of the telencephalic ventricles.

Similarly, the number of DCX-ir cells decreased significantly with age in the LP (r =-0.9243; P<0.0001; Fig 5.4 A), MP (r = -0.9244; P<0.0001, Fig 5.4B), S (r =-0.9641; P<0.0001; Fig 5.4C) and St (r =-0.9905; P<0.0001; Fig 5.4D).

Figure 5.3: Photomicrographs and graphs showing age-related changes in the number of PCNA-ir cells in the dorsal (A) and ventral (B) ventricular zones of the *X. laevis* telencephalon. Generally, the number of PCNA-ir cells in both the dorsal (A) and ventral (B) ventricular zones of the *X. laevis* telencephalon significantly declined with age. Error bars correspond to the standard error of the mean (SEM).

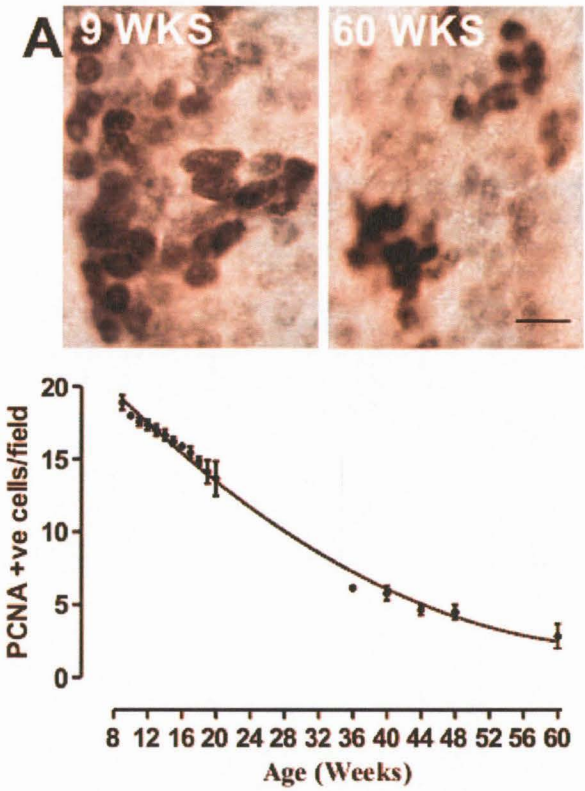
A
9 WKS
60 WKS
PCNA +ve cells/field
0
5
10
15
20
8 12 16 20 24 28 32 36 40 44 48 52 56 60
Age (Weeks)

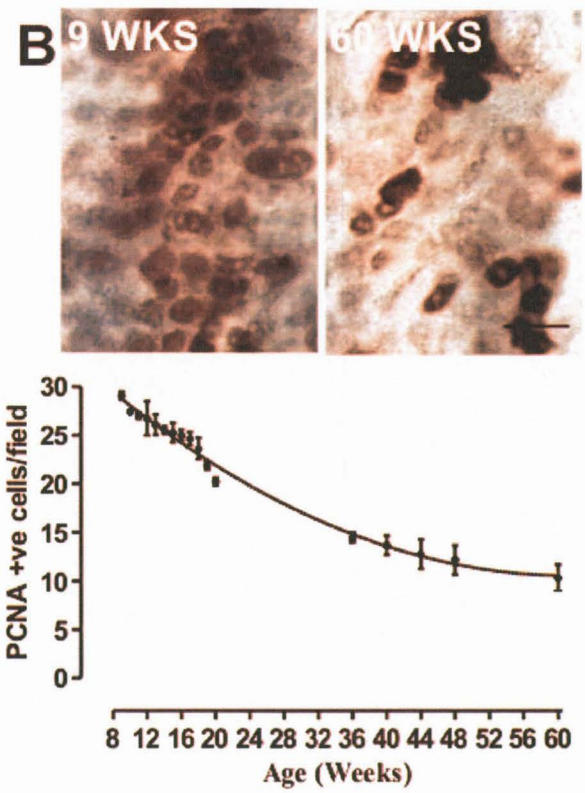
B
9 WKS
60 WKS
PCNA +ve cells/field
0
5
10
15
20
25
30
8 12 16 20 24 28 32 36 40 44 48 52 56 60
Age (Weeks)

Figure 5.4: Photomicrographs and graphs showing age-related changes in the number of DCX-ir cells in the LP (A), MP (B), S (C) and St (D) of the *X. laevis* telencephalon. Generally, the number of DCX-ir cells in all the areas of the *X. laevis* telencephalon quantified significantly declined with age. Error bars correspond to the standard error of the mean (SEM). See list of abbreviations for abbreviations used in this figure legend.

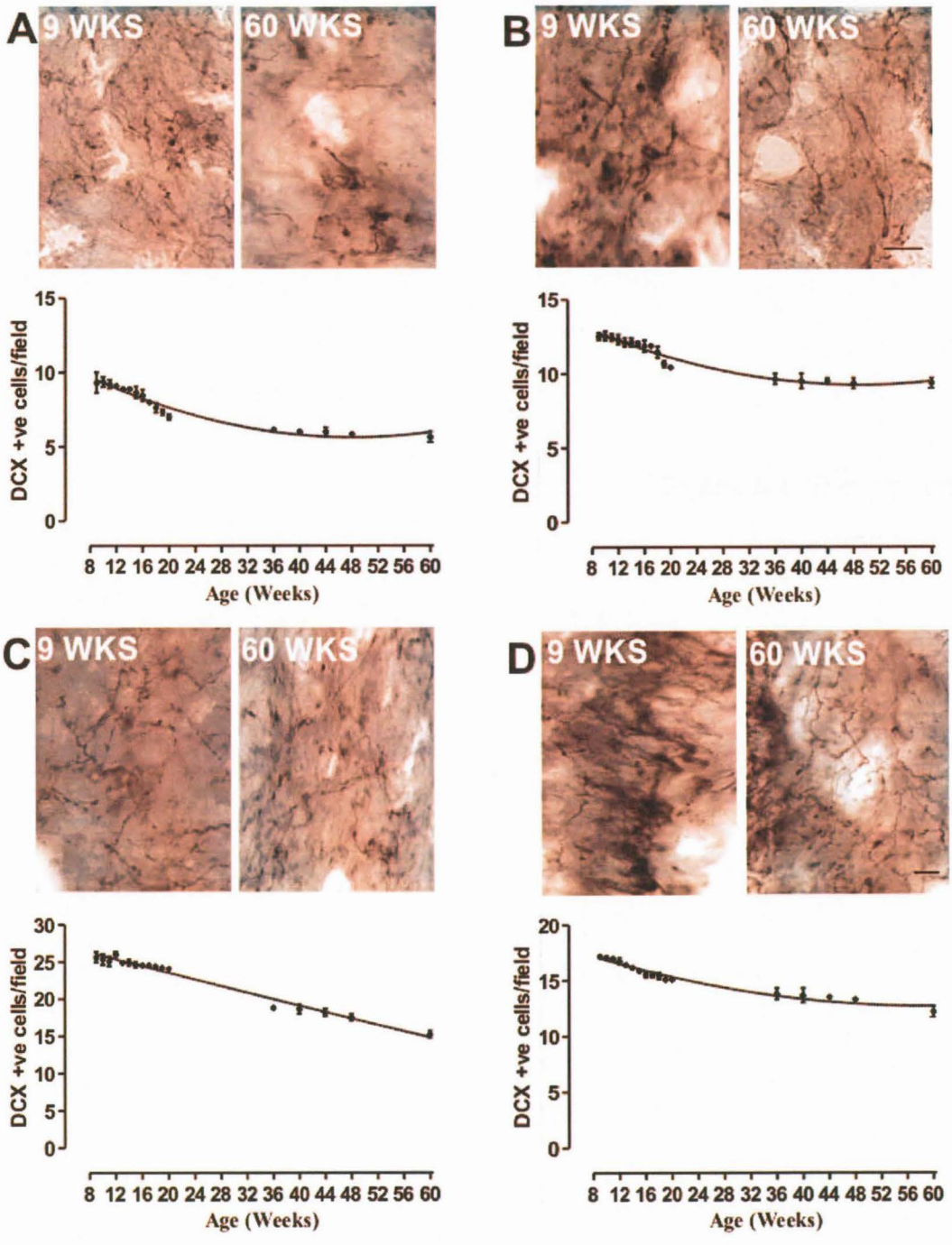
A
9 WKS
60 WKS
B
9 WKS
60 WKS
DCX +ve cells/field
15
10
5
0
8 12 16 20 24 28 32 36 40 44 48 52 56 60
Age (Weeks)
C
9 WKS
60 WKS
D
9 WKS
60 WKS
DCX +ve cells/field
30
25
20
15
10
5
0
8 12 16 20 24 28 32 36 40 44 48 52 56 60
Age (Weeks)

5.3.4 Life-history stage dependent changes in PCNA and DCX immunoreactivity in the telencephalon

Analysis of variance (ANOVA) revealed significant differences in the number of PCNA-ir cells among the different life history stages in the ventral (F= 101.2; P<0.0001, Fig 5.5A) and dorsal (F=205.7; P<0.0001; Fig 5.5B) ventricular zones. Furthermore, Bonferroni *post hoc* analysis revealed that the number of PCNA-ir cells significantly declined by approximately 48% in the ventral (P<0.0001) and 66% in the dorsal (P<0.0001) ventricular zones between the juvenile and sub adult life-history stages. However, no significant differences were found in the number of PCNA-ir cells in the ventral and dorsal ventricles between the sub adult and adult life-history stages (P>0.05).

Significant differences were also found in the number of DCX-ir cells among the different life-history stages in the LP (F=37.6; P<0.0001, Fig 5.6A), MP (F=43.1; P<0.0001, Fig 5.6B), St (F= 277.3; P<0.0001, Fig 5.6C) and S (F=52.9; P<0.0001, Fig 5.6D). Bonferroni *post hoc* analysis revealed that the number of DCX-ir cells significantly decreased by approximately 15% in the S (P<0.0001); 20% in the MP (P<0.0001) and 30% in the St (P<0.0001) & the LP (P<0.0001) between juvenile and sub adult life-history stages. However, no significant differences were found in all the telencephalic areas quantified except for the St between the sub adult and adult life-history stages (P>0.05). In the St, DCX-ir cells significantly decreased by approximately 12%.

Figure 5.5: Graphical representation of life-history stage related changes in PCNA immunoreactivity in ventral and dorsal ventricular zones of the *X. laevis* telencephalon. Generally, the number of PCNA-ir cells was significantly higher in juvenile group compared to the sub adult and adult groups in both the ventral and dorsal ventricular zones of the telencephalon. However, no significant differences were found in the number of PCNA-ir cells in the ventral and dorsal ventricular zones of the telencephalon between the sub adult and adult groups. Error bars correspond to the SEM. *P<0.01. **P<0.001 ***P<0.0001 #P>0.005. See list of abbreviations for abbreviations used in this figure legend.

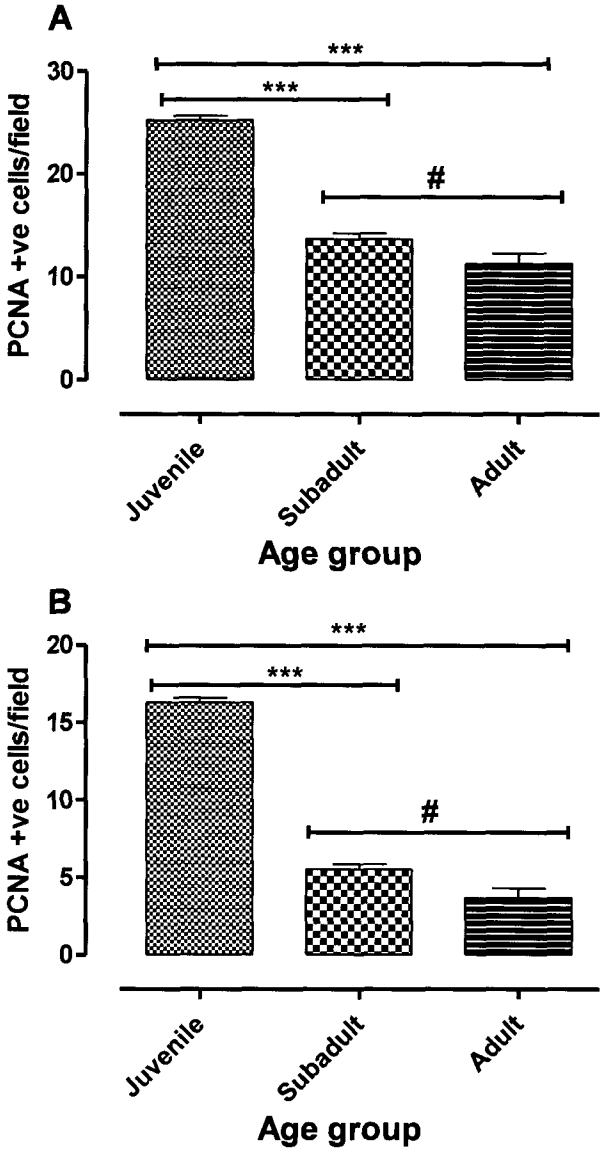
A
***
***
#
30
20
10
0
PCNA +ve cells/field
Juvenile
Subadult
Adult
Age group
B
***
***
#
20
15
10
5
0
PCNA +ve cells/field
Juvenile
Subadult
Adult
Age group

Figure 5.6: Graphical representation of life-history stage related changes in DCX immunoreactivity in parenchyma of the *X. laevis* telencephalon. Generally, the number of DCX-ir cells was significantly higher in juvenile group compared to the sub adult and adult groups in the LP (A), MP (B), St (C) and S (D) areas of the *X. laevis* telencephalon. However, no significant differences were found in the number of DCX-ir cells in the LP, MP, St and S between the sub adult and adult groups. Error bars correspond to the SEM. **P*<0.01. ***P*<0.001 ****P*<0.0001 #*P*>0.005. See list of abbreviations for abbreviations used in this figure legend.

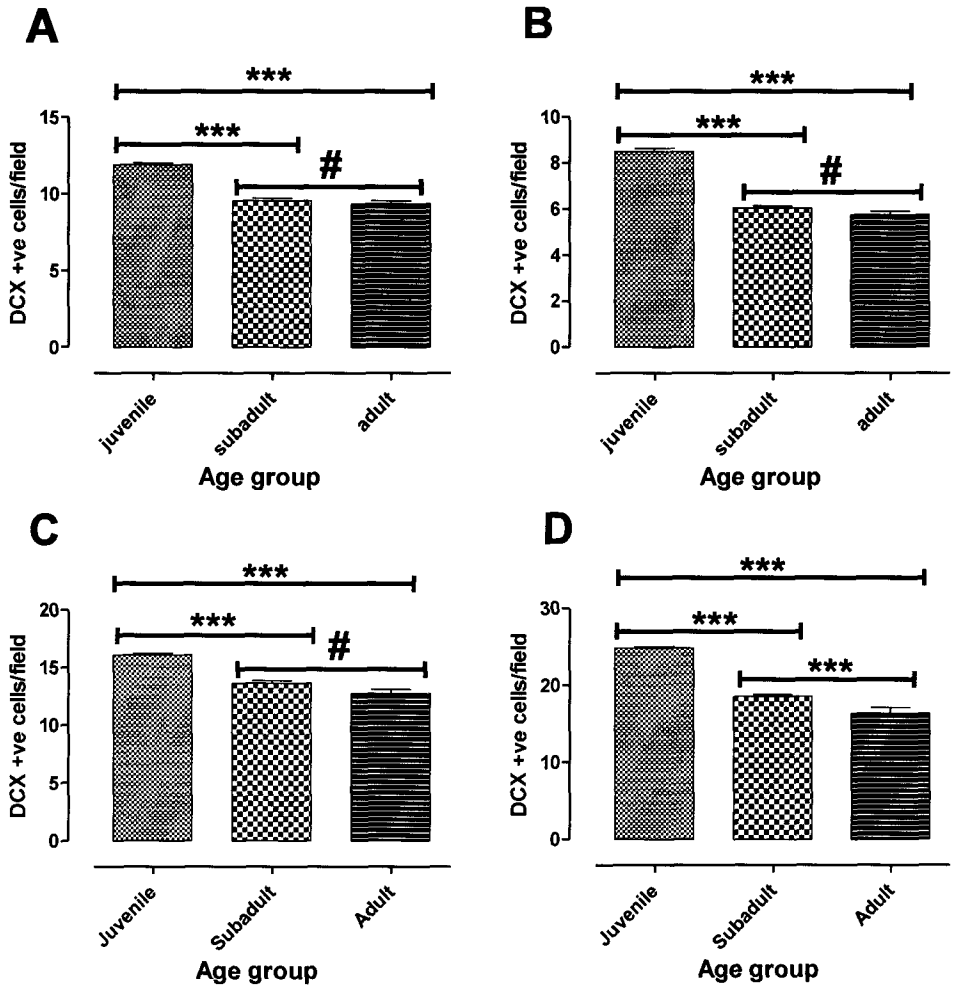
A
B
C
D
***
#
DCX +ve cells/field
juvenile
subadult
adult
Juvenile
Subadult
Adult
Age group

5.4 DISCUSSION

Our study used PCNA and DCX immunohistochemistry to investigate cell proliferation and neuronal incorporation in the post-metamorphic *X. laevis* brain and to determine how expression of these markers changes with age and life history stage.

5.4.1 Methodological considerations

Proliferating cell nuclear antigen (PCNA) is a protein associated with catalytic activity of DNA polymerase A and is expressed during the G1 and S phases of the cell cycle (Balthazart and Ball, 2014b). In addition, PCNA expression is highly conserved among eukaryotes (Charvet and Striedter, 2008) and was used in the current study as a marker for cell proliferation in the post-metamorphic *X. laevis* brain. Indeed, PCNA immunohistochemistry was previously used for neuroanatomical mapping of cell proliferation in the anuran amphibian brain (Raucci et al., 2006; Cerri et al., 2009; D'Amico et al., 2011). Additionally, double labelling experiments have shown that the pattern of PCNA expression coincides with that of BrdU in the *X. laevis* brain at short survival times (D'Amico et al., 2011).

On the other hand, DCX is a microtubule-associated protein that binds to microtubules, increasing their bundling and stabilization (Horesh et al., 1999). DCX controls the polymerization of the leading process and stabilization of the cytoskeleton during neuroblast migration (Balthazart and Ball, 2014a, 2014b). DCX immunohistochemistry was previously used to demonstrate neuroblast migration and incorporation in the amphibian brain (D'Amico et al., 2011; Maden et al., 2013). In this study, DCX immunolabelling was used as a marker for neuronal incorporation in the post-metamorphic *X. laevis* brain.

5.4.2 PCNA and DCX expression in the *X. laevis* brain

Proliferative activity was observed in the olfactory bulb, telencephalon, diencephalon and cerebellum of the *X. laevis* across all ages studied. More specifically, mitotic activity was mainly observed in the ventricular lining of the olfactory bulb, ventricles of the telencephalon, ventricular lining associated with the ventral hypothalamus, pre-optic area and the granule layer of the cerebellum. The neuro-anatomical mapping of cell proliferation observed in our study is largely comparable to the findings reported by other researchers except for a few differences in the location of proliferating cells and discussed below.

The highest concentrations of proliferating cells were observed in the telencephalic ventricular 'hot spots'. This observation is in perfect agreement with findings reported from studies in other anurans (Bernocchi et al., 1990; Filoni et al., 1995; Wullimann et al., 2005; Raucci et al., 2006; Almli and Wilczynski, 2007; D'Amico et al., 2011) and other non-mammalian vertebrates (Alvarez-Buylla, 1992; García-Verdugo et al., 2002; Nottebohm, 2002; Lindsey and Tropepe, 2006; Chapouton et al., 2007; González-Granero et al., 2011; Nkomozepi et al., 2018). In addition, abundant proliferative activity was observed mainly in the ventral ventricular 'hot spot' adjacent to the sub pallium. This observation is in agreement with findings made in other anuran studies using *X. laevis* (D'Amico et al., 2011) or other species such as *H. cinerea* (Almli and Wilczynski, 2007). Interestingly, cell proliferation was also found to be extremely abundant in the telencephalic ventricular areas adjacent to the sub pallium in other classes of vertebrates such as fish and birds (Alvarez-Buylla et al., 1990; Cayre et al., 2002; Nottebohm, 2002; Lindsey and Tropepe, 2006; Chapouton et al., 2007; Pellegrini et al., 2007; Kaslin et al., 2008; Mazengenya et al., 2017; Nkomozepi et al., 2018). However, proliferative activity in adult *R. esculenta* was reported to be more abundant along the dorsal ventricular zones (Raucci et al., 2006; Cerri et al., 2009). This variation in the distribution of proliferative cells could reflect species specific differences in neurogenic activity as different studies used different anuran species.

In this study, fewer proliferating cells were also observed in the ventricular linings adjacent to the preoptic area, ventral hypothalamus and cerebellum. Similar findings were also reported in other studies. Indeed, proliferative cells were observed in the ventricular lining of the preoptic area of the *R. temporaria*, *R.esculenta* and *X. laevis* (Bernocchi et al., 1990; Chetverukhin and Polenov, 1993; Raucci et al., 2006; D'Amico et al., 2011), ventral hypothalamus of *R.catesbiana, R.esculenta, H.cinerea* and *X.laevis* (Bernocchi et al., 1990; Polenov and Chetverukhin, 1993; Almli and Wilczynski, 2007; Simmons et al., 2008; D'Amico et al., 2011) and cerebellum of *R. esculenta* and *X. laevis* (Raucci et al., 2006; D'Amico et al., 2011).

These findings confirm that proliferative activity is more widespread in the anuran compared to mammalian brain. This high proliferative activity is probably related to the need to provide neuronal substrates for the continuous brain growth observed in amphibians. Additionally, it has also been suggested that the widespread neurogenesis observed in amphibians presumably underlies the high regenerative capacity reported in these animals (Endo et al., 2007). Similarly, widespread mitotic brain activity is also a characteristic observed in other anamniotic vertebrates such as fish that exhibit continuous brain growth throughout life (Lindsey and Tropepe, 2006; Zupanc, 2006). Contrarily, cell proliferation is mostly restricted to the forebrain in amniotic vertebrates such as mammals, birds and reptiles (Alvarez-Buylla and Kirn, 1997; García-Verdugo et al., 2002; Nottebohm, 2002; González-Granero et al., 2011; Kempermann, 2011). The cell proliferation pattern exhibited by anurans is somewhat intermediate between that observed in fish and reptiles (Almli and Wilczynski, 2007).

Neuroblasts were observed in the parenchymal areas of the olfactory bulb, telencephalon, hypothalamus and cerebellum adjacent to the respective proliferative ventricular walls. In the telencephalon, the highest concentration of neuroblasts was observed in sub pallium, more specifically, the striatum, septum and nucleus accumbens. These neuroblasts appeared to have migrated from the ventrally located telencephalic ventricular areas that exhibit high proliferative activity. This observation is in perfect agreement with reports from other anuran studies using the *H. cinerea, R. catesbeiana* and *X. laevis* (Almli and Wilczynski, 2007; Simmons et al., 2008; D'Amico et al., 2011). Indeed, these studies revealed that after two weeks following BrdU injection, the majority of BrdU-ir cells migrate from the ventral regions of the

lateral ventricles to the sub pallial parenchyma. D'Amico et al. (2011), using BrdU/DCX double labelling technique provided further evidence that these BrdU-ir cells observed in the sub pallium are neuroblasts.

DCX positive neuroblasts were also observed in the medial, lateral and dorsal pallial areas although their density was lower compared to the sub pallium. Of the pallial areas, the medial pallium had the highest concentration followed by the lateral pallium. Our results are comparable to the findings of D'Amico et al. (2011) in the *X. laevis* brain but contrary to those of Almli and Wilczynski (2007) in the *H. cinerea* brain. In the *H. cinerea*, Almli and Wilczynski (2007) reported that the lateral pallium exhibited more BrdU-ir cells than the medial pallium following long survival times post BrdU injection. The disparity could be a reflection of species specific differences in neuronal incorporation.

Compared to the telencephalon, fewer DCX-ir neuroblasts were also identified in the parenchyma of the preoptic area, ventral hypothalamus and the granular layer of the cerebellum. These observations corroborate findings in the *H. cinerea* and *X. laevis* (Almli and Wilczynski, 2007; D'Amico et al., 2011). Contrary to reports by Almli and Wilczynski (2007), we did not observe any proliferating cells or neuroblasts in the thalamus, optic tectum, torus and reticular formation. Interestingly, the granular layer of cerebellum appears to continue to recruit neuroblasts across all vertebrates studied so far (Lindsey and Tropepe, 2006; Grandel and Brand, 2013).

5.4.3 Age and life-history stage dependent changes in PCNA and DCX expression

The quantification of PCNA and DCX-ir cells was carried out in areas of the telencephalon that showed strong neurogenic activity. More specifically, PCNA was quantified in the dorsal and ventral reaches or 'hot spots' of the lateral ventricles. On the other hand, DCX was quantified in the striatum, septum, medial and lateral pallia. Across all ages studied, abundant neurogenic activity was observed in all brain regions quantified even though the activity was comparatively less in adult than juvenile frogs. Indeed, our study revealed that the number of proliferating cells and

neuroblasts decreased significantly with post-metamorphic age in the *X. laevis* telencephalon. Although no quantitative age dependent studies have been reported before this study, all studies in anurans to date agree that post-metamorphic juvenile froglets exhibit higher neurogenic activity compared to adult frogs (Raucci et al., 2006; D'Amico et al., 2011). Based on qualitative observations, D'Amico et al. (2011) reported higher neurogenic activity in brain of juvenile compared to adult *X. laevis*. In addition, pre-metamorphic larvae have been shown to display even greater neurogenic activity than post-metamorphic frogs (Filoni et al., 1995; Wullimann et al., 2005; Raucci et al., 2006; D'Amico et al., 2011). The climax of metamorphosis appears to be the point where the reduction in proliferative potential in the anuran brain begins (Filoni et al., 1995; Chapman et al., 2006; Raucci et al., 2006). Indeed, Raucci et al. (2006) reported drastic post-metamorphic decline in proliferative activity in the *R. esculanta* brain. Similarly, Chapman et al. (2006) reported a significant increase in the number of proliferating cells in the auditory medulla of *R. catesbeiana* before metamorphic climax followed by a decrease during the post-metamorphic period. These observations in the anuran amphibian brain corroborate reports that age related decreases in neurogenic activity are a characteristic observed at all taxonomic levels of vertebrates (Lindsey and Tropepe, 2006).

Our study further revealed that post metamorphic neurogenic activity in all the *X. laevis* brain areas quantified sharply declines during the transition from juvenile to sub adult life history stages. Therefore, it appears that neurogenic activity begins to decline during the metamorphic climax but sharply declines during the transition from juvenile to sub adult stages as the frogs attain sexual maturity. Although no studies have reported or identified the cause of the age dependent decline in neurogenic activity in amphibian brain, changes in the composition of the neurogenic niches are most likely involved. Studies in other vertebrate animals have identified age related lengthening of the cell cycle or changes in production of growth factors, certain hormones and neurotransmitters as potential intrinsic mechanisms for the observed age related decline (Lindsey and Tropepe, 2006). Indeed, Thuret et al. (2015) identified age dependent lengthening of the cell cycle in the pre-metamorphic *X. laevis* central nervous system as a potential culprit.

5.5 CONCLUSION

The *X. laevis* brain exhibits widespread cell proliferation and neuronal recruitment. Even though neurogenic activity in the *X. laevis* brain remains high throughout the different life history stages, it declines with increasing age. Furthermore, this decline in neurogenic activity is more pronounced during the transition from juvenile to sub adult life-history stages compared to the adult stage.

CHAPTER 6: GENERAL DISCUSSION AND CONCLUSIONS

6.1 Observations from the different vertebrate taxa studied

The current study was designed with an aim to determine time-course changes in cell proliferation, differentiation and cell death in the mammalian, avian and amphibian brains. In addition, time-course in this study was defined as increasing chronological age spanning different life-history stages of the animal. However, changes in cell death could not be established using the techniques that were proposed for this study. As already alluded to in Chapter 1, neurogenesis involves many steps including proliferation of neuronal stem cells, differentiation, migration and neuronal incorporation into target areas (Barnea and Pravosudov, 2011). In this study, we evaluated neuronal stem cell proliferation, neuronal differentiation and incorporation in the brains of the BALB/c mouse, Japanese quail and African clawed frog using Ki-67 or PCNA and DCX immunohistochemistry respectively. This study further evaluated how neurogenesis in the brains of each of these vertebrates changes with chronological age and life-history stage. Analysis of the data on neurogenesis from these different animals belonging to different vertebrate taxa revealed both shared and divergent characteristics.

Firstly, there appears to be a phylogenetic reduction in the number of proliferative zones in the brains of vertebrates. In the amphibian and avian brains, proliferative activity was observed in the olfactory bulb, telencephalon, diencephalon and rhombencephalon of the brain (Table 6.1). On the contrary, proliferative activity was mainly restricted to the telencephalon, cerebellum and to a lesser extent the olfactory bulb of the BALB/c mouse brain (Table 6.1). Indeed, proliferative activity in the BALB/c mouse olfactory bulb is most likely related to the production of neuroglia since most of the new bulbar interneurons are derived from the sub ventricular zones of the lateral ventricle. Across all the species studied, however, it appears that proliferation along the ventricular zones is highly conserved. Indeed, neuronal stem proliferation was observed in areas associated with the ventricles in all the vertebrates investigated in this study (Table 6.1). In the African clawed frog, cell proliferation was restricted to the ventricular lining of the olfactory bulb, telencephalon, diencephalon and the rhombencephalon. In the Japanese quail, neuronal stem proliferative activity was mainly observed in the lining of the telencephalic ventricles although fewer cells were also observed in the lining of 3rd, 4th and mesencephalic aqueduct. In mammals, proliferation was also found in the sub

ventricular zones of the lateral ventricles. In the avian and amphibian telencephalic ventricles, the distribution of proliferating cells is not uniform as they form clusters along the ventral and dorsal reaches of the lateral ventricles. The location of these clusters correspond to the proliferative "hot spots" described by Alvarez-Buylla et al. (1994).

However, other "secondary proliferative sites" were also observed in the BALB/c mouse and Japanese quail brains. In the BALB/c mouse, the sub granular zone of the dentate gyrus is the main secondary proliferative site. In the quail, however, "secondary proliferative sites" were observed in the diencephalon and mesencephalon (Table 6.1). These "secondary proliferative sites" are located in the parenchyma of the brain and are believed to originate from the proliferating cells situated along the ventricles ("primary sites") during embryonic development (Chernoff et al., 2002; Lindsey and Tropepe, 2006). Since no DCX expression was observed in all these "secondary proliferative sites" in the avian brain, it is unlikely that the proliferative activity is related to neurogenesis. Therefore, proliferative activity observed in the diencephalon and mesencephalon divisions of the quail brain is presumably related to the production of neuroglia. However, this presumption needs to be confirmed through double-labelling experiments involving PCNA and a glia cell marker.

Table 6.1: A comparison of proliferative brain areas among vertebrates studied

			Mammalian	Avian	Amphibian
Olfactory Bulb	OB parenchyma/ventricle		+	+	+
Telencephalon	Lateral ventricle/SVZ		+	+	+
	Pallium	DP, LP	-	-	-
		HP/MP	-	-	-
	Sub pallium	Striatum	-	-	-
		Septum	-	-	-
Diencephalon	3rd Ventricle		-	+	+
	Preoptic region		-	+	+
	Hypothalamus		-	+	+
	Thalamus		-	-	-
Mesencephalon	Mesencephalic aqueduct		-	+	+
	Tectum		+	-	-
	Midbrain		-	+	-
Rhombencephalon	4th ventricle		-	+	+
	Cerebellum		+	+	+

+ Indicates presence - indicates absence

Secondly, it also appears that there is a progressive reduction in the number of brain areas incorporating new neurons as species evolve. In the amphibian brain, new neurons are incorporated in the olfactory bulb, telencephalon, diencephalon (pre-optic and ventral hypothalamic areas) and the rhombencephalon (cerebellum). In the avian brain, neuronal incorporation is restricted to the olfactory bulb, telencephalon and cerebellum. In the mammalian brain, neuronal incorporation is restricted to the olfactory bulb and telencephalon only (Table 6.2).

In the avian and amphibian telencephalon, neuronal incorporation is more widespread, having been observed in both pallial and sub pallial areas, compared to mammals (Table 6.2). In fact, the striatal division of both the amphibian and avian sub pallium incorporates more neuroblasts than the rest of the telencephalon. Contrarily, neuronal incorporation in the mammalian telencephalon is only restricted to the granule cell layer of the dentate gyrus and the olfactory bulb (Table 6.2). However, a few previous studies have reported neuronal incorporation in the mammalian striatum under normal physiological conditions (Bédard et al., 2002; Ernst et al., 2014)

Table 6.2: A comparison of brain areas that incorporate new neurons among vertebrates studied

			Mammalian	Avian	Amphibian
Olfactory Bulb	OB parenchyma		+	+	+
Telencephalon	Lateral ventricle/SVZ		+	+	+
	Pallium	DP, LP/CTX	+	+	+
		HP/MP	+	+	+
	Sub pallium	Striatum	-	+	+
		Septum	-	+	+
Diencephalon	Preoptic region		-	-	+
	Hypothalamus		-	-	+
	Thalamus		-	-	-
Mesencephalon	Tectum		-	-	-
	Midbrain		-	-	-
Rhombencephalon	Cerebellum		-	+	+

+ Indicates presence - indicates absence

Interestingly, the presence of neurogenesis in the olfactory bulb and hippocampus appears to be conserved in all the vertebrates investigated in this study. Although the olfactory bulb is very consistent throughout evolution, homologies observed for the hippocampus are complex and not fully understood for all vertebrates. Based on evidence from hodological, gene expression, immunohistochemistry and electrophysiology studies, the avian hippocampus is believed to be homologous to the mammalian hippocampus (Jarvis et al., 2005). More specifically, the dorsomedial and v-shaped ventral regions of the avian hippocampus have been proposed to be homologous to the mammalian Ammon's horn and dentate gyrus respectively (Atoji and Wild, 2004). Similarly, the medial pallium of the amphibian brain is also viewed to be homologous to the mammalian and avian hippocampi (Bruce and Neary, 1995; Broglio et al., 2015; Sotelo et al., 2016). However, the whole amphibian medial pallium was reported to be only homologous to the mammalian subiculum and Ammon's horn and that no part of it is homologous to the mammalian dentate gyrus (Roth and Westhoff, 1999). In summary, the study revealed that there is a phylogenetic reduction in brain areas that support neurogenesis from amphibians to mammals.

Thirdly, it also appears that age-related decline in neurogenic activity is a common feature of all vertebrates investigated. Although age-related decline in neurogenesis was observed in all vertebrates investigated, the sharpest and most rapid decline was observed in the mammalian neurogenic areas. Regardless of the age-related decline, neurogenic activity remained comparatively high in the amphibian and avian brains. It appears that there is a more rapid neuronal stem cell "deforestation" (Encinas and Sierra, 2012) or a rapid decline in neurogenesis supporting factors (Hamilton et al., 2013) in the mammalian neurogenic niches compared to either the avian or amphibian niches.

Fourthly, this study revealed differences in the life-history stage related changes in neurogenesis. In the avian and amphibian brains, neurogenic activity declined at a steady state during the juvenile stages and only drastically declined at an age when the animals attained sexual maturity. In mammals, however, neurogenesis declined at a rapid rate from the first week without defining any plateau stages when neurogenesis was stable. This study made two assumptions in this regard: Firstly, that all the animal species used in this study become sexually reproductive at a

certain point in their lifespan. Secondly, that the age at which sexual maturity is attained is the beginning of adulthood. Reproductive maturity is deemed to be a reasonable physiological indicator of the attainment of adulthood (Lindsey and Tropepe, 2006). However, the exact age in the life-history of a given species at which sexual maturity is attained is variable and depends on a variety of individual factors. In addition, not all species become sexually reproductive in their life-span. For instance, non-dominant rodents in a unit or group may never reproduce because only the dominant male services all the females in a given unit.

Finally, nothing in this study suggested that postnatal neurogenesis is a vestigial remnant of the embryonic process. In all the animals investigated in this study, neurogenesis persisted throughout the ages and life-history stages studied. Indeed, if neurogenesis was just a vestige of the embryonic process it would have stopped at some point during the animal's life-span and certainly would not be related to specific functions for instance song-learning in songbirds (Nottebohm, 2011) or spatial memory in rodents (Drapeau et al., 2003).

6.2 Limitations of the study

Firstly, we had proposed to investigate time-course changes in cell turnover in the different vertebrate brains used in this study using the flourojade C technique. However, due to circumstances beyond our control we could not get flourojade C from the local manufacturers. We also attempted to use Giemsa staining to identify the apoptotic cells but our efforts were fruitless.

Secondly, only laboratory bred animals were used in this study. The biggest concern that arises is how representative the findings from laboratory bred animal models are compared to animals living in natural populations. Indeed, Barnea and Nottebohm (1994) reported an approximately two-fold reduction in adult neurogenesis in the hippocampus of captive compared to wild black capped chickadees. Laboratory environments lack an adequate assortment of environmental stimuli that characterise natural environments. Thus, caution must be taken when interpreting findings from laboratory animals. However, age-dependent studies are not practical when using wild living animals as it is always difficult to accurately determine the age of the

animals. Therefore, the use of laboratory bred animals in our study enabled us to ascertain the ages and life-history stages of the animals.

Thirdly, as already pointed out above this study assumed the age at which sexual maturity is expected to be the landmark for attaining adulthood. However, the age at which sexual maturity is attained in a given species is highly variable depending several factors such as the social hierarchy, environment to mention just a few. In addition, some species never attain sexual maturity throughout their lifespan (Lindsey and Tropepe, 2006).

Fourthly, the current study used one species to represent each of the amphibian, avian and mammalian vertebrate groups. However, variation in the characteristics of neurogenesis exists among animal species within each taxonomic group. Regardless of this fact, significant differences still exist in the characteristic features of neurogenesis such as the rate, location, number of neurogenic niches and migratory pathways across the different vertebrate (Lindsey and Tropepe, 2006). The findings from this study therefore establish a baseline for future comparative studies including more animal models for each vertebrate class.

Lastly, in brain areas where PCNA or Ki-67 but not DCX-ir cells were observed it was generally presumed that the cell proliferation was related to production of neuroglia. Without evidence from double-labelling experiments using PCNA and a glial cell marker such as GFAP, caution must be exercised when making such conclusions. However, reactivity of some conventional glial cell markers such GFAP or S100 has been shown to unreliable in the non-mammalian central nervous system (Castagna et al., 2003; Bardet et al., 2012). This finding should therefore inspire future studies to investigate the exact nature of these newly formed cells.

6.3 Recommendations

Firstly, we recommend that a similar interclass study be extended to wild living natural populations of these species. The natural environment provides a unique set of environmental stimuli that is not present in laboratory environments. Such studies are important to determine whether findings from laboratory animals are upheld in

natural populations. If not, the next step would be to determine the exogenous factors responsible for the observed disparity.

Secondly, attempts should be made to include more members of each vertebrate taxa so as to determine intra-class as well as inter-class shared and divergent characteristics of neurogenesis. Thirdly, more research needs to be done using double labelling experiments of Ki-67 or PCNA proliferation markers with a wide range of glial cell markers so as to ascertain the phenotype of proliferating cells in non-neurogenic brain areas.

Fourthly, cell death is a major component in neurogenesis under normal physiological conditions. However, information on this process is only available for mammalian species (Amrein et al., 2004; Nada et al., 2010). In the hippocampi of rodents investigated thus far, formation of new neurons is balanced by neuronal death leading to no changes in the granule cell population (Amrein et al., 2004; Nada et al., 2010). Similar investigations on cell death should also be extended to amphibian and avian animal models so as to determine the relationship between neurogenesis and neuronal turnover. Cell death studies have now been planned to become a component of the postdoctoral studies arising from this study.

Lastly, comparative interclass and age-dependent studies focussing on the changes in neurogenesis promoting and inhibiting factors in each neurogenic niche should will be considered for further investigation. In addition, the investigation should also be extended to changes in neuronal stem cell populations in all the niches. These studies will establish the exact mechanisms underlying interclass differences as well age-dependent changes in neurogenesis.

6.4 Conclusions

The current study yielded some important conclusions and opened opportunities for future research. In all vertebrates, the ventricular lining is the main site of neuronal birth. In the amphibian brain, neuronal birth takes place in the ventricular lining of the olfactory bulb, telencephalon, diencephalon and rhombencephalon. In the avian brain, neuronal birth is restricted to the ventricular lining of the olfactory bulb and telencephalon, and the cerebellum (Nkomozepi et al., 2018). In mammals, however,

neuronal birth is restricted to the telencephalon, specifically the sub ventricular zone of the lateral ventricles, rostral migratory stream and the sub granular zone of the dentate gyrus. This reflects a phylogenetic reduction in the brains regions exhibiting proliferative activity.

Similarly, neuronal incorporation is more widespread in the amphibian and avian brains compared to the mammalian brain. In the amphibian brain, new neurons are incorporated in the olfactory bulb, telencephalon, diencephalon and cerebellum. In the avian brain, neuronal incorporation takes place mainly in different parts of the telencephalon, and to a lesser extent the olfactory bulb and cerebellum (Nkomozepi et al., 2018). In mammals, neuronal incorporation is mainly restricted to the olfactory bulb and the hippocampal dentate gyrus. It therefore appears that as vertebrates evolve, there is a reduction in the number of brain regions incorporating new neurons.

In addition, this study also revealed that neurogenesis decreases with chronological age in all the vertebrates studied. In the amphibian and avian brains, the rate of neurogenesis is relatively stable during the juvenile period and then declines steeply during the transition from sub adult to adult life-history stages as the animal attains sexual maturity. In mammals, however, the decline in neurogenesis is very rapid and steep from early postnatal life to adulthood. Thus neurogenesis declines at a slower pace in the amphibian and avian brains compared to their mammalian counterparts.

REFERENCES

Absil P, Pinxten R, Balthazart J, Eens M. 2003. Effect of age and testosterone on autumnal neurogenesis in male European starlings (Sturnus vulgaris). Behavioural Brain Research 143:15-30.

Aimone JB, Li Y, Lee SW, Clemenson GD, Deng W, Gage FH. 2014. Regulation and function of adult neurogenesis: from genes to cognition. Physiological reviews 94:991-1026.

Ainsworth SJ, Stanley RL, Evans DJ. 2010. Developmental stages of the Japanese quail. Journal of anatomy 216:3-15.

Aitken S. 2015. The effects of housing conditions on neurogenesis in the black-capped chickadee. MSc dissertation, Dalhousie University, Canada.

Akbar Z, Qureshi AS. 2012. Effects of Seasonal Variation in Different Reproductive Phases on the Cellular Response of Bursa and Testes in Japanese Quail (Coturnix japonica). Pakistan Veterinary Journal 32: 525-529.

Allen E. 1912. The cessation of mitosis in the central nervous system of the albino rat: Journal of Comparative Neurology 22:547-568.

Almli LM, Wilczynski W. 2007. Regional distribution and migration of proliferating cell populations in the adult brain of Hyla cinerea (Anura, Amphibia). Brain research 1159:112-118.

Altman J. 1972. Postnatal development of the cerebellar cortex in the rat. I. The external germinal layer and the transitional molecular layer. Journal of Comparative Neurology 145:353-397.

Altman J, Das GD. 1965. Autoradiographic and histological evidence of postnatal hippocampal neurogenesis in rats. Journal of Comparative Neurology 124:319-335.

Alunni A, Bally-Cuif L. 2016. A comparative view of regenerative neurogenesis in vertebrates. Development 143:741-753.

Alvarez-Buylla A. 1990. Mechanism of neurogenesis in adult avian brain. Experientia 46:948-955.

Alvarez-Buylla A. 1992. Neurogenesis and plasticity in the CNS of adult birds. Experimental neurology 115:110-114.

Alvarez-Buylla A, García-Verdugo JM, Mateo AS, Merchant-Larios H. 1998. Primary neural precursors and intermitotic nuclear migration in the ventricular zone of adult canaries. Journal of Neuroscience 18:1020-1037.

Alvarez-Buylla A, Kirn JR. 1997. Birth, migration, incorporation, and death of vocal control neurons in adult songbirds. Journal of neurobiology 33:585-601.

Alvarez-Buylla A, Nottebohm F. 1988. Migration of young neurons in adult avian brain. Nature 335:353-354.

Alvarez-Buylla A, Seri B, Doetsch F. 2002. Identification of neural stem cells in the adult vertebrate brain. Brain research bulletin 57:751-758.

Alvarez-Buylla A, Theelen M, Nottebohm F. 1990. Proliferation "hot spots" in adult avian ventricular zone reveal radial cell division. Neuron 5:101-109.

Alvarez-Buylla A, Ling CY, Nottebohm F. 1992. High vocal center growth and its relation to neurogenesis, neuronal replacement and song acquisition in juvenile canaries. Journal of neurobiology 23:396-406.

Alvarez-Buylla A, Ling CY, Yu WS. 1994. Contribution of neurons born during embryonic and adult life to the brain of adult canaries: Regional specificity and delayed birth of neurons in the song-control nuclei. Journal of Comparative Neurology 347:233-248.

Amamoto R, Huerta VGL, Takahashi E, Dai G, Grant AK, Fu Z, Arlotta P. 2016. Adult axolotls can regenerate original neuronal diversity in response to brain injury. Elife 5:e13998.

Amrein I, Becker AS, Engler S, Huang S-h, Müller J, Slomianka L, Oosthuizen MK. 2014. Adult neurogenesis and its anatomical context in the hippocampus of three mole-rat species. Frontiers in neuroanatomy 8:39.

Amrein I, Slomianka L, Lipp HP. 2004. Granule cell number, cell death and cell proliferation in the dentate gyrus of wild-living rodents. European Journal of Neuroscience 20:3342-3350.

Atkinson R, Bevilaqua LR, Rostas JA, Hunter M. 2003. Discriminative taste aversion learning: A learning task for older chickens. Neurobiology of learning and memory 79:25-31.

Atkinson R, Migues PV, Cammarota M, Kavanagh JM, Hunter M, Rostas JA. 2008. Biochemical, behavioural and electrophysiological investigations of brain maturation in chickens. Brain research bulletin 76:217-223.

Atoji Y, Wild JM. 2004. Fiber connections of the hippocampal formation and septum and subdivisions of the hippocampal formation in the pigeon as revealed by tract tracing and kainic acid lesions. Journal of Comparative Neurology 475:426-461.

Baird GS, Nelson SK, Keeney TR, Stewart A, Williams S, Kraemer S, Peskind ER, Montine TJ. 2012. Age-dependent changes in the cerebrospinal fluid proteome by slow off-rate modified aptamer array. The American journal of pathology 180:446-456.

Balthazart J, Ball GF. 2014a. Doublecortin is a highly valuable endogenous marker of adult neurogenesis in canaries. Brain, behavior and evolution 84:1-4.

Balthazart J, Ball GF. 2014b. Endogenous versus exogenous markers of adult neurogenesis in canaries and other birds: advantages and disadvantages. Journal of Comparative Neurology 522:4100-4120.

Balthazart J, Ball GF. 2016. Endocrine and social regulation of adult neurogenesis in songbirds. Frontiers in neuroendocrinology 41:3-22

Balthazart J, Boseret G, Konkle A, Hurley LL, Ball GF. 2008. Doublecortin as a marker of adult neuroplasticity in the canary song control nucleus HVC. European Journal of Neuroscience 27:801-817.

Balthazart J, Charlier TD, Barker JM, Yamamura T, Ball GF. 2010. Sex steroid-induced neuroplasticity and behavioral activation in birds. European Journal of Neuroscience 32:2116-2132.

Balu DT, Lucki I. 2009. Adult hippocampal neurogenesis: regulation, functional implications, and contribution to disease pathology. Neuroscience & Biobehavioral Reviews 33:232-252.

Bardet SM, Mouriec K, Balthazart J. 2012. Birth of neural progenitors during the embryonic period of sexual differentiation in the Japanese quail brain. Journal of Comparative Neurology 520:4226-4253.

Barkan S, Ayali A, Nottebohm F, Barnea A. 2007. Neuronal recruitment in adult zebra finch brain during a reproductive cycle. Developmental neurobiology 67:687-701.

Barkan S, Roll U, Yom-Tov Y, Wassenaar LI, Barnea A. 2016. Possible linkage between neuronal recruitment and flight distance in migratory birds. Scientific reports 6:21983.

Barker JM, Ball GF, Balthazart J. 2014. Anatomically discrete sex differences and enhancement by testosterone of cell proliferation in the telencephalic ventricle zone of the adult canary brain. Journal of chemical neuroanatomy 55:1-8.

Barker JM, Boonstra R, Wojtowicz JM. 2011. From pattern to purpose: how comparative studies contribute to understanding the function of adult neurogenesis. European Journal of Neuroscience 34:963-977.

Barnea A, Nottebohm F. 1994. Seasonal recruitment of hippocampal neurons in adult free-ranging black-capped chickadees. Proceedings of the National Academy of Sciences 91:11217-11221.

Barnea A, Pravosudov V. 2011. Birds as a model to study adult neurogenesis: bridging evolutionary, comparative and neuroethological approaches. European Journal of Neuroscience 34:884-907.

Bayer S. 1983. 3 H-thymidine-radiographic studies of neurogenesis in the rat olfactory bulb. Experimental Brain Research 50:329-340.

Baylé J, Ramade F, Oliver J. 1974. Stereotaxic topography of the brain of the quail (Coturnix coturnix japonica). Journal de physiologie 68:219.

Bédard A, Cossette M, Lévesque M, Parent A. 2002. Proliferating cells can differentiate into neurons in the striatum of normal adult monkey. Neuroscience letters 328:213-216.

Bennett G Galef J, White DJ. 1998. Mate-choice copying in Japanese quail, Coturnix coturnix japonica. Animal Behaviour 55:545-552.

Bernocchi G, Scherini E, Giacometti S, Mareš V. 1990. Premitotic DNA synthesis in the brain of the adult frog (Rana esculenta L.): An autoradiographic 3H-thymidine study. The Anatomical Record 228:461-470.

Bodnar AG, Ouellette M, Frolkis M, Holt SE, Chiu C-P, Morin GB, Harley CB, Shay JW, Lichtsteiner S, Wright WE. 1998. Extension of life-span by introduction of telomerase into normal human cells. science 279:349-352.

Bond AM, Ming G-l, Song H. 2015. Adult mammalian neural stem cells and neurogenesis: five decades later. Cell stem cell 17:385-395.

Bonfanti L, Peretto P. 2011. Adult neurogenesis in mammals–a theme with many variations. European Journal of Neuroscience 34:930-950.

Boseret G, Ball GF, Balthazart J. 2007. The microtubule-associated protein doublecortin is broadly expressed in the telencephalon of adult canaries. Journal of chemical neuroanatomy 33:140-154.

Boxem M. 2006. Cyclin-dependent kinases in C. elegans. Cell division 1:6.

Brenowitz EA. 2004. Plasticity of the adult avian song control system. Annals of the New York Academy of Sciences 1016:560-585.

Brenowitz EA. 2013. Testosterone and brain-derived neurotrophic factor interactions in the avian song control system. Neuroscience 239:115-123.

Brenowitz EA. 2015. Transsynaptic trophic effects of steroid hormones in an avian model of adult brain plasticity. Frontiers in neuroendocrinology 37:119-128.

Brenowitz EA, Larson TA. 2015. Neurogenesis in the adult avian song-control system. Cold Spring Harbor perspectives in biology 7:a019000.

Broglio C, Martín-Monzón I, Ocaña F, Gómez A, Durán E, Salas C, Rodríguez F. 2015. Hippocampal pallium and map-like memories through vertebrate evolution. Journal of Behavioral and Brain Science 5:109.

Brown JP, Couillard-Després S, Cooper-Kuhn CM, Winkler J, Aigner L, Kuhn HG. 2003. Transient expression of doublecortin during adult neurogenesis. Journal of Comparative Neurology 467:1-10.

Bruce LL, Neary TJ. 1995. The limbic system of tetrapods: a comparative analysis of cortical and amygdalar populations. Brain, Behavior and Evolution 46:224-234.

Buchwalder T, Wechsler B. 1997. The effect of cover on the behaviour of Japanese quail (Coturnix japonica). Applied Animal Behaviour Science 54:335-343.

Bullwinkel J, Baron-Lühr B, Lüdemann A, Wohlenberg C, Gerdes J, Scholzen T. 2006. Ki-67 protein is associated with ribosomal RNA transcription in quiescent and proliferating cells. Journal of cellular physiology 206:624-635.

Cameron H, Gould E. 1994. Adult neurogenesis is regulated by adrenal steroids in the dentate gyrus. Neuroscience 61:203-209.

Cameron H, Woolley C, McEwen B, Gould E. 1993. Differentiation of newly born neurons and glia in the dentate gyrus of the adult rat. Neuroscience 56:337-344.

Cameron HA, McKay RD. 1999. Restoring production of hippocampal neurons in old age. Nature neuroscience 2:894-897.

Capes-Davis A, Tolhurst O, Dunn JM, Jeffrey PL. 2005. Expression of doublecortin (DCX) and doublecortin-like kinase (DCLK) within the developing chick brain. Developmental dynamics 232:457-467.

Caporaso GL, Lim DA, Alvarez-Buylla A, Chao MV. 2003. Telomerase activity in the subventricular zone of adult mice. Molecular and Cellular Neuroscience 23:693-702.

Castagna C, Viglietti-Panzica C, Panzica GC. 2003. Protein S100 immunoreactivity in glial cells and neurons of the Japanese quail brain. Journal of chemical neuroanatomy 25:195-212.

Cattan A, Ayali A, Barnea A. 2015. The cell birth marker BrdU does not affect recruitment of subsequent cell divisions in the adult avian brain. BioMed research international: 126078

Cayre M, Malaterre J, Scotto-Lomassese S, Strambi C, Strambi A. 2002. The common properties of neurogenesis in the adult brain: from invertebrates to vertebrates. Comparative Biochemistry and Physiology Part B: Biochemistry and Molecular Biology 132:1-15.

Cerri S, Bottiroli G, Bottone MG, Barni S, Bernocchi G. 2009. Cell proliferation and death in the brain of active and hibernating frogs. Journal of anatomy 215:124-131.

Chapman JA, Weinstein JL, Simmons AM. 2006. Cell proliferation in the Rana catesbeiana auditory medulla over metamorphic development. Developmental Neurobiology 66:115-133.

Chapouton P, Jagasia R, Bally-Cuif L. 2007. Adult neurogenesis in non-mammalian vertebrates. Bioessays 29:745-757.

Charvet CJ, Striedter GF. 2008. Developmental species differences in brain cell cycle rates between northern bobwhite quail (Colinus virginianus) and parakeets (Melopsittacus undulatus): implications for mosaic brain evolution. Brain, behavior and evolution 72:295-306.

Chawana R, Patzke N, Kaswera C, Gilissen E, Ihunwo AO, Manger P. 2013. Adult neurogenesis in eight megachiropteran species. Neuroscience 244:159-172.

Chen G, Bonder EM, Cheng MF. 2006. Lesion-induced neurogenesis in the hypothalamus is involved in behavioral recovery in adult ring doves. Journal of neurobiology 66:537-551.

Chen G, Cheng M-F. 2007. Inhibition of lesion-induced neurogenesis impaired behavioral recovery in adult ring doves. Behavioural brain research 177:358-363.

Chen X-H, Iwata A, Nonaka M, Browne KD, Smith DH. 2003. Neurogenesis and glial proliferation persist for at least one year in the subventricular zone following brain trauma in rats. Journal of neurotrauma 20:623-631.

Chen Z, Ye R, Goldman SA. 2013. Testosterone modulation of angiogenesis and neurogenesis in the adult songbird brain. Neuroscience 239:139-148.

Chernoff EA, Sato K, Corn A, Karcavich RE. 2002. Spinal cord regeneration: intrinsic properties and emerging mechanisms. In: Seminars in cell & developmental biology: Elsevier. p 361-368.

Chetverukhin VK, Polenov AL. 1993. Ultrastructural radioautographic analysis of neurogenesis in the hypothalamus of the adult frog, Rana temporaria, with special reference to physiological regeneration of the preoptic nucleus. Cell and tissue research 271:341-350.

Correa SM, Horan CM, Johnson PA, Adkins-Regan E. 2011. Copulatory behaviors and body condition predict post-mating female hormone concentrations, fertilization success, and primary sex ratios in Japanese quail. Hormones and behavior 59:556-564.

D'Amico LA, Boujard D, Coumailleau P. 2011. Proliferation, migration and differentiation in juvenile and adult Xenopus laevis brains. Brain research 1405:31-48.

Dalm S, Enthoven L, Meijer OC, van der Mark MH, Karssen AM, de Kloet ER, Oitzl MS. 2005. Age-related changes in hypothalamic-pituitary-adrenal axis activity of male C57BL/6J mice. Neuroendocrinology 81:372-380.

Dermon C, Zikopoulos B, Panagis L, Harrison E, Lancashire C, Mileusnic R, Stewart M. 2002. Passive avoidance training enhances cell proliferation in 1-day-old chicks. European Journal of Neuroscience 16:1267-1274.

DeWulf V, Bottjer SW. 2002. Age and sex differences in mitotic activity within the zebra finch telencephalon. The Journal of neuroscience 22:4080-4094.

Dong HW. 2008. The Allen reference atlas: A digital color brain atlas of the C57Bl/6J male mouse: John Wiley & Sons Inc.

Drapeau E, Mayo W, Aurousseau C, Le Moal M, Piazza P-V, Abrous DN. 2003. Spatial memory performances of aged rats in the water maze predict levels of hippocampal neurogenesis. Proceedings of the National Academy of Sciences 100:14385-14390.

Encinas JM, Michurina TV, Peunova N, Park J-H, Tordo J, Peterson DA, Fishell G, Koulakov A, Enikolopov G. 2011. Division-coupled astrocytic differentiation and age-related depletion of neural stem cells in the adult hippocampus. Cell stem cell 8:566-579.

Encinas JM, Sierra A. 2012. Neural stem cell deforestation as the main force driving the age-related decline in adult hippocampal neurogenesis. Behavioural brain research 227:433-439.

Endo T, Yoshino J, Kado K, Tochinai S. 2007. Brain regeneration in anuran amphibians. Development, growth & differentiation 49:121-129.

Enwere E, Shingo T, Gregg C, Fujikawa H, Ohta S, Weiss S. 2004. Aging results in reduced epidermal growth factor receptor signaling, diminished olfactory neurogenesis, and deficits in fine olfactory discrimination. Journal of Neuroscience 24:8354-8365.

Eriksson PS, Perfilieva E, Björk-Eriksson T, Alborn A-M, Nordborg C, Peterson DA, Gage FH. 1998. Neurogenesis in the adult human hippocampus. Nature medicine 4:1313-1317.

Ernst A, Alkass K, Bernard S, Salehpour M, Perl S, Tisdale J, Possnert G, Druid H, Frisén J. 2014. Neurogenesis in the striatum of the adult human brain. Cell 156:1072-1083.

Essers J, Theil AF, Baldeyron C, van Cappellen WA, Houtsmuller AB, Kanaar R, Vermeulen W. 2005. Nuclear dynamics of PCNA in DNA replication and repair. Molecular and cellular biology 25:9350-9359.

Fernández-Flores F, García-Verdugo JM, Martín-Ibáñez R, Herranz C, Fondevila D, Canals JM, Arús C, Pumarola M. 2018. Characterization of the canine rostral ventricular-subventricular zone: Morphological, immunohistochemical, ultrastructural, and neurosphere assay studies. Journal of Comparative Neurology 526:721-741.

Ferretti P, Prasongchean W. 2015. Adult neurogenesis and regeneration: focus on nonmammalian vertebrates. In: Neural Stem Cells in Development, Adulthood and Disease: Springer. p 1-21.

Ferrón S, Mira H, Franco S, Cano-Jaimez M, Bellmunt E, Ramírez C, Fariñas I, Blasco MA. 2004. Telomere shortening and chromosomal instability abrogates proliferation of adult but not embryonic neural stem cells. Development 131:4059-4070.

Filoni S, Bernardini S, Cannata S. 1995. Differences in the decrease in regenerative capacity of various brain regions of Xenopus laevis are related to differences in the undifferentiated cell populations. Journal fur Hirnforschung 36:523-529.

Freeman FM, Rose SP. 1999. Expression of Fos and Jun proteins following passive avoidance training in the day-old chick. Learning & Memory 6:389-397.

Frynta D, Slabova M, Vachova H, Volfova R, Munclinger P. 2005. Aggression and commensalism in house mouse: a comparative study across Europe and the Near East. Aggressive Behavior 31:283-293.

Gage FH. 2000. Mammalian neural stem cells. Science 287:1433-1438.

Gage FH, Temple S. 2013. Neural stem cells: generating and regenerating the brain. Neuron 80:588-601.

García-Verdugo JM, Ferrón S, Flames N, Collado La, Desfilis E, Font E. 2002. The proliferative ventricular zone in adult vertebrates: a comparative study using reptiles, birds, and mammals. Brain research bulletin 57:765-775.

García-Verdugo JM, Doetsch F, Wichterle H, Lim DA, Alvarez-Buylla A. 1998. Architecture and cell types of the adult subventricular zone: in search of the stem cells. Developmental Neurobiology 36:234-248.

Garcia A, Steiner B, Kronenberg G, Bick-Sander A, Kempermann G. 2004. Age-dependent expression of glucocorticoid-and mineralocorticoid receptors on neural precursor cell populations in the adult murine hippocampus. Aging cell 3:363-371.

Goldman SA, Nottebohm F. 1983. Neuronal production, migration, and differentiation in a vocal control nucleus of the adult female canary brain. Proceedings of the National Academy of Sciences 80:2390-2394.

González-Granero S, Lezameta M, García-Verdugo JM. 2011. Adult neurogenesis in reptiles. In: Neurogenesis in the Adult Brain I: Springer. p 169-189.

Grandel H, Brand M. 2013. Comparative aspects of adult neural stem cell activity in vertebrates. Development genes and evolution 223:131-147.

Gray SJ, Hurst JL. 1997. Behavioural mechanisms underlying the spatial dispersion of commensalMus domesticusand grasslandMus spretus. Animal Behaviour 53:511-524.

Guigueno MF, MacDougall-Shackleton SA, Sherry DF. 2016. Sex and seasonal differences in hippocampal volume and neurogenesis in brood-parasitic brown-headed cowbirds (Molothrus ater). Developmental Neurobiology.

Guitar NA. 2016. Spatial Memory in Black-capped Chickadees: Studies of Adult Hippocampal Neurogenesis and Win-Shift/Win-Stay Spatial Search. In: The University of Western Ontario.

Hall ZJ, Bauchinger U, Gerson AR, Price ER, Langlois LA, Boyles M, Pierce B, McWilliams SR, Sherry DF, MacDougall-Shackleton SA. 2014. Site-specific regulation of adult neurogenesis by dietary fatty acid content, vitamin E and flight exercise in European starlings. European Journal of Neuroscience 39:875-882.

Hamilton LK, Joppé SE, M Cochard L, Fernandes KJ. 2013. Aging and neurogenesis in the adult forebrain: what we have learned and where we should go from here. European journal of neuroscience 37:1978-1986.

Hastings NB, Gould E. 1999. Rapid extension of axons into the CA3 region by adult-generated granule cells. Journal of Comparative Neurology 413:146-154.

Herrgen L, Akerman CJ. 2016. Mapping neurogenesis onset in the optic tectum of Xenopus laevis. Developmental neurobiology 76:1328-1341.

Horesh D, Sapir T, Francis F, Wolf SG, Caspi M, Elbaum M, Chelly J, Reiner O. 1999. Doublecortin, a stabilizer of microtubules. Human molecular genetics 8:1599-1610.

Hoshooley JS, Sherry DF. 2004. Neuron production, neuron number, and structure size are seasonally stable in the hippocampus of the food-storing black-capped chickadee (Poecile atricapillus). Behavioral neuroscience 118:345.

Hubrecht RC, Kirkwood J. 2010. The UFAW handbook on the care and management of laboratory and other research animals: John Wiley & Sons.

Ihunwo A, Pillay S. 2007. Neurogenic sites in the adult mammalian central nervous system. Res J Biol Sci 2:170-177.

Ihunwo AO, Tembo LH, Dzamalala C. 2016. The dynamics of adult neurogenesis in human hippocampus. Neural regeneration research 11:1869.

Jarvis ED, Güntürkün O, Bruce L, Csillag A, Karten H, Kuenzel W, Medina L, Paxinos G, Perkel DJ, Shimizu T. 2005. Avian brains and a new understanding of vertebrate brain evolution. Nature Reviews Neuroscience 6:151.

Jaskelioff M, Muller FL, Paik J-H, Thomas E, Jiang S, Adams AC, Sahin E, Kost-Alimova M, Protopopov A, Cadinanos J. 2011. Telomerase reactivation reverses tissue degeneration in aged telomerase-deficient mice. Nature 469:102.

Jessberger S, Clark RE, Broadbent NJ, Clemenson GD, Consiglio A, Lie DC, Squire LR, Gage FH. 2009. Dentate gyrus-specific knockdown of adult neurogenesis impairs spatial and object recognition memory in adult rats. Learning & memory 16:147-154.

Jin K, Sun Y, Xie L, Batteur S, Mao XO, Smelick C, Logvinova A, Greenberg DA. 2003. Neurogenesis and aging: FGF-2 and HB-EGF restore neurogenesis in hippocampus and subventricular zone of aged mice. Aging cell 2:175-183.

Jinno S. 2011. Decline in adult neurogenesis during aging follows a topographic pattern in the mouse hippocampus. Journal of Comparative Neurology 519:451-466.

Kaplan MS, Bell DH. 1984. Mitotic neuroblasts in the 9-day-old and 11-month-old rodent hippocampus. Journal of Neuroscience 4:1429-1441.

Kaplan MS, Hinds JW. 1977. Neurogenesis in the adult rat: electron microscopic analysis of light radioautographs. Science 197:1092-1094.

Kaslin J, Ganz J, Brand M. 2008. Proliferation, neurogenesis and regeneration in the non-mammalian vertebrate brain. Philosophical Transactions of the Royal Society of London B: Biological Sciences 363:101-122.

Kempermann G. 2011. Seven principles in the regulation of adult neurogenesis. European Journal of Neuroscience 33:1018-1024.

Kempermann G, Kuhn HG, Gage FH. 1997. More hippocampal neurons in adult mice living in an enriched environment. Nature 386:493.

Kim HJ, Kim JY, Sun W. 2012. Age-dependent changes in the subcallosal zone neurogenesis of mice. Neurochemistry international 61:879-884.

Kim WY, Sharpless NE. 2006. The regulation of INK4/ARF in cancer and aging. Cell 127:265-275.

Kim Y-H, Peregrine J, Arnold AP. 2006. The distribution of expression of doublecortin (DCX) mRNA and protein in the zebra finch brain. Brain research 1106:189-196.

Kippin TE, Martens DJ, van der Kooy D. 2005. p21 loss compromises the relative quiescence of forebrain stem cell proliferation leading to exhaustion of their proliferation capacity. Genes & development 19:756-767.

Kirkham M, Hameed LS, Berg DA, Wang H, Simon A. 2014. Progenitor cell dynamics in the newt telencephalon during homeostasis and neuronal regeneration. Stem cell reports 2:507-519.

Kirn J, Nottebohm F. 1993. Direct evidence for loss and replacement of projection neurons in adult canary brain. The Journal of neuroscience 13:1654-1663.

Kirn JR. 2010. The relationship of neurogenesis and growth of brain regions to song learning. Brain and language 115:29-44.

Kirn JR, Alvarez-Buylla A, Nottebohm F. 1991. Production and survival of projection neurons in a forebrain vocal center of adult male canaries. Journal of Neuroscience 11:1756-1762.

Klempin F, Kronenberg G, Cheung G, Kettenmann H, Kempermann G. 2011. Properties of doublecortin-(DCX)-expressing cells in the piriform cortex compared to the neurogenic dentate gyrus of adult mice. PloS one 6:e25760.

Knoth R, Singec I, Ditter M, Pantazis G, Capetian P, Meyer RP, Horvat V, Volk B, Kempermann G. 2010. Murine features of neurogenesis in the human hippocampus across the lifespan from 0 to 100 years. PloS one 5:e8809.

Kondo K, Suzukawa K, Sakamoto T, Watanabe K, Kanaya K, Ushio M, Yamaguchi T, Nibu KI, Kaga K, Yamasoba T. 2010. Age-related changes in cell dynamics of the postnatal mouse olfactory neuroepithelium: Cell proliferation, neuronal differentiation, and cell death. Journal of Comparative Neurology 518:1962-1975.

Kremer T, Jagasia R, Herrmann A, Matile H, Borroni E, Francis F, Kuhn HG, Czech C. 2013. Analysis of adult neurogenesis: evidence for a prominent "non-neurogenic" DCX-protein pool in rodent brain. PloS one 8:e59269.

Kronenberg G, Bick-Sander A, Bunk E, Wolf C, Ehninger D, Kempermann G. 2006. Physical exercise prevents age-related decline in precursor cell activity in the mouse dentate gyrus. Neurobiology of aging 27:1505-1513.

Kuenzel WJ, Masson M. 1988. A stereotaxic atlas of the brain of the chick (Gallus domesticus): Johns Hopkins University Press.

Kuhn HG, Dickinson-Anson H, Gage FH. 1996. Neurogenesis in the dentate gyrus of the adult rat: age-related decrease of neuronal progenitor proliferation. Journal of Neuroscience 16:2027-2033.

Kuhn HG, Eisch AJ. 2014. Neural Stem Cells in Development, Adulthood and Disease: Springer.

LaDage LD, Roth TC, Pravosudov VV. 2011. Hippocampal neurogenesis is associated with migratory behaviour in adult but not juvenile sparrows (Zonotrichia leucophrys ssp.). Proceedings of the Royal Society of London B: Biological Sciences 278:138-143.

Lai M, Hibberd CJ, Gluckman PD, Seckl JR. 2000. Reduced expression of insulin-like growth factor 1 messenger RNA in the hippocampus of aged rats. Neuroscience letters 288:66-70.

Lazzari M, Franceschini V, Ciani F. 1997. Glial fibrillary acidic protein and vimentin in radial glia of Ambystoma mexicanum and Triturus carnifex: an immunocytochemical study. Journal fur Hirnforschung 38:187-194.

Lee DA, Blackshaw S. 2012. Functional implications of hypothalamic neurogenesis in the adult mammalian brain. International journal of developmental neuroscience 30:615-621.

Lee DW, Miyasato LE, Clayton NS. 1998. Neurobiological bases of spatial learning in the natural environment: neurogenesis and growth in the avian and mammalian hippocampus. Neuroreport 9:R-15-R-27.

Legrier M-E, Ducray A, Propper A, Kastner A. 2001. Region-specific expression of cell cycle inhibitors in the adult brain. Neuroreport 12:3127-3131.

Lemasson M, Saghatelyan A, Olivo-Marin J-C, Lledo P-M. 2005. Neonatal and adult neurogenesis provide two distinct populations of newborn neurons to the mouse olfactory bulb. Journal of Neuroscience 25:6816-6825.

Li X, Tang X, Jablonska B, Aguirre A, Gallo V, Luskin MB. 2009. P27KIP1 regulates neurogenesis in the rostral migratory stream and olfactory bulb of the postnatal mouse. Journal of Neuroscience 29:2902-2914.

Lindsey BW, Tropepe V. 2006. A comparative framework for understanding the biological principles of adult neurogenesis. Progress in neurobiology 80:281-307.

Ling C, Cheng M-F. 1995. Sex differences in cell proliferation in the ventricular zone of young ring doves. Brain research bulletin 37:657-662.

Ling C, Zuo M, Alvarez-Buylla A, Cheng MF. 1997. Neurogenesis in juvenile and adult ring doves. Journal of Comparative Neurology 379:300-312.

Liu X-S, Tilwalli S, Ye G-l, Lio PA, Pasternak JF, Trommer BL. 2000. Morphologic and electrophysiologic maturation in developing dentate gyrus granule cells. Brain research 856:202-212.

Lois C, Alvarez-Buylla A. 1994. Long-distance neuronal migration in the adult mammalian brain. Science 264:1145-1148.

Luo J, Daniels SB, Lennington JB, Notti RQ, Conover JC. 2006. The aging neurogenic subventricular zone. Aging cell 5:139-152.

Lupien SJ, McEwen BS, Gunnar MR, Heim C. 2009. Effects of stress throughout the lifespan on the brain, behaviour and cognition. Nature reviews neuroscience 10:434-445.

Maddin HC, Eckhart L, Jaeger K, Russell AP, Ghannadan M. 2009. The anatomy and development of the claws of Xenopus laevis (Lissamphibia: Anura) reveal alternate pathways of structural evolution in the integument of tetrapods. Journal of anatomy 214:607-619.

Maden M, Manwell LA, Ormerod BK. 2013. Proliferation zones in the axolotl brain and regeneration of the telencephalon. Neural development 8:1.

Maheu ME, Devorak J, Freibauer A, Davoli MA, Turecki G, Mechawar N. 2015. Increased doublecortin (DCX) expression and incidence of DCX-immunoreactive multipolar cells in the subventricular zone-olfactory bulb system of suicides. Frontiers in neuroanatomy 9.

Mandal PK, Blanpain C, Rossi DJ. 2011. DNA damage response in adult stem cells: pathways and consequences. Nature Reviews Molecular Cell Biology 12:198.

Markakis EA, Gage FH. 1999. Adult-generated neurons in the dentate gyrus send axonal projections to field CA3 and are surrounded by synaptic vesicles. Journal of comparative neurology 406:449-460.

Maslov AY, Barone TA, Plunkett RJ, Pruitt SC. 2004. Neural stem cell detection, characterization, and age-related changes in the subventricular zone of mice. Journal of Neuroscience 24:1726-1733.

Mattson MP, Maudsley S, Martin B. 2004. BDNF and 5-HT: a dynamic duo in age-related neuronal plasticity and neurodegenerative disorders. Trends in neurosciences 27:589-594.

Mazengenya P, Bhagwandin A, Manger PR, Ihunwo AO. 2018. Putative adult neurogenesis in old world parrots: the Congo African grey parrot (Psittacus erithacus) and Timneh grey parrot (Psittacus timneh). Frontiers in Neuroanatomy 12:7.

Mazengenya P, Bhagwandin A, Nkomozepi P, Manger PR, Ihunwo AO. 2017. Putative adult neurogenesis in two domestic pigeon breeds (Columba livia domestica): racing homer versus utility carneau pigeons. Neural Regeneration Research 12:1086.

McCabe B, Horn G. 1994. Learning-related changes in Fos-like immunoreactivity in the chick forebrain after imprinting. Proceedings of the National Academy of Sciences 91:11417-11421.

Melleu F, Pinheiro M, Lino-de-Oliveira C, Marino-Neto J. 2016. Defensive behaviors and prosencephalic neurogenesis in pigeons (Columba livia) are affected by environmental enrichment in adulthood. Brain Structure and Function 221:2287-2301.

Melleu F, Santos T, Lino-de-Oliveira C, Marino-Neto J. 2013. Distribution and characterization of doublecortin-expressing cells and fibers in the brain of the adult pigeon (Columba livia). Journal of chemical neuroanatomy 47:57-70.

Meskenaite V, Krackow S, Lipp H-P. 2016. Age-Dependent Neurogenesis and Neuron Numbers within the Olfactory Bulb and Hippocampus of Homing Pigeons. Frontiers in Behavioral Neuroscience 10:126

Mezey S, Krivokuca D, Bálint E, Adorján A, Zachar G, Csillag A. 2012. Postnatal changes in the distribution and density of neuronal nuclei and doublecortin antigens in domestic chicks (Gallus domesticus). Journal of Comparative Neurology 520:100-116.

Miller RA, Harper JM, Dysko RC, Durkee SJ, Austad SN. 2002. Longer life spans and delayed maturation in wild-derived mice. Experimental Biology and Medicine 227:500-508.

Mills AD, Crawford LL, Domjan M, Faure JM. 1997. The behavior of the Japanese or domestic quail Coturnix japonica. Neuroscience & Biobehavioral Reviews 21:261-281.

Ming G-l, Song H. 2011. Adult neurogenesis in the mammalian brain: significant answers and significant questions. Neuron 70:687-702.

Mirich JM, Williams NC, Berlau DJ, Brunjes PC. 2002. Comparative study of aging in the mouse olfactory bulb. Journal of Comparative Neurology 454:361-372.

Mirzadeh Z, Merkle FT, Soriano-Navarro M, Garcia-Verdugo JM, Alvarez-Buylla A. 2008. Neural stem cells confer unique pinwheel architecture to the ventricular surface in neurogenic regions of the adult brain. Cell stem cell 3:265-278.

Mobley AS, Rodriguez-Gil DJ, Imamura F, Greer CA. 2014. Aging in the olfactory system. Trends in neurosciences 37:77-84.

Molofsky AV, Pardal R, Iwashita T, Park I-K, Clarke MF, Morrison SJ. 2003. Bmi-1 dependence distinguishes neural stem cell self-renewal from progenitor proliferation. nature 425:962.

Molofsky AV, Slutsky SG, Joseph NM, He S, Pardal R, Krishnamurthy J, Sharpless NE, Morrison SJ. 2006. Increasing p16 INK4a expression decreases forebrain progenitors and neurogenesis during ageing. Nature 443:448.

Montaron M, Drapeau E, Dupret D, Kitchener P, Aurousseau C, Le Moal M, Piazza P, Abrous D. 2006. Lifelong corticosterone level determines age-related decline in neurogenesis and memory. Neurobiology of aging 27:645-654.

Montaron M, Petry K, Rodriguez J, Marinelli M, Aurousseau C, Rougon G, Le Moal M, Abrous D. 1999. Adrenalectomy increases neurogenesis but not PSA-NCAM expression in aged dentate gyrus. European Journal of Neuroscience 11:1479-1485.

Moreno N, González A. 2004. Localization and connectivity of the lateral amygdala in anuran amphibians. Journal of Comparative Neurology 479:130-148.

Moreno N, González A. 2017. Pattern of neurogenesis and identification of neuronal progenitor subtypes during pallial development in Xenopus laevis. Frontiers in neuroanatomy 11:24.

Mouriec K, Balthazart J. 2013. Peripubertal proliferation of progenitor cells in the preoptic area of Japanese quail (Coturnix japonica). Brain research 1516:20-32.

Nacher J, Crespo C, McEwen BS. 2001. Doublecortin expression in the adult rat telencephalon. European Journal of Neuroscience 14:629-644.

Nada M-B, Slomianka L, Vyssotski AL, Lipp H-P. 2010. Early age-related changes in adult hippocampal neurogenesis in C57 mice. Neurobiology of aging 31:151-161.

Nakamori T, Maekawa F, Sato K, Tanaka K, Ohki-Hamazaki H. 2013. Neural basis of imprinting behavior in chicks. Development, growth & differentiation 55:198-206.

Newman AE, MacDougall-Shackleton SA, An YS, Kriengwatana B, Soma KK. 2010. Corticosterone and dehydroepiandrosterone have opposing effects on adult neuroplasticity in the avian song control system. Journal of Comparative Neurology 518:3662-3678.

Nikolakopoulou A, Dermon C, Panagis L, Pavlidis M, Stewart M. 2006a. Passive avoidance training is correlated with decreased cell proliferation in the chick hippocampus. European Journal of Neuroscience 24:2631-2642.

Nikolakopoulou AM, Parpas A, Panagis L, Zikopoulos B, Dermon CR. 2006b. Early post-hatching sex differences in cell proliferation and survival in the quail telencephalic ventricular zone and intermediate medial mesopallium. Brain research bulletin 70:107-116.

Nishino J, Kim I, Chada K, Morrison SJ. 2008. Hmga2 promotes neural stem cell self-renewal in young but not old mice by reducing p16 Ink4a and p19 Arf expression. Cell 135:227-239.

Nkomozepi P, Mazengenya P, Ihunwo AO. 2018. Changes in neurogenesis with post-hatching age in the male Japanese quail (Cortunix japonica) brain. Acta neurobiologiae experimentalis 78:173-186.

Nottebohm F. 1980. Testosterone triggers growth of brain vocal control nuclei in adult female canaries. Brain research 189:429-436.

Nottebohm F. 1984. Birdsong as a model in which to study brain processes related to learning. Condor:227-236.

Nottebohm F. 1996. A white canary on Mount Acropolis. Journal of Comparative Physiology A 179:149-156.

Nottebohm F. 2002. Why are some neurons replaced in adult brain? Journal of Neuroscience 22:624-628.

Nottebohm F. 2011. Song learning in birds offers a model for neuronal replacement in adult brain. In: Neurogenesis in the Adult Brain I: Springer. p 47-84.

Obiorah M, McCandlish E, Buckley B, DiCicco-Bloom E. 2015. Hippocampal developmental vulnerability to methylmercury extends into prepubescence. Frontiers in neuroscience 9:150.

Olaleye OO, Ihunwo AO. 2014. Adult neurogenesis in the four-striped mice (Rhabdomys pumilio). Neural regeneration research 9:1907.

Olude AM, Olopade JO, Ihunwo AO. 2014. Adult neurogenesis in the African giant rat (Cricetomysgambianus, waterhouse). Metabolic brain disease 29:857-866.

Ottinger MA, Abdelnabi M, Li Q, Chen K, Thompson N, Harada N, Viglietti-Panzica C, Panzica GC. 2004. The Japanese quail: a model for studying reproductive aging of hypothalamic systems. Experimental gerontology 39:1679-1693.

Ottinger MA, Brinkley HJ. 1979. Testosterone and sex related physical characteristics during the maturation of the male Japanese quail (Coturnix coturnix japonica). Biology of reproduction 20:905-909.

Paredes, M.F., Sorrells, S.F., Garcia-Verdugo, J.M. and Alvarez-Buylla, A., 2016. Brain size and limits to adult neurogenesis. Journal of Comparative Neurology, 524(3), pp.646-664.

Parish CL, Beljajeva A, Arenas E, Simon A. 2007. Midbrain dopaminergic neurogenesis and behavioural recovery in a salamander lesion-induced regeneration model. Development 134:2881-2887.

Pellegrini E, Mouriec K, Anglade I, Menuet A, Le Page Y, Gueguen MM, Marmignon MH, Brion F, Pakdel F, Kah O. 2007. Identification of aromatase-positive radial glial cells as progenitor cells in the ventricular layer of the forebrain in zebrafish. Journal of Comparative Neurology 501:150-167.

Pierce AA, Xu AW. 2010. De novo neurogenesis in adult hypothalamus as a compensatory mechanism to regulate energy balance. Journal of Neuroscience 30:723-730.

Pino A, Fumagalli G, Bifari F, Decimo I. 2017. New neurons in adult brain: distribution, molecular mechanisms and therapies. Biochemical Pharmacology.8 (17): 30480

Polenov AL, Chetverukhin VK. 1993. Ultrastructural radioautographic analysis of neurogenesis in the hypothalamus of the adult frog, Rana temporaria, with special reference to physiological regeneration of the preoptic nucleus. Cell and tissue research 271:351-362.

Puelles L. 2007. chick brain in stereotaxic coordinates: Academic Press.

Pytte CL, Gerson M, Miller J, Kirn JR. 2007. Increasing stereotypy in adult zebra finch song correlates with a declining rate of adult neurogenesis. Developmental Neurobiology 67:1699-1720.

Quiñones-Hinojosa A, Sanai N, Soriano-Navarro M, Gonzalez-Perez O, Mirzadeh Z, Gil-Perotin S, Romero-Rodriguez R, Berger MS, Garcia-Verdugo JM, Alvarez-Buylla A. 2006. Cellular composition and cytoarchitecture of the adult human subventricular zone: a niche of neural stem cells. Journal of Comparative Neurology 494:415-434.

Rai KS, Hattiangady B, Shetty AK. 2007. Enhanced production and dendritic growth of new dentate granule cells in the middle-aged hippocampus following intracerebroventricular FGF-2 infusions. European Journal of Neuroscience 26:1765-1779.

Rasika S, Alvarez-Buylla A, Nottebohm F. 1999. BDNF mediates the effects of testosterone on the survival of new neurons in an adult brain. Neuron 22:53-62.

Raucci F, Di Fiore MM, Pinelli C, D'Aniello B, Luongo L, Polese G, Rastogi RK. 2006. Proliferative activity in the frog brain: a PCNA-immunohistochemistry analysis. Journal of chemical neuroanatomy 32:127-142.

Reiner A, Perkel DJ, Bruce LL, Butler AB, Csillag A, Kuenzel W, Medina L, Paxinos G, Shimizu T, Striedter G. 2004. Revised nomenclature for avian telencephalon and some related brainstem nuclei. Journal of Comparative Neurology 473:377-414.

Rostas J, Kavanagh J, Dodd P, Heath J, Powis D. 1991. Mechanisms of synaptic plasticity. Molecular Neurobiology 5:203-216.

Roth G, Westhoff G. 1999. Cytoarchitecture and connectivity of the amphibian medial pallium. European journal of morphology 37:166-171.

Sapolsky RM. 1992. Do glucocorticoid concentrations rise with age in the rat? Neurobiology of aging 13:171-174.

Sapolsky RM, Meaney MJ. 1986. Maturation of the adrenocortical stress response: neuroendocrine control mechanisms and the stress hyporesponsive period. Brain Research Reviews 11:65-76.

Schneider CA, Rasband WS, Eliceiri KW. 2012. NIH Image to ImageJ: 25 years of image analysis. Nature methods 9:671-675.

Scholzen T, Gerdes J. 2000. The Ki-67 protein: from the known and the unknown. Journal of cellular physiology 182:311-322.

Seidenfaden R, Desoeuvre A, Bosio A, Virard I, Cremer H. 2006. Glial conversion of SVZ-derived committed neuronal precursors after ectopic grafting into the adult brain. Molecular and cellular neuroscience 32:187-198.

Seki T, Arai Y. 1995. Age-related production of new granule cells in the adult dentate gyrus. Neuroreport 6:2479-2482.

Seki T, Sawamoto K, Parent JM, Alvarez-Buylla A. 2011. Neurogenesis in the adult brain I: Neurobiology: Springer Science & Business Media.

Seri B, Garcıa-Verdugo JM, McEwen BS, Alvarez-Buylla A. 2001. Astrocytes give rise to new neurons in the adult mammalian hippocampus. Journal of Neuroscience 21:7153-7160.

Seri B, García-Verdugo JM, Collado-Morente L, McEwen BS, Alvarez-Buylla A. 2004. Cell types, lineage, and architecture of the germinal zone in the adult dentate gyrus. Journal of Comparative Neurology 478:359-378.

Sherr CJ, Roberts JM. 1999. CDK inhibitors: positive and negative regulators of G1-phase progression. Genes & development 13:1501-1512.

Shetty AK, Hattiangady B, Shetty GA. 2005. Stem/progenitor cell proliferation factors FGF-2, IGF-1, and VEGF exhibit early decline during the course of aging in the hippocampus: Role of astrocytes. Glia 51:173-186.

Shihabuddin LS, Horner PJ, Ray J, Gage FH. 2000. Adult spinal cord stem cells generate neurons after transplantation in the adult dentate gyrus. Journal of Neuroscience 20:8727-8735.

Shook BA, Manz DH, Peters JJ, Kang S, Conover JC. 2012. Spatiotemporal changes to the subventricular zone stem cell pool through aging. Journal of Neuroscience 32:6947-6956.

Simmons AM, Chapman JA, Brown RA. 2006. Developmental changes in cell proliferation in the auditory midbrain of the bullfrog, Rana catesbeiana. Journal of neurobiology 66:1212-1224.

Simmons AM, Horowitz SS, Brown RA. 2008. Cell proliferation in the forebrain and midbrain of the adult bullfrog, Rana catesbeiana. Brain, behavior and evolution 71:41-53.

Soma KK, Tramontin AD, Featherstone J, Brenowitz EA. 2004. Estrogen contributes to seasonal plasticity of the adult avian song control system. Journal of neurobiology 58:413-422.

Sotelo MI, Daneri MF, Bingman VP, Muzio RN. 2016. Telencephalic Neuronal Activation Associated with Spatial Memory in the Terrestrial Toad Rhinella arenarum: Participation of the Medial Pallium during Navigation by Geometry. Brain, behavior and evolution 88:149-160.

Spritzer MD, Galea LA. 2007. Testosterone and dihydrotestosterone, but not estradiol, enhance survival of new hippocampal neurons in adult male rats. Developmental neurobiology 67:1321-1333.

Stamatakis A, Barbas H, Dermon CR. 2004. Late granule cell genesis in quail cerebellum. Journal of Comparative Neurology 474:173-189.

Striedter GF, Charvet CJ. 2008. Developmental origins of species differences in telencephalon and tectum size: morphometric comparisons between a parakeet (Melopsittacus undulatus) and a quail (Colinus virgianus). Journal of Comparative Neurology 507:1663-1675.

Sun Y, Jin K, Childs JT, Xie L, Mao XO, Greenberg DA. 2006. Vascular endothelial growth factor-B (VEGFB) stimulates neurogenesis: evidence from knockout mice and growth factor administration. Developmental biology 289:329-335.

Szenczi P, Bánszegi O, Groó Z, Altbäcker V. 2012. Development of the social behavior of two mice species with contrasting social systems. Aggressive behavior 38:288-297.

Tang YP, Wade J. 2012. 17β-Estradiol regulates the sexually dimorphic expression of BDNF and TrkB proteins in the song system of juvenile zebra finches. PloS one 7:e43687.

Tang YP, Wade J. 2016. Sex and age differences in brain-derived neurotrophic factor and vimentin in the zebra finch song system: Relationships to newly generated cells. Journal of Comparative Neurology 524:1081-1096.

Thuret R, Auger H, Papalopulu N. 2015. Analysis of neural progenitors from embryogenesis to juvenile adult in Xenopus laevis reveals biphasic neurogenesis and continuous lengthening of the cell cycle. Biology open:bio. 013391.

Tropepe V, Craig CG, Morshead CM, van der Kooy D. 1997. Transforming growth factor-α null and senescent mice show decreased neural progenitor cell proliferation in the forebrain subependyma. Journal of Neuroscience 17:7850-7859.

Tsai HM, Garber BB, Larramendi LM. 1981. 3H-Thymidine autoradiographic analysis of telencephalic histogenesis in the chick embryo: I. Neuronal birthdates of telencephalic compartments in situ. Journal of Comparative Neurology 198:275-292.

Ünal B, Bradley PM, Sahin B, Canan S, Aslan H, Kaplan S. 2002. Estimation of numerical density and mean synaptic height in chick hippocampus 24 and 48 hours after passive avoidance training. Developmental brain research 136:135-144.

und Halbach OvB. 2010. Involvement of BDNF in age-dependent alterations in the hippocampus. Frontiers in aging neuroscience 2:36

Van Praag H, Kempermann G, Gage FH. 1999. Running increases cell proliferation and neurogenesis in the adult mouse dentate gyrus. Nature neuroscience 2:266.

Vellema M, Hertel M, Urbanus SL, Linden A, Gahr M. 2014. Evaluating the predictive value of doublecortin as a marker for adult neurogenesis in canaries (Serinus canaria). Journal of Comparative Neurology 522:1299-1315.

Vellema M, Van der Linden A, Gahr M. 2010. Area-specific migration and recruitment of new neurons in the adult songbird brain. Journal of Comparative Neurology 518:1442-1459.

Villeda SA, Luo J, Mosher KI, Zou B, Britschgi M, Bieri G, Stan TM, Fainberg N, Ding Z, Eggel A. 2011. The ageing systemic milieu negatively regulates neurogenesis and cognitive function. Nature 477:90.

Wada H, Newman AE, Hall ZJ, Soma KK, MacDougall-Shackleton SA. 2014. Effects of corticosterone and DHEA on doublecortin immunoreactivity in the song control system and hippocampus of adult song sparrows. Developmental neurobiology 74:52-62.

Wada M, Urano A, Gorbman A. 1980. A stereotaxic atlas for diencephalic nuclei of the frog, Rana pipiens. Archivum histologicum japonicum 43:157-173.

Wang N, Hurley P, Pytte C, Kirn JR. 2002. Vocal control neuron incorporation decreases with age in the adult zebra finch. The Journal of neuroscience 22:10864-10870.

Wang S, Scott BW, Wojtowicz JM. 2000. Heterogenous properties of dentate granule neurons in the adult rat. Journal of neurobiology 42:248-257.

Westhoff G, Roth G. 2002. Morphology and projection pattern of medial and dorsal pallial neurons in the frog Discoglossus pictus and the salamander Plethodon jordani. Journal of Comparative Neurology 445:97-121.

Whitman MC, Fan W, Rela L, Rodriguez-Gil DJ, Greer CA. 2009. Blood vessels form a migratory scaffold in the rostral migratory stream. Journal of Comparative Neurology 516:94-104.

Wilbrecht L, Kirn JR. 2004. Neuron addition and loss in the song system: regulation and function. Annals of the New York Academy of Sciences 1016:659-683.

Wong K-K, Maser RS, Bachoo RM, Menon J, Carrasco DR, Gu Y, Alt FW, DePinho RA. 2003. Telomere dysfunction and Atm deficiency compromises organ homeostasis and accelerates ageing. Nature 421:643.

Wullimann MF, Rink E, Vernier P, Schlosser G. 2005. Secondary neurogenesis in the brain of the African clawed frog, Xenopus laevis, as revealed by PCNA, Delta-1, Neurogenin-related-1, and NeuroD expression. Journal of Comparative Neurology 489:387-402.

y Cajal SR. 1913. Contribucion al conocimiento de la neuroglia del cerebro humano.

Yamamura T, Barker JM, Balthazart J, Ball GF. 2011. Androgens and estrogens synergistically regulate the expression of doublecortin and enhance neuronal recruitment in the song system of adult female canaries. The Journal of Neuroscience 31:9649-9657.

Zuo MX. 1998. The studies on neurogenesis induced by brain injury in adult ring dove. Cell research 8:151-158.

Zupanc G. 2006. Neurogenesis and neuronal regeneration in the adult fish brain. Journal of Comparative Physiology A 192:649.

APPENDICES

STRICTLY CONFIDENTIAL

ANIMAL ETHICS SCREENING COMMITTEE (AESC)

CLEARANCE CERTIFICATE NO. 2012/53/01

APPLICANT: **Professor. P Manger**

DEPARTMENT: **Anatomical Sciences**

PROJECT TITLE: **Comparative Neuroanatomy of Vertebrate Species - establishing a world-class brain bank at Wits**

Number and Species

Approved: Various species of vertebrates, to be detailed in M&Es as they become available

Approval was given for to the use of animals for the project described above at an AESC meeting held on **27 November 2012**. This approval remains valid until **30 November 2014**.

The use of these animals is subject to AESC guidelines for the use and care of animals, is limited to the procedures described in the application.

Signed: _____ (Chairperson, AESC) Date: 5/12/12

I am satisfied that the persons listed in this application are competent to perform the procedures therein, in terms of Section 23 (1) (c) of the Veterinary and Para-Veterinary Professions Act (19 of 1982)

Signed: _____ (Registered Veterinarian) Date: 5/12/12

cc: Supervisor:
Director: CAS

STRICTLY CONFIDENTIAL

ANIMAL ETHICS SCREENING COMMITTEE (AESC)

CLEARANCE CERTIFICATE NO. 2014/35/A

APPLICANT: Mr P Nkomozepi

SCHOOL: Anatomical Sciences

LOCATION: Faculty of Health Sciences

PROJECT TITLE: *Time-course changes in cell proliferation and neurogenesis in the African clawed frog (Xenopus laevis) and Balb C mouse (Mus musculus) brains*

Number and Species

36 African Clawed frogs
36 Laboratory Mice

Approval was given for to the use of animals for the project described above at an AESC meeting held on 27 May 2014 . This approval remains valid until 26 May 2016.

The use of these animals is subject to AESC guidelines for the use and care of animals, is limited to the procedures described in the application form and is subject to any additional conditions listed below:

None.

Signed: _____ (Chairperson, AESC) Date: 1/7/2014

I am satisfied that the persons listed in this application are competent to perform the procedures therein, in terms of Section 23 (1) (c) of the Veterinary and Para-Veterinary Professions Act (19 of 1982)

Signed: _____ (Registered Veterinarian) Date: 1 July 2014

cc: Supervisor: Profs A Ihunwo & P Manger

Director: CAS

Works 2000/lain0015/AESCCert.wps

Pilani PhD

ORIGINALITY REPORT

22%	15%	18%	3%
SIMILARITY INDEX	INTERNET SOURCES	PUBLICATIONS	STUDENT PAPERS

PRIMARY SOURCES

1	Pilani Nkomozepi, Pedzisai Mazengenya, Amadi O. Ihunwo. "Changes in neurogenesis with post-hatching age in the male Japanese quail (Cortunix japonica) brain", Acta Neurobiologiae Experimentalis, 2018 Publication	3%
2	tel.archives-ouvertes.fr Internet Source	1%
3	papyrus.bib.umontreal.ca Internet Source	1%
4	www.scribd.com Internet Source	1%
5	Neurogenesis in the Adult Brain I, 2011. Publication	1%
6	researchspace.auckland.ac.nz Internet Source	1%
7	www.frontiersin.org Internet Source	<1%
	link.springer.com	

8	Internet Source	<1%
9	Jan Kaslin. "Proliferation, neurogenesis and regeneration in the non-mammalian vertebrate brain", Philosophical Transactions of The Royal Society B Biological Sciences, 01/12/2008 Publication	<1%
10	www.ncbi.nlm.nih.gov Internet Source	<1%
11	onlinelibrary.wiley.com Internet Source	<1%
12	pdfs.semanticscholar.org Internet Source	<1%
13	cshperspectives.cshlp.org Internet Source	<1%
14	Pedzisai Mazengenya, Adhil Bhagwandin, Paul R. Manger, Amadi O. Ihunwo. "Putative Adult Neurogenesis in Old World Parrots: The Congo African Grey Parrot (Psittacus erithacus) and Timneh Grey Parrot (Psittacus timneh)", Frontiers in Neuroanatomy, 2018 Publication	<1%
15	hal-univ-rennes1.archives-ouvertes.fr Internet Source	<1%
16	academic.oup.com	

	Internet Source	<1%
17	www-brs.ub.ruhr-uni-bochum.de Internet Source	<1%
18	www.dbbe.fcen.uba.ar Internet Source	<1%
19	www.jneurosci.org Internet Source	<1%
20	journal.frontiersin.org Internet Source	<1%
21	Stem Cell Biology and Regenerative Medicine, 2015. Publication	<1%
22	Cayre, M.. "Cell migration in the normal and pathological postnatal mammalian brain", Progress in Neurobiology, 200905 Publication	<1%
23	Ruth Morona, José Luis Ferran, Luis Puelles, Agustín González. " Gene expression analysis of developing cell groups in the pretectal region of ", Journal of Comparative Neurology, 2017 Publication	<1%
24	Submitted to Boston University Student Paper	<1%
	www.eneuro.org	

25	Internet Source	<1%
26	neuraldevelopment.biomedcentral.com Internet Source	<1%
27	open.bu.edu Internet Source	<1%
28	Laure Anne D'Amico, Daniel Boujard, Pascal Coumailleau. "Proliferation, migration and differentiation in juvenile and adult Xenopus laevis brains", Brain Research, 2011 Publication	<1%
29	Christina Herold, Philipp Schlömer, Isabelle Mafoppa-Fomat, Julia Mehlhorn, Katrin Amunts, Markus Axer. "The hippocampus of birds in a view of evolutionary connectomics", Cortex, 2018 Publication	<1%
30	www.karger.com Internet Source	<1%
31	www.nature.com Internet Source	<1%
32	dev.biologists.org Internet Source	<1%
33	mediatum.ub.tum.de Internet Source	<1%

34	neuroviisas.med.uni-rostock.de Internet Source	<1%
35	www.spn.org.pt Internet Source	<1%
36	ecommons.usask.ca Internet Source	<1%
37	Submitted to Federal University of Technology Student Paper	<1%
38	d-nb.info Internet Source	<1%
39	Rebecca A. Ihrie. "Cells in the astroglial lineage are neural stem cells", Cell and Tissue Research, 01/2008 Publication	<1%
40	Meskenaite, Virginia, Sven Krackow, and Hans-Peter Lipp. "Age-Dependent Neurogenesis and Neuron Numbers within the Olfactory Bulb and Hippocampus of Homing Pigeons", Frontiers in Behavioral Neuroscience, 2016. Publication	<1%
41	www.jove.com Internet Source	<1%
42	Taylor Gordon, J.. "The 2006 Benjamin Franklin Medal in Life Science presented to Fernando Nottebohm, Ph.D. for demonstration of Central	<1%

	Neurogenesis in Adult Avians, with Concomitant Implications for the Theory of Memory and for the Future of Neurological Repair in Injury and Disease", Journal of the Franklin Institute, 201005 Publication	
43	G. Jean Harry. "Neurogenesis and Brain Repair", Neuroimmune Pharmacology, 2008 Publication	<1%
44	Tang, Yu Ping, and Juli Wade. "Sex and Age Differences in Brain Derived Neurotrophic Factor and Vimentin in the Zebra Finch Song System: Relationships to Newly Generated Cells : Song system differentiation: BDNF and vimentin", The Journal of Comparative Neurology, 2015. Publication	<1%
45	www.dtic.mil Internet Source	<1%
46	Submitted to Queen Mary and Westfield College Student Paper	<1%
47	www.fitex.co.nz Internet Source	<1%
48	media.proquest.com Internet Source	<1%

	Neurogenesis in Adult Avians, with Concomitant Implications for the Theory of Memory and for the Future of Neurological Repair in Injury and Disease", Journal of the Franklin Institute, 201005 Publication	
43	G. Jean Harry. "Neurogenesis and Brain Repair", Neuroimmune Pharmacology, 2008 Publication	<1%
44	Tang, Yu Ping, and Juli Wade. "Sex and Age Differences in Brain Derived Neurotrophic Factor and Vimentin in the Zebra Finch Song System: Relationships to Newly Generated Cells : Song system differentiation: BDNF and vimentin", The Journal of Comparative Neurology, 2015. Publication	<1%
45	www.dtic.mil Internet Source	<1%
46	Submitted to Queen Mary and Westfield College Student Paper	<1%
47	www.fitex.co.nz Internet Source	<1%
48	media.proquest.com Internet Source	<1%

RESEARCH PAPER

Acta Neurobiol Exp 2018, 78: 173–186
DOI: 10.21307/ane-2018-016

ACTA NEUROBIOLOGIÆ EXPERIMENTALIS

Changes in neurogenesis with post-hatching age in the male Japanese quail (*Cortunix japonica*) brain

Pilani Nkomozepi[1,2], Pedzisai Mazengenya[1] and Amadi O. Ihunwo[1]*

[1] *School of Anatomical Sciences, Faculty of Health Sciences, University of the Witwatersrand, Johannesburg, South Africa,*
[2] *Department of Human Anatomy and Physiology, University of Johannesburg, Doornfontein, Johannesburg, South Africa,*
** Email : amadi.ihunwo@wits.ac.za*

Most avian neurogenesis studies have previously focused on the song control system and little attention has been given to non-song birds. The objective of this study was to assess changes in neurogenesis associated with post-hatching age (3-12 weeks) in the Japanese quail brain using proliferating cell nuclear antigen (PCNA) and doublecortin (DCX) immunohistochemistry. PCNA-immunoreactive (ir) cells were observed mainly in the olfactory bulb ventricular zone, telencephalic ventricular zones and cerebellum. Fewer PCNA-ir cells were also observed in the hypothalamus, thalamus and bed nucleus of the stria terminalis. In telencephalic ventricular zones, PCNA-ir cells were concentrated ventrally and dorsally adjacent to the mesopallium and medial striatum, respectively. DCX-ir cells were observed in the olfactory bulb, telencephalon and cerebellum. Furthermore, DCX-ir cells were scattered throughout the pallium except in the entopallium and arcopallium, septal nuclei and striatum. Fewer DCX-ir cells were also observed in the hippocampus and bed nucleus of stria terminalis. The density of PCNA-ir cells and DCX-ir cells in all brain areas declined with post-hatching age. In conclusion, cell proliferation appears to be restricted to the ventricular zones whereas neuronal recruitment is more widespread in the olfactory bulb, telencephalon and cerebellum. Postnatal neuronal incorporation appears to be absent in the diencephalon and mesencephalon.

Key words: neurogenesis, proliferating cell nuclear antigen, doublecortin, post-hatching, Japanese quail brain, neuronal recruitment

INTRODUCTION

Across all vertebrate species, the central nervous system harbours constitutively active neuronal progenitors that are responsible for producing new neurons throughout life (Alunni and Bally-Cuif 2016). The process through which new neurons are formed from these progenitors is termed neurogenesis and involves cell proliferation, differentiation, migration and integration of the newly formed neurons into the existing neuronal circuitry (Barnea and Pravosudov 2011). In mammalian adult brains, neurogenesis is restricted to the subgranular zone of the hippocampus and the subventricular zone of the lateral ventricle (Kaslin et al. 2008, Olaleye and Ihunwo 2014). However, in avian brains new neurons are generated along the walls of the lateral ventricle and migrate radially to be integrated into the different circuits of the telencephalon (Hall et al. 2014, Vellema et al. 2010).

The songbird species such as the canary and zebra finch have been used extensively in post-hatching neurogenesis studies (Brenowitz 2004, Brenowitz and Larson 2015, Nottebohm 1984, 2011). Although neurogenesis in songbird brains was observed to be widespread, the focus of most studies has been almost exclusively on neuronal recruitment and integration into telencephalic circuits involved in song production (Alvarez-Buylla et al. 1992, 1994, Balthazart et al. 2008, Balthazart and Ball 2016, Boseret et al. 2007, Nottebohm 2011). However, songbirds constitute only about 2% of all avian species (Ling et al. 1997). Furthermore, previous studies have revealed that the neurogenesis observed in the telencephalon is not only specific to songbirds but also occurs in other avian species belonging to other orders such as ring doves (Ling et al. 1997, Ling and Cheng

Received 18 September 2017, accepted 17 April 2018

exeley

© 2018 by Acta Neurobiologiæ Experimentalis

1995), pigeons (Melleu et al. 2013, 2016, Meskenaite et al. 2016) chicken (Mezey et al. 2012, Nikolakopoulou et al. 2006a) and quails (Balthazart et al. 2010, Bardet et al. 2012, Mouriec and Balthazart 2013, Nikolakopoulou et al. 2006b).

Neurogenesis in the avian brain has been shown to be regulated by several internal and external factors including levels of circulating sex steroids (e.g. testosterone, estradiol), variations in day length, seasonal changes and age (Barker et al. 2014, DeWulf and Bottjer 2002, Guigueno et al. 2016, Meskenaite et al, 2016, Mouriec and Balthazart 2013, Yamamura et al. 2011).

Age-related decline in the production and recruitment of neuronal cells has been reported in the telencephalon and song control nuclei of canaries (Alvarez-Buylla et al. 1994) and zebra finches (DeWulf and Bottjer 2002, Pytte et al. 2007, Wang et al. 2002). In addition, neurogenesis was reported to decline with age in the telencephalic ventricular zones of the ring doves (Ling et al. 1997), the hippocampus and olfactory bulb (OB) of the pigeon (Meskenaite et al. 2016), and the telencephalon of the chicken (Mezey et al. 2012). Interestingly, Mouriec and Balthazart (2013) reported an age-dependent decline in cell proliferation in the medial preoptic nucleus (POM) of the Japanese quail brain during the pre-pubertal stages (postnatal day, PND 1 to 43) which was followed by an increase in cell proliferation at puberty (PND 44 to 56).

The majority of neurogenesis studies in quails focussed on the sex steroid sensitive areas like the POM (Bardet et al. 2012), intermediate medial mesopallium and lateral septal nucleus (Nikolakopoulou et al. 2006b) with little attention given to neurogenesis in other quail brain areas like the telencephalon.

The aim of the present study was therefore to determine the effect of post-hatching age on cell proliferation and neuronal recruitment in the male Japanese quail (*Cortunix japonica*) brain. Japanese quails are precocial birds that belong to the order galliformes. In addition, male quails exhibit crowing, a testosterone dependent behaviour. However, crowing is considered a non-learned vocalisation in contrast to the learned song of songbirds.

To achieve this aim, proliferating cell nuclear antigen (PCNA) and doublecortin (DCX) were used to assess cell proliferation and neuronal recruitment respectively in quail brains.

METHODS

Experimental Animals

Thirty male Japanese quails with post-hatching ages ranging from 3 to 12 weeks obtained from the agricultural research centre (ARC, Irene, South Africa) were used in this study. All animals were treated and used according to the guidelines of the University of the Witwatersrand Animal Ethics Committee, which corresponds with those of the National Institute of Health (NIH) for care and use of animals in scientific experimentation. All protocols were approved by the University of the Witwatersrand Animal Ethics Screening Committee (AESC/2012/53/01).

Throughout their life, the birds were maintained on a photoperiod simulating long days (16:8 h, light:dark) with access to food and water *ad libitum*. During the first 3 weeks after hatching, chicks were kept in mixed groups in brooder cages at 30°C. Temperature was then progressively reduced to room temperature by the 5th week. From post-hatching age 3 weeks, 3 birds were collected every week up until the 12th week. The quails were allocated to groups according to their sexual maturity as follows: juvenile (sexually immature, 3-5 weeks old, n=9), subadult (sexually matured, 6-8 weeks old, n=9) and adult (sexually active, 9-12 weeks old, n=12).

Tissue collection and processing

All birds were given a dose of heparin (1 ml i.m.) 5 min prior to euthanasia to prevent blood clotting followed by an intraperitoneal injection of Euthapent (0.5–1 ml/kg). Animals were then perfusion-fixed transcardially, initially with 0.9% cold saline solution, followed by 4% paraformaldehyde in 0.1 M phosphate buffer (PB, pH 7.4) solution. After perfusion, brains were carefully removed from the skull, post-fixed overnight in 4% paraformaldehyde in 0.1 M PB and weighed before being transferred into 30% sucrose in 0.1 M PB until equilibration was reached. The brains were sectioned in a coronal plane at 50 µm using a cryostat (Shandon Cryotome E, Thermo Fischer scientific, UK) at -24°C and repeated series of 5 sections were collected free-floating into 24 multi-well plates containing 0.1 M PB. The first series of sections was mounted on gelatin coated slides before staining with 1% cresyl violet for anatomical orientation, the second series for PCNA and the third for DCX immunohistochemistry. The remaining two series were stored in a cryoprotectant solution at -20°C for future use.

Immunohistochemistry

Brain sections were pre-treated for 30 min at room temperature under gentle shaking with an endogenous peroxidase inhibitor (0.1 M PB, 100% meth-

anol and 30% H_2O_2 in the ratio 49.2 : 49.2 : 1.66). Following three 10 min rinses in 0.1 M PB, the sections were subsequently pre-incubated in a blocking buffer solution (3% normal horse serum or 3% normal rabbit serum, 2% bovine serum albumin, 0.25% Triton X-100 in 0.1 M PB) for 2 h under gentle shaking at room temperature to prevent non-specific binding. Sections were then transferred into a primary antibody solution 1 : 500, mouse anti-PCNA, clone PC 10; NCL-L-PCNA, Novocastra, UK or 1 : 300, goat anti-DCX, C-18 : SC-8066, Santa Cruz Biotechnology, Inc, USA, in the blocking buffer solution, and were incubated for 48 h at 4°C under gentle shaking. Following incubation, sections were subjected to three 10 min rinses in 0.1 M PB before being incubated in secondary antibody solution 1 : 1000 biotinylated anti-mouse IgG, Novocastra, UK or 1 : 1000 dilution of biotinylated anti-goat IgG, BA-5000; Vector Laboratories, USA in blocking buffer solution, for 2 h at room temperature under gentle shaking. Following three 10 min rinses in 0.1 M PB, the sections were incubated in an avidin-biotin solution 1 : 125, Vector Laboratories in 0.1 M PB for 1 h. The sections were then transferred into three 10 min 0.1 M PB rinses before being placed in a solution containing 0.05% 3, 3 Di-amino-benzidine tetrachloride (DAB) in 0.1 M PB for 5 min. To each 1 ml of this solution, 3.3 µl of 30% H_2O_2 was added, and chromatic precipitation was visually monitored under a low power stereomicroscope.

Development was subsequently stopped by placing the sections in 0.1 M PB, followed by a final 10 min rinse in 0.1 M PB. Sections were mounted on 0.5% gelatinised slides, left to dry overnight, dehydrated in a graded series of alcohols, cleared in xylene and cover slipped with Depex. To ensure that non-specific staining did not affect the results, control sections taken at random were processed in the same manner, but either the primary or the secondary antibody was omitted. No labeled cells were observed in either case.

Data Analysis

Sections were analysed qualitatively with both low and high power microscopy to yield a comparative description of the distribution of PCNA and DCX-ir neurons. Brain structures were identified based on the atlas of the quail or chicken brain (Baylé et al. 1974, Kuenzel and Masson 1988, Puelles 2007) and we adopted the nomenclature by the Avian Brain Forum (Reiner et al., 2004). High power microscopic observations were used to determine the relative densities of stained structures throughout the different regions of the brain. The relative densities of immunostained structures were visually compared and recorded on a scale ranging from absent (-) to low (+) to moderate (++) to high (+++). A second observer was used to eliminate observer bias.

High resolution microscopic images were digitally captured using an AxioCam HRC digital camera on a Zeiss Axioplan 2 compound microscope and a Zeiss Discovery SteREO v20 Stereomicroscope connected to a PC running Axiovision software. Composite images were prepared with the Adobe Photoshop 7.0 software (Adobe Systems, Mountain View, CA). No pixilation adjustment or manipulation of the captured images was undertaken, except for the adjustment of contrast and brightness levels.

RESULTS

We report here changes in PCNA-ir and DCX-ir from post-hatching age 3 weeks to 12 weeks.

Age related changes in PCNA expression in the Japanese quail brain

Olfactory bulb

In juvenile quails, a high density of PCNA-ir cells was observed in the ependymal and subependymal lining of the olfactory ventricles (Fig. 1A, B). In addition, a few PCNA-ir cells were observed extending dorsally into the hyperpallium densocellulare (HD) (Fig. 1C). The distribution of PCNA-ir cells in the OB of subadult and adult quails was similar to that observed in juvenile quails except that no PCNA-ir cells were observed extending into the HD in adult quails older than 9 weeks (Fig. 3A-C, Table I).

Telencephalon

In the juvenile telencephalon, a high density of PCNA-ir cells was observed throughout the rostrocaudal extent of the lateral ventricles (Fig. 1D-L). In the ventricular zones, PCNA-ir cells were mostly abundant ventrally adjacent to the medial striatum (Mst) and dorsally adjacent to the mesopallium (M) (Fig. 1D, E). In addition, a few PCNA-ir cells were observed in the M (arrows in Fig. 1E) of quails aged 3 and 4 weeks. However, no PCNA-ir cells were observed in the rest of the pallial areas. In the subpallium, a low density of PCNA-ir cells was observed in the Mst adjacent to the lateral ventricles (Fig. 1H, I). Fewer cells were also observed in the bed nucleus of stria terminalis (bed nucleus of the stria terminalis, medial division, BSTM and bed nucleus of the stria terminalis, lateral division, BSTL) (arrows in Fig. 1L).

The distribution of PCNA-ir cells in the telencephalon of subadult and adult quails was similar to that observed in the juvenile group although the density of PCNA-ir cells was lowest in the adult group (Figs 3D-I). However, no PCNA-ir cells were observed in the pallial areas of the subadult and adult quails. In addition, PCNA-ir cells were absent in the BSTM and BSTL of adults older than 9 weeks or in the Mst of adult quails (Table 1).

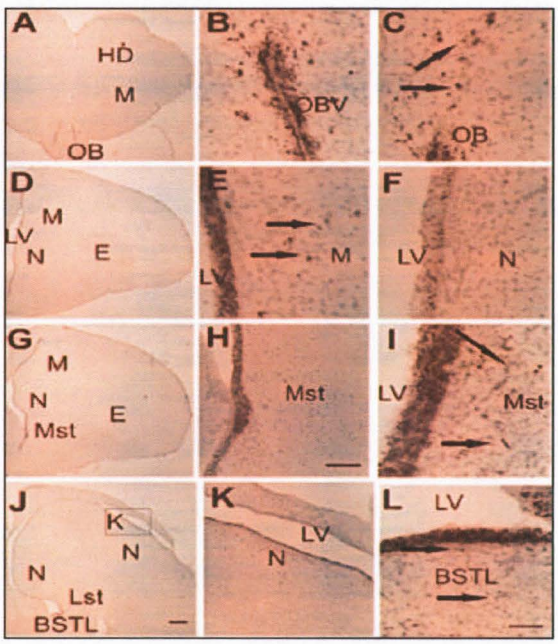

Fig. 1. Photomicrographs showing distribution of PCNA-ir cells in the olfactory bulb (OB) and telencephalon of the juvenile Japanese quail brain. (A) Low power photomicrograph showing distribution of PCNA-ir cells in the OB. (B) High power photomicrograph showing distribution of PCNA-ir cells along the OB ventricular lining. (C) High power photomicrograph showing PCNA-ir cells (black arrows) extending from the OB to the hyperpallium densocellulare (HD). (D) Low power image showing distribution of PCNA-ir cells long the lining of the lateral ventricle (LV) of the rostral telencephalon. (E) High power image showing distribution PCNA-ir cells along the lining of the LV adjacent to the mesopallium (M) (black arrows showing PCNA-ir cells in the M). (F) High power image showing distribution PCNA-ir cells in the lining of the lateral ventricle adjacent to the nidopallium (N). (G) Low power image showing distribution of PCNA-ir cells long the lining of the lateral ventricle of the mid telencephalon. (H) Photomicrograph showing an increase in PCNA-ir cells on the ventral reach of the lateral ventricular zones adjacent to medial striatum (Mst). (I) High power image showing PCNA-ir cells in the Mst (black arrows) adjacent to the lateral ventricle. (J) Low power photomicrograph showing distribution of PCNA-ir cells long the lining of the lateral ventricle of the caudal telencephalon (insert shows part of the lateral ventricle magnified in figure K). (K) High power image showing distribution of PCNA-ir cells along the lateral ventricular lining of the caudal telencephalon. (L) High power photomicrograph showing the distribution of PCNA-ir cells in the bed nucleus of the stria terminalis lateral division (BSTL) (black arrows). E, entopallium; OBV, olfactory bulb ventricle. Scale bars: J=500 μm and applies to A, D, G; L=50 μm and applies to B, C, E, F, I, K and H=200 μm.

Diencephalon

In the hypothalamus of juvenile quails, medium densities of PCNA-ir cells were observed in the POM (Figs 2A, 3J), nucleus paraventricularis (PVN), nucleus ventromedialis hypothalami (VMN) and nucleus tuberis (Tu). In the thalamus, low densities of PCNA-ir cells were observed in the nucleus rotundus (Rt), nucleus ovoidalis (OV), nucleus dorsolateralis anterior thalami (DLA), nucleus dorsomedialis anterior thalami (DMA) and nucleus geniculatus lateralis pars ventralis (Glv) (Fig. 2B). A low density of PCNA-ir cells was also observed lining the ventricular zones of the 3rd ventricle of the diencephalon. The pattern of expression of PCNA in the diencephalon of subadult and adult quails was identical to that observed in juvenile quails although the density of PCNA-ir cells appeared to decline with age (Table 1).

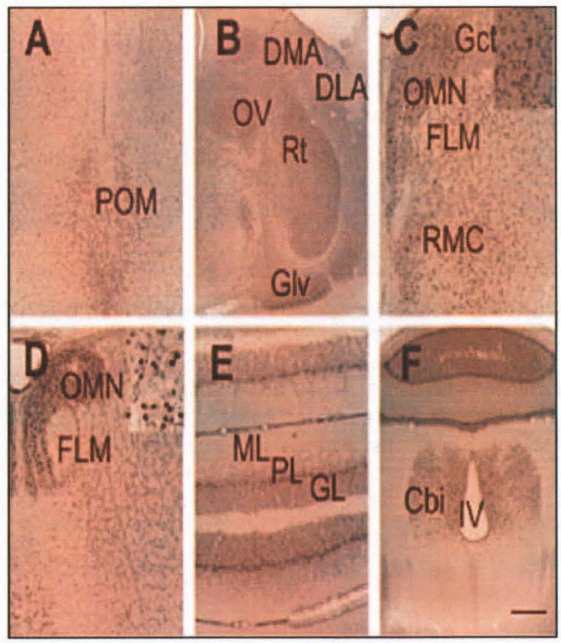

Fig. 2. Photomicrographs showing distribution of PCNA-ir cells in the nucleus preopticus medialis (POM) (A), thalamic nuclei (B), mesencephalic nuclei (C, D) nuclei, cerebellar cortex (E) and the nucleus cerebellum internum (Cbi) (F) of the juvenile Japanese quail brain. Inserts in figures C and D represent high magnifications of the griseum centrale (Gct) and oculomotor nucleus (OMN) respectively. DLA, nucleus dorsolateralis anterior thalami; DMA, nucleus dorsomedialis anterior thalami; FLM, fasciculus longitudinalis medialis; GL, granule cell layer; Glv, nucleus geniculatus lateralis, pars ventralis; ML, molecular cell layer; OV, nucleus ovoidalis; PL, Purkinje cells; Rt, nucleus rotundus; RMC, red nucleus magnocellular part; IV, fourth ventricle. Scale bars: F=200 μm and applies to images A-F; inserts in C and D=20 μm.

Mesencephalon and optic tectum

In the juvenile mesencephalon, a high density of strongly stained PCNA-ir cells was observed in the oculomotor nucleus (OMN) and red nucleus magnocellular part (RMC) located ventral to the OMN (Figs 2C-D, 3M). In addition, a high density of small weakly stained PCNA-ir cells was also observed in the griseum centrale (Gct) (Fig. 2C). Furthermore, a low density of PCNA-ir cells was observed in the lining of the mesencephalic aqueduct. The distribution of PCNA-ir cells in the mesencephalon of subadult and adult groups was similar to that of the juvenile groups. However, the density of PCNA-ir cells was lowest in the adult group. In the optic tectum, no PCNA-ir cells were observed in all age-groups (Table 1).

Cerebellum

In the cerebellum of juvenile quails, a high density of PCNA-ir cells was observed in the Purkinje and granule cell layers of the cerebellum (Figs 2E, 3P). In addition to this, fewer PCNA-ir cells were found in the nucleus cerebellum internum (Cbi) situated on either side of the cerebellar recess of the fourth ventricle (Fig. 2F). A similar pattern of PCNA expression was observed in subadult quails although the number of PCNA-ir cells decreased with age. In the adult quails, fewer PCNA-ir cells were observed in the cerebellar layers whereas no PCNA-ir cells were observed in the Cbi (Table 1).

Age-related changes in DCX expression in the Japanese quail brain

Two main types of DCX-ir cells were observed in the Japanese quail brain. Type 1 cells were round multipolar cells that displayed spherical or triangular shapes with cytoplasm filled with DCX and pale nuclei devoid of DCX staining. Long DCX-ir fibres extending from the cell bodies were also observed (Fig. 4A). The type 1 pattern of staining was mostly observed in the pallial (towards the external surface) and striatal parts of the telencephalon. In addition, smaller type 1 cells were observed in the cerebellum.

Type 2 cells were either unipolar or bipolar cells that displayed elongated DCX-ir cell bodies with long

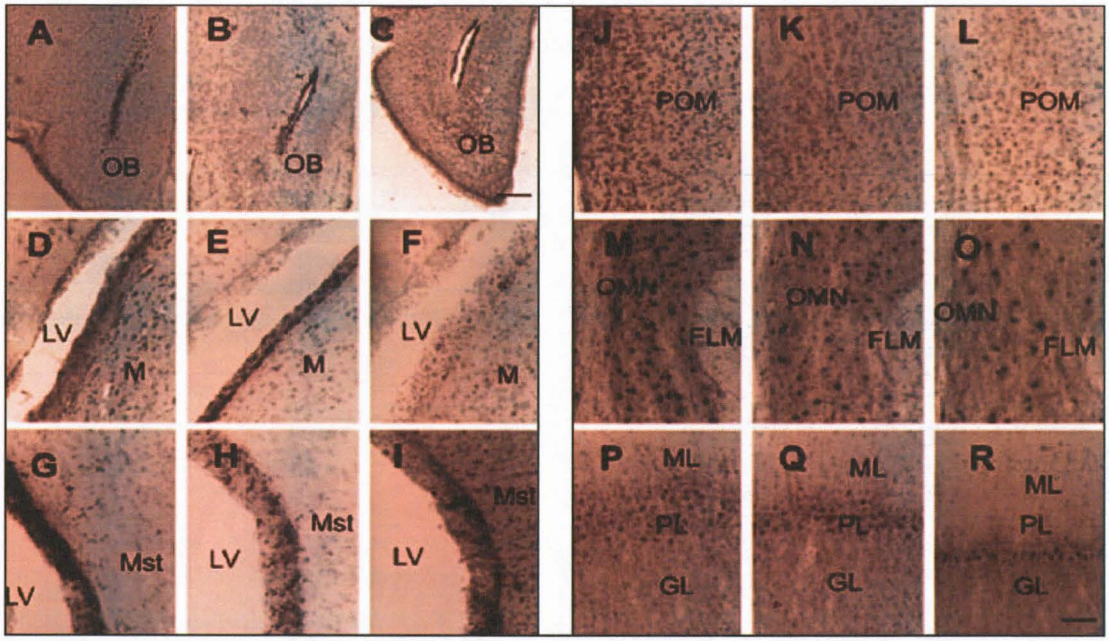

Fig. 3. Photomicrographs showing the distribution of PCNA-ir cells in the different parts of the brain of juvenile (A, D, G, J, M and P), subadult (B, E, H, K, N and Q) and adult (C, F, I, L, O and R) Japanese quails. Ventricular lining of olfactory bulb (OB) (A-C), ventricular lining adjacent to mesopallium (M) (D-F), ventricular lining adjacent to medial striatum (Mst) (G-I), nucleus preopticus medialis (POM) (J-L), oculomotor nucleus (OMN) (M-O) and cerebellum (P-R). FLM, fasciculus longitudinalis medialis; GL, granule cell layer; LV, lateral ventricle; ML, molecular cell layer; PL, Purkinje cell layer. Scale bars: C=200 μm and applies to A and C; R=50 μm and applies to D-Q.

fibres originating from one or both ends. Furthermore, the cell bodies of type 2 cells displayed elongated pale staining nuclei (Fig. 4B). The type 2 staining pattern was mostly observed in the pallial areas adjacent to the lateral ventricles, striatum, septum, and cerebellar cortex.

Olfactory bulb

In juvenile quails, the OB was intensely stained with a compact plexus of DCX-ir fibres interspersed with small round or fusiform (types 1 and 2) weakly stained cell bodies in the ependymal and subependymal linings of the olfactory ventricles (Figs 5A-B, 7A). In addition, a dense network of DCX-ir fibres extended dorsally into the HD (Fig. 5C). The pattern of DCX staining in the OB of subadult and adult animals was identical to that observed in juvenile animals, although there was a marked decline in the density of DCX-ir cells and fibres with age (Fig. 7A-C). In contrast to juvenile and subadult quails, no DCX-ir fibres were observed extending into the HD in adult quails.

Telencephalon

In juvenile quails, the highest density of DCX-ir cells and fibres were observed in the pallial part (hyperpallium apicale, HA, HD, M and nidopallium, N) of the telencephalon, although the density of positive cells varied across different pallial areas (Fig. 5D-N). Type 1 cells were mostly observed near the external surfaces of the pallium, whereas type 2 cells were observed near the lateral ventricles. The HA, HD, M and N were densely populated by types 1 and 2 DCX-ir cells. A much higher density of type 1 and 2 DCX-ir cells was observed on the ventral aspect of the nidopallium caudale (NC). In addition, a high density of DCX-ir fibres was observed in the pallial areas adjacent to the lateral ventricles with the highest densities observed in the M and Mst. The hippocampus (HP) had the lowest density of DCX-ir cells in the pallium (Fig. 5G, H). However, DCX-ir elements (cells or fibres) were absent in the entopallium (Fig. 5D, K) and arcopallium.

In the subpallium, a high density of type 1 and 2 cells was observed in the Mst (Fig. 5D, G, I) and lateral striatum (Lst) (Fig. 5G, J, K). A low density of type 2 cell bodies was also observed in the septum (lateral septum, SL and medial septum, SM) (Fig. 5J) and in the bed nucleus of stria terminalis (BSTM and BSTL) (Fig. 5N). However, no DCX-ir cells or fibres were observed in the globus pallidus (Fig. 5G).

Throughout the entire telencephalon, the lateral ventricular walls were lined with a high density of DCX-ir elements. The distribution of DCX-ir cells in the pallium of subadult and adult quails was similar to that observed in juvenile quails except for a reduction in the density of DCX-ir elements with age (Figs 7D-I, Table II). Similarly, the density of DCX-ir elements declined with age in the subpallium of subadult and adult quails (Figs 7J-O, Table II). However, no DCX-ir elements were observed in the BSTM and BSTL of adult quails older than 9 weeks (Table II).

Diencephalon, mesencephalon and optic tectum

At all ages studied, no type 1 or type 2 DCX-ir cells were observed in the ventricular or parenchymal areas of the diencephalon, mesencephalon and optic tectum (Fig. 6A-C).

Cerebellum

A high density of small bipolar DCX-ir cells (type 2) was observed in the granular and Purkinje layers of the juvenile quail cerebellar cortex (Fig. 6D, F, G). In addition, a few type 2 cells with long fibres were also observed in the molecular layer of the cerebellum (Fig. 6D, E).

In the subadult and adult quail cerebellar cortex, the pattern of DCX-ir cells was similar to that observed

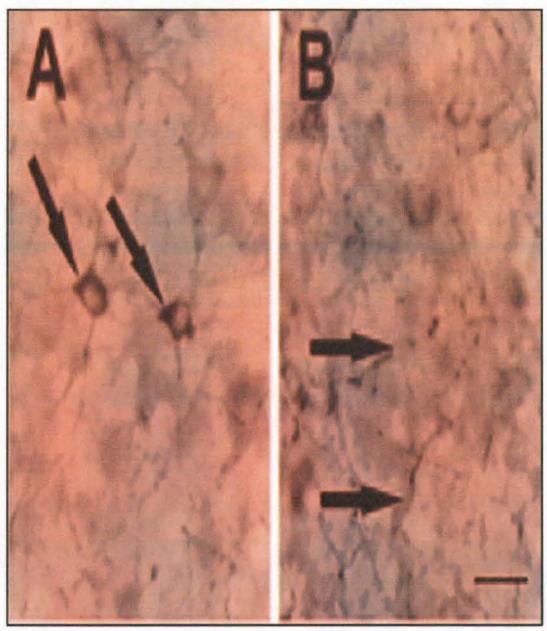

Fig. 4. Photomicrographs showing type 1 (A) and type 2 (B) DCX-ir cells in the Japanese quail brain (black arrows). Scale bar: B=20 μm and also applies to A.

in juveniles although the densities declined with age (Fig. 7P-R, Table II). However, no type 1 or type 2 DCX-ir cells were observed in the Cbi at all ages studied (Fig. 6H).

Table I. Age-related changes in PCNA immunoreactivity in the Japanese quail brain.

			Post hatching age									
			3 weeks	4 weeks	5 weeks	6 weeks	7 weeks	8 weeks	9 weeks	10 weeks	11 weeks	12 weeks
Olfactory Bulb	OBV		+++	+++	+++	++	++	++	++	+	+	+
Telencephalon	LV		+++	+++	+++	+++	+++	+++	++	++	++	++
	Pallium	HA	-	-	-	-	-	-	-	-	-	-
		HD	-	-	-	-	-	-	-	-	-	-
		M	-*	-*	-	-	-	-	-	-	-	-
		N	-	-	-	-	-	-	-	-	-	-
		E	-	-	-	-	-	-	-	-	-	-
		A	-	-	-	-	-	-	-	-	-	-
		HP	-	-	-	-	-	-	-	-	-	-
	Subpallium	Mst	-**	-**	-	-	-	-	-	-	-	-
		Lst	-	-	-	-	-	-	-	-	-	-
		GP	-	-	-	-	-	-	-	-	-	-
		SL	-	-	-	-	-	-	-	-	-	-
		SM	-	-	-	-	-	-	-	-	-	-
		BSTM	+	+	+	+	+	+	+	-	-	-
		BSTL	+	+	+	+	+	+	+	-	-	-
Diencephalon	Hypothalamus	POM	++	++	++	+	+	+	+	+	+	+
		PVN	+	+	+	+	+	+	+	+	+	+
		VMN	+	+	+	+	+	+	+	+	+	+
		Tu	+	+	+	+	+	+	+	+	+	+
	Thalamus	Rt	+++	+++	+++	++	++	++	++	+	+	+
		OV	+++	+++	+++	++	++	++	++	+	+	+
		DLA	++	++	++	+	+	+	+	+	+	+
		DMA	++	++	++	+	+	+	+	+	+	+
		Glv	+++	+++	+++	++	++	++	++	+	+	+
Mesencephalon		Gct	+++	+++	+++	++	++	++	++	++	+	+
		OMN	+++	+++	+++	++	++	++	++	++	+	+
		RMC	++	++	++	+	+	+	+	+	+	+
Optic Tectum			-	-	-	-	-	-	-	-	-	-
Cerebellum		CB	+++	+++	+++	++	++	++	+	+	+	+
		Cbi	+++	+++	+++	++	++	++	+	+	+	+

+++- high density, ++- medium density, +- low density. PCNA-ir cells in the mesopallium (*) and medial striatum (**). - No positive PCNA-ir.

DISCUSSION

Our study used PCNA and DCX to investigate cell proliferation and neuronal incorporation in the Japanese quail brain to determine how these processes change with post-hatching age.

Methodological considerations

Proliferating cell nuclear antigen, also known as cyclin, is a protein associated with catalytic activity of DNA polymerase A and is critical to the extension of the DNA strand during replication (Balthazart and Ball 2014b). PCNA is therefore expressed during the G1 and S phases of the cell cycle and not in G0 or the resting phase. In addition, PCNA expression is highly conserved among eukaryotes (Charvet and Striedter 2008) and has been employed in the current study as a marker of cell proliferation in the Japanese quail brain. PCNA immunolabelling was used previously in the avian brain to compare cell proliferation during ontogeny in birds that possess large (Parakeets) *vs.* small (Bobwhite quails) brains in adulthood (Charvet and Striedter 2008). Additionally, Bardet et al. (2012) and Mouriec and Balthazart (2013) also used PCNA to demonstrate age dependent changes in cell proliferation in the POM of Japanese quail brains. In the quail

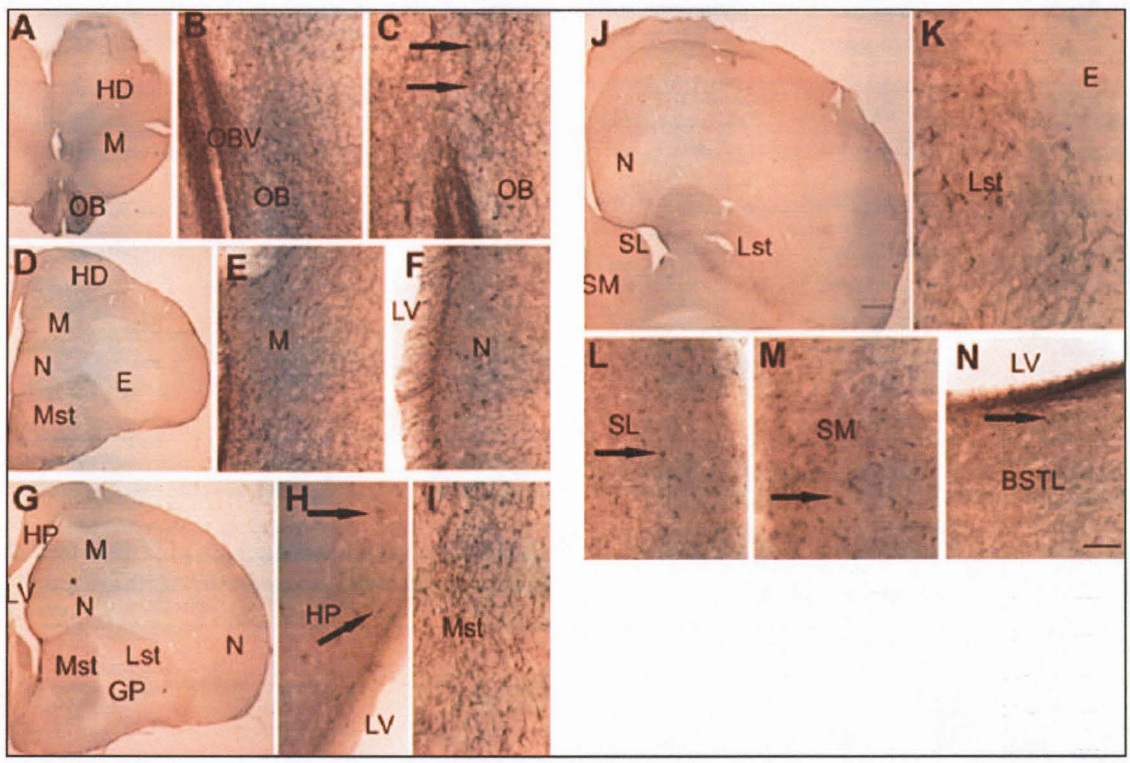

Fig. 5. Photomicrographs showing distribution of DCX-ir cells in the olfactory bulb and telencephalon of the Japanese quail brain. (A) Low power photomicrograph showing distribution of DCX-ir cells in the olfactory bulb (OB). (B) High power photomicrograph showing distribution of DCX-ir cells along the OB. (C) High power photomicrograph showing DCX-ir cells (black arrows) extending from the OB to the hyperpallium densocellulare (HD). (D) Low power image showing distribution of DCX-ir cells in the rostral telencephalon, E-high power image showing distribution DCX-ir cells in the mesopallium (M). (F) High power image showing distribution DCX-ir cells in the nidopallium (N). (G) Low power image showing distribution of DCX cells in the mid telencephalon. (H) Photomicrograph showing DCX-ir cells in the hippocampus (HP) (black arrows). (I) High power image showing DCX-ir cells in the medial striatum (Mst). (J) Low power photomicrograph showing distribution of DCX-ir cells in the caudal telencephalon. (K) High power image showing distribution of DCX-ir cells in the Lst near the lateral striatal- entopallial junction. (L) High power photomicrograph showing the distribution of DCX-ir cells in the lateral septum (SL) (black arrow). (M) High power photomicrograph showing the distribution of DCX-ir cells in the medial septum (SM) (black arrow). (N) High power photomicrograph showing the distribution of DCX-ir cells in the bed nucleus of the stria terminalis lateral division (BSTL) (black arrow). GP, globus pallidus; Lst, lateral striatum; LV, lateral ventricle; OBV, olfactory bulb ventricle. Scale bars: J=500 μm and applies to A, D, G; N=50 μm and applies to B, C, E, F, H, I, K, L, M.

specifically, the pattern of PCNA staining was reported to coincide with bromodeoxyuridine (BrdU) labelling observed after injections with short survival times (Bardet et al. 2012, Striedter and Charvet 2008) and this therefore justifies its use as a marker of cell proliferation in the current study.

Table II. Age-related changes in DCX immunoreactivity in the Japanese quail brain.

			Post hatching age									
			3 weeks	4 weeks	5 weeks	6 weeks	7 weeks	8 weeks	9 weeks	10 weeks	11 weeks	12 weeks
Olfactory Bulb	OB		+++	+++	+++	+++	++	++	++	+	+	+
Telencephalon	LV		+++	+++	+++	+++	+++	+++	++	++	+	+
	Pallium	HA	+++	+++	+++	++	++	++	+	+	+	+
		HD	+++	+++	+++	+++	+++	+++	++	++	++	++
		M	+++	+++	+++	+++	+++	+++	++	++	++	++
		N	+++	+++	+++	+++	+++	+++	++	++	++	++
		E	-	-	-	-	-	-	-	-	-	-
		A	-	-	-	-	-	-	-	-	-	-
		HP	++	++	+	+	+	+	+	+	+	+
	Subpallium	Mst	+++	+++	+++	+++	+++	+++	++	++	+	+
		Lst	+++	+++	+++	++	++	++	+	+	+	+
		GP	-	-	-	-	-	-	-	-	-	-
		SL	++	++	++	+	+	+	+	+	+	+
		SM	+	+	+	+	+	+	+	+	+	+
		BSTM	+	+	+	+	+	+	+	-	-	-
		BSTL	+	+	+	+	+	+	+	-	-	-
Diencephalon	Hypothalamus	POM	-	-	-	-	-	-	-	-	-	-
		PVN	-	-	-	-	-	-	-	-	-	-
		VMN	-	-	-	-	-	-	-	-	-	-
		Tu	-	-	-	-	-	-	-	-	-	-
	Thalamus	Rt	-	-	-	-	-	-	-	-	-	-
		OV	-	-	-	-	-	-	-	-	-	-
		DLA	-	-	-	-	-	-	-	-	-	-
		DMA	-	-	-	-	-	-	-	-	-	-
		Glv	-	-	-	-	-	-	-	-	-	-
Mesencephalon		Gct	-	-	-	-	-	-	-	-	-	-
		OMN	-	-	-	-	-	-	-	-	-	-
		RMC	-	-	-	-	-	-	-	-	-	-
Optic tectum			-	-	-	-	-	-	-	-	-	-
Cerebellum		CB	+++	+++	+++	++	++	++	+	+	+	+
		Cbi	-	-	-	-	-	-	-	-	-	-

+++ - high density, ++ - medium density, + - low density of DCX-ir type 1 and 2 cells only. - No positive DCX-ir.

DCX is a microtubule-associated protein that binds to microtubules, increasing their bundling and stabilization (Horesh et al. 1999). DCX controls the polymerization of the leading process and stabilization of the cytoskeleton during neuronal migration (Balthazart and Ball 2014a, 2014b) thus playing a critical role in the positioning of new born neurons. However, mammalian studies have also shown that DCX is not only a marker of neurogenesis but is also related to the extensive neuronal plasticity present in the adult brain (Brown et al. 2003, Klempin et al. 2011, Kremer et al. 2013, Nacher et al. 2001). Given the role of DCX in microtubule reorganization, DCX also supports the reorganization of the dendritic arbour, neurite outgrowth and synaptogenesis in plastic neurons.

The DCX antibody has been validated for both mammals and birds and it has been established that it is specific to the DCX protein (Balthazart et al. 2008, Balthazart and Ball 2014b). In galliformes, DCX has been identified in the developing or post- hatching brain of the chicken (Capes-Davis et al. 2005, Mezey et al. 2012) and Japanese quail (Balthazart et al. 2010). In this study, DCX immunolabelling was also used to investigate neuronal incorporation in the Japanese quail brain.

Two main types of DCX-ir elements were observed in this study. Type 1 cells were observed mostly near the external surfaces of the brain and are presumably differentiating neurons that have reached their destination following migration since DCX expression begins in late mitotic neuronal precursors and extends to early post mitotic neurons (Balthazart et al. 2008, Brown et al. 2003). Type 2 cells were mostly observed in the telencephalic areas adjacent to the lateral ventricles and resemble migrating neurons with leading and trailing processes that will presumably transform into multipolar morphology on reaching their target area (Boseret et al. 2007, Mezey et al. 2012).

Ontogenetic considerations

Japanese quails are precocial birds and therefore require minimal parental care after hatching. For precocial birds it is vital to have a highly developed brain by the time of hatching especially subtelencephalic areas that are important for homeostatic processes and simple behavioural tasks (Mezey et al. 2012). Neurogenesis in the quail brain is therefore supposed to be complete before

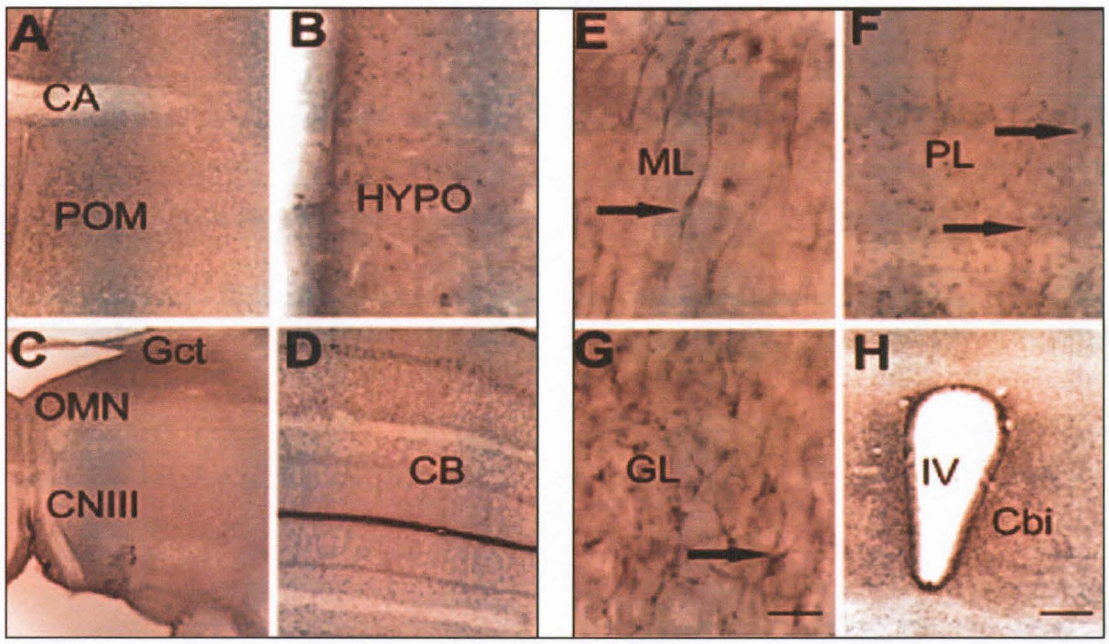

Fig. 6. Photomicrographs showing Japanese brain sections through the nucleus preopticus medialis (POM), hypothalamus (HYPO), mesencephalon and cerebellum. DCX-ir cells were absent in the POM (A), hypothalamus (B), mesencephalon (C) and nucleus cerebellum internum (Cbi) (H). DCX-ir cells (black arrows) were observed in all the layers (molecular cell layer (ML), Purkinje cell layer (PL) and granule cell layer (GL) of the cerebellar cortex (D, E, F and G). IV, fourth ventricle, CA, anterior commissure; CB, cerebellum; Gct, griseum centrale; OMN, oculomotor nucleus. Scale bars: G=20 μm and applies to E and F; H=200 μm and applies to A, B, C and D.

hatching (Tsai et al. 1981). In galliformes such as quails and chicks, neurogenesis starts at about 16-30% of hatching time and is presumed to be complete for the medulla by 30%, the tectum by 50% and the telencephalon by 50% of hatching time (Mezey et al. 2012). However Bardet et al. (2012) reported that neurons in most brain areas in the quail except for the telencephalon and the cerebellum are born and become post-mitotic before embryonic day 6 (E6). Even if neurogenesis persists throughout life in the telencephalon of adult birds, the bulk of neurons in this part of the brain are produced before E6 in quails (Bardet et al. 2012) and E7-E9 in chicks (Tsai et al. 1981). Our results reveal that the post hatch development of higher order brain areas such as the telencephalon and cerebellum is protracted in precocial birds in a similar way as observed in other birds and mammals.

Age-related changes in PCNA and DCX expression in different brain regions

PCNA-ir and DCX-ir elements were observed in the OB of juvenile, subadult and adult quails. Our findings suggest that the lining of the olfactory ventricle is the birth site of neurons that are incorporated in the OB. This is in contrast with the situation in mammals where neurons are born in the lateral ventricular zones and migrate through the rostral migratory stream to reach the OB (Maheu et al. 2015). A qualitative analysis of the results revealed an age-dependent decline in PCNA-ir and DCX-ir cells in the OB especially in the subadult and adult groups. A similar age-dependent decline in DCX expression was also reported by Mezey et al. (2012) in chicks and Meskenaite et al. (2016) in pigeons. DCX-ir cells and fibres running between the OB and the HD have been previously observed in the adult chick (Mezey et al. 2012) and in the pigeon (Melleu et al. 2013). These fibres may represent an extensive network of newly generated neurons being continuously exchanged along the rostrocaudal extension of the olfactory pathways (Melleu et al. 2013). The presence of neuronal production and incorporation in the OB of the quail is not surprising as this bird has been reported to have a keen sense of smell and is known to be able to detect the presence of certain pesticides, as well as avoid food containing a toxic chemical called lectin, using only the sense of smell (Mills et al. 1997).

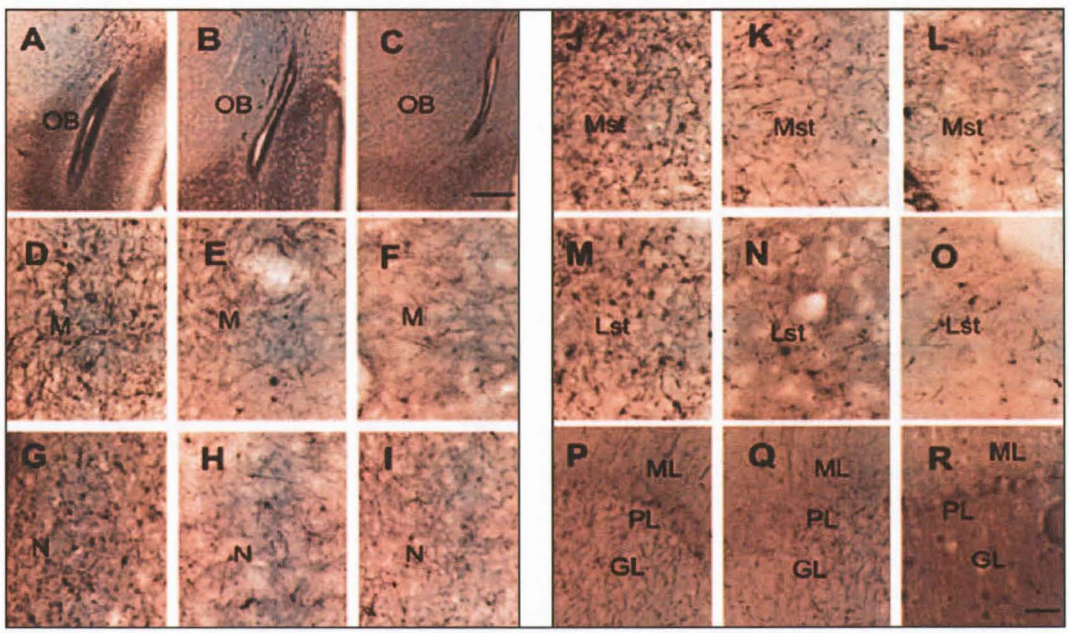

Fig. 7. Photomicrographs showing the distribution of DCX-ir cells the different parts of the brain of juvenile (A, D, G, J, M and P), subadult (B, E, H, K, N and Q) and adult (C, F, I, L, O and R) Japanese quails. Olfactory bulb (OB) (A-C), mesopallium (M) (D-F), nidopallium (N) (G-I), medial striatum (Mst) (J-L), lateral striatum (Lst) (M-O) and cerebellum (P-R). GL, granule cell layer; ML, molecular cell layer; PL, Purkinje cell layer. Scale bars: C=200 μm and applies to A-C; R=50 μm and applies to D-Q.

In the pallium, the majority of PCNA-ir cells observed throughout the rostrocaudal extent of the lateral ventricles appeared to decline with post-hatching age. PCNA-ir cells were mostly found to be abundant ventrally and dorsally in the ventricular zones adjacent to the medial striatum and mesopallium, respectively, corresponding to the proliferative "hotspots" described by Alvarez-Buylla et al. (1990). In juvenile quails, very few PCNA-ir cells were observed in the mesopallium and caudal part of the nidopallium adjacent to the lateral ventricles. Similarly, Bardet et al. (2012) reported the presence of a few PCNA and BrdU labelled cells in the quail pallium and concluded that these could be slow cycling progenitors. Alternatively, the presence of PCNA-ir cells in the parenchyma may not be related to cell proliferation but to DNA repair in mature neurons as proposed by Essers et al. (2005). Apart from those few cells in the pallial parenchyma of juvenile quails, cell proliferation in the subadult and adult Japanese quails appears to be restricted to the lateral ventricular zones.

DCX-ir cells were observed throughout the pallium except for the entopallium and the arcopallium. DCX expression in the pallium suggests that the Japanese quail, like other birds, continues to recruit neurons into the pallium throughout life although at a slower rate in adult as compared to juvenile and subadult quails. The very low density of DCX-ir cells in the quail hippocampus throughout juvenile, subadult and adult stages is not surprising given that spatial memory is not as major a factor in the life of quails as it is for food storing birds (Mezey et al. 2012) or homing pigeons (Meskenaite et al. 2016).

In the subpallium, PCNA-ir cells declined with post hatching age eventually disappearing in the medial striatum and in the bed nucleus of stria terminalis (BSTM and BSTL) in adult quails older than 9 and 10 weeks respectively. DCX expression ceased in the BSTL and BSTM at 11 weeks suggesting that these brain structures reach full maturation at 10 weeks after which no new neurons are incorporated. However the striatum continues to express DCX throughout the juvenile, subadult and adult ages.

The observation that DCX is expressed in the septum and the striatum, areas where PCNA is not expressed, implies that there could be another source for neurons that are added to these brain areas, presumably the adjacent lateral ventricles. Furthermore, our findings suggest that the septum continues to recruit neurons throughout the ages studied. This is contrary to the findings by Nikolakopoulou et al. (2006b) who reported an early maturation of the SL in the quail at post-hatching day 20 (P20) using BrdU staining. They reported that about 50% of BrdU-ir cells in the SL were of an unknown phenotype as they neither co-expressed with neuronal or glial markers. Since the SL is a steroid sensitive brain area, this population of BrdU-ir cells could be slow cyclin progenitors that are quiescent at P20 but may be reactivated at puberty when the level of circulating steroids increases as observed by Mouriec and Balthazart (2013).

Given the fact that no type 1 or type 2 DCX-ir cells were observed in the diencephalon, the PCNA immunoreactivity observed in this region is presumably related to glial cell production. Additionally, Balthazart et al. (2010) also reported a lack of DCX immunoreactivity in the adult quail POM. In support of our observation, Bardet et al. (2012) reported that neuronal production in this region of the quail brain is complete by embryonic day 6 and that further cell proliferation after this date is related to production of glial cells. However, previous attempts to test this hypothesis through double labelling experiments in birds proved to be technically challenging because many antibodies available to identify glial cells in mammals (S100, GFAP or CD11) either do not label any cell in birds or only label subpopulations of glial cells in specific brain regions (Castagna et al. 2003, Bardet et al. 2012).

As was the case with the diencephalon, no type 1 or type 2 DCX-ir cells were observed in these two regions of the quail brain. As a result, it can be concluded that the intense PCNA immunoreactivity observed in the oculomotor nucleus, griseum centrale and the red nucleus of the mesencephalon may not have related to neurogenesis but possibly related to glial cell production. No PCNA-ir or DCX-ir cells were observed in the optic tectum in any of the quails suggesting that this structure reaches full maturity before hatching.

Our findings suggest that neuronal birth and incorporation continue to take place in the cerebellum of juvenile, subadult and adult quails just like other birds species (Bardet et al. 2012, Stamatakis et al. 2004,). The PCNA immunoreactivity observed in the Cbi of juvenile and subadult quails may be related to glial cell production since no type 1 or type 2 DCX-ir cells were observed in that nucleus.

In conclusion, post-hatch neuronal production appears to be restricted to olfactory and telencephalic ventricles whereas neuronal incorporation is restricted to the telencephalon and cerebellum. In addition, both processes continue into adulthood and appear to decline with post-hatching age beginning from the 6th week. Furthermore, subtelencephalic regions such as the diencephalon, mesencephalon and optic tectum appear to reach full maturity prior to hatching and post-hatching proliferation observed in these regions is most likely related to glial cell production.

ACKNOWLEDGEMENTS

We express our most sincere gratitude to Mrs Hasiena Ali, School of Anatomical Sciences, University of the Witwatersrand for assistance with immunohistochemistry, the University of Witwatersrand Central Animal Service for providing excellent care of animals, and to Dr Umar M Bello for his assistance in sourcing the animals.

This work was supported by the Swiss-South Africa Joint Research Programme (SSAJRP) awarded to Prof Amadi O Ihunwo.

REFERENCES

Alunni A, Bally-Cuif L (2016) A comparative view of regenerative neurogenesis in vertebrates. Development 143: 741–753.

Alvarez-Buylla A, Theelen M, Nottebohm F (1990) Proliferation "hot spots" in adult avian ventricular zone reveal radial cell division. Neuron 5: 101–109.

Alvarez-Buylla A, Ling CY, Nottebohm F (1992) High vocal center growth and its relation to neurogenesis, neuronal replacement and song acquisition in juvenile canaries. J Neurobiol 23: 396–406.

Alvarez-Buylla A, Ling CY, Yu WS (1994) Contribution of neurons born during embryonic and adult life to the brain of adult canaries: Regional specificity and delayed birth of neurons in the song-control nuclei. J Comp Neurol 347: 233–248.

Balthazart J, Boseret G, Konkle A, Hurley IL, Ball GF (2008) Doublecortin as a marker of adult neuroplasticity in the canary song control nucleus HVC. Eur J Neurosci 27: 801–817.

Balthazart J, Charlier TD, Barker JM, Yamamura T, Ball GF (2010) Sex steroid-induced neuroplasticity and behavioral activation in birds. Eur J Neurosci 32: 2116–2132.

Balthazart J, Ball GF (2014a) Doublecortin is a highly valuable endogenous marker of adult neurogenesis in canaries. Brain Bev Evol 84: 1–4.

Balthazart J, Ball GF (2014b) Endogenous versus exogenous markers of adult neurogenesis in canaries and other birds: advantages and disadvantages. J Comp Neurol 522: 4100–4120.

Balthazart J, Ball GF (2016) Endocrine and social regulation of adult neurogenesis in songbirds. Front Neuroendocrinol 41: 3–22.

Bardet SM, Mouriec K, Balthazart J (2012) Birth of neural progenitors during the embryonic period of sexual differentiation in the Japanese quail brain. J Comp Neurol 520: 4226–4253.

Barker JM, Ball GF, Balthazart J (2014) Anatomically discrete sex differences and enhancement by testosterone of cell proliferation in the telencephalic ventricle zone of the adult canary brain. J Chem Neuroanat 55: 1–8.

Barnea A, Pravosudov V (2011) Birds as a model to study adult neurogenesis: bridging evolutionary, comparative and neuroethological approaches. Eur J Neurosci 34: 884–907.

Baylé J, Jamade F, Oliver J (1974) Stereotaxic topography of the brain of the quail (*Coturnix coturnix japonica*). J Physiol 68: 219–241.

Boseret G, Ball GF, Balthazart J (2007) The microtubule-associated protein doublecortin is broadly expressed in the telencephalon of adult canaries. J Chem Neuroanat 33: 140–154.

Brenowitz EA (2004) Plasticity of the adult avian song control system. Ann N Acad Sci 1016: 560–585.

Brenowitz EA, Larson TA (2015) Neurogenesis in the adult avian song-control system. Cold Spring Harb Persepct Biol 7: a019000.

Brown JP, Couillard-Després S, Cooper-Kuhn CM, Winkler J, Aigner l, Kuhn HG (2003) Transient expression of doublecortin during adult neurogenesis. J Comp Neurol 467: 1–10.

Capes-Davis A, Tolhurst O, Dunn JM, Jeffrey PL (2005) Expression of doublecortin (DCX) and doublecortin-like kinase (DCLK) within the developing chick brain. Dev Dyn 232: 457–467.

Castagna C, Viglietti-Panzica C, Panzica GC (2003) Protein S100 immunoreactivity in glial cells and neurons of the Japanese quail brain. J Chem Neuroanat 25: 195–212.

Charvet CJ, Striedter GF (2008) Developmental species differences in brain cell cycle rates between northern bobwhite quail (*Colinus virginianus*) and parakeets (*Melopsittacus undulatus*): implications for mosaic brain evolution. Brain Behav Evol 72: 295–306.

DeWulf V, Bottjer SW (2002) Age and sex differences in mitotic activity within the zebra finch telencephalon. J Neurosci 22: 4080–4094.

Essers J, Theil AF, Baldeyron C, Van Cappellen WA, Houtsmuller AB, Kanaar R, Vermeulen W (2005) Nuclear dynamics of PCNA in DNA replication and repair. Mol Cell Biol 25: 9350–9359.

Guigueno MF, Macdougall-Shackleton SA, Sherry DF (2016) Sex and seasonal differences in hippocampal volume and neurogenesis in brood-parasitic brown-headed cowbirds (*Molothrus ater*). Dev Neurobiol 76: 1226–1240.

Hall ZJ, Bauchinger U, Gerson AR, Price ER, Langlois IA, Boyles M, Pierce B, Mcwilliams SR, Sherry DF, Macdougall-Shackleton SA (2014) Site-specific regulation of adult neurogenesis by dietary fatty acid content, vitamin E and flight exercise in European starlings. Eur J Neurosci 39: 875–882.

Horesh D, Sapir T, Francis F, Wolf SG, Caspi M, Elbaum M, Chelly J, Reiner O (1999) Doublecortin, a stabilizer of microtubules. Hum Mol Genet 8: 1599–1610.

Kaslin J, Ganz J, Brand M (2008) Proliferation, neurogenesis and regeneration in the non-mammalian vertebrate brain. Philos Trans R Soc Lond B Biol Sci 363: 101–122.

Klempin F, Kronenberg G, Cheung G, Kettenmann H, Kempermann G (2011) Properties of doublecortin-(DCX)-expressing cells in the piriform cortex compared to the neurogenic dentate gyrus of adult mice. PloS One 6: e25760.

Kremer T, Jagasia R, Herrmann A, Matile H, Borroni E, Francis F, Kuhn HG, Czech C (2013) Analysis of adult neurogenesis: evidence for a prominent "non-neurogenic" DCX-protein pool in rodent brain. PloS One 8: e59269.

Kuenzel WJ, Masson M (1988) A stereotaxic atlas of the brain of the chick (*Gallus domesticus*). Johns Hopkins University Press, Maryland, USA.

Ling C, Cheng MF (1995) Sex differences in cell proliferation in the ventricular zone of young ring doves. Brain Res Bull 37: 657–662.

Ling C, Zuo M, Alvarez-Buylla A, Cheng MF (1997) Neurogenesis in juvenile and adult ring doves. J Comp Neurol 379: 300–312.

Maheu ME, Devorak J, Freibauer A, Davoli MA, Turecki G, Mechawar N (2015) Increased doublecortin (DCX) expression and incidence of DCX-immunoreactive multipolar cells in the subventricular zone-olfactory bulb system of suicides. Front Neuroanat 9: 74.

Melleu F, Pinheiro M, Lino-De-Oliveira C, Marino-Neto J (2016) Defensive behaviors and prosencephalic neurogenesis in pigeons (*Columba livia*) are affected by environmental enrichment in adulthood. Brain Struct Funct 221: 2287–2301.

Melleu F, Santos T, Lino-De-Oliveira C, Marino-Neto J (2013) Distribution and characterization of doublecortin-expressing cells and fibers in the brain of the adult pigeon (*Columba livia*). J Chem Neuroanat 47: 57–70.

Meskenaite V, Krackow S, Lipp H-P (2016) Age-Dependent Neurogenesis and Neuron Numbers within the Olfactory Bulb and Hippocampus of Homing Pigeons. Front Behav Neurosci 10: 126.

Mezey S, Krivokuca D, Bálint E, Adorján A, Zachar G, Csillag A (2012) Postnatal changes in the distribution and density of neuronal nuclei and doublecortin antigens in domestic chicks (*Gallus domesticus*). J Comp Neurol 520: 100–116.

Mills AD, Crawford IL, Domjan M, Faure JM (1997) The behavior of the Japanese or domestic quail *Coturnix japonica*. Neurosci Biobehav Rev 21: 261–281.

Mouriec K, Balthazart J (2013) Peripubertal proliferation of progenitor cells in the preoptic area of Japanese quail (*Coturnix japonica*). Brain Res 1516: 20–32.

Nacher J, Crespo C, Mcewen BS (2001) Doublecortin expression in the adult rat telencephalon. Eur J Neurosci 14: 629–644.

Nikolakopoulou A, Dermon C, Panagis I, Pavlidis M, Stewart M (2006a) Passive avoidance training is correlated with decreased cell proliferation in the chick hippocampus. Eur J Neurosci 24: 2631–2642.

Nikolakopoulou A, Parpas A, Panagis I, Zikopoulos B, Dermon C (2006b) Early post-hatching sex differences in cell proliferation and survival in the quail telencephalic ventricular zone and intermediate medial mesopallium. Brain Res Bull 70: 107–116.

Nottebohm F (1984) Birdsong as a model in which to study brain processes related to learning. Condor 86: 227–236.

Nottebohm F (2011) Song learning in birds offers a model for neuronal replacement in adult brain. In: Neurogenesis in the Adult Brain I. Springer, Japan, p. 47–84.

Olaleye OO, Ihunwo AO (2014) Adult neurogenesis in the four-striped mouse (Rhabdomys pumilio). Neural Regen Res 9: 1907–1911.

Puelles L (2007) Chick brain in stereotaxic coordinates, Academic Press, San Diego, USA.

Pytte CL, Gerson M, Miller J, Kirn JR (2007) Increasing stereotypy in adult zebra finch song correlates with a declining rate of adult neurogenesis. Dev Neurobiol 67: 1699–1720.

Reiner A, Perkel DJ, Bruce IL, Butler AB, Csillag A, Kuenzel W, Medina I, Paxinos G, Shimizu T, Striedter G (2004) Revised nomenclature for avian telencephalon and some related brainstem nuclei. J Comp Neurol 473: 377–414.

Stamatakis A, Barbas H, Dermon C (2004) Late granule cell genesis in quail cerebellum. J Comp Neurol 474: 173–189.

Striedter GF, Charvet CJ (2008) Developmental origins of species differences in telencephalon and tectum size: morphometric comparisons between a parakeet (*Melopsittacus undulatus*) and a quail (*Colinus virgianus*). J Comp Neurol 507: 1663–1675.

Tsai HM, Garber BB, Larramendi IM (1981) 3H-Thymidine autoradiographic analysis of telencephalic histogenesis in the chick embryo: I. Neuronal birthdates of telencephalic compartments in situ. J Comp Neurol 198: 275–292.

Vellema M, Van der Linden A, Gahr M (2010) Area-specific migration and recruitment of new neurons in the adult songbird brain. J Comp Neurol 518: 1442–1459.

Wang N, Hurley P, Pytte C, Kirn IR (2002) Vocal control neuron incorporation decreases with age in the adult zebra finch. J Neurosci 22: 10864–10870.

Yamamura T, Barker JM, Balthazart J, Ball GF (2011) Androgens and estrogens synergistically regulate the expression of doublecortin and enhance neuronal recruitment in the song system of adult female canaries. J Neurosci 31: 9649–9657.

International Journal of Developmental Neuroscience 72 (2019) 36–47

Contents lists available at ScienceDirect

International Journal of Developmental Neuroscience

journal homepage: www.elsevier.com/locate/ijdevneu

Age-related changes in Ki-67 and DCX expression in the BALB/ c mouse (*Mus Musculus*) brain

Pilani Nkomozepi[a,b], Pedzisai Mazengenya[a], Amadi O. Ihunwo[a,*]

[a] School of Anatomical Sciences, Faculty of Health Sciences, University of the Witwatersrand, 7 York Road, Parktown, Johannesburg, 2190, South Africa
[b] Department of Human Anatomy and Physiology, Faculty of Health Sciences, University of Johannesburg, Cnr Siemert and Bet Streets, Doornfontein, 2094, Johannesburg, South Africa

ARTICLE INFO

Keywords:
Age
Life-history stage
Ki-67
DCX
Brain
BALB/c mouse

ABSTRACT

Several studies have identified age as one of the strongest regulators of neurogenesis in the mammalian brain. However, previous age-related studies focused mainly on changes in neurogenesis during different stages of adulthood and did not describe changes in neurogenesis through the different life history stages of the animal. The aim of this study was therefore to determine time course changes in neurogenesis in the male BALB/c mouse brain at postnatal ages 1 week to 12 weeks, spanning juvenile, sub adult and adult life history stages. To achieve this, Ki-67 and DCX immunohistochemistry was used to assess changes in cell proliferation and neuronal incorporation respectively. Ki-67 expression was mainly observed in the olfactory bulb, rostral migratory stream, sub ventricular zone of lateral ventricle and the sub granular zone of the dentate gyrus. In addition, fewer Ki-67 positive cells were also observed in the neocortex, cerebellum and tectum. DCX was expressed in similar regions as Ki-67 except for the cerebellum and tectum. Expression of both Ki-67 and DCX sharply decreased with advancing age or life history stages in the sub ventricular zone, rostral migratory stream and sub granular zone of the BALB/c mouse brain. Neurogenesis therefore persists throughout all life history stages in the BALB/c mouse brain although it decreases with age.

1. Introduction

Neurogenesis in the mammalian brain was thought to be complete before or soon after birth. Today it is widely accepted that the mammalian brain, just like other vertebrates, continues to produce new neurons throughout life. The process through which new neurons are added to the brain after birth is termed postnatal or secondary neurogenesis (Thuret et al., 2015). To date, postnatal neurogenesis has been reported in the brains of several laboratory bred and wild living mammalian species including laboratory mice (Kondo et al., 2010; Nada et al., 2010; Encinas et al., 2011; Mobley et al., 2014), four striped mice (Olaleye and Ihunwo, 2014), rats (Kuhn et al., 1996; Jessberger et al., 2009), voles (Amrein et al., 2004), African giant rats (Olude et al., 2014), mole rats (Amrein et al., 2014), bats (Chawana et al., 2013), dogs (Fernández-Flores et al., 2018) and humans (Eriksson et al., 1998).

Neurogenesis is a complex multi-step process that involves proliferation of neuronal stem cells, differentiation, migration and integration into existing neuronal circuits (Barnea and Pravosudov, 2011). Under normal physiological conditions, new neurons are formed in the sub ventricular zone (SVZ) of the lateral ventricles and the sub granular zones (SGZ) of the hippocampal dentate gyrus of the mammalian brain (Ihunwo and Pillay, 2007). Neurons formed in the SVZ

Abbreviations: AESC, animal and ethics screening committee; ANOVA, analysis of variance; CA, anterior commissure; CB, cerebellum; CC, corpus callosum; CP, caudoputamen; DAB, 3, 3' di-amino-benzidine tetrachloride; DCX, doublecortin; DCX-ir, doublecortin immunoreactive cells; DG, dentate gyrus; DIEN, diencephalon; dRMS, dorsal band of the rostral migratory stream; EGFR, epidermal growth factor receptor; EGF, epidermal growth factor; FGF 2, Fibroblast growth factor 2; HL-RMS, Horizontal limb of the rostral migratory stream; HPA, hypothalamo-pituitary axis; H_2O_2, hydrogen peroxide; IC, inferior colliculus; IGF-1, insulin-like growth factor-1; IgG, immunoglobulin G; Ki-67, Kiel 67; Ki-67-ir, Kiel 67 immunoreactive cells; LV, lateral ventricle; nAcc, nucleus accumbens; MED, medulla; MES, mesencephalon; NC, neocortex; NIH, National Institute of Health; NRF, National Research Foundation; OBc-RMS, olfactory bulb core of the rostral migratory stream; OB, olfactory bulb; PB, phosphate buffer; RMS, rostral migratory stream; SCZ, sub callosal zone; SEM, standard error of mean; SGZ, sub granular zone; SSAJRP, Swiss-South Africa joint research programme; SVZ, sub ventricular zone; SVZa, anterior part of the sub ventricular zone; TECT, tectum; TGF, transforming growth factor; VEGF, vascular endothelial growth factor; VL-RMS, ventral limb of the rostral migratory stream; vRMS, ventral band of the rostral migratory stream

* Corresponding author at: School of Anatomical Sciences, Faculty of Health Sciences, University of the Witwatersrand, 7 York Road, Parktown, 2193, Johannesburg, South Africa.
E-mail address: amadi.ihunwo@wits.ac.za (A.O. Ihunwo).

https://doi.org/10.1016/j.ijdevneu.2018.11.005
Received 2 October 2018; Received in revised form 2 November 2018; Accepted 19 November 2018
Available online 22 November 2018
0736-5748/ © 2018 ISDN. Published by Elsevier Ltd. All rights reserved.

migrate long distances through the rostral migratory stream (RMS) to reach the olfactory bulb (OB) where they integrate into the local circuitry as granule cells and periglomerular cells (Mobley et al., 2014). On the other hand, neurons born in the SGZ travel short distances to integrate into the granule cell layer of the dentate gyrus (Nada et al., 2010; Amrein et al., 2014). However, other potential neurogenic sites have been reported in the mammalian brain including the hypothalamus, cortex, septum, subcallosal zone (SCZ), 3rd ventricle and 4th ventricle (Brown et al., 2003; Ihunwo and Pillay, 2007; Pierce and Xu, 2010; Kim et al., 2012; Lee and Blackshaw, 2012).

Several intrinsic and extrinsic factors have been shown to regulate neurogenesis including growth factors, hormones, physical activity, environmental enrichment, learning and age (reviewed by Aimone et al. (2014)). Although neurogenesis persists throughout life in the mammalian brain, several studies have identified chronological age as one of the strongest of its regulators. In mice specifically, age-related decline in neurogenesis was reported in the dentate gyrus (Kuhn et al., 1996; Nada et al., 2010; Encinas et al., 2011; Jinno, 2011),SVZ (Enwere et al., 2004; Luo et al., 2006; Shook et al., 2012), RMS (Mobley et al., 2014), OB (Enwere et al., 2004; Kondo et al., 2010) and the SCZ (Kim et al., 2012). However, these age- related studies focused only on neurogenesis at different phases of adulthood, that is young or early (1–3 months old), mid (6–12 months old) and late (20–24 months old) adulthood. Findings from such studies only represent changes at the tail end of postnatal neurogenesis and do not provide insight on how postnatal neurogenesis changes across different life history stages of the animal, that is juvenile, sub adult and adult stages. Given that age-related decreases in neurogenesis likely commences during early postnatal life, the current study analyzed age and life-history stage related changes in this process in the male BALB/c mouse brain. Ki-67 and DCX immunohistochemistry was used to assess changes in cell proliferation and neuronal incorporation respectively. Ki-67 is a chromosomal associated protein that is expressed during the cell cycle whereas DCX is a microtubule-associated protein which labels immature and migrating neuroblasts in the brain (Jinno, 2011; Balthazart and Ball, 2014).

2. Materials and methods

2.1. Animals

Male BALB/c mice obtained from the Central Animal Services, University of the Witwatersrand with ages ranging from 1 to 12 weeks (n = 36) were used in this study. The animals were treated and used according to the guidelines of the University of the Witwatersrand Animal Ethics Committee which correspond with those of the National Institute of Health (NIH) for care and use of animals in scientific experimentation. All protocols were approved by the University of the Witwatersrand Animal Ethics Screening Committee (AESC/2014/35/A).

Throughout the study, the mice were maintained under a 12 h: 12 h light dark cycle with access to food and water *ad libitum*. For the 12 weeks, 3 mice were collected and sacrificed every week. The mice were randomly allocated to groups according to their sexual maturity as follows: juvenile (1–5 weeks old, n = 15), sub adult (6–8 weeks old, n = 9) and young adult (9–12 weeks old, n = 12).

2.2. Tissue collection and processing

All animals were injected intraperitoneally with Euthapent (0.5–1 ml/kg). Animals were then perfused transcardially, initially with 0.9% cold saline solution, followed by 4% paraformaldehyde in 0.1 M phosphate buffer (PB, pH 7.4) solution. After perfusion, brains were carefully removed from the skull, post-fixed overnight in 4% paraformaldehyde in 0.1 M PB, weighed before being transferred into 30% sucrose in 0.1 M PB until equilibration. The brains were sectioned in a sagittal plane at 50 μm using a cryostat (Shandon Cryotome E, Thermo Fischer Scientific, UK) at -24°C and repeated series of 5 sections were collected free-floating into 24 multi-well plates containing 0.1 M PB. The first series of sections was mounted on gelatin- coated slides before staining with 1% cresyl violet for anatomical orientation. The second and third series were used for Ki-67 and DCX immunohistochemistry respectively. The remaining two series were stored in a cryoprotectant solution at -20° C for future use.

2.3. Immunohistochemistry

Brain sections were pre-treated for 30 min at room temperature under gentle shaking with an endogenous peroxidase inhibitor solution [0.1 M PB, 100% methanol, 30% H_2O_2 in the ratio of 49.2: 49.2: 1.66]. Following three 10-min rinses in 0.1 M PB, the sections were subsequently pre-incubated in a blocking buffer solution [3% normal goat serum, 2% bovine serum albumin, 0.25% Triton X-100 in 0.1 M PB] for 2 h under gentle shaking at room temperature to prevent non-specific binding. Sections were then transferred into a primary antibody solution [1:1000, rabbit anti-Ki-67 (AB15580, Abcam, UK) or 1: 2000, rabbit anti-DCX (AB18723, Abcam, UK), in the blocking buffer solution] and were incubated for 48 h at 4 °C under gentle shaking. Following incubation, sections were subjected to three 10-min rinses in 0.1 M PB before being incubated in secondary antibody solution [1,000 dilution of biotinylated anti-rabbit IgG (BA-5000; Vector Laboratories, USA) in blocking buffer solution] for 2 h at room temperature under gentle shaking. Following three 10-min rinses in 0.1 M PB, the sections were incubated in an avidin-biotin solution [1: 125 A and 1: 125 B (Vector Laboratories) in 0.1 M PB] for 1 h. The sections were then transferred into three 10-min 0.1 M PB rinses before being placed in a solution containing 0.05% 3, 3′ di-amino-benzidine tetrachloride (DAB) in 0.1 M PB for 5 min. To each 1 ml of this solution, 3.3 μl of 30% H_2O_2 were added, and chromatic precipitation was visually monitored under a low power stereomicroscope.

Development was subsequently stopped by placing the sections in 0.1 M PB, followed by a final 10-min rinse in 0.1 M PB. Sections were mounted on 0.5% gelatinised slides, left to dry overnight, dehydrated in a graded series of alcohols, cleared in xylene and cover slipped with DPX. To ensure that non-specific staining was not affecting the results, control sections taken at random were processed in the same manner, but either the primary or the secondary antibody was omitted. No labelled cells were observed in either case.

2.4. Data analysis

2.4.1. Qualitative analysis

Sections were analysed qualitatively with both low and high power microscopy to yield a comparative description of the distribution of Ki-67 and DCX-immunoreactive (-ir) cells. Anatomical brain structures were identified based on the Allen's reference atlas of the mouse brain (Dong, 2008). High power microscopic observation was used to determine the relative densities of Ki-67 and DCX immunostained structures throughout the different regions of the brain. The relative densities of immunostained structures were visually compared and recorded on a scale ranging from absent (-) to low (+) to moderate (++) to high (+++) (Chawana et al., 2013; Mazengenya et al., 2018; Nkomozepi et al., 2018).

2.4.2. Quantitative analysis

The quantification of Ki-67 and DCX-ir cells was done using computer assisted image analysis by the first author (PN) who was blinded to the ages of the animals. Sections were digitized using a AxioCam HRC video camera linked to a Zeiss Axioplan 2 microscope and Ki-67 and DCX-ir cells in each brain region of interest were manually counted using the cell counter function of ImageJ (Schneider et al., 2012). Ki-67 and DCX quantification was carried out in the following brain regions:

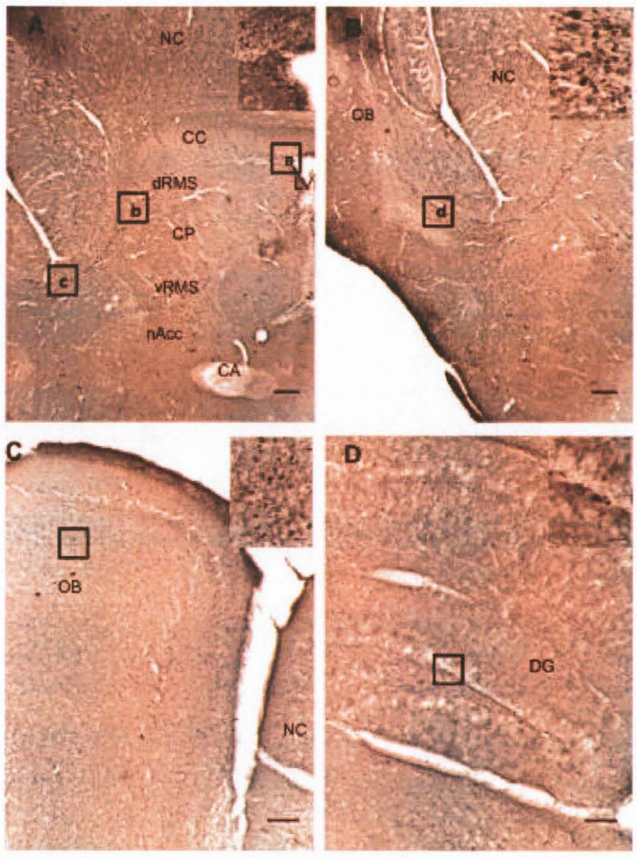

Fig. 1. Photomicrographs showing distribution of Ki-67-ir cells in the telencephalon and olfactory bulb of the BALB/c mouse brain. (A) Ki-67-ir cells in the sub ventricular zone (SVZ) and the rostral migratory streams (dRMS & vRMS), (B) Ki-67-ir cells in terminal portion of the rostral migratory stream in the core of the olfactory bulb (OBc-RMS), (C) Ki-67- ir cells in the olfactory bulb (OB) and (D) Ki-67-ir cells in the dentate gyrus of the hippocampus (DG). The inserts in the upper right corner of each image represent higher magnification photomicrographs. In all images dorsal is to the top and rostral to the left. Squares a, b, c & d in photomicrographs A and B show brain regions where quantification was carried out. Squares in photomicrographs A (a), B, C and D show regions where the inserts were magnified from. Scale bar in A and B = 200 μm; in C and D = 100 μm. Scale bar in all inserts = 20 μm. See list of abbreviations for abbreviations used on the figure.

2.4.3. Sub ventricular zone and rostral migratory stream

Quantification of Ki-67 and DCX-ir cells was carried out in all the brain sections per animal exhibiting the complete SVZ- RMS- OB continuum (two sections in this case) following the method described by Li et al. (2009). The first brain section corresponded to sagittal level 15 (lateral 1.10 mm) of Allen's reference atlas of the mouse brain (Dong, 2008) and the second one was situated 250 μm medial to the first section. For the SVZ, the enlarged region overlying the anterior horn of the lateral ventricle (SVZa) was quantified (Fig. 1 A). For the RMS, three regions were quantified: the short vertical segment which descends ventrally from the SVZ (VL-RMS), the rostral horizontal extension of the RMS (HL-RMS) (Fig. 1 A) and the terminal portion of the RMS in the centre of the olfactory bulb (OBc-RMS) (Fig. 1B). In each of these brain regions, three quantification fields at a magnification of 100X (each one equal to 0.013 mm^2) were used per section.

2.4.4. Sub granular zone of the dentate gyrus

Ki-67 and DCX-ir cells were quantified in 6 corresponding sections/per animal (approximately 250 μm apart) containing the dentate gyrus following a method modified from Obiorah et al. (2015). The first section was situated at a level corresponding to sagittal level 12 (lateral 1.725 mm) of Allen's reference atlas of the mouse brain (Dong, 2008) and the rest were placed medial to the first one. In each section, all Ki-67 and DCX-ir in the SGZ of the entire dentate gyrus were quantified at a magnification of 40 ×.

High resolution microscopic images digitally captured with an AxioCam HRC digital camera on a Zeiss Axioplan 2 compound microscope were processed with the Adobe Photoshop 7.0 software (Adobe Systems, Mountain View, CA). No pixelation adjustment or manipulation of the captured images was undertaken, except for the adjustment of brightness and contrast.

2.4.5. Statistical analysis

Ki-67 and DCX-ir cell counts were averaged where multiple quantification fields were used at the same or different medio-lateral levels of the same brain region. The Shapiro-Wilks normality test was used to test the normality of data in all the variables. For all the variables, the data followed a normal distribution ($P > 0.05$). The correlation between age and either Ki-67 or DCX-ir cell counts for each brain region was tested using Pearson's correlation analysis.

For each brain area quantified, the mean counts of Ki-67 or DCX ir cells for each life-history stage were computed and compared using one-way analysis of variance (ANOVA) followed by Bonferroni's *post hoc* test. All analyses were performed using Graphpad prism 5 software (Graphpad software, CA). All results were expressed as means ± standard deviation and a significance level of $P < 0.05$ was used.

Table 1
Age-related changes in Ki-67 expression in the BALB/c mouse brain.

	Ki-67 Immunoreactivity											
	1 week	2 weeks	3weeks	4weeks	5weeks	6weeks	7weeks	8weeks	9weeks	10weeks	11weeks	12weeks
OB	+++	+++	++	++	+	+	+	+	+	+	+	+
RMS	+++	+++	+++	+++	+++	+++	+++	+++	++	++	++	++
SVZ	+++	+++	+++	+++	+++	+++	+++	+++	++	++	++	++
SGZ	+++	+++	++	++	++	++	++	+	+	+	+	+
NC	+	+	+	+	+	+	+	+	+	+	+	+
TECT	++	++	++	+	+	+	+	+	+	+	+	+
DIEN	–	–	–	–	–	–	–	–	–	–	–	–
MES	–	–	–	–	–	–	–	–	–	–	–	–
MED	–	–	–	–	–	–	–	–	–	–	–	–
CB	++	++	++	++	++	++	++	+	+	+	+	+

+++ high density ++ medium density + low density - absent. See list of abbreviations for abbreviations used in the table.

3. Results

3.1. Distribution of Ki-67 and DCX immunoreactive cells in the BALB/c mouse brain

The distributive pattern of Ki-67 and DCX-ir was similar across all the ages studied except for variations in the density of labelled cells (Tables 1 and 2). Thus the following description applies to all ages studied.

Ki-67-ir cells were mainly observed in the sub ventricular zones (SVZ) of the lateral ventricles, the rostral migratory stream (RMS), olfactory bulbs (OB) and sub granular zone (SGZ) of the dentate gyrus.

In the SVZ, Ki-67-ir cells occupied the dorsal and ventral proliferative zones which were separated by the lateral ventricular bulge of the corpus striatum (Fig. 1 A). From the dorsal proliferative zone a band of Ki-67-ir cells (dorsal RMS) coursed along the dorsal border of the corpus striatum between the caudoputamen and the corpus callosum. In this region, some Ki-67-ir cells appeared to migrate from the dorsal RMS and traverse the substance of the corpus callosum to reach the neocortex (Fig. 2A). Ki-67-ir cells from the ventral proliferative zone (ventral RMS) coursed along the ventral border of the corpus striatum between the nucleus accumbens and the caudoputamen. The dorsal RMS and ventral RMS merged rostrally into one RMS before turning sharply upwards to enter the OB (Fig. 1 B). In the OB, Ki-67-ir cells were observed in all the five layers although they were mostly abundant in the granule cell layer (Fig. 1 C).

Ki-67-ir cells were mostly observed in the SGZ, a region located between the granule cell layer and the hilus of the dentate gyrus of the hippocampus (Fig. 1 D). In addition, fewer Ki- 67-ir cells were observed in the granule cell layer of the dentate gyrus. Few Ki-67-ir cells were occasionally observed in the different layers of the neocortex (Fig. 2 B); the cerebellar cortex and peduncles (Fig. 2 C), superior and inferior colliculi of the tectum (Fig. 2 D). The density of Ki-67-ir cells decreased with advancing age (Table 1).

Similarly, DCX-ir cells were observed mainly in the SVZ of the lateral ventricles, RMS (Fig. 3 A & B), OB (Fig. 3C) and SGZ (Fig. 3 D) at all ages studied. In these areas, DCX-ir cells were observed in corresponding locations as the Ki-67-ir cells. The majority of DCX-ir cells observed in the SVZ and RMS were bipolar in morphology with short leading processes and appeared to migrate from the SVZ towards the OB. In the OB, numerous small bipolar cells with short processes were observed in the granule cell layer (Insert, Fig. 3 C). In addition, fewer cells with longer processes were observed in the internal plexiform and glomerular layers of the OB.

In the dentate gyrus, DCX-ir cells were mostly observed in the SGZ and granule layer with their processes extending towards the granule cell layer and molecular layers respectively (Insert, Fig. 3D). Fewer DCX-ir cells were occasionally observed in the layers of the neocortex (Fig. 3E). The density of DCX-ir cells decreased with advancing age (Table 2).

3.2. Age-related changes in the number of Ki-67 and DCX immunoreactive cells in the BALB/c mouse brain

Pearson's correlation analysis revealed that the number of Ki-67-ir cells sharply declined with postnatal age in the VL-RMS ($r = -0.9884$; $P < 0.0001$, Fig. 4A), HL-RMS ($r = -0.9910$; $P < 0.0001$, Fig. 4C), OBc-RMS ($r = -0.9951$; $P < 0.0001$, Fig. 5A), SVZa ($r = -0.9940$; $P < 0.0001$, Fig. 6A) and SGZ ($r = -0.9838$; $P < 0.0001$, Fig. 6C)

Similarly, the number of DCX-ir cells decreased significantly with postnatal age in the VL-RMS ($r = -0.9811$; $P < 0.0001$, Fig. 4B), HL-RMS ($r = -0.9830$; $P < 0.0001$, Fig. 4D), OBc-RMS ($r = -0.9858$; $P < 0.0001$, Fig. 5B), SVZa ($r = -0.9722$; $P < 0.0001$, Fig. 6B) and SGZ ($r = -0.9767$; $P < 0.0001$, Fig. 6D).

Table 2
Age-related changes in DCX expression in the BALB/c mouse brain.

	DCX Immunoreactivity											
	1 week	2 weeks	3weeks	4weeks	5weeks	6weeks	7weeks	8weeks	9weeks	10weeks	11weeks	12weeks
OB	+++	+++	+++	+++	+++	+++	+++	+++	++	++	++	++
RMS	+++	+++	+++	+++	+++	+++	++	++	++	++	++	+
SVZ	+++	+++	+++	+++	+++	+++	++	++	++	++	++	++
SGZ	+++	+++	+++	+++	+++	++	++	++	++	+	+	+
NC	++	++	+	+	+	+	+	+	+	+	+	+
TECT	–	–	–	–	–	–	–	–	–	–	–	–
DIEN	–	–	–	–	–	–	–	–	–	–	–	–
MES	–	–	–	–	–	–	–	–	–	–	–	–
MED	–	–	–	–	–	–	–	–	–	–	–	–
CB	–	–	–	–	–	–	–	–	–	–	–	–

+++ high density ++ medium density + low density - absent. See list of abbreviations for abbreviations used in the table.

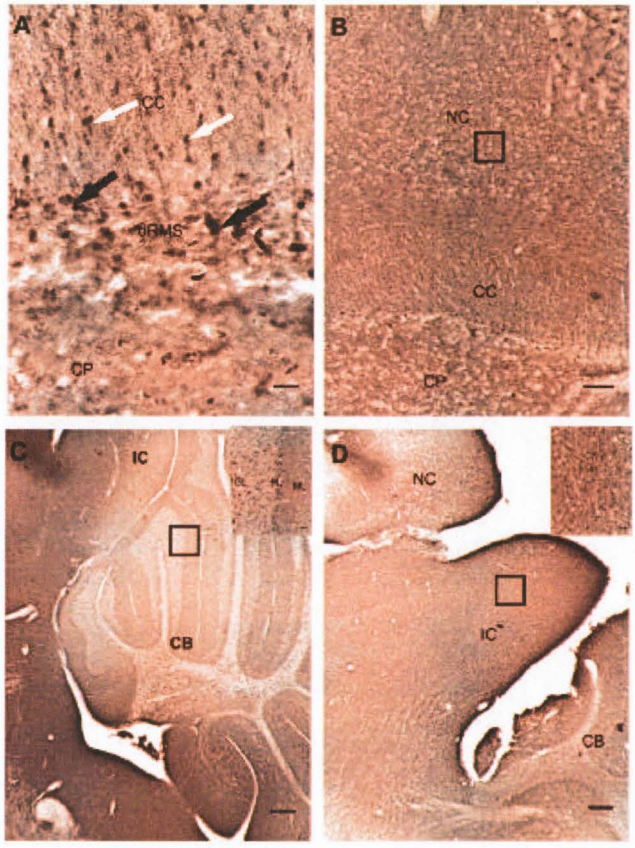

Fig. 2. Photomicrographs showing distribution of Ki-67-ir cells in the dorsal RMS & corpus callosum (A), neocortex (B), cerebellum (C) and inferior colliculus (D) of the BALB/c mouse brain. The inserts in the upper right corner of images B, C and D represent higher magnification photomicrographs of the respective region to demonstrate cellular morphology. In all images dorsal is to the top and rostral to the left. Squares in images B, C and D represent areas where images in inserts were obtained from. Black arrows show Ki-67-ir cells in the dRMS and white arrows show Ki-67-ir cells migrating through the corpus callosum. Scale bar in A = 20 μm; in B = 100 μm; in C and D = 200 μm. Scale bar in inserts B, C and D = 20 μm. See list of abbreviations for abbreviations used on the figure.

3.3. Life-history stage related changes in Ki-67 and DCX immunoreactivity in the BALB/c mouse brain

One way analysis of variance (ANOVA) revealed significant differences in the number of Ki-67-ir cells at different life-history stages in the VL-RMS ($F = 137.7$; $P < 0.0001$, Fig. 7A), HL-RMS ($F = 153.9$; $P < 0.0001$, Fig. 7C), OBc-RMS ($F = 197.0$; $P < 0.0001$, Fig. 7E), SVZa ($F = 135.2$; $P < 0.0001$, Fig. 8A) and SGZ ($F = 119.6$; $P < 0.0001$, Fig. 8C). Between juvenile and sub adult life-history stages, Bonferroni *post hoc* analysis revealed that the number of Ki-67-ir cells significantly declined by approximately 20% in the VL-RMS ($P < 0.0001$), HL-RMS ($P < 0.0001$) & SVZa ($P < 0.0001$) and approximately 25% in the OBc-RMS ($P < 0.0001$) & SGZ ($P < 0.0001$). Similarly, the numbers of Ki-67 positive cells declined by approximately 25% in the SVZa ($P < 0.0001$) & SGZ ($P < 0.0001$), approximately 30% in the VL-RMS ($P < 0.0001$) and approximately 35% in the HL-RMS ($P < 0.0001$) & OBc-RMS ($P < 0.0001$) between the sub adult and adult life-history stages.

Using ANOVA, significant differences were found in the number of DCX-ir cells at different life-history stages in the VL RMS ($F = 134.5$; $P < 0.0001$, Fig. 7B), HL-RMS ($F = 139.6$; $P < 0.0001$, Fig. 7D), OBc-RMS ($F = 145.3$; $P < 0.0001$, Fig. 7F), SVZa ($F = 141.3$; $P < 0.0001$, Fig. 8B) and SGZ ($F = 153.5$; $P < 0.0001$, Fig. 8D). Bonferroni *post hoc* analysis revealed that the number of DCX-ir cells significantly declined by approximately 30% in the VL-RMS ($P < 0.0001$), HL-RMS ($P < 0.0001$), OBc-RMS ($P < 0.0001$), SVZa ($P < 0.0001$) and SGZ ($P < 0.0001$) between the juvenile and sub adult life-history stages. Similarly, the numbers of DCX-ir cells declined by approximately 20% in the VL-RMS ($P < 0.0001$), HL-RMS ($P < 0.0001$), OBc-RMS ($P < 0.0001$), SVZa ($P < 0.0001$) and SGZ ($P < 0.0001$) between sub adult and adult life-history stages.

4. Discussion

In the current study, Ki-67 and DCX immunohistochemistry was used to identify proliferating cells and immature neurons respectively in the BALB/c mouse brain. Ki-67, is a nuclear protein that is associated with ribosomal transcription and is found in the nucleus during interphase (Bullwinkel et al., 2006). However, during mitosis Ki-67 becomes associated with the surface of chromosomes (Balthazart and Ball, 2014). Ki-67 is expressed during all active phases of the cell cycle (G1, S, G2 and mitosis) but is absent in cells that are not cycling (Scholzen and Gerdes, 2000). However, Ki-67 labelling is related to both neurogenesis and gliogenesis. DCX is a microtubule associated protein that controls polymerisation of the leading process and stabilisation of the neuroblast cytoskeleton during migration (Horesh et al., 1999). DCX, therefore, plays a critical role in the migration of immature neurons from the birth site to final positioning at the recruitment site.

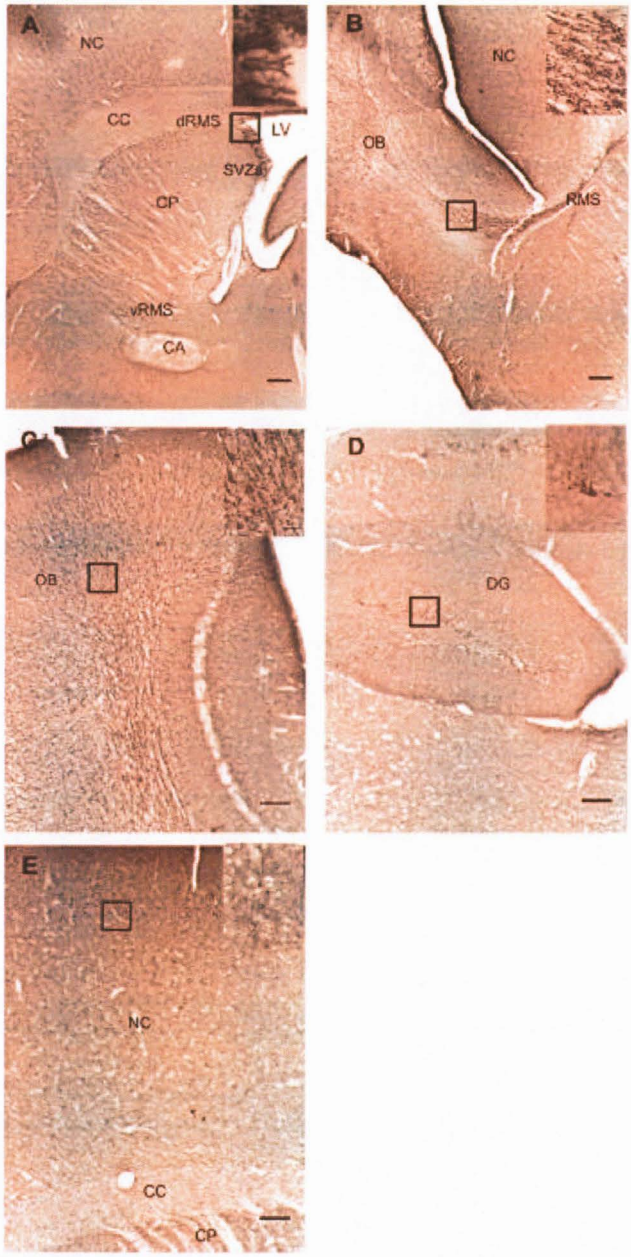

Fig. 3. Photomicrographs showing distribution of DCX-ir cells in the telencephalon and olfactory bulb of the BALB/c mouse brain. (A) DCX-ir cells in the sub ventricular zone (SVZ) and the rostral migratory streams (dRMS & vRMS), (B) DCX-ir cells in the terminal portion of the rostral migratory stream that projects into the olfactory bulb (OBc-RMS), (C) DCX- ir cells in the olfactory bulb (OB), (D) DCX-ir cells in the dentate gyrus of the hippocampus (DG) and (E) DCX-ir cells in the neocortex (NC). The inserts in the upper right corner of each image represent higher magnification photomicrographs of each region to demonstrate cellular morphology. In all images dorsal is to the top and rostral to the left. Squares in photomicrographs A, B, C, D and E represent areas where images in inserts were obtained from. Scale bar in A and B = 200 μm; in C and D = 100 μm. Scale bar in all inserts = 20 μm. See list of abbreviations for abbreviations used on the figure.

4.1. Distribution of Ki-67 and DCX immunoreactive cells in the BALB/c mouse brain

Proliferating cells and immature neurons were observed at all ages in the sub ventricular zone of the lateral ventricles, rostral migratory stream, olfactory bulb and sub granular zone of the hippocampal dentate gyrus. Expression of both Ki-67 and DCX confirmed that these brain regions are indeed neurogenic sites and these findings extend earlier observations made by previous researchers in mammals (Kuhn et al., 1996; Enwere et al., 2004; Kondo et al., 2010; Nada et al., 2010; Encinas et al., 2011; Jinno, 2011; Kempermann, 2011; Mobley et al., 2014; Olaleye and Ihunwo, 2014; Olude et al., 2014; Fernández-Flores et al., 2018).

New neurons produced in the sub ventricular zone migrate along

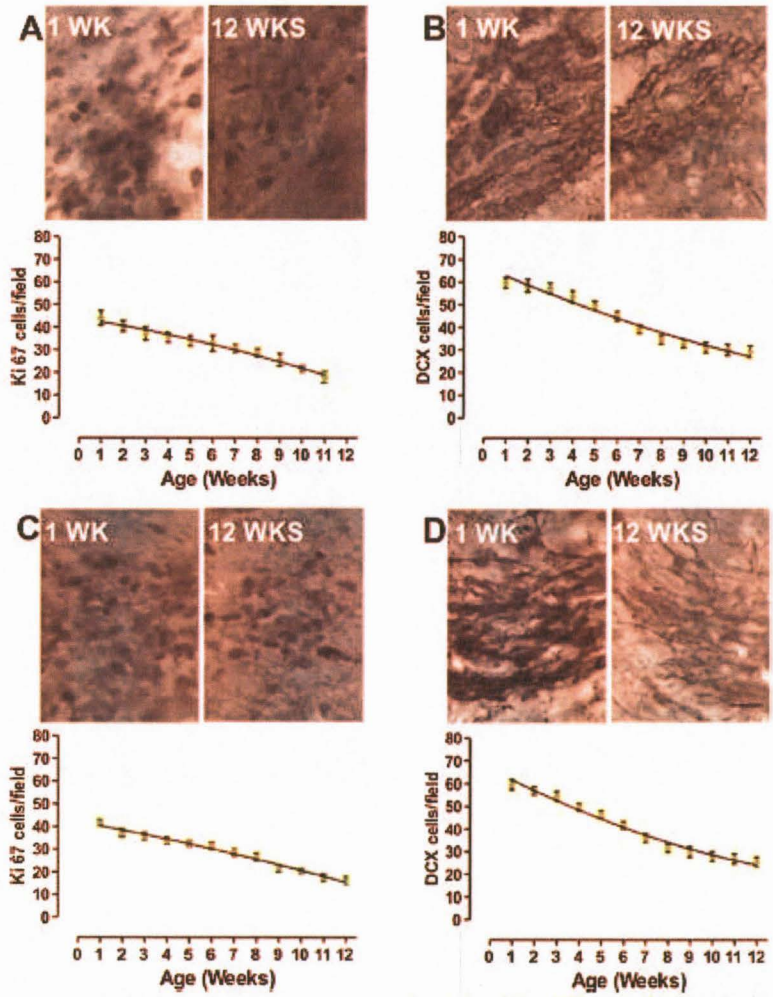

Fig. 4. Photomicrographs and graphs showing age-related changes in numbers of Ki-67-ir (A & C) and DCX-ir (B & D) cells in the different parts of the rostral migratory stream of the BALB/c mouse brain. The number of Ki-67-ir cells sharply decreased with age in the VL-RMS (A) and HL-RMS (C). Similarly, DCX-ir cells decreased with age in the VL-RMS (B) and HL-RMS (D). In each figure, the photomicrographs represent the same brain region in the youngest (1 week old) and the oldest (12 weeks old) animals used in this study. Scale bar in D = 20 μm and applies to all photomicrographs. Error bars correspond to the standard error of the mean (SEM).

the lateral wall of the lateral ventricles and through the rostral migratory stream guided by the astrocytic scaffolding to reach the olfactory bulb where they differentiate into granule and periglomerular interneurons (Mobley et al., 2014). As the neuroblasts migrate through the rostral migratory stream, they retain their ability to proliferate (Mobley et al., 2014) and possibly explains the expression of Ki-67 in RMS observed in the current study.

In the olfactory bulb, mitral and tuft cells are born during embryonic development. However, granule and periglomerular interneurons are mainly born postnatally (Mirich et al., 2002). In fact, only about 25% of the bulbar interneurons are born prenatally (Bayer, 1983). The bulk of bulbar interneurons are born locally within the olfactory bulb before postnatal day 7. In addition, proliferation in the olfactory bulb after the first postnatal week is most likely related to production of glial cells as the SVZ and RMS become the major sources of new bulbar interneurons(Lemasson et al., 2005). Therefore, the Ki-67 expression in the olfactory bulb we observed in this study is most likely related to formation of neuroglia.

Within the hippocampus, Ki-67 and DCX-ir cells were also observed in the sub granular zone of the dentate gyrus at all ages investigated confirming the presence of neurogenesis in this region. In this region, new neurons are born in the sub granular zone, migrate a short distance and integrate into the granule cell layer.

In the neocortex, a few cells expressing Ki-67 and DCX were also observed. In addition, we observed Ki-67 cells migrating from the dorsal RMS through the corpus callosum to reach the neocortex (Fig. 2A) suggesting that the proliferating cells and immature neurons observed in the cortex could have migrated from the dorsal RMS. These observations confirmed that the neocortex continues to recruit new neurons at all ages studied. Our observations are in agreement with the

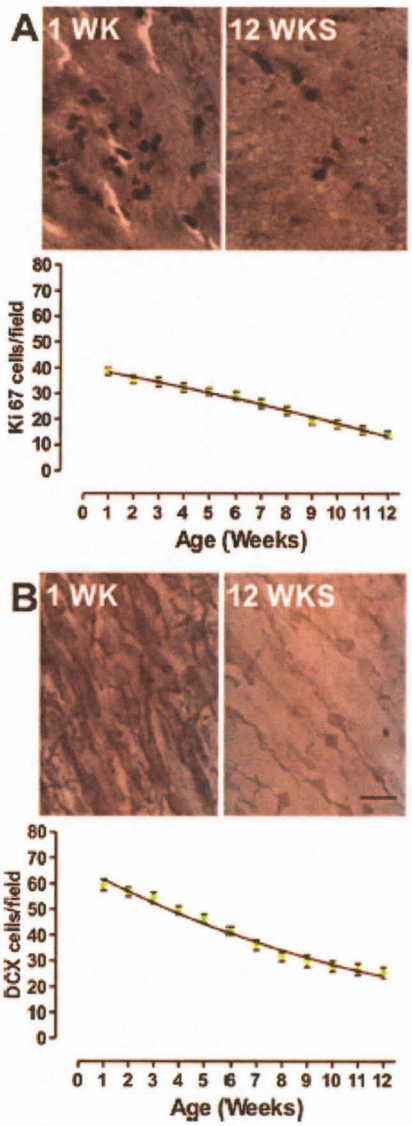

Fig. 5. Photomicrographs and graphs showing age-related changes in the number of Ki-67-ir (A) and DCX-ir (B) cells in the terminal portion of the rostral migratory stream that extends into the core of the olfactory bulb (OBc-RMS) of the BALB/c mouse. The number of Ki-67-ir cells sharply decreased with age in the OBc-RMS (A). Similarly, DCX-ir cells decreased with age in the OBc-RMS (B). In each figure, the photomicrographs represent the same brain region in the youngest (1 week old) and the oldest (12 weeks old) animals used in this study. Scale bar in B = 20 μm and applies to all photomicrographs. Error bars correspond to the standard error of the mean (SEM).

findings of other authors who have reported presence of neurogenesis in the mammalian neocortex (Ihunwo and Pillay, 2007; Chawana et al., 2013; Olude et al., 2014). In contrast to our findings, Olaleye and Ihunwo (2014) observed only DCX but not Ki-67 immunoreactivity in the four striped mouse neocortex. This variation could possibly reflect species (four striped mouse vs BALB/c mouse) and habitat (wild vs laboratory bred) specific differences.

Ki-67 but not DCX immunoreactivity was observed in the tectum and cerebellum. The proliferation observed in these brain regions is presumably related to production of neuroglial cells and not neurons since no immature neurons were observed.

4.2. Age and life-history stage related changes in Ki-67 and DCX expression in the BALB/c mouse brain

In this study, the number of proliferating cells and immature neurons in the SVZ and RMS significantly decreased with postnatal age and life history periods (i.e higher during juvenile periods and lower during adulthood) of the BALB/c mouse brain. Our results further revealed that there was no period during the first 12 postnatal weeks where neurogenesis was stable over extended periods defining life-history stages corresponding to juvenile, sub adult and adult. Age-related decreases in neurogenesis in the SVZ and RMS have been reported previously in laboratory mice (Enwere et al., 2004; Luo et al., 2006; Shook et al., 2012; Mobley et al., 2014), laboratory rats (Chen et al., 2003), the giant African rat (Olude et al., 2014) and more recently dogs (Fernández-Flores et al., 2018). These age-related decreases in neurogenesis in the SVZ and RMS have also been proposed to be functionally linked to the olfactory dysfunction that is observed during aging (Enwere et al., 2004). The decreases in neurogenesis in the SVZ and RMS with age are thought to be as a consequence of either a reduction in the neuronal stem cell proliferation (Kuhn et al., 1996; Tropepe et al., 1997; Enwere et al., 2004; Luo et al., 2006)or lengthening of the cell cycle (Tropepe et al., 1997; Maslov et al., 2004). The decline in cell proliferation observed in the SVZ and RMS has been reported to be related in part to a reduction in epidermal growth factor receptor (EGFR) signaling, fibroblast growth factor 2 (FGF 2) and transforming growth factor (TGF), all of which have been shown to decline with age (Jin et al., 2003; Enwere et al., 2004; Sun et al., 2006). Intracerebral infusions of FGF 2 or heparin binding EGF in aged rodents was reported to restore SVZ and RMS neurogenesis to levels found in young rodents (Jin et al., 2003). In addition, this ability to respond to exogenous factors suggests that neuronal stem cells in the SVZ and RMS become quiescent with aging but retain their capacity to form new neurons when appropriately stimulated. Furthermore, age dependent reductions in telomerase activity have also been implicated in age-related down regulation of neurogenesis in the SVZ. Caporaso et al. (2003) reported that the young rodent SVZ contains higher telomerase activity compared to the adults. Interestingly, telomerase activity appears to mirror proliferation levels in the SVZ (Caporaso et al., 2003).

In the SGZ of the dentate gyrus, a similar relationship between age or life-history stage and the number of proliferating cells or immature neurons was also observed. Similar age-related changes in hippocampal neurogenesis were previously reported in several mammals including laboratory mice (Kronenberg et al., 2006; Nada et al., 2010), wild mice (Amrein et al., 2004), laboratory rats (Drapeau et al., 2003; Jessberger et al., 2009) African giant rats (Olude et al., 2014), mole rats (Amrein et al., 2014) and Humans (Knoth et al., 2010). These observed age-related reductions in neurogenesis in the dentate gyrus could be functionally related to the spatial memory deficits observed in aged animals (Kuhn et al., 1996; Drapeau et al., 2003).

Although the exact mechanisms underlying age-related reductions in hippocampal neurogenesis are poorly understood, a few processes have been singled out. These include a reduction in the neuronal stem cell pool, reduced proliferation of neuronal stem cells or progenitors, reduced survival of neuronal stem cells or progenitors and reduced neuronal lineage commitment (Encinas et al., 2011). Encinas et al. (2011) reported division coupled conversion of neuronal stem cells into mature astrocytes in the hippocampus of aged rodents.

Several factors have been implicated in age-related down regulation of hippocampal neurogenesis among them glucocorticoids and growth

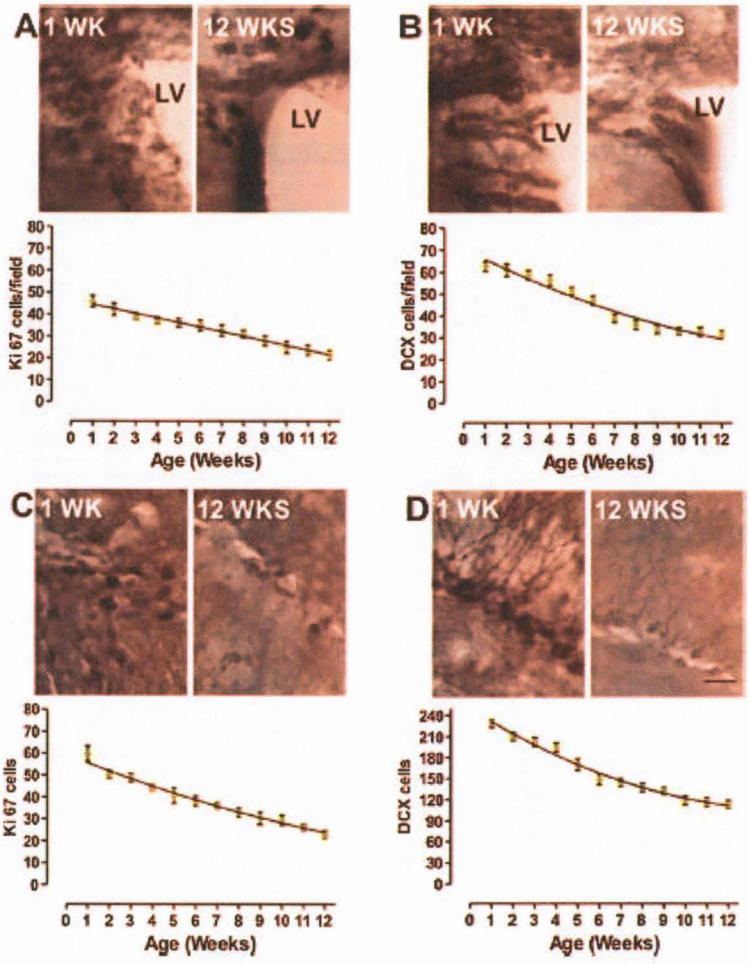

Fig. 6. Photomicrographs and graphs showing age-related changes in the number of Ki-67-ir (A & C) and DCX-ir (B & D) cells in the anterior part of the sub ventricular (SVZa) and sub granular (SGZ) zones of the BALB/c mouse brain. The number of Ki-67-ir cells sharply decreased with age in the SVZa (A) and SGZ (C). Similarly, DCX-ir cells decreased with age in the SVZa (B) and SGZ (D). In each figure, the photomicrographs represent the same brain region in the youngest (1 week old) and the oldest (12 weeks old) animals used in this study. Scale bar in D = 20 μm and applies to all photomicrographs. Error bars correspond to the standard error of the mean (SEM).

factors such as insulin-like growth factor-1 (IGF-I), FGF-2 and vascular endothelial growth factor (VEGF).

Glucocorticoid receptors are strongly expressed in the granule cells of the hippocampus and in neuronal stem cells (Garcia et al., 2004). During the early postnatal period, rodents have been shown to exhibit very low levels of circulating glucocorticoids and to be relatively resistant to stress (Sapolsky and Meaney, 1986). Incidentally, this early postnatal period is also associated with high levels of hippocampal neurogenesis (Bayer, 1983). Furthermore, previous studies have shown that glucocorticoid levels naturally rise with increasing postnatal age in rodents as the hypothalamic-pituitary-adrenal (HPA) axis matures (Sapolsky, 1992; Dalm et al., 2005) and this rise coincides with a reduction in the numbers of newly generated neurons (Cameron and Gould, 1994; Seki and Arai, 1995; Kuhn et al., 1996; Cameron and McKay, 1999).The HPA axis matures during adolescence, thereby providing increased levels of glucocorticoids which have drastic effects on hippocampal neurogenesis in adult animals (Lupien et al., 2009). Conversely, elimination of glucocorticoids by adrenalectomy increases proliferation of neuronal progenitors and formation of new neurons in the hippocampus (Cameron and McKay, 1999; Montaron et al., 1999, 2006).

Growth factors (IGF-I, FGF-2 and VEGF) increase neuronal stem cell proliferation in the hippocampal dentate gyrus and the concentration of these factors in serum or expression of their receptors in the hippocampus have reported to be reduced in adults and aged animals compared to juvenile animals (Lai et al., 2000; Jin et al., 2003; Shetty et al., 2005; Sun et al., 2006). In addition, intraventricular infusion of these growth factors were reported to increase neurogenesis in the adult or aging hippocampus (Lai et al., 2000; Jin et al., 2003; Sun et al., 2006; Rai et al., 2007).

5. Conclusion

Neurogenesis persists throughout the life-history periods of the BALB/c mouse in the sub ventricular zone of the lateral ventricles, rostral migratory stream, olfactory bulb, sub granular zone of the dentate gyrus and the neocortex. In addition, neurogenesis declines sharply with postnatal age in the SVZ, RMS and SGZ of the BALB/c mouse brain. Although cell proliferation persists in the tectum and cerebellum of the BALB/c mouse, it is presumably related to the

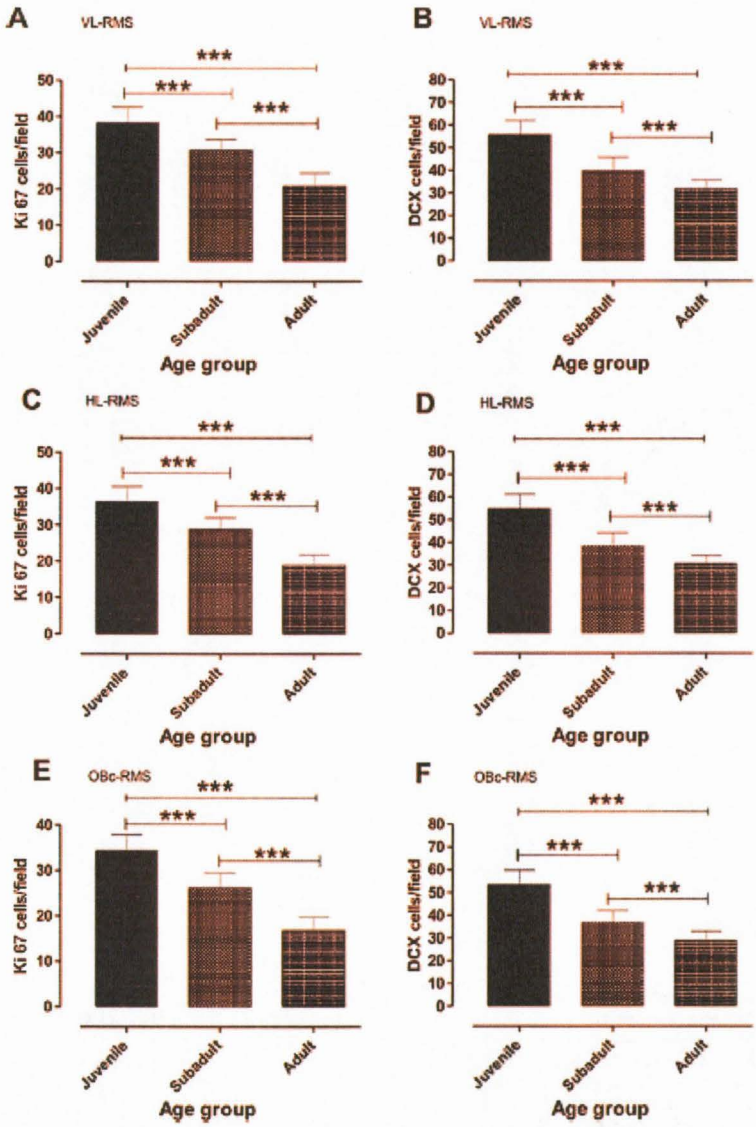

Fig. 7. Graphical representation of the life-history stage related changes in the number of Ki-67-ir (A, C &E) and DCX-ir (B, D & F) cells in the rostral migratory of the BALB/c mouse brain. The number of Ki-67-ir cells decreased with advancing life-history stages in the VL-RMS (A), HL-RMS (C) and OBc-RMS (E). Similarly, DCX-ir cells decreased with advancing life-history stages in the VL-RMS (B), HL-RMS (D) and OBc-RMS (F). Error bars correspond to the mean (SEM). ***$P < 0.0001$.

production of neuroglia.

Funding

This work was supported by the Swiss-South Africa Joint Research Programme (SSAJRP) and the National Research Foundation (NRF) grants awarded to Professor Amadi O Ihunwo.

Conflict of interest

The authors declare no conflict of Interest

Acknowledgements

We express our most sincere gratitude to Mrs Hassiena Ali, Dr Adhil Bangwandin and Professor Paul Manger, of the School of Anatomical Sciences, University of the Witwatersrand for their assistance with animal perfusions, extraction of the brains and immunohistochemistry.

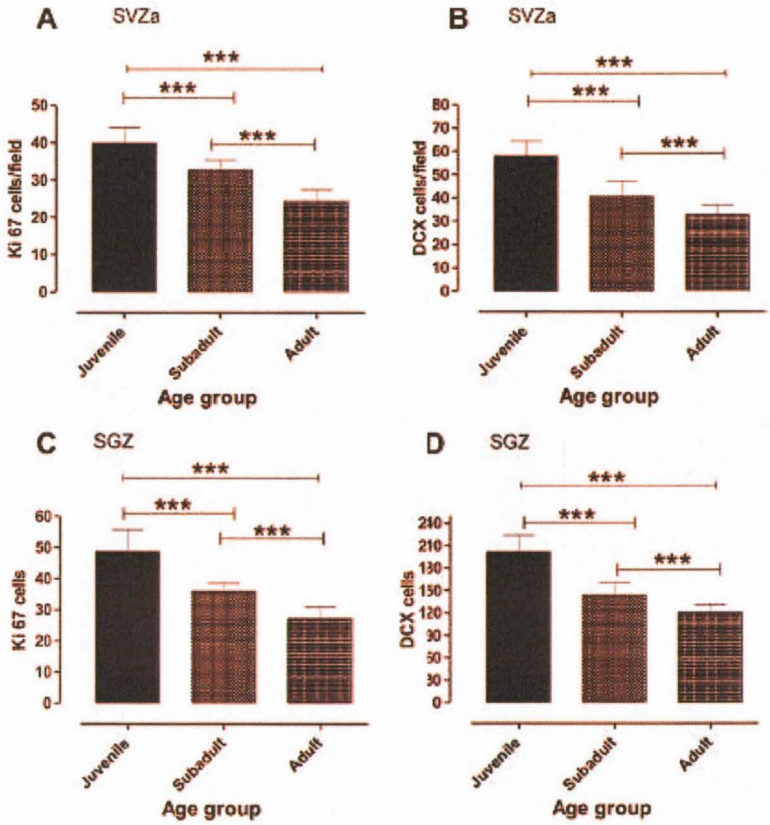

Fig. 8. Graphical representation of the life-history stage related changes in the number of Ki-67-ir (A&C) and DCX-ir (B&D) cells the SVZa and SGZ of the BALB/c mouse brain. The number of Ki-67-ir cells decreased with advancing life-history stages in the SVZa (A) and SGZ (C). Similarly, DCX-ir cells decreased with advancing life-history stages in the SVZa (B) and SGZ (D). Error bars correspond to the standard error of the mean (SEM). ***$P < 0.0001$.

We also extend our gratitude to the University of Witwatersrand Central Animal Service for the care of the animals during the experimental period.

References

Aimone, J.B., Li, Y., Lee, S.W., Clemenson, G.D., Deng, W., Gage, F.H., 2014. Regulation and function of adult neurogenesis: from genes to cognition. Physiol. Rev. 94, 991–1026.

Amrein, I., Becker, A.S., Engler, S., Sh, Huang, Müller, J., Slomianka, L., Oosthuizen, M.K., 2014. Adult neurogenesis and its anatomical context in the hippocampus of three mole-rat species. Front. Neuroanat. 8.

Amrein, I., Slomianka, L., Lipp, H.P., 2004. Granule cell number, cell death and cell proliferation in the dentate gyrus of wild-living rodents. Eur. J. Neurosci. 20, 3342–3350.

Balthazart, J., Ball, G.F., 2014. Endogenous versus exogenous markers of adult neurogenesis in canaries and other birds: advantages and disadvantages. J. Comp. Neurol. 522, 4100–4120.

Barnea, A., Pravosudov, V., 2011. Birds as a model to study adult neurogenesis: bridging evolutionary, comparative and neuroethological approaches. Eur. J. Neurosci. 34, 884–907.

Bayer, S., 1983. 3 H-thymidine-radiographic studies of neurogenesis in the rat olfactory bulb. Exp. Brain Res. 50, 329–340.

Brown, J.P., Couillard-Despres, S., Cooper-Kuhn, C.M., Winkler, J., Aigner, L., Kuhn, H.G., 2003. Transient expression of doublecortin during adult neurogenesis. J. Comp. Neurol. 467, 1–10.

Bull-Winkel, J., Baron-Uhlig, B., Lüdemann, A., Wohlenberg, C., Gerdes, J., Scholzen, T., 2006. Ki-67 protein is associated with ribosomal RNA transcription in quiescent and proliferating cells. J. Cell. Physiol. 206, 624–635.

Cameron, H., Gould, E., 1994. Adult neurogenesis is regulated by adrenal steroids in the dentate gyrus. Neuroscience 61, 203–209.

Cameron, H.A., McKay, R.D., 1999. Restoring production of hippocampal neurons in old age. Nat. Neurosci. 2, 894–897.

Caporaso, G.L., Lim, D.A., Alvarez-Buylla, A., Chao, M.V., 2003. Telomerase activity in the subventricular zone of adult mice. Mol. Cell. Neurosci. 23, 693–702.

Chawana, R., Patzke, N., Kaswera, C., Gilissen, E., Ihunwo, A.O., Manger, P., 2013. Adult neurogenesis in eight megachiropteran species. Neuroscience 244, 159–172.

Chen, X.-H., Iwata, A., Nonaka, M., Browne, K.D., Smith, D.H., 2003. Neurogenesis and glial proliferation persist for at least one year in the subventricular zone following brain trauma in rats. J. Neurotrauma 20, 623–631.

Dalm, S., Enthoven, L., Meijer, O.C., van der Mark, M.H., Karssen, A.M., de Kloet, E.R., Oitzl, M.S., 2005. Age-related changes in hypothalamic-pituitary-adrenal axis activity of male C57BL/6J mice. Neuroendocrinology 81, 372–380.

Dong, H.W., 2008. The Allen Reference Atlas: a Digital Color Brain Atlas of the C57Bl/6J Male Mouse. John Wiley & Sons Inc.

Drapeau, E., Mayo, W., Aurousseau, C., Le Moal, M., Piazza, P.-V., Abrous, D.N., 2003. Spatial memory performances of aged rats in the water maze predict levels of hippocampal neurogenesis. Proc. Natl. Acad. Sci. 100, 14385–14390.

Encinas, J.M., Michurina, T.V., Peunova, N., Park, J.-H., Tordo, J., Peterson, D.A., Fishell, G., Koulakov, A., Enikolopov, G., 2011. Division-coupled astrocytic differentiation and age-related depletion of neural stem cells in the adult hippocampus. Cell Stem Cell 8, 566–579.

Enwere, E., Shingo, T., Gregg, C., Fujikawa, H., Ohta, S., Weiss, S., 2004. Aging results in reduced epidermal growth factor receptor signaling, diminished olfactory neurogenesis, and deficits in fine olfactory discrimination. J. Neurosci. 24, 8354–8365.

Eriksson, P.S., Perfilieva, E., Björk-Eriksson, T., Alborn, A.-M., Nordborg, C., Peterson, D.A., Gage, F.H., 1998. Neurogenesis in the adult human hippocampus. Nat. Med. 4.

Fernández-Flores, P., García-Verdugo, J.M., Martín-Ibáñez, R., Herranz, C., Fondevila, D., Ginés, J.M., Arús, C., Pumarola, M., 2008. Characterization of the canine rostral ventricular-subventricular zone: morphological, immunohistochemical, ultrastructural, and neurosphere assay studies. J. Comp. Neurol. 526, 721–741.

García, A., Steiner, B., Kronenberg, G., Bick-Sander, A., Kempermann, G., 2004.

Age-dependent expression of glucocorticoid and mineralocorticoid receptors on neural precursor cell populations in the adult murine hippocampus. Aging Cell 3, 363–371.
Horesh, D., Sapir, T., Francis, F., Wolf, S.G., Caspi, M., Elbaum, M., Chelly, J., Reiner, O., 1999. Doublecortin, a stabilizer of microtubules. Hum. Mol. Genet. 8, 1599–1610.
Ihunwo, A., Pillay, S., 2007. Neurogenic sites in the adult mammalian central nervous system. Res. J. Biol. Sci. 2, 170–177.
Jessberger, S., Clark, R.E., Broadbent, N.J., Clemenson, G.D., Consiglio, A., Lie, D.C., Squire, L.R., Gage, F.H., 2009. Dentate gyrus-specific knockdown of adult neurogenesis impairs spatial and object recognition memory in adult rats. Learn. Mem. 16, 147–154.
Jin, K., Sun, Y., Xie, L., Batteur, S., Mao, X.O., Smelick, C., Logvinova, A., Greenberg, D.A., 2003. Neurogenesis and aging: FGF-2 and HB-EGF restore neurogenesis in hippocampus and subventricular zone of aged mice. Aging Cell 2, 175–183.
Jinno, S., 2011. Decline in adult neurogenesis during aging follows a topographic pattern in the mouse hippocampus. J. Comp. Neurol. 519, 451–466.
Kempermann, G., 2011. Seven principles in the regulation of adult neurogenesis. Eur. J. Neurosci. 33, 1018–1024.
Kim, H.J., Kim, J.Y., Sun, W., 2012. Age-dependent changes in the subcallosal zone neurogenesis of mice. Neurochem. Int. 61, 879–884.
Knoth, R., Singec, I., Ditter, M., Pantazis, G., Capetian, P., Meyer, R.P., Horvat, V., Volk, B., Kempermann, G., 2010. Murine features of neurogenesis in the human hippocampus across the lifespan from 0 to 100 years. PLoS One 5, e8809.
Kondo, K., Suzukawa, K., Sakamoto, T., Watanabe, K., Kanaya, K., Ushio, M., Yamaguchi, T., Nibu, K.I., Kaga, K., Yamasoba, T., 2010. Age-related changes in cell dynamics of the postnatal mouse olfactory neuroepithelium: cell proliferation, neuronal differentiation, and cell death. J. Comp. Neurol. 518, 1962–1975.
Kronenberg, G., Bick-Sander, A., Bunk, E., Wolf, C., Ehninger, D., Kempermann, G., 2006. Physical exercise prevents age-related decline in precursor cell activity in the mouse dentate gyrus. Neurobiol. Aging 27, 1505–1513.
Kuhn, H.G., Dickinson-Anson, H., Gage, F.H., 1996. Neurogenesis in the dentate gyrus of the adult rat: age-related decrease of neuronal progenitor proliferation. J. Neurosci. 16, 2027–2033.
Lai, M., Hibberd, C.J., Gluckman, P.D., Seckl, J.R., 2000. Reduced expression of insulin-like growth factor I messenger RNA in the hippocampus of aged rats. Neurosci. Lett. 288, 66–70.
Lee, D.A., Blackshaw, S., 2012. Functional implications of hypothalamic neurogenesis in the adult mammalian brain. Int. J. Dev. Neurosci. 30, 615–621.
Lemasson, M., Saghatelyan, A., Olivo-Marin, J.C., Lledo, P.-M., 2005. Neonatal and adult neurogenesis provide two distinct populations of newborn neurons to the mouse olfactory bulb. J. Neurosci. 25, 6816–6825.
Li, X., Tang, X., Jablonska, B., Aguirre, A., Gallo, V., Luskin, M.B., 2009. P27KIP1 regulates neurogenesis in the rostral migratory stream and olfactory bulb of the postnatal mouse. J. Neurosci. 29, 2902–2914.
Luo, J., Daniels, S.B., Lennington, J.B., Notti, R.Q., Conover, J.C., 2006. The aging neurogenic subventricular zone. Aging Cell 5, 139–152.
Lupien, S.J., McEwen, B.S., Gunnar, M.R., Heim, C., 2009. Effects of stress throughout the lifespan on the brain, behaviour and cognition. Nat. Rev. Neurosci. 10, 434–445.
Maslov, A.Y., Barone, T.A., Plunkett, R.J., Pruitt, S.C., 2004. Neural stem cell detection, characterization, and age-related changes in the subventricular zone of mice. J. Neurosci. 24, 1726–1733.
Matengenya, P., Bhagwandin, A., Manger, P.R., Ihunwo, A.O., 2018. Putative adult neurogenesis in old world parrots: the Congo African grey parrot (Psittacus erithacus) and Timneh grey parrot (Psittacus timneh). Front. Neuroanat. 12, 7.
Mirich, J.M., Williams, N.C., Berlau, D.J., Brunjes, P.C., 2002. Comparative study of aging in the mouse olfactory bulb. J. Comp. Neurol. 454, 361–372.
Mobley, A.S., Rodriguez-Gil, D.J., Imamura, F., Greer, C.A., 2014. Aging in the olfactory system. Trends Neurosci. 37, 77–84.
Montaron, M., Drapeau, E., Dupret, D., Kitchener, P., Aurousseau, C., Le Moal, M., Piazza, P., Abrous, D., 2006. Lifelong corticosterone level determines age-related decline in neurogenesis and memory. Neurobiol. Aging 27, 645–654.
Montaron, M., Petry, K., Rodriguez, J., Marinelli, M., Aurousseau, C., Rougon, G., Le Moal, M., Abrous, D., 1999. Adrenalectomy increases neurogenesis but not PSA-NCAM expression in aged dentate gyrus. Eur. J. Neurosci. 11, 1479–1485.
Nada, M.-B., Slomianka, L., Vyssotski, A.L., Lipp, H.-P., 2010. Early age-related changes in adult hippocampal neurogenesis in C57 mice. Neurobiol. Aging 31, 151–161.
Nkomozepi, P., Matengenya, P., Ihunwo, A.O., 2018. Changes in neurogenesis with post-hatching age in the male Japanese quail (Coturnix japonica) brain. Acta Neurobiol. Exp. (Wars) 78, 173–186.
Obiorah, M., McCandlish, E., Buckley, B., DiCicco-Bloom, E., 2015. Hippocampal developmental vulnerability to methylmercury extends into prepubescence. Front. Neurosci. 9, 150.
Olaleye, O.O., Ihunwo, A.O., 2014. Adult neurogenesis in the four-striped mice (Rhabdomys pumilio). Neural Regen. Res. 9, 1907.
Olude, A.M., Olopade, J.O., Ihunwo, A.O., 2014. Adult neurogenesis in the African giant rat (Cricetomys gambianus, waterhouse). Metab. Brain Dis. 29, 857–866.
Pierce, A.A., Xu, A.W., 2010. De novo neurogenesis in adult hypothalamus as a compensatory mechanism to regulate energy balance. J. Neurosci. 30, 723–730.
Rai, K.S., Hattiangady, B., Shetty, A.K., 2007. Enhanced production and dendritic growth of new dentate granule cells in the middle-aged hippocampus following intracerebroventricular FGF-2 infusions. Eur. J. Neurosci. 26, 1765–1779.
Sapolsky, R.M., 1992. Do glucocorticoid concentrations rise with age in the rat? Neurobiol. Aging 13, 171–174.
Sapolsky, R.M., Meaney, M.J., 1986. Maturation of the adrenocortical stress response: neuroendocrine control mechanisms and the stress hyporesponsive period. Brain Res. Rev. 11, 65–76.
Schneider, C.A., Rasband, W.S., Eliceiri, K.W., 2012. NIH Image to ImageJ: 25 years of image analysis. Nat. Methods 9, 671–675.
Scholzen, T., Gerdes, J., 2000. The Ki-67 protein: from the known and the unknown. J. Cell. Physiol. 182, 311–322.
Seki, T., Arai, Y., 1995. Age-related production of new granule cells in the adult dentate gyrus. Neuroreport 6, 2479–2482.
Shetty, A.K., Hattiangady, B., Shetty, G.A., 2005. Stem/progenitor cell proliferation factors FGF-2, IGF-1, and VEGF exhibit early decline during the course of aging in the hippocampus: role of astrocytes. Glia 51, 173–186.
Shook, B.A., Manz, D.H., Peters, J.J., Kang, S., Conover, J.C., 2012. Spatiotemporal changes to the subventricular zone stem cell pool through aging. J. Neurosci. 32, 6947–6956.
Sun, Y., Jin, K., Childs, J.T., Xie, L., Mao, X.O., Greenberg, D.A., 2006. Vascular endothelial growth factor-B (VEGFB) stimulates neurogenesis: evidence from knockout mice and growth factor administration. Dev. Biol. 289, 329–335.
Thuret, S., Auger, H., Papalopulu, N., 2015. Analysis of neural progenitors from embryogenesis to juvenile adult in Xenopus laevis reveals biphasic neurogenesis and continuous lengthening of the cell cycle. Biology open bio, 013391.
Tropepe, V., Craig, C.G., Morshead, C.M., van der Kooy, D., 1997. Transforming growth factor-α null and senescent mice show decreased neural progenitor cell proliferation in the forebrain subependyma. J. Neurosci. 17, 7850–7859.

From: Stefano Stifani (International Journal of Developmental Neuroscience) <EviseSupport@elsevier.com>
Sent: Monday, March 11, 2019 3:13 PM
To: Amadi Ihunwo <Amadi.Ihunwo@wits.ac.za>
Subject: Your manuscript DN_2018_231_R1 has been accepted

Ref: DN_2018_231_R1
Title: Quantitative analysis of age and life-history stage related changes in DCX expression in the male Japanese quail (Cortunix Japonica) telencephalon
Journal: International Journal of Developmental Neuroscience

Dear Professor Ihunwo,

I am pleased to inform you that your paper has been accepted for publication.

Your accepted manuscript will now be transferred to our production department. We will create a proof which you will be asked to check. You can read more about this here. Meanwhile, you will be asked to complete a number of online forms required for publication. If we need additional information from you during the production process, we will contact.

Thank you for submitting your work to International Journal of Developmental Neuroscience. We hope you consider us again for future submissions.

Kind regards,

Stefano Stifani, PhD
Editor-in-Chief
International Journal of Developmental Neuroscience

Have questions or need assistance?
For further assistance, please visit our Customer Support site. Here you can search for solutions on a range of topics, find answers to frequently asked questions, and learn more about EVISE® via interactive tutorials. You can also talk 24/5 to our customer support team by phone and 24/7 by live chat and email.

Copyright © 2018 Elsevier B.V. | Privacy Policy

Elsevier B.V., Radarweg 29, 1043 NX Amsterdam, The Netherlands, Reg. No. 33156677.